AD-A130 540 AIRBORNE SYSTEMS COURSE TEXTBOOK NAVIGATION SYSTEMS TEST AND EVALUATION(U) NAVAL TEST PILOT SCHOOL PATUXENT RIVER MD G W MASTERS 01 SEP 81 1/3

UNCLASSIFIED F/G 5/9 NL

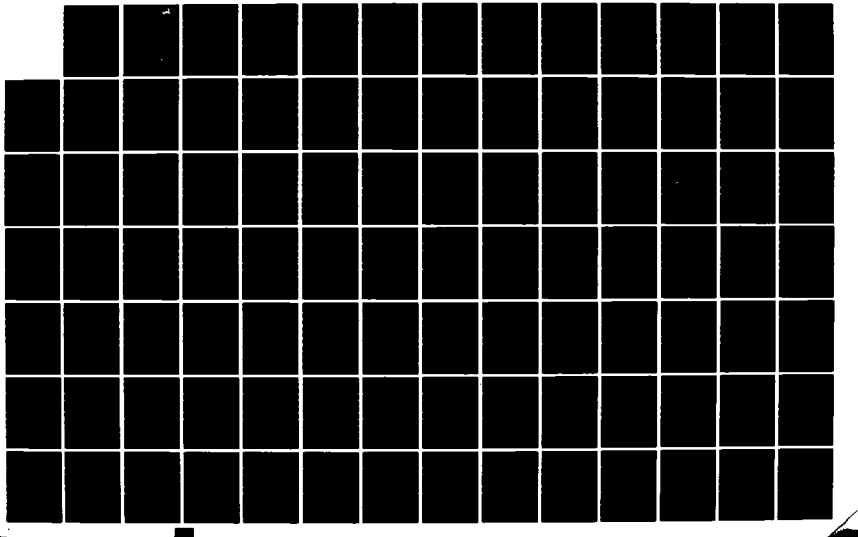

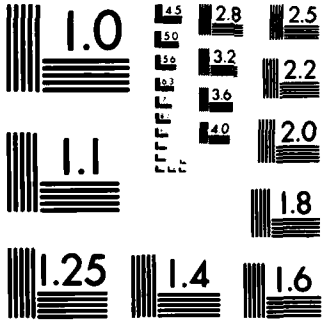

MICROCOPY RESOLUTION TEST CHART
NATIONAL BUREAU OF STANDARDS-1963-A

UNITED STATES NAVAL
TEST PILOT SCHOOL

AIRBORNE SYSTEMS COURSE TEXTBOOK

NAVIGATION SYSTEMS TEST AND EVALUATION

By

George W. Masters

1 September, 1981

UNCLASSIFIED

SECURITY CLASSIFICATION OF THIS PAGE *(When Data Entered)*

REPORT DOCUMENTATION PAGE		READ INSTRUCTIONS BEFORE COMPLETING FORM
1. REPORT NUMBER -	2. GOVT ACCESSION NO. AD-A130 548	3. RECIPIENT'S CATALOG NUMBER -
4. TITLE *(and Subtitle)* Navigation Systems Test and Evaluation		5. TYPE OF REPORT & PERIOD COVERED - 6. PERFORMING ORG. REPORT NUMBER -
7. AUTHOR(s) George W. Masters		8. CONTRACT OR GRANT NUMBER(s) -
9. PERFORMING ORGANIZATION NAME AND ADDRESS U. S. Naval Test Pilot School Naval Air Test Center Patuxent River, Maryland 20670		10. PROGRAM ELEMENT, PROJECT, TASK AREA & WORK UNIT NUMBERS -
11. CONTROLLING OFFICE NAME AND ADDRESS Academics Branch U. S. Naval Test Pilot School		12. REPORT DATE 1 September 1981 13. NUMBER OF PAGES 238
14. MONITORING AGENCY NAME & ADDRESS*(if different from Controlling Office)* -		15. SECURITY CLASS. *(of this report)* UNCLASSIFIED 15a. DECLASSIFICATION/DOWNGRADING SCHEDULE -

16. DISTRIBUTION STATEMENT *(of this Report)*
Approved for public release; distribution unlimited

17. DISTRIBUTION STATEMENT *(of the abstract entered in Block 20, if different from Report)*
-

18. SUPPLEMENTARY NOTES
-

19. KEY WORDS *(Continue on reverse side if necessary and identify by block number)*
Navigation, Inertial Navigation, Doppler Navigation, Radio Navigation, Satellite Navigation, Avionics, Airborne Systems, Test and Evaluation, Flight Testing

20. ABSTRACT *(Continue on reverse side if necessary and identify by block number)*
Textbook for teaching test and evaluation of navigation systems, including theory of operation, operating characteristics and test methodology. Topics include basic airborne navigation principles, inertial navigation systems, doppler navigation systems, radio navigation systems, satellite navigation systems, navigation system hardware and test equipment, and test methods.

DD FORM 1 JAN 73 1473 EDITION OF 1 NOV 65 IS OBSOLETE

UNCLASSIFIED

SECURITY CLASSIFICATION OF THIS PAGE *(When Data*

NAVIGATION SYSTEMS

TEST AND EVALUATION

TABLE OF CONTENTS

AIRBORNE NAVIGATION SYSTEM
TEST AND EVALUATION

1.0 Introduction

1.1 The Nature of Airborne Navigation

Navigation is the process of determining the position, velocity, and orientation of a vehicle, with respect to a specified reference position, and in a specified coordinate system. (The process of determining the direction in which to proceed to arrive at a specified position is termed guidance. The process of executing the guidance commands is termed flight control.) The reference position and coordinate system may be fixed in inertial space, fixed with respect to the earth, or fixed with respect to a moving (translating and/or rotating) reference, such as another vehicle. Long range airborne navigation (position) information is typically presented in terms of latitude, longitude, and altitude (in spherical coordinates). Short range navigation information often is presented, in Cartesian coordinates, as linear distance from a local, specified reference. The usual attitude reference directions are north, east, and the local vertical. It should be noted that a navigation system often does not sense motion or compute position in the same reference system in which the information is presented to the user.

Modern aircraft require continuously available, accurate, "real-time" navigational information. These requirements are a result of the nature of modern aircraft (e.g. speed and range) and of the missions they perform (e.g. rendezvous and weapon delivery). The need for "real-time" information, combined with the need for an automated navigational process, imposes restrictions upon the manner in which the various methods of navigation are employed in modern aircraft. Systems which possess long-term accuracy but which entail an appreciable delay

between the sensing of input data and the presentation of output data, (such as those employing the Transit satellite and those employing intermittent celestial fixes), require an independent means of extrapolating between measurements. Such extrapolation is best accomplished by a system with good short-term accuracy and continuous output, such as an inertial navigation system. The best characteristics of both systems can be exploited by using the system with intermittent, long-term-accuracy data to periodically update the system with continuous, short-term-accurate data. Such "integrated" navigation systems are commonly employed in aircraft. The integration of the performance characteristics of two or more systems in this manner requires correspondingly integrated test procedures for evaluation of the composite system.

1.2 Position Fixing versus Dead Reckoning

Two basically different methods of navigation exist: position fixing and dead reckoning. Position fixing entails a direct, independent determination of position at each point in time. Each determination is independent of those at other time points. Dead reckoning, (derived from DEDUCED RECKONING), entails the deduction of position at a specified point in time from a known position at a previous time and the measurement of velocity between the two time points. That is:

$$\vec{P}(t_1) = P(t_0) + \int_{t_0}^{t_1} \vec{V}(t)\, dt$$

where:

$\vec{P}$ = Position Vector

$\vec{V}$ = Velocity Vector

Because of the time integration and dependence on initial conditions evidenced by the above equation, dead reckoning navigation systems are susceptible to the accumulation of errors. They, therefore, exhibit relatively poor long-term accuracy. Position fixing systems, however, do not accumulate errors in this manner and, therefore, exhibit relatively good long-term accuracy. However, the error characteristics of the two types of systems tend to be reversed with respect to short-term errors. That is, dead reckoning systems tend to exhibit good short-term accuracy and position fixing systems tend to exhibit poor short-term accuracy. These complementary error characteristics are the principal reason for the widespread use of composite systems as discussed in Section 1.1 of this text. (Currently operational radio navigation systems are position-fixing systems while inertial navigation is a dead reckoning technique). These differences in short - and long-term accuracy strongly influence the test methods appropriate to the two types of navigational systems.

1.3 The Basic Methods of Position Fixing

Position fixing navigation systems generally determine position as the intersection of two or more lines (or curves) of position as shown in Figure 1.3.1. Four basic geometric configurations are commonly encountered as shown in that figure. The method of position fixing illustrated in Figure 1.3.1-a utilizes a polar coordinate system and involves the determination of range and bearing of the vehicle from a single, known reference point. The TACAN system, discussed in Section 2.3.6 of this text, is an example of such a system. The method illustrated in Figure 1.3.1-b, called triangulation, determines position as the intersection of the two lines of constant bearing from two known reference points. A position fix determined solely by radio direction finding, as discussed in Section 2.3.3 of this text, is an example of triangulation. The method illustrated in Figure 1.3.1-c, called trilateration, determines vehicle position as the common intersection of the three circles of constant range from three known reference points. (The intersections yielded by only two such circles are ambiguous as shown in the figure.) A position fix determined by ranges from Distance Measuring Equipment (DME) stations, as discussed in Section 2.3.4 of this text, is an example of trilateration. The method of position fixing illustrated in Figure 1.3.1-d utilizes the difference in the ranges from the vehicle to two (or three) pairs of known reference points. (The fix provided by only two pairs of reference points is, in general, ambiguous, but the geometry generally is such that the ambiguity is easily resolved without the use of a third pair of reference points.) The individual lines-of-position are hyperbolic as shown in the figure. Loran and omega, discussed in Sections 2.3.7 and 2.3.8 of this text, respectively, are examples of hyperbolic systems. (Omega also has a ρ,ρ mode as discussed in Section 2.3.8).

a.

a. Polar coordinate (ρ, α)

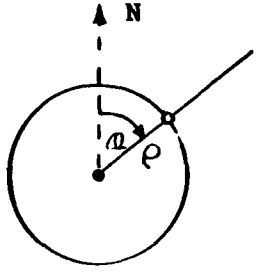

b. Triangulation (α, α)

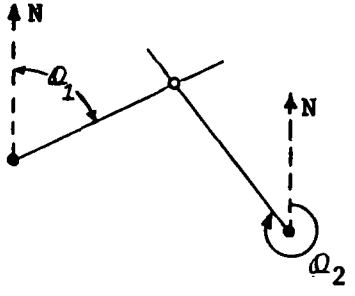

c. Trilateration (ρ, ρ)

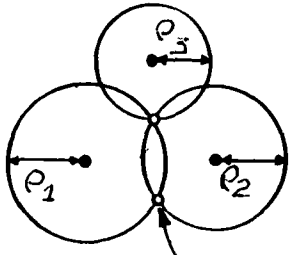

Ambiguous fix due to the use of two stations

d. Hyperbolic $(\Delta \rho)$

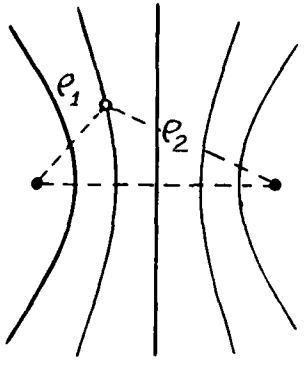

$\rho_2 - \rho_1$ is constant on any one line.
Three pairs of stations provide a fix.

Figure 1.3.1 -- Basic Methods of Position Fixing

The transit and Global Positioning System (GPS) navigation systems employ modified or hybrid methods of position fixing. The Transit system utilizes Doppler shift (satellite-to-vehicle range rate) to determine the vehicle distances from the satellite ground track and the satellite sub-orbital point corresponding to the point of closest approach. The system is ambiguous, yielding a fix on each side of the satellite ground track. With favorable geometry, the ambiguity is easily resolved by independent data. (The Transit system is discussed in Section 2.4.1 of this text.) The GPS system utilizes both range and range rate from known satellite positions to obtain a best estimate of vehicle position in three dimensions. (The GPS navigation system is discussed in Section 2.4.2 of this text.)

The nature of a navigation system (position fixing or dead reckoning) and the geometric configuration of the lines of position determine the system error model (how the measurement and instrument errors affect navigational accuracy). The error model, in turn, determines the performance testing required for a given system.

1.4 The Principal Airborne Navigation Systems

Because of the nature of modern aircraft and the missions they perform, the principal airborne navigation systems of interest here are listed below. (Other methods of navigation, such as celestial navigation and dead reckoning utilizing air data (airspeed) and a magnetic compass, are used primarily as adjunct or back-up systems for those listed here.)

Inertial Navigation
Doppler Radar Navigation
Instrument Low-Approach System (ILS)
Microwave Landing System (MLS)
Airborne Direction Finder (ADF)
Distance Measuring Equipment (DME)
VHF Omnidirectional Range (VOR)
Tactical Air Navigation (TACAN)
Long Range Navigation (LORAN)
Omega
Transit Satellite Navigation
Global Positioning System (GPS)

These navigation systems are discussed in the following paragraphs.

2.0 Navigation System Theory of Operation

2.1 Inertial Navigation Systems

2.1.1 Basic Principles of Operation -- Inertial navigation is a dead reckoning technique based upon the fact that, if vehicle acceleration is known as a function of time, the change in vehicle position can be computed by doubly integrating the acceleration. That is:

$$x(t_1) = x(t_0) + v(t_0)[t_1 - t_0] + \int_{t_0}^{t_1}\int \ddot{x}(t)\, dt\, dt$$

where:

$X(t_1)$ = Vehicle Position at $t \approx t_1$

$X(t_0)$ = Vehicle Position at $t \approx t_0$

$V(t_0)$ = Vehicle Velocity at $t \approx t_0$

$\ddot{X}(t)$ = Vehicle Acceleration

The determination of vehicle acceleration, unfortunately, is complicated by a number of factors including the maintenance of directional references, the fact that ordinary accelerometers cannot detect accelerations due to gravitation, gravitational anomalies, geodetic anomalies, and centrifugal and coriolis accelerations due to navigating on a rotating earth. In the following discussions, these factors will be investigated by introducing them into the inertial navigation problem, one at a time, starting with the simplest possible model.

Linear Motion in Inertial Space -- Inertial space is defined as a hypothetical non-rotating, non-accelerating frame of reference (coordinate system). It is

the frame of reference in which Newtons laws of motion hold. In particular, it is the frame of reference in which, for a rigid body:

$$\sum \vec{F} = m \vec{a}$$

where:

$\vec{F}$ = The Vector Sum of the Forces Applied to the body

M = The Mass of the body

$\vec{a}$ = The Acceleration of the body

Note that here we are neglecting relativistic effects. Because the accelerometers commonly used in inertial guidance systems cannot sense gravitational accelerations, we will, in the following treatment, distinguish between gravitational forces, $m\vec{g}$, and non-gravitational forces (also called specific forces), $\sum \vec{F}$, acting on the vehicle. Thus, Newton's second law becomes:

$$\sum \vec{F} + m\vec{g} = m \ddot{\vec{x}}$$

where:

$\sum \vec{F}$ = Sum of Non-Gravitational (Specific) Forces Acting on Rigid Body

$\vec{g}$ = Acceleration due to Gravitation

m = Mass of Body

$\ddot{\vec{X}}$ = Total Acceleration of Body

In order to compute the body linear velocity, $\dot{X}$, and position, X, the total acceleration, $\ddot{X}$, must be integrated with respect to time. That is:

$$\ddot{\vec{x}}(t) = \frac{1}{m} \sum \vec{F}(t) + g(t)$$

$$\dot{\vec{x}}(t) = \dot{\vec{x}}(t_0) + \int_{t_0}^{t} \ddot{\vec{x}}(t)\, dt$$

$$\vec{x}(t) = \vec{x}(t_0) + \int_{t_0}^{t} \dot{\vec{x}}(t)\, dt$$

The rotational motion equivalent to Newton's Second Law for linear motion is expressed by the equation:

$$\sum \vec{M}(t) = I \ddot{\vec{\theta}}(t)$$

where:

I = Rigid Body Moment of Inertia

$\sum \vec{M}$ = Vector Sum of Torques Acting on Body

$\ddot{\vec{\theta}}$ = Angular Acceleration of Body

The rotational velocity, $\dot{\vec{\theta}}$, and position (attitude), $\vec{\theta}$, of a rigid body can be computed from its rotational acceleration by integration. That is:

$$\ddot{\vec{\theta}}(t) = \frac{1}{I} \sum \vec{M}(t)$$

$$\dot{\vec{\theta}}(t) = \dot{\vec{\theta}}(t_0) + \int_{t_0}^{t} \ddot{\vec{\theta}}(t)\, dt$$

$$\vec{\theta}(t) = \vec{\theta}(t_0) + \int_{t_0}^{t} \dot{\vec{\theta}}(t)\, dt$$

Inertial Navigation for a Flat, Non-Rotating Earth -- Consider the case of inertial navigation for a vehicle in planar motion above a "flat" earth. The situation is then as depicted in Figure 2.1.1.1-a. Employing Cartesian coordinates, the x axis is parallel to the earth's surface, the z axis is perpendicular to the surface, and the motion is constrained to the x-z plane. The gravitational vector, $\bar{g}$, is independent of both x and z and is directed in the (-z) direction. Thus, the equations of motion for the x and z axes are:

(a) Vehicle Trajectory

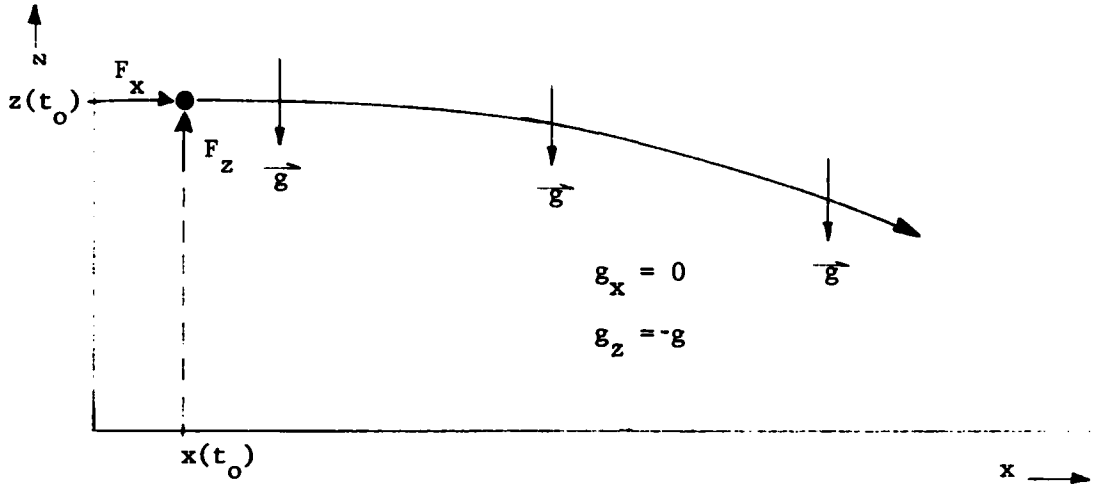

(b) Inertial Navigation System Block Diagram (Flat Earth)

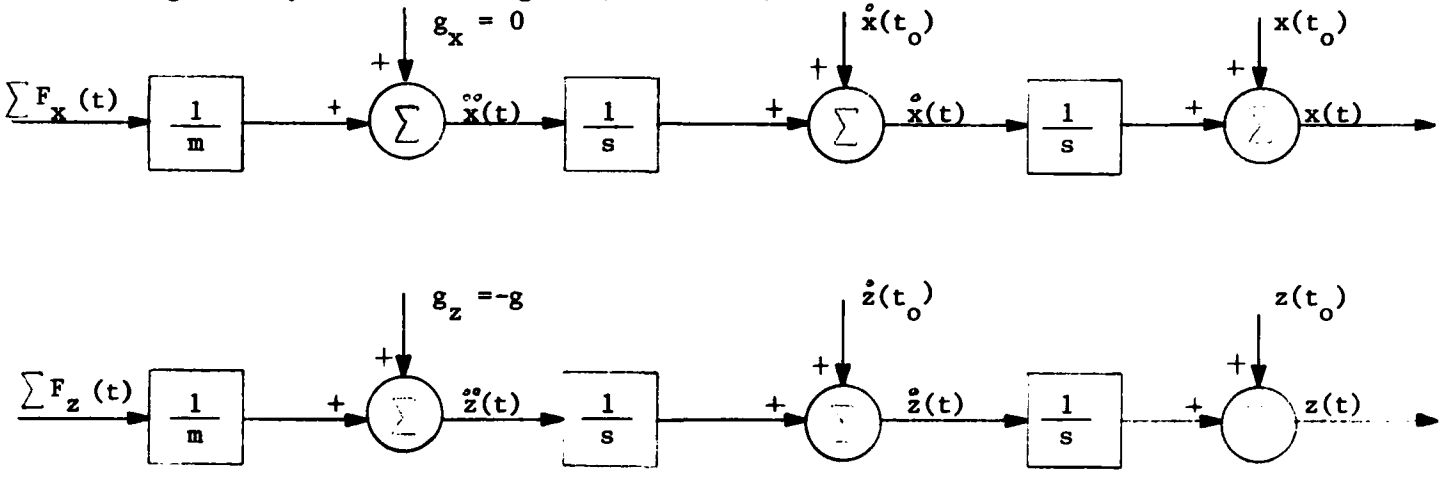

Figure 2.1.1.1 -- Planar Inertial Navigation Above a Flat Earth

$$\ddot{x}(t) = \frac{1}{m}\sum F_x(t) + g_x = \frac{1}{m}\sum F_x(t)$$

$$\dot{x}(t) = \dot{x}(t_0) + \int_{t_0}^{t} \ddot{x}(t)\,dt$$

$$x(t) = x(t_0) + \int_{t_0}^{t} \dot{x}(t)\,dt$$

$$\ddot{z}(t) = \frac{1}{m}\sum F_z(t) + g_z(t) = \frac{1}{m}\sum F_z(t) - g$$

$$\dot{z}(t) = \dot{z}(t_0) + \int_{t_0}^{t} \ddot{z}(t)\,dt$$

$$z(t) = z(t_0) + \int_{t_0}^{t} \dot{z}(t)\,dt$$

In order to compute position for this simplified case, an inertial navigation system performs the following steps.

(1) Measure the non-gravitational accelerations (due to the specific forces).

(2) Add the (constant) gravitational acceleration in the z-direction.

(3) Integrate the total acceleration to get incremental velocity.

(4) Add the initial velocity to get total velocity.

(5) Integrate the total velocity to get incremental position.

(6) Add the initial position to get current position.

(7) Repeat Step (1) through (6) to update position and velocity continuously.

The above process can best be visualized by means of the block diagram shown in Figure 2.1.1.1 (b).

Inertial Navigation for a Spherical, Non-Rotating Earth -- Now consider the case of inertial navigation for a vehicle in planar motion above a spherical, non-rotating earth. The situation is then as depicted in Figure 2.1.1.2-a. Still employing cartesian coordinates, the x axis is parallel to the surface of the earth at the initial vehicle position, the z axis is perpendicular to the surface

(a) Vehicle Trajectory

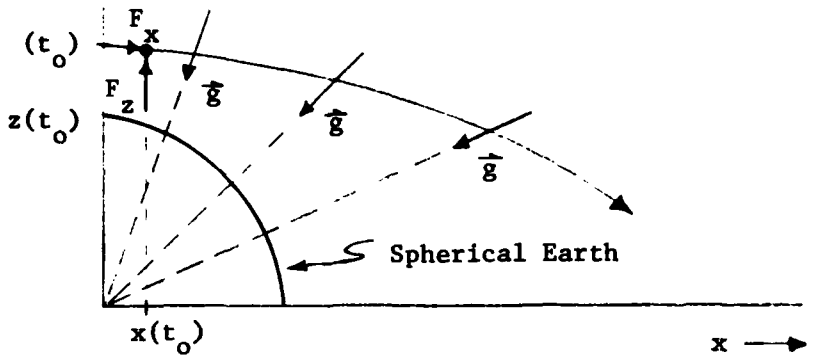

$$g_x(x, z) = \frac{-gx}{\sqrt{x^2 + z^2}}$$

$$g_y(x, z) = \frac{-gz}{\sqrt{x^2 + z^2}}$$

(b) Inertial Navigation System Block Diagram (Spherical Earth)

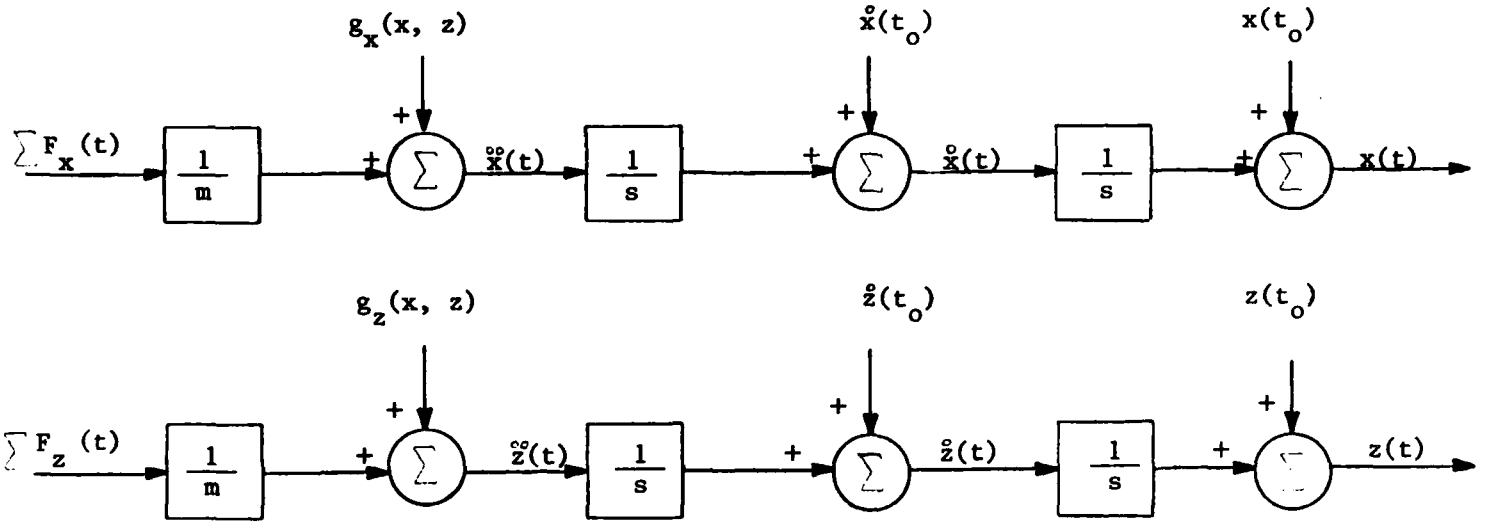

Figure 2.1.1.2 -- Planar Inertial Navigation Above a Spherical Earth

at that point, and the motion is constrained to the x-z plane. (Note that x and z no longer correspond to distance traveled on the surface of the earth and to altitude. If such quantities are required, coordinate transformations must be performed on the x and z quantities.) The gravitation vector for a spherical, homogeneous earth is directed toward the center of the earth and is given by the equations in Figure 2.1.1.2-a. The equations of motion for a spherical earth are:

$$\ddot{x}(t) = \frac{1}{m}\sum F_x(t) + g_x(x,z)$$

$$\dot{x}(t) = \dot{x}(t_o) + \int_{t_o}^{t} \ddot{x}(t)\,dt$$

$$x(t) = x(t_o) + \int_{t_o}^{t} \dot{x}(t)\,dt$$

$$\ddot{z}(t) = \frac{1}{m}\sum F_z(t) + g_z(x,z)$$

$$\dot{z}(t) = \dot{z}(t_o) + \int_{t_o}^{t} \ddot{z}(t)\,dt$$

$$z(t) = z(t_o) + \int_{t_o}^{t} \dot{z}(t)\,dt$$

These equations can be represented by the block diagrams shown in Figure 2.1.1.2-b. Note that the INS computations for a spherical earth are identical to those for a flat earth with the exception that, for a spherical earth, the components of gravity are functions of x and z, thus coupling the x and z channels.

Inertial Navigation for a Rotating Earth -- The inertial navigation equations presented in the preceding sections for a non-rotating earth were expressed in a coordinate system fixed in inertial space. Some inertial navigation systems, called analytic systems, perform in that frame of reference. Most terrestrial inertial navigation systems, however, called semi-analytic systems, measure and compute in a frame of reference fixed to the rotating earth. As indicated in Figure 2.1.1.3, velocities and accelerations measured (or computed) in a rotating coordinate system contain terms due to Coriolis and centrifugal accelerations. The equations relating quantities in a rotating system to those in a non-rotating (inertial) coordinate system can be derived from the expression for the time rate-of-change of a vector in a rotating frame of reference. That is:

$$\dot{\vec{r}}_I = \dot{\vec{r}}_R + \vec{\omega} \times \vec{r}_R$$

and:

$$\ddot{\vec{r}}_I = \ddot{\vec{r}}_R + 2\vec{\omega} \times \dot{\vec{r}}_R + \vec{\omega} \times (\vec{\omega} \times \vec{r}_R)$$

where:

$\vec{r}_I$ = Position Vector in Inertial Coordinates

$\vec{r}_R$ = Position Vector in Rotating Coordinates

$\vec{\omega}$ = Angular Velcoty Vector of Rotating Coordinate System

$\vec{\omega} \times \vec{r}_R$ = Cross Product of Vectors $\vec{\omega}$ and $\vec{r}_R$

An adequate understanding of the origin of the coriolis and centrigugal terms can be achieved, however, by means of the following intuitive derivation.

Assume, (without loss of generality), that, at the instant of observation, the inertial and rotating axes concide. That is, $\vec{\omega} = 0$, and:

$$X_I = X_R$$

$$Z_I = Z_R$$

$$x_I = x_L$$

$$z_I = z_L$$

$$\dot{x}_I = \dot{x}_L - \omega z_L$$

$$\dot{z}_I = \dot{z}_L + \omega x_L$$

$$\ddot{x}_I = \ddot{x}_L + 2\omega \dot{z}_L - \omega^2 x_L$$

$$\ddot{z}_I = \ddot{z}_L - 2\omega \dot{x}_L - \omega^2 z_L$$

I = Inertial Frame

L = Rotating Frame

m = Mass (Object)

δ = Incremental Angle of Rotation

ω = Angular Rate of Rotation

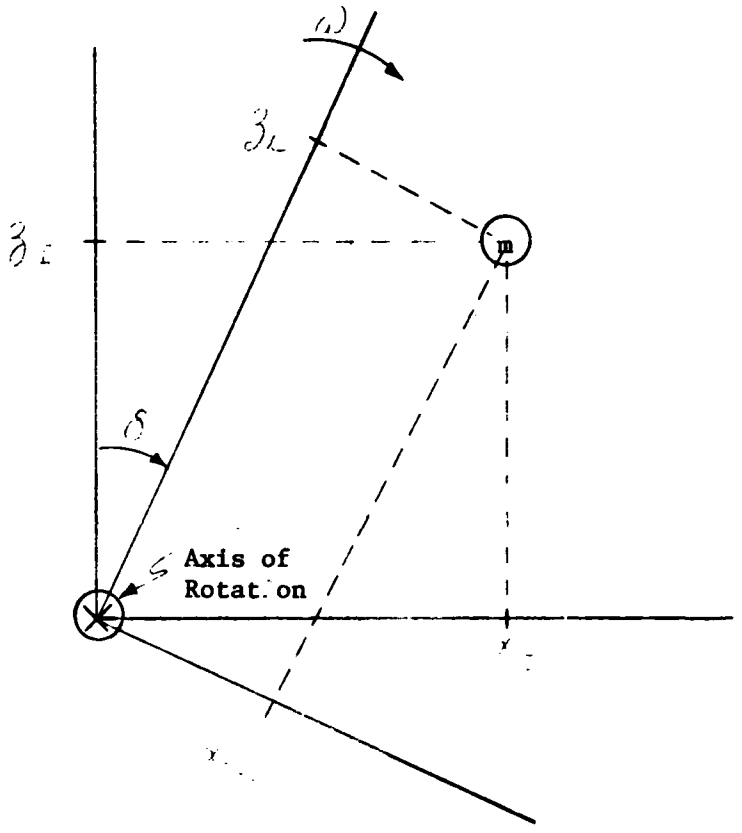

Assume:

Figure 2.1.1.3 -- Motion in a Rotating Frame of Reference

By inspection of Figure 2.1.1.3, it can be seen that an object at rest in the rotating coordinate system will have components of velocity in the inertial coordinate system proportional to the rate of rotation, ω. That is:

$$\dot{x}_I = \dot{x}_R + \omega z_R$$

$$\dot{z}_I = \dot{z}_R - \omega x_R$$

The inertial accelerations acting upon an object at rest (or moving with a constant velocity) in the rotating coordinate system are somewhat less obvious than are the velocities. They are, however, the centrigugal acceleration (equal to the product of the square of the angular rate of rotation and the distance from the center of rotation) and the coriolis force (equal to twice the product of the angular rate of rotation and the cross-velocity). That is:

$$\ddot{x}_I = \ddot{x}_R + 2\omega \dot{z}_R - \omega^2 x_R$$

$$\ddot{z}_I = \ddot{z}_R - 2\omega \dot{x}_R - \omega^2 z_R$$

(The centrifugal acceleration is caused by the time rate of change in the direction of the velocity vector, due to the rotation. The Coriolos acceleration is caused by the time rate of change in the magnitude of the velocity vector due to the rate of change in distance from the axis of rotation, produced by the cross-velocity.)

For an inertial navigation system sensing and computing in the hypothetical rotating coordinate system shown in Figure 2.1.1.3, the total accelerations would be given by:

$$\ddot{x}_R = \frac{1}{m}\sum F_x + g_x - 2\omega \dot{y}_R + \omega^2 x_R$$

$$\ddot{y}_R = \frac{1}{m}\sum F_y + g_y + 2\omega \dot{x}_R + \omega^2 y_R$$

Centrifugal Acceleration

Coriolis Acceleration

Gravitational Acceleration

Non-Gravitational Acceleration

The block diagram of such an inertial navigation system is shown in Figure 2.1.1.4. As indicated in the figure, an INS would determine the vehicle earth-referenced position by performing the following operations.

(1) Measure (sense) the non-gravitational (specific) accelerations.

(2) Compute and add the gravitational accelerations (because they are not sensed by the accelerometers).

(3) Compute and subtract the coriolis and centrifugal accelerations (because they are sensed by the accelerometers but do not represent accelerations with respect to an earth-fixed coordinate system).

(4) Integrate the total acceleration to get incremental velocity change.

(5) Add initial velocity to get total velocity.

(6) Integrate total velocity to get incremental position change.

(7) Add initial position to get new position.

(8) Repeat Steps (1) through (7).

Note that the rotating coordinate system employed in Figure 2.1.1.3 is a hypothetical system intended only to illustrate the origins of the coriolis and centrifugal terms in the accelerations sensed by an INS. The equations and INS

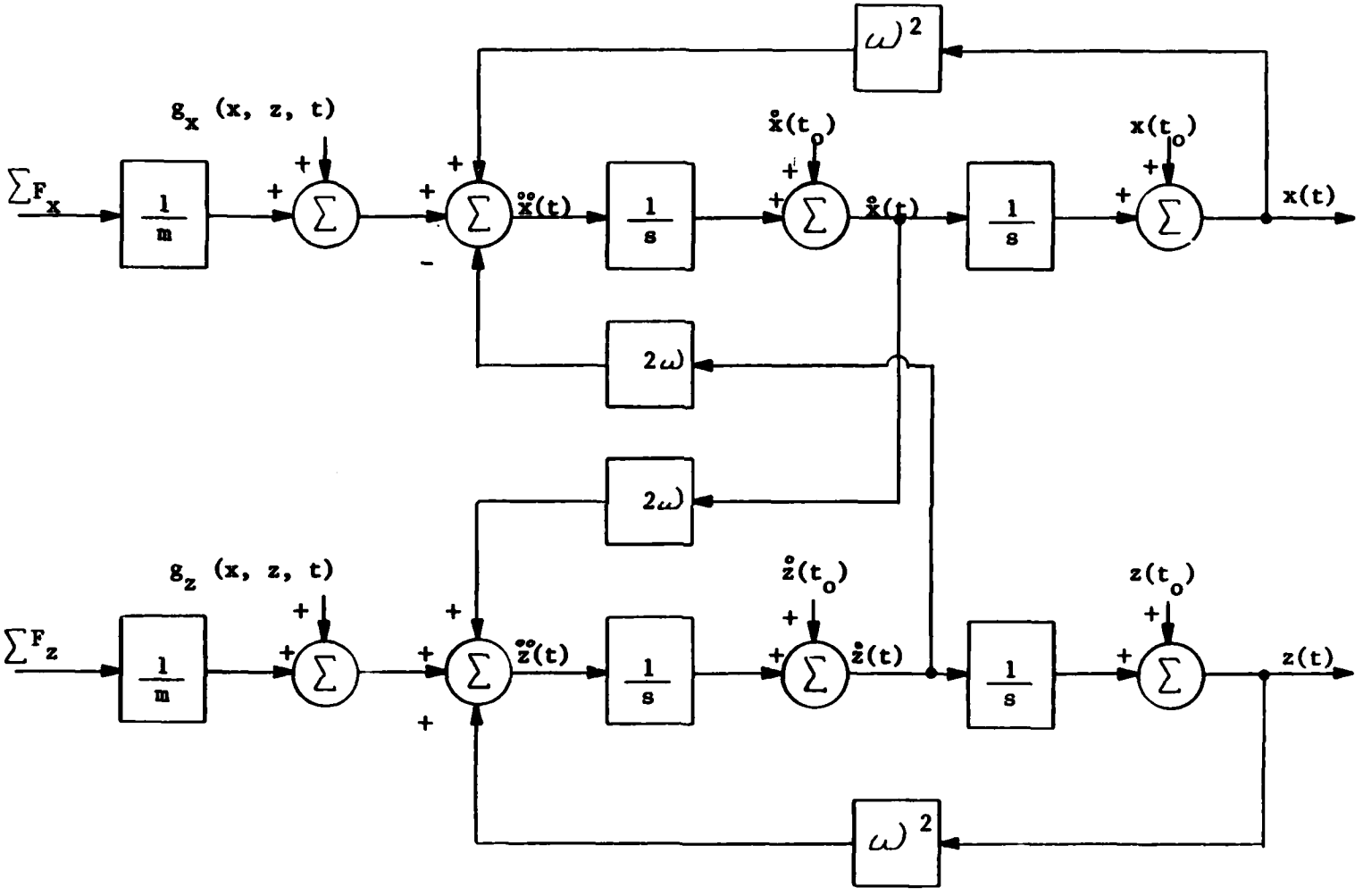

Figure 2.1.1.4 -- Block Diagram, Inertial Navigation System Operating in a Rotating Coordinate System

operation based upon that system are, however, very similar to those applicable to an actual inertial navigating system. The principal differences arise from the fact that, in an actual INS, the axes are not generally perpendicular to the earth's angular velocity vector (except on the equator) and the fact that the origin of the coordinate system is not generally located on the axis of rotation. In a terrestrial semi-analytic, (local-vertical-tracking), inertial navigation system, the inertial platform (on which the gyros and accelerometers are mounted) is rotated, in accordance with earth rate and vehicle movement with respect to the earth, so as to maintain the vertical axis aligned with the local vertical. The origin and orientation of the INS sensing and computing coordinate system are fixed to the inertial platform. Thus, the INS navigates in a rotating coordinate system centered at vehicle position. The local vertical is the direction of the gravity vector at that particular location. The direction of the gravity vector is affected by the fact that the earth is non-homogeneous and is an oblate spheroid. Corrections for these factors must be incorporated into the "gravity model" for an accurate INS.

2.1.2 INS Components and Subsystems

The Linear Accelerometer -- The linear accelerometer is a transducer, the output of which is a measure of the linear acceleration of its case (second rate of change of position with respect to time in the direction of its input axis), with respect to inertial space. (Inertial space is a non-accelerating, non-rotating frame of reference. For purposes of visualization, inertial space can be considered stationary with respect to the "fixed" stars.)

Conceptually, (and, in some cases, actually), an accelerometer consists of a "seismic" or "proof" mass mounted inside a case, and restrained by springs, as shown in Figure 2.1.2.1. In addition to the restraining force of the springs, the motion of the mass with respect to the case is restrained by viscous damping between the mass and the case. The relative motion between the proof mass and the case, (the output of the device), is converted to an electrical output by a potentiometer the arm of which is mechanically attached to the mass. As a result of the inertia of the proof mass, an acceleration of the accelerometer case due to an applied specific force will result in a relative displacement between the proof mass and the case. Summing forces on the proof mass and applying Newton's Second Law:

$$\sum F_x = m \ddot{x}_{mI}$$

or:

$$-k(x_{mI} - x_{cI}) - c_d(\dot{x}_{mI} - \dot{x}_{cI}) = m\ddot{x}_{mI}$$

where:

$\sum F_x$ = Sum of Forces on Proof Mass (Dynes)

C_d = Damping Coefficient (Dynes-Sec/Cm)

k = Spring Constant (Dynes/Cm)

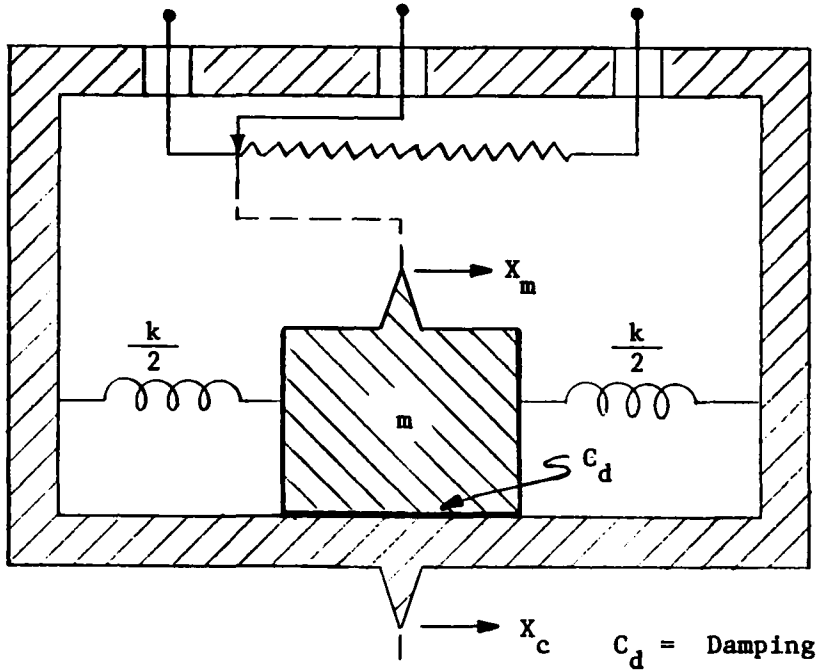

C_d = Damping Coefficient

k = Spring Constant

m = Proof Mass Mass

X_c = Displacement of Case

X_m = Displacement of Proof Mass

Figure 2.1.2.1 -- Linear Accelerometer

m = Mass of Proof Mass (Dynes-Sec^2/Cm)

X_{C_I} = Displacement of Case with respect to Inertial Space (Cm)

X_{M_I} = Displacement of Proof Mass with respect to Inertial Space (Cm)

$\dot{X}$ = Velocity (Cm/Sec)

$\ddot{X}$ = Acceleration (Cm/Sec^2)

Defining the displacement of the proof mass with respect to the case by the equations:

$$x_{mc} = x_{mI} - x_{cI}$$

and collecting terms, the equation of motion becomes:

$$m\ddot{x}_{mc} + c_d\dot{x}_{mc} + kx_{mc} = m\ddot{x}_{cI}$$

$m\ddot{x}_{mc}$	$c_d\dot{x}_{mc}$	kx_{mc}	$m\ddot{x}_{cI}$
Inertial Reaction Force	Damping Force	Spring Force	Input Acceleration Force

This equation is that of a linear, damped, second-order system. An accelerometer is, in fact, characterized by such a response. In the steady state ($\ddot{X}_{M_C} = \dot{X}_{M_C} = 0$):

$$x_{mc} = (m/k)\ddot{x}_{cI}$$

Thus, the displacement of the proof mass with respect to the case is a linear measure of the acceleration of the case with respect to inertial space, as required.

In a gravitational field, both the proof mass and the accelerometer case (and the object to which the case is attached) are accelerated. To assess the effects of such an acceleration, one can add a force, equal to mg, to those acting on the proof mass, and add an acceleration, equal to g, to the case acceleration, $\ddot{X}_{CI}$. Thus:

$$m\ddot{x}_{mc} + C_d\dot{x}_{mc} + kx_{mc} + mg = m(\ddot{x}_{cI} + g)$$

It can be seen that the terms mg on both sides of the equation cancel, leaving the output of the accelerometer unaffected. Such an accelerometer is thus unable to sense gravitational accelerations.

The accelerometers employed in most modern inertial navigation systems are not constructed exactly as shown in Figure 2.1.2.1. Most employ rotating, pendulous masses and detect their motion by means of induction-type motion sensors. Many incorporate gyroscopic and viscous damping elements for smoothing or integration of the output acceleration (integrating accelerometers). Many do not permit the mass to move, employing force-balancing transducers to null that motion. (The output of the accelerometer is then the current or voltage required to balance the forces.) Two - and three-input-axis accelerometers are sometimes used.

The Gyroscope -- The gyroscope is a transducer the output of which is a measure of the rotational motion of its case, about the input axis, with respect to inertial space. Position gyros sense angular displacement. Rate gyros sense angular rate (rate of change of angular position with respect to time). All gyros are based upon the fact that a rotating (spinning) element tends to maintain its spin axis in a direction fixed with respect to inertial space.

Conceptually, a two-degree-of-freedom displacement gyro is configured as shown in Figure 2.1.2.2. Neglecting bearing friction, structural asymmetries, and mass unbalances, the orientation of the spin axis of the spinning element remains fixed in inertial space despite rotations, translations, and accelerations of the gyro case. The orientations of the inner and outer gimbals about the input axes are, then, also fixed in inertial space, thus providing stable inertial references about those two axes. (A two-gimbal gyro has two degrees of freedom and senses angular motion about any axis perpendicular to the spin axis.) Any rotation of the gyro case about the input axes produces relative displacements of the corresponding gimbals, thereby producing output indications from the pick-offs shown in the figure.

Due to Coriolis effects produced by the spinning element, a gyro responds to applied torques about an axis perpendicular to the axis about which the torque is applied. Furthermore, the resulting motion is not an angular acceleration, (as it would be for a non-gyroscopic body), but an angular velocity. The relative directions of the applied torque, the spin vector, and the angular velocity vector obey the "right-hand" rule as depicted in Figure 2.1.2.3. Thus, if a torque $\vec{M}_y$ is applied to the outer gimbal of the gyro, about the y-axis, (perhaps due to friction in the bearings between the outer gimbal and the case), there will result an angular velocity of the inner gimbal, $\vec{\omega}_z$. The magnitude of the angular velocity is given by the equation:

$$\omega_z = M_y / H_x \qquad \text{(Rad/Sec)}$$

where M_y is the applied torque in Dyne-Cm and Hx is the angular momentum of the gyro spinning element, given by:

$$H_x = I_s \omega_s \qquad \text{(Dyne-Cm-Sec)}$$

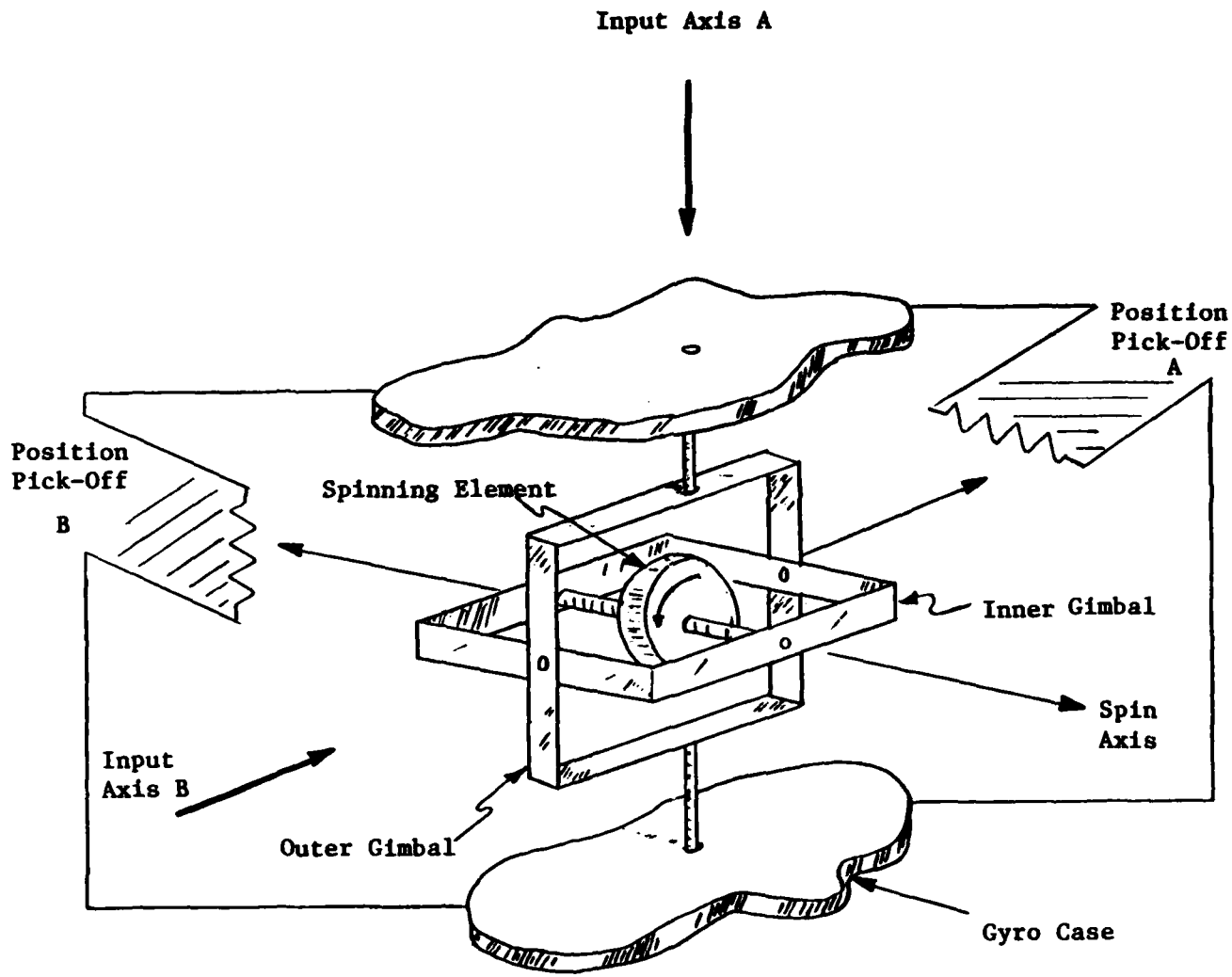

Figure 2.1.2.2 -- The Displacement Gyroscope

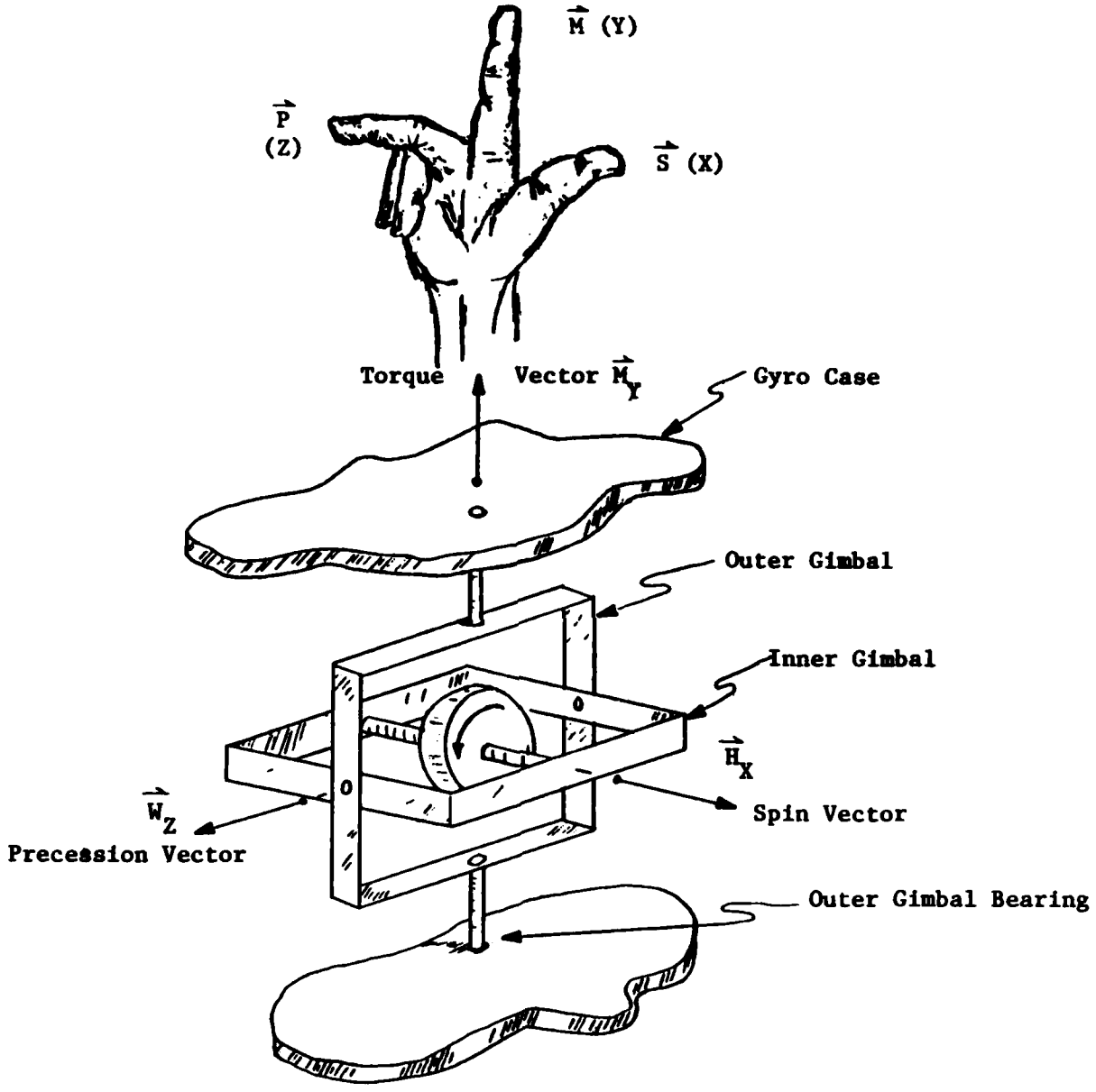

Figure 2.1.2.3 -- Precession of a Torqued Gyro

where I_s is the moment of inertia of the spinning member about the spin axis in Dyne-Cm-Sec^2 and ω_s is the angular velocity of spin in Rad/Sec.

Two-degree-of-freedom displacement (unrestrained) gyros are rarely employed in modern inertial navigation systems. For that reason, a detailed analysis of their operation will not be presented here. There is, however, a phenomenon peculiar to two-degree-of-freedom gyros that should be mentioned--nutation. When the angular orientation of the spin vector of a two-degree-of-freedom gyro is disturbed, there is a coupling between the two output axes such that an oscillatory transfer of energy occurs between the two gimbals. The resulting lightly-damped "coning" motion of the spin axis, called nutation, can produce catastrophic effects in a system incorporating the gyro in question. Specifically, if mechanical disturbances exist near the nutation frequency, large-scale oscillations can occur in the gyro outputs unless a nutation damper is provided to stop the oscillatory motion. The nutation frequency is given by the equation:

$$f_N = \left(\frac{I_{SA}}{I_{OA}}\right) \frac{\omega_s}{2\pi} \quad \text{(Hertz)}$$

where:

I_{SA} = Moment of Inertia about Gyro Spin Axis

I_{OA} = Moment of Inertia about Gyro Output Axis

ω_s = Angular Spin Rate of Gyro (Rad/Sec.)

When the outer gimbal of the gyro in Figure 2.1.2.2 is affixed to the case as shown in Figure 2.1.2.4, the result is a single-degree-of-freedom displacement gyro. If, in addition, the inner gimbal is restrained by a spring between the inner gimbal and the case, as also shown in Figure 2.1.2.4, the deflection of the

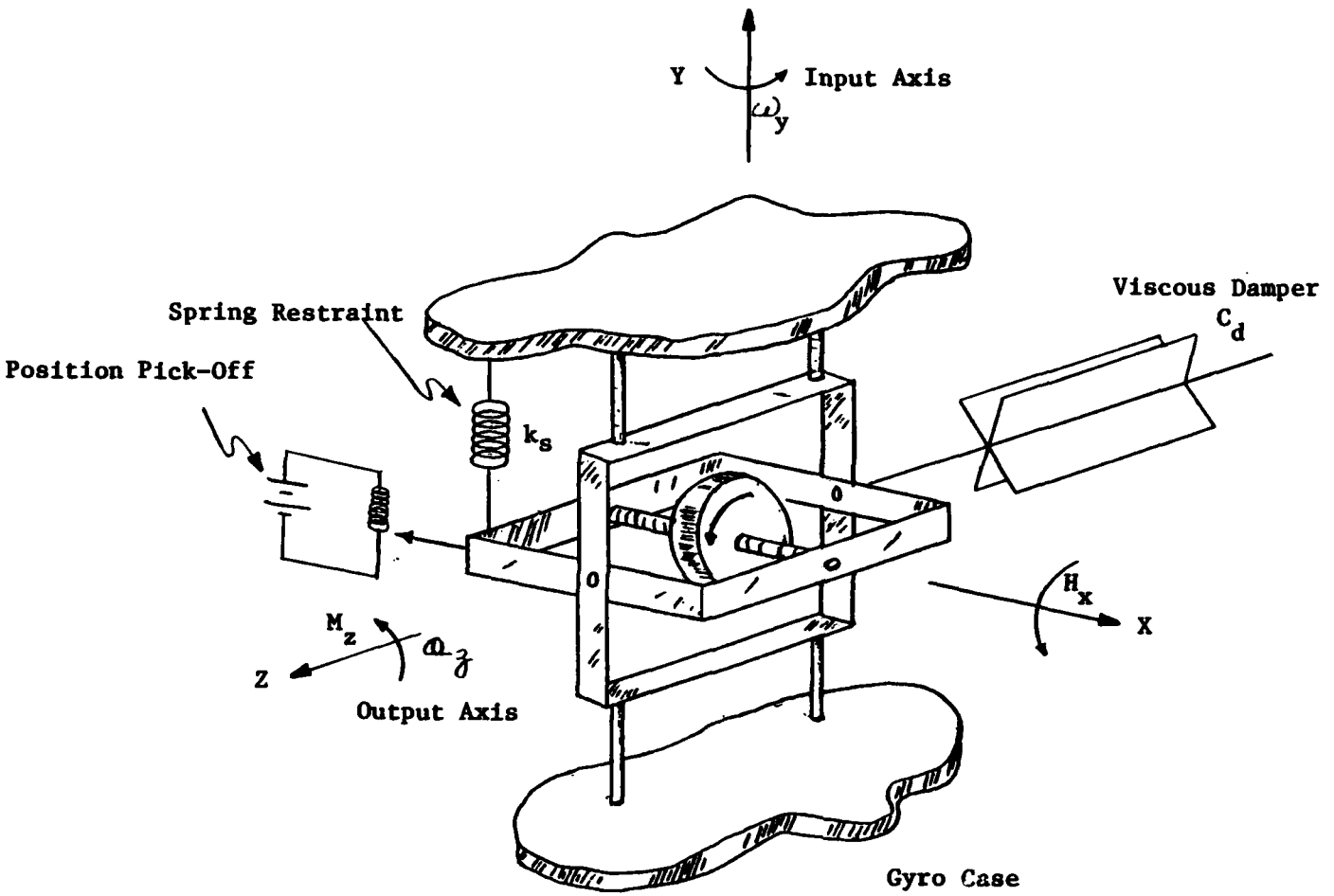

Figure 2.1.2.4 -- The Elastically-Restrained (Rate) Gyro

inner gimbal (gyro output) is proportional to the angular rate, rather than the angular displacement, of the case, about the input axis. That is, the gyro becomes a rate gyro. If, in addition, a viscous damper is placed on the gyro output axis as shown in the figure, there are then three torques acting on the inner gimbal about the output axis. These torques are:

(1) the gyroscopic torque, due to the input angular velocity of the gyro case about the input axis, given by:

$$M_{zg} = \omega_y H_x \qquad \text{(Dyne-Cm)}$$

where:

ω_y = Input Angular Rate (Rad/Sec)

H_x = Angular Momentum of Spinning Element (Dyne-Cm-Sec)

(2) the restraining torque due to the spring, given by:

$$M_{zs} = -k_s \theta_z \qquad \text{(Dyne-Cm)}$$

where:

k_s = Restraining Spring Constant (Dyne-Cm/Radian)

θ_z = Angular Deflection of Inner Gimbal about Output Axis (Rad.)

(3) the restraining torque due to the viscous damper, given by:

$$M_{zd} = -C_d \dot{\theta}_z \qquad \text{(Dyne-Cm)}$$

where:

C_d = Damping Coefficient (Dyne-Cm-Sec/Rad)

$\dot{\theta}_z$ = Angular Velocity of Inner Gimbal about Output Shaft (Rad/Sec.)

Summing torques about the output axis and setting them equal to the inertial reaction torque, the equation of motion of the inner gimbal about the output axis is:

$$I_{OA} \ddot{\theta}_z + C_d \dot{\theta}_z + k_s \theta_z = H_x \omega_y$$

where:

I_{OA} = Moment of Inertia about the Output Axis (Dyne-Cm-Sec^2)

$\ddot{\theta}_z$ = Angular Acceleration about Output Axis (Rad/Sec^2)

This equation is that of a linear, damped, second-order system. Thus, the gyroscope is characterized by a second-order response. In the steady state $(\ddot{\theta}_z = \dot{\theta}_z = 0)$:

$$\theta_z = \left(\frac{H_x}{k_s}\right) \omega_y \qquad \text{(Radians)}$$

Thus, the angular displacement of the rate gyro (the output of the device) is proportional to the angular velocity (rate) of the case with respect to inertial space, as required.

If the damping coefficient, D_c, is increased and the spring constant, k_s, is decreased until the damping torque becomes dominant, the rate gyro equation becomes:

$$C_d \dot{\theta}_z = H_x \omega_y \qquad \text{(Dyne-Cm)}$$

Then:

$$\dot{\theta}_z = \left(\frac{H_x}{C_d}\right) \omega_y \qquad \text{(Rad/Sec)}$$

or:

$$\theta_z = \left(\frac{H_x}{C_d}\right) \int \omega_y \, dt \qquad \text{(Rad)}$$

Thus, the output of the gyro is proportional to the integral of the angular velocity of the gyro case about its input axis, and the gyro becomes a rate-integrating (displacement) gyro.

The gyroscopes employed in most modern inertial navigation systems are not constructed exactly as shown in Figures 2.1.2.3 and 2.1.2.4. Many are single-degree-of-freedom devices similar to the drawing in Figure 2.1.2.5. The gyroscopic (spinning) element is housed in a drum which floats in damping fluid, thus simultaneously providing damping and greatly reducing the forces applied to the output axis bearings. The "spring" torque is applied by means of an electromagnetic torque generator, and the output angle sensor is a low-friction inductive pickoff. As with the output-motion-nulling accelerometer, the modern rate gyroscope generally nulls the angular displacement about the output shaft. A two-degree-of-freedom gyro based upon similar principles is shown in Figure 2.1.2.6.

The Stable Platform -- An INS stable platform is a physical member the orientation of which is controlled with respect to inertial space. In analytic systems, the stable platform is "fixed" in inertial space. In semi-analytic systems, the orientation of the stable platform with respect to inertial space is controlled in such a way as to maintain the vertical axis of the platform aligned with the local vertical at that longitude and latitude. The purpose of the stable platform is to provide a platform upon which to mount the accelerometers in such a way that their input axes are maintained in the proper directions. (For a north-pointing, semi-analytic INS, the "proper" directions are east, north, and up.) The orientation of a stable platform is maintained by the gyros, also mounted on the

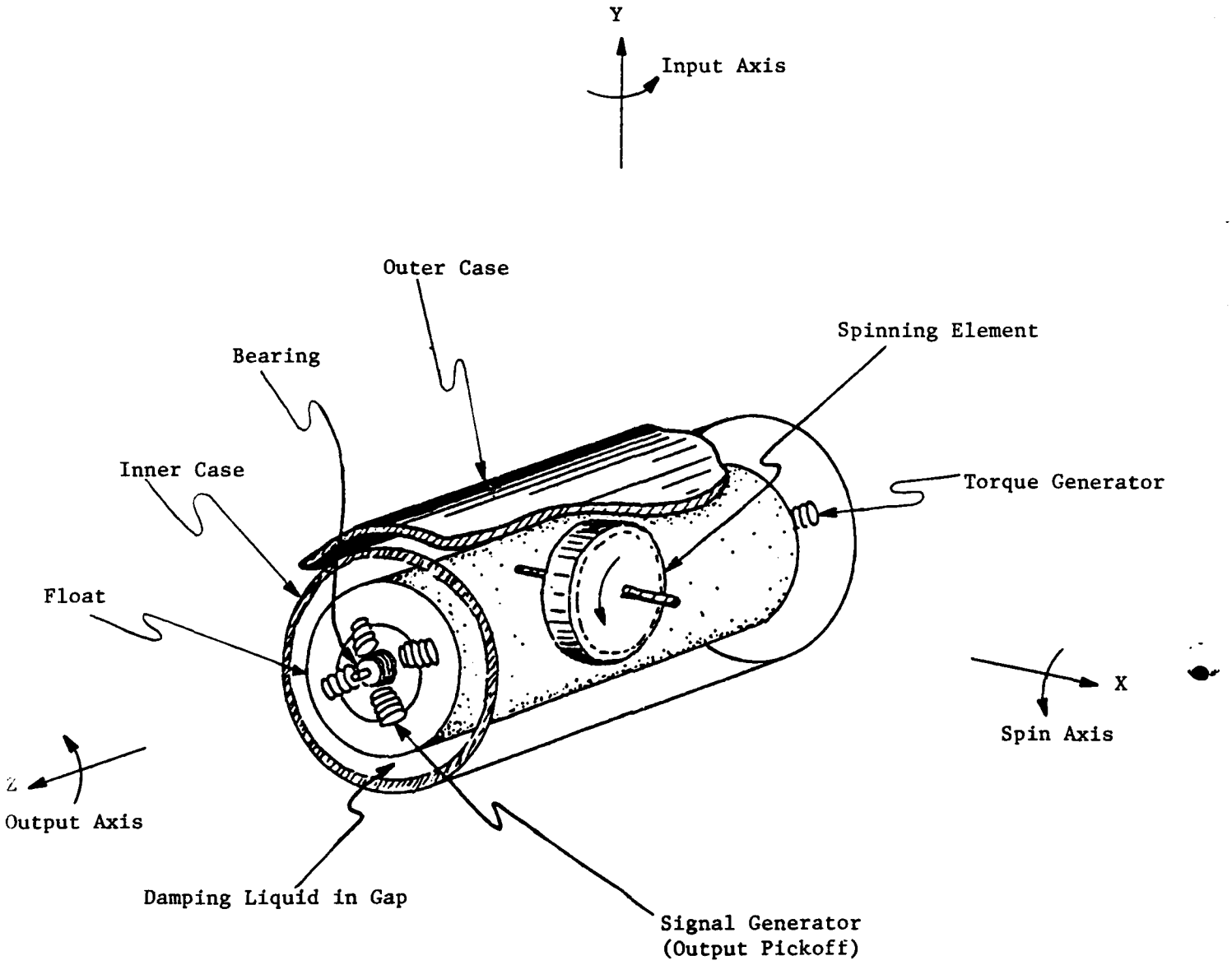

Figure 2.1.2.5 -- Typical Single Degree of Freedom Gyro

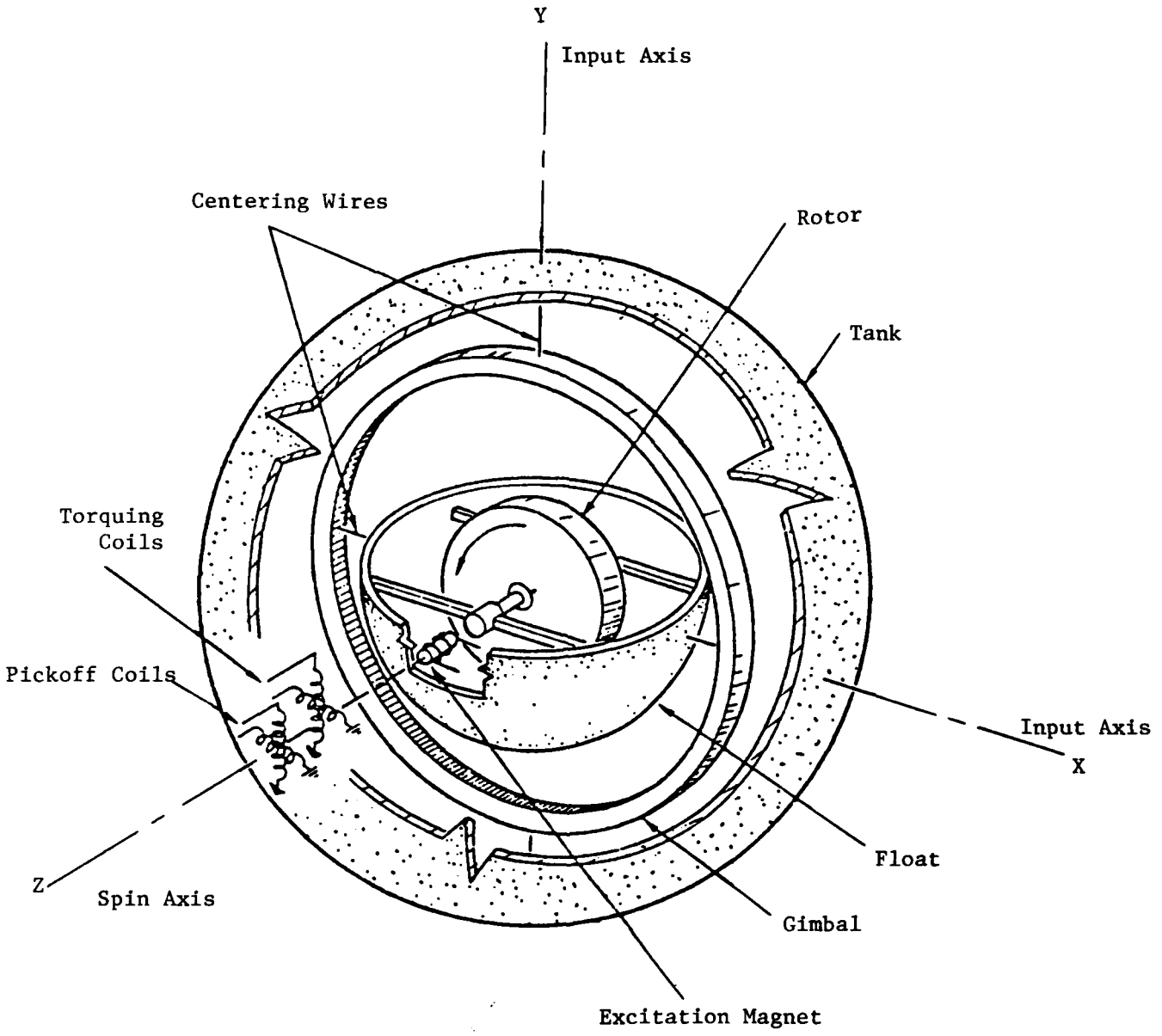

Figure 2.1.2.6 -- Two-Degree of Freedom Floated Gyro

platform, with their input axes mutually perpendicular. Any angular deviation of the platform is sensed by the gyros. The resulting signal is amplified and used, via a drive motor, to restore the platform to the proper orientation. A single-axis stable platform is depicted in Figure 2.1.2.7. The stable platform is an angular positional feedback servo and can be represented by the block diagram shown in Figure 2.1.2.8.

A schematic drawing of a three-axis stable platform is shown in Figure 2.1.2.9. As indicated in the drawing, three gimbals are required to achieve three-axis platform stabilization. There is a problem, however, with the three gimbal system shown in Figure 2.1.2.9, as illustrated in Figure 2.1.2.10. If aircraft maneuvers result in all of the gimbals in a three-gimbal system being in the same plane as shown in Figure 2.1.2.10a, any further rotation about an axis perpendicular to that plane will result in the stable platform being disoriented. That is, the stable platform is no longer isolated from that particular aircraft motion. The solution to the gimbal-lock problem is to employ a fourth (redundant) gimbal as shown in Figure 2.1.2.10b. The orientation of the redundant gimbal is controlled in such a way that all four gimbals are never in the same plane. Thus, there is always a gimbal with freedom about any possible axis of rotation, thereby providing an all-attitude stable platform. A more detailed drawing of a four-gimbal system is presented in Figure 2.1.2.11.

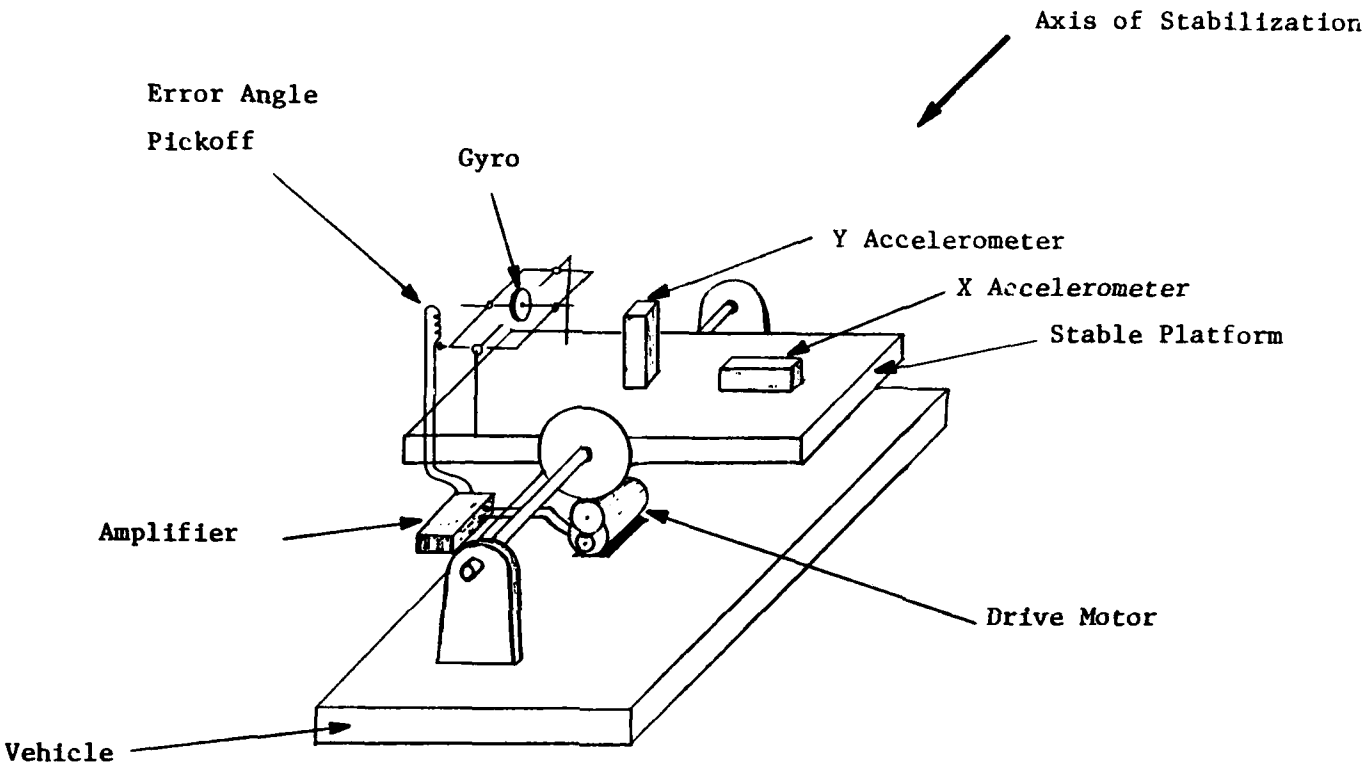

Figure 2.1.2.7 -- A Single-Axis Stable Platform

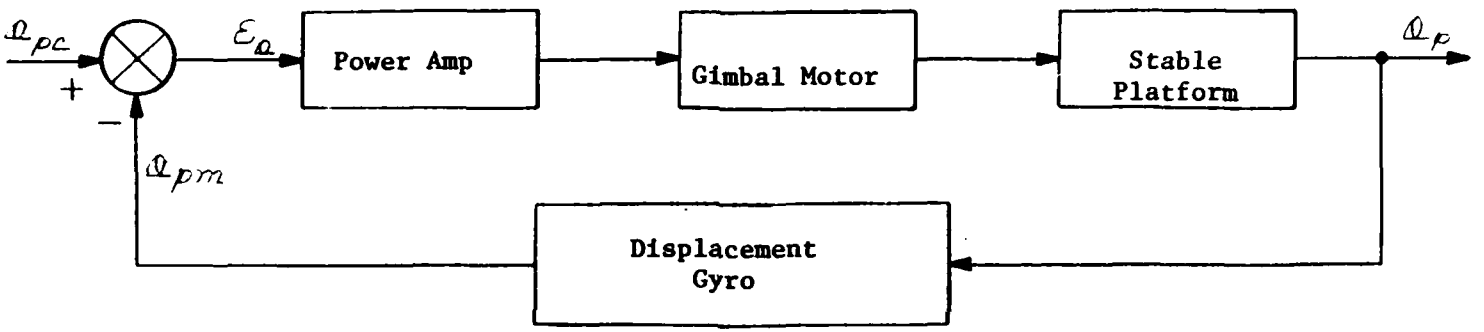

$\mathcal{Q}_p$ = Platform Orientation Angle

$\mathcal{Q}_{pc}$ = Commanded Platform Orientation Angle

$\mathcal{Q}_{pm}$ = Measured Platform Orientation Angle

$\mathcal{E}_{\mathcal{Q}}$ = Platform Orientation Angle Error

Figure 2.1.2.8 -- Block Diagram, Single-Axis Stable Platform

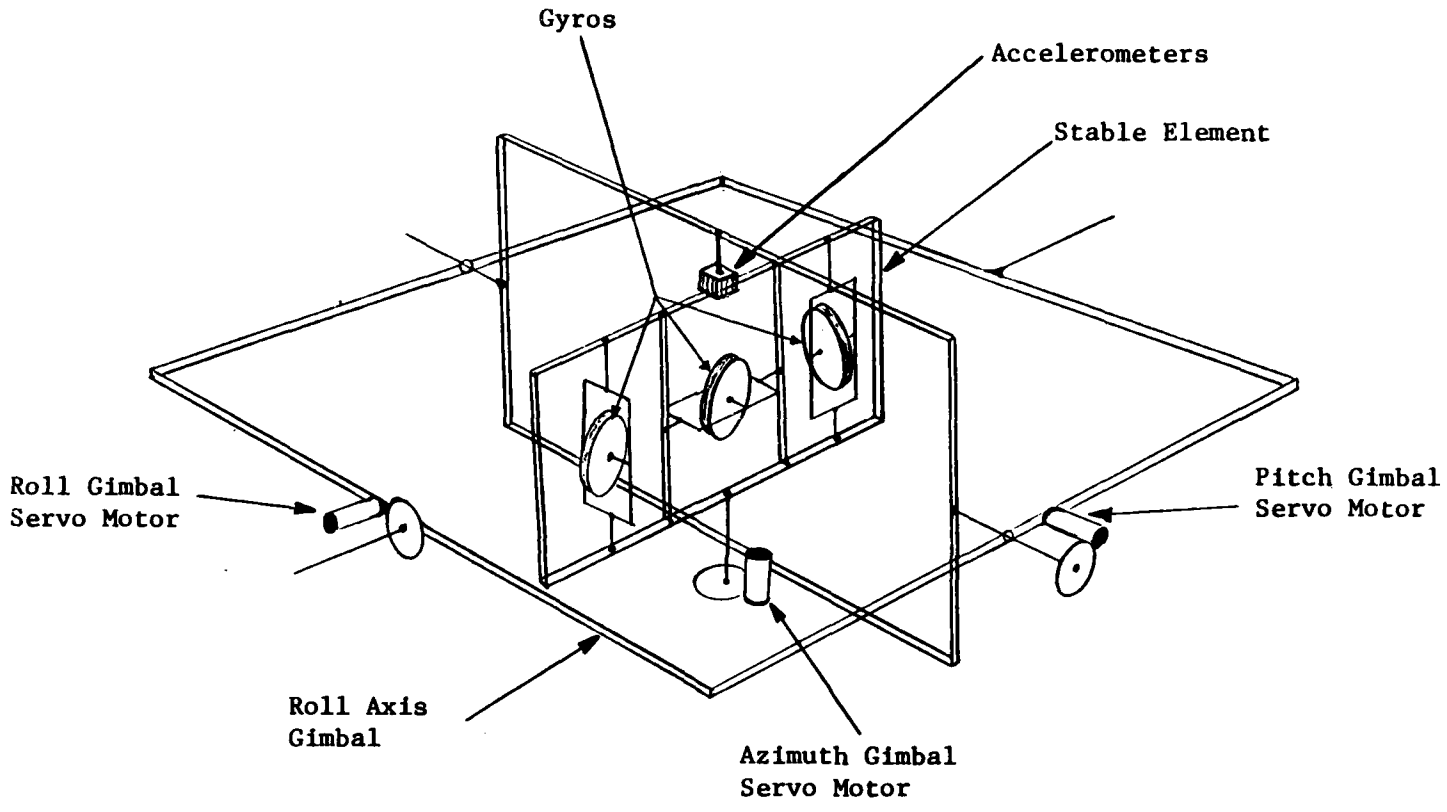

Figure 2.1.2.9 -- Three-Axis Stable Platform

(a) 3-Gimbal Platform (Locked)

(b) 4-Gimbal Platform

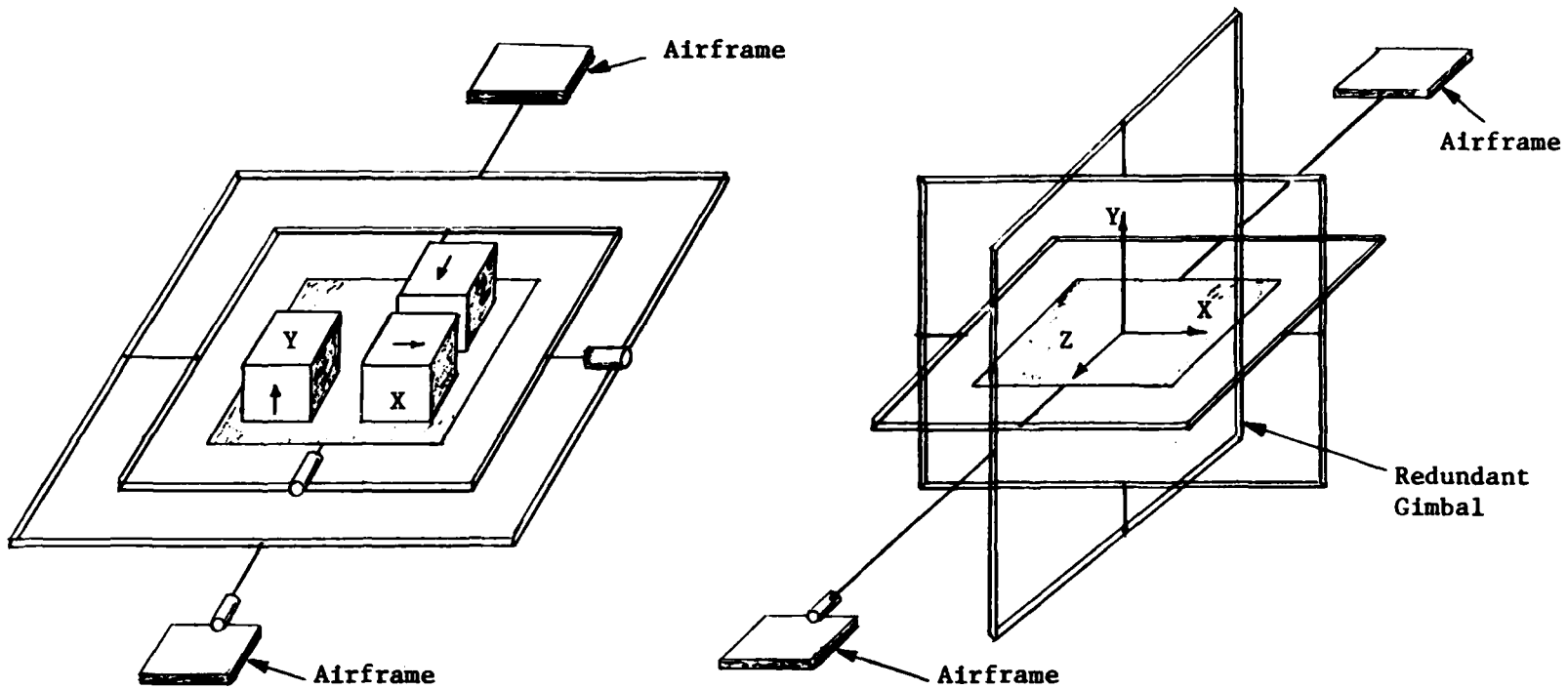

Figure 2.1.2.10 -- Illustration of Gimbal Lock in a Three-Gimbal System

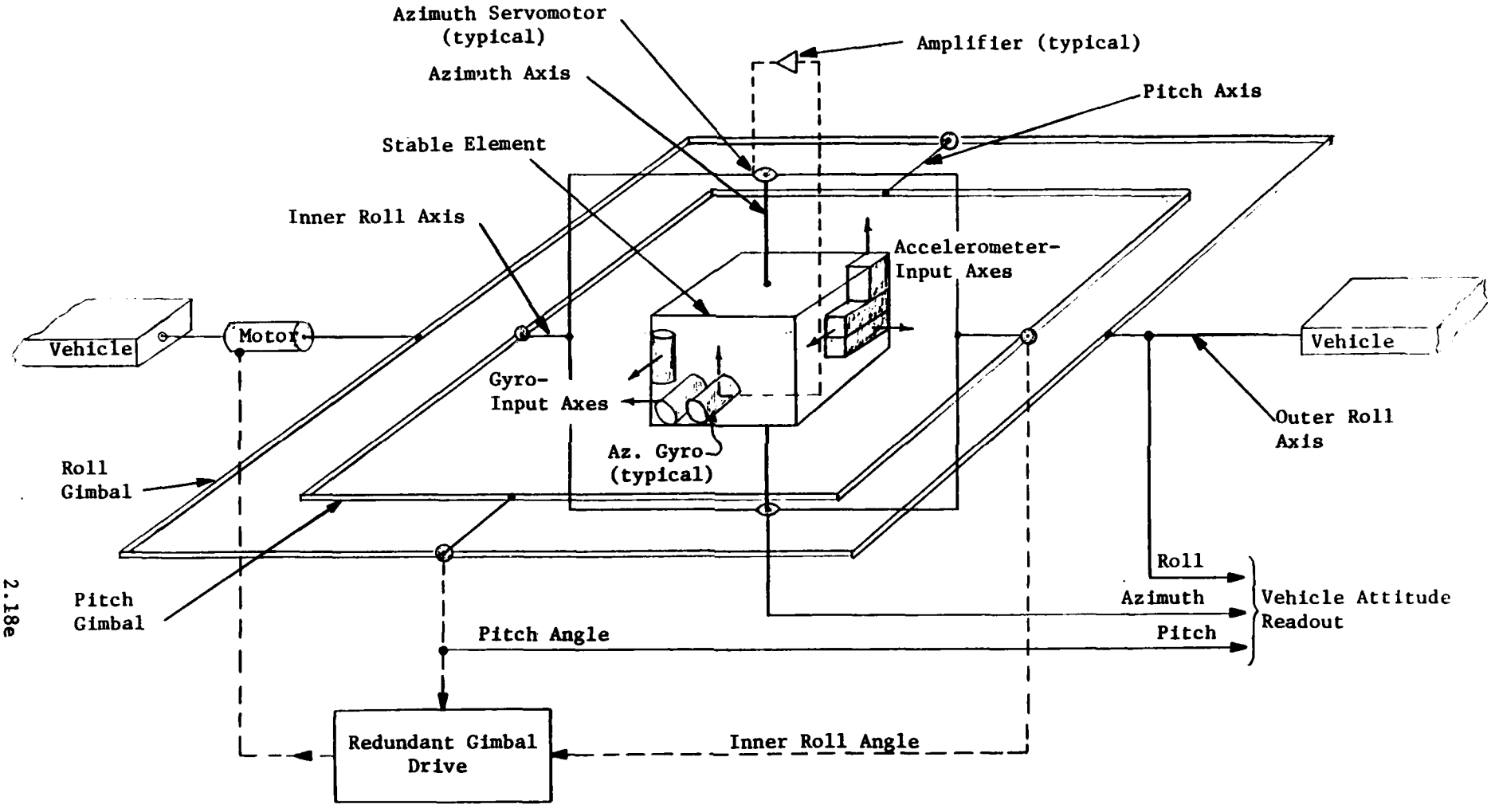

Figure 2.1.2.11 -- A Four-Gimbal Stable Platform

2.1.3 The Local-Vertical Tracker -- As previously indicated, the stable platform in a semi-analytic INS is controlled in such a way as to maintain the vertical axis aligned with the local vertical. A theoretical device, the Schuler pendulum, also maintains such an orientation. The Schuler pendulum consists of a weight on the end of a weightless rod of length equal to the radius of the earth. (It is assumed, in the following discussion, that the earth is a homogeneous, spherical solid.) If the length, L, of the pendulum were less than the radius of the earth, R_E, an acceleration of the pivot point, around the surface of the earth, would result in the pendulum (initially) leading the vertical as shown in Figure 2.1.3(a). If the length of the pendulum were greater than the radius of the earth, the pendulum would (initially) lag the vertical as shown in Figure 2.1.3.1(b). If, however, the length of the pendulum were exactly equal to the radius of the (spherical) earth, the mass, m, would remain at the center of the earth (center of gravitation), and the pendulum rod would remain aligned with the local vertical as shown in Figure 2.1.3.1(c). Furthermore, it would be unaffected by the rotation of the earth and, therefore, would require no centrifugal or coriolis corrections. If it were possible to construct such a device, it could be employed as a local-vertical tracker in a semi-analytic inertial navigation system. It is, obviously, impossible to suspend a mass at the center of the earth. Fortunately, it is not necessary to do so in order to construct a local-vertical tracker. The essential characteristic of the Schuler pendulum is not the mass at the center of the earth; it is the period of a pendulum of length equal to the radius of the earth, given by the equation:

$$T_S = 2\pi\sqrt{\frac{L}{g}} = 2\pi\sqrt{\frac{R_E}{g}}$$

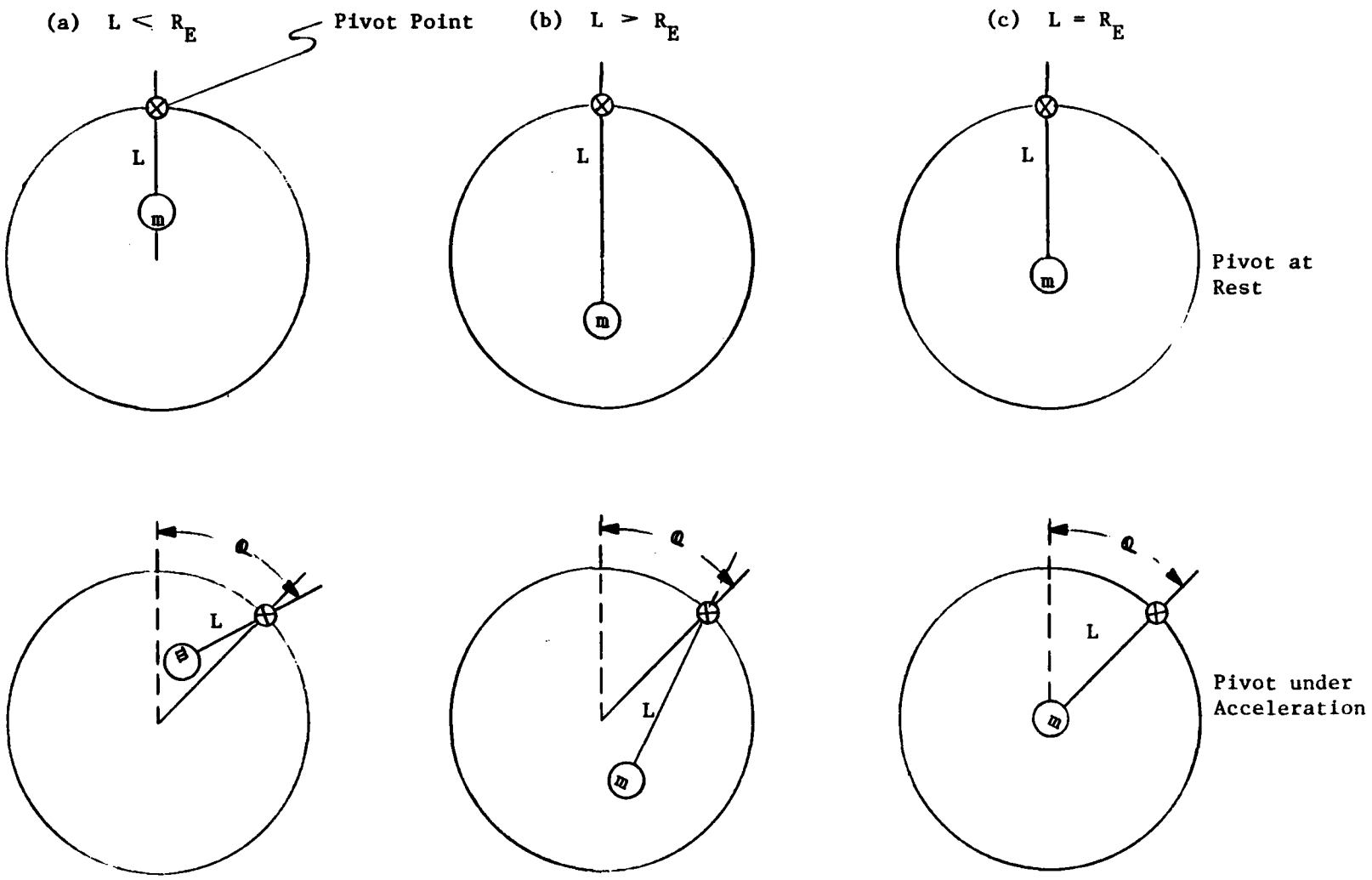

Figure 2.1.3.1 -- The Schuler Pendulum

where:

g	=	Acceleration due to Gravity	(Meters/Sec^2)
L	=	Length of Pendulum	(Meters)
R_E	=	Radius of the Earth	(Meters)

(If the pivot of the pendulum is located in a vehicle above the surface of the earth, the altitude of the vehicle must be included in the value of R_E.)
That period (the Schuler period) is 84.4 minutes. Any pendulum with an 84.4 minute period will, under displacement of its pivot point from one earth location to another, swing through exactly the required angle to maintain its supporting shaft pointing at the center of the (homogeneous, spherical) earth. Theoretically, it is possible to construct a pendulum with an 84.4 minute period utilizing the configuration, called a physical pendulum, shown in Figure 2.1.3.2. A physical pendulum consists of a solid bar suspended by a pivot slightly offset from its center of mass as shown in the figure. The period of a physical pendulum is given by the equation:

$$T = 2\pi \sqrt{\frac{I}{mgd}} \qquad \text{(Seconds)}$$

where:

d	=	Distance from Pivot Point to Center of Mass
g	=	Acceleration due to Gravity
I	=	Moment of Inertia of Bar about the Pivot
m	=	Mass of Bar

The period of a simple pendulum is determined by its length (and the acceleration due to gravity). The period of a physical pendulum, however, is a function of

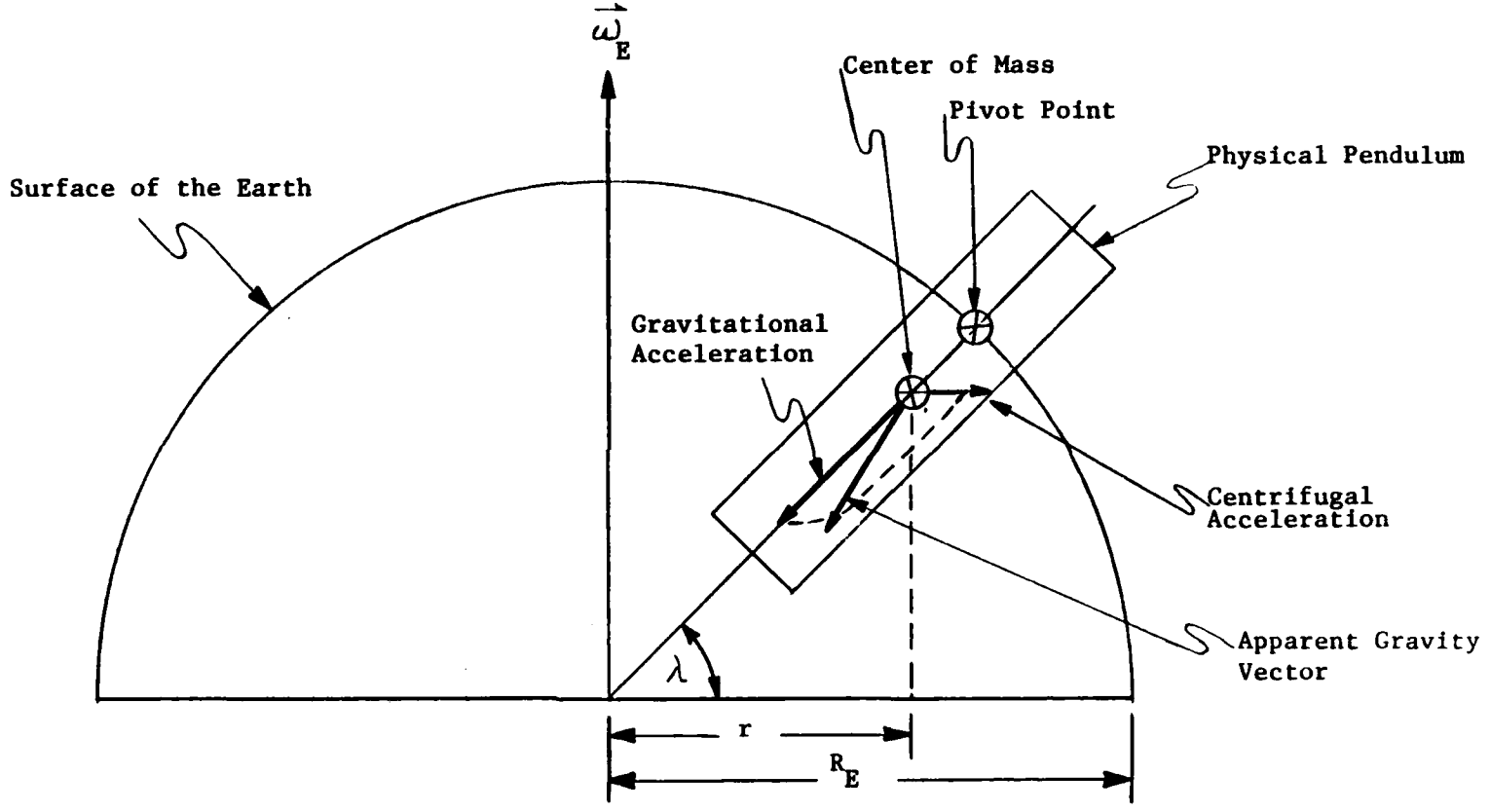

Figure 2.1.3.2 -- The Physical Pendulum Vertical Tracker

the distance between its pivot point and its center of mass. Theoretically, a physical pendulum with an 84.4 minute period can be constructed. Unfortunately, however, the distance, d, for a reasonably-sized 84.4 minute physical pendulum is only a few thousandths of an inch. Since the tuning of the Schuler pendulum would be critical to the operation of an INS, structural stability would be a major problem. In short, a physical Schuler pendulum is not practical for use in an INS. The properties of such a pendulum are, however, worth examining, because they closely resemble those of the stable platform in an actual semi-analytic INS. In particular, the physical pendulum is subject to precisely the same coriolis and centrifugal effects that must be removed in an INS. The simplicity of the physical pendulum, however, allows the origin of these effects to be seen more clearly.

Referring to Figure 2.1.3.2, it can be seen that the centrifugal acceleration due to earth rate, ω_E, directed outward perpendicular to the earth's spin axis, will cause the pendulum to swing outward, aligning itself with the apparent gravity vector. The magnitude of the northerly component of the centrifugal acceleration, a_{ce}, is given by the equation:

$$a_{ce} = r\,\omega_E^2 \cos(\lambda) = R_E\,\omega_E^2 \cos^2(\lambda)$$

where:

r = Radial Distance of Vehicle from Earth's Spin Axis

R_E = Radius of Earth

ω_E = Earth Spin Rate

λ = Latitude of Vehicle

Note that, if the vehicle possesses an easterly transport velocity (an easterly velocity with respect to the earth) the effective rotation rate must be added to ω_E.

Again referring to Figure 2.1.3.2, it can be seen that a north velocity, V_N, of the pendulum pivot point will result in a decreasing value of the radius r. The rate of change of r will, in turn, produce a rate of change in that component of east velocity produced by earth rate ($r\omega_E$). Thus, a north velocity will produce an easterly Coriolis acceleration, a_{co}, given by the equation:

$$a_{co} = -2\,\omega_E\,v_N\,\sin(\lambda)$$

The coriolis acceleration, as did the centrifugal acceleration, will cause the pendulum to swing in such a way as to align itself with the "apparent gravity vector". The centrifugal and coriolis acceleration terms presented above exemplify those that must be computed and cancelled in an actual semi-analytic inertial navigation system.

As previously stated, a physical pendulum cannot practicably be employed as the stable platform in an inertial navigation system. There is, however, a way to construct a "pendulum" with an 84.4 minute period--the electromechanical-servo stable platform already discussed in Section 2.1.2 of this text. As stated therein, the orientation of the stable platform in a semi-analytic INS is controlled in such a way as to maintain its vertical axis aligned with the local vertical. Control of platform orientation about each horizontal axis is accomplished by a closed-loop servomechanism similar to the one shown in the block diagram of Figure 2.1.3.3. As indicated in Figure 2.1.3.3(a), a horizontal

(a) Geometric Relationship between Platform Angle and Range

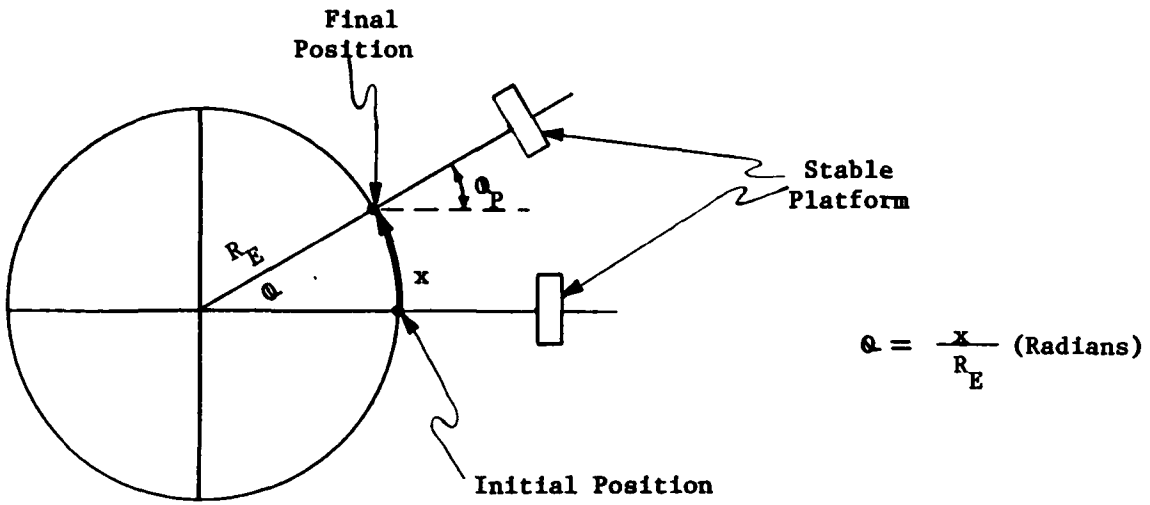

(b) Block Diagram

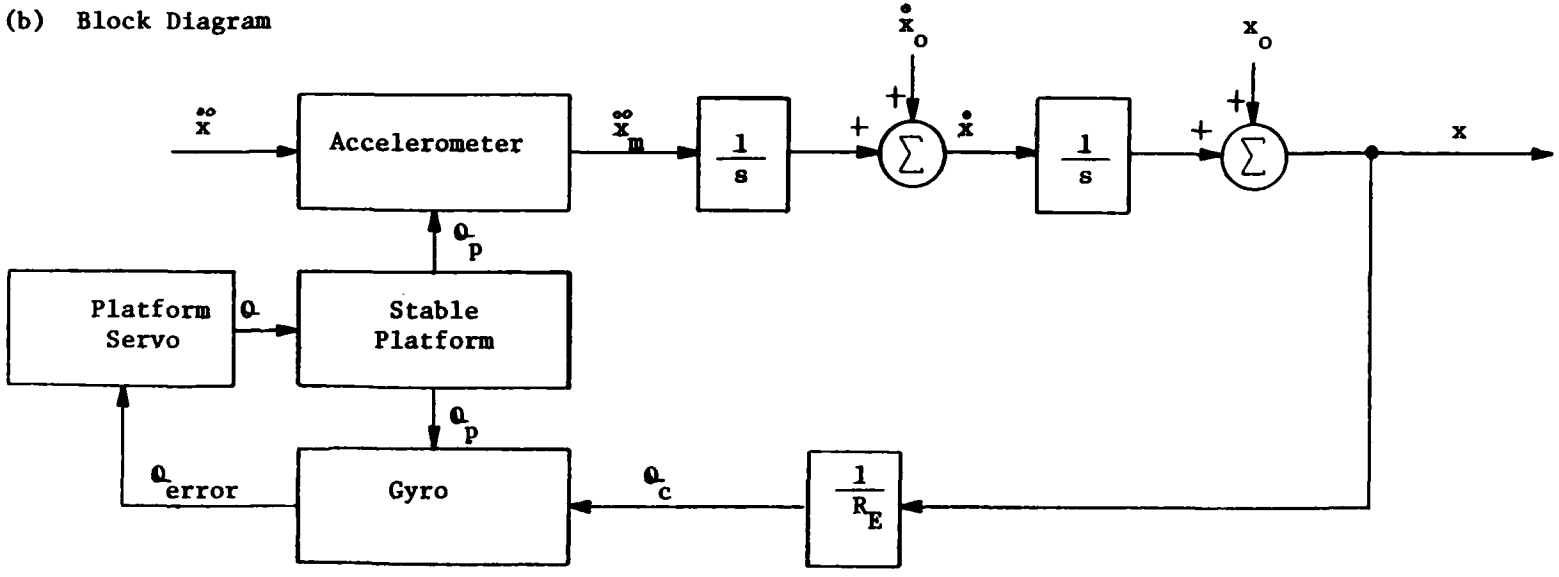

Figure 2.1.3.3 -- Vertical-Tracking Electromechanical Servo

channel in a semi-analytic INS determines distance traveled along the earth's surface--that is, arc length (x). The angle through which the stable platform must be rotated in order to maintain its vertical axis aligned with the local vertical is then given by the equation:

$$\theta_P = \frac{X}{R_E} \qquad \text{(Radians)}$$

(Note that this analysis does not consider the required corrections for earth rate, coriolis and centrifugal accelerations, or gravitational anomalies.) In the vertical-tracking servo shown in Figure 2.1.3.3(b), the computed value of platform angle, θ_c, is obtained by dividing the computed value of x by R_E as required. The computed value of platform angle is then used to drive a torque motor in the gyro so as to re-orient the spin axis of the gyro (thereby changing the reference angle of the gyro by an amount θ_c), thus creating an output (error) signal from the gyro. The output of the gyro is the error signal for the stable platform servo described in Section 2.1.2 of this text. The platform servo therefore nulls the error signal by rotating the platform through the angle θ_c, thus maintaining the platform's vertical orientation, as required.

The preceding analysis assumes that the platform vertical is, in fact, maintained in alignment with the local vertical, thereby preventing vertical accelerations from entering the horizontal channels. Of special interest is the effect on the system if the platform is allowed to "tilt". In level flight, (or on the ground), the altitude of the vehicle is maintained constant by externally-applied forces (aerodynamic lift or weight-on-wheels). These external (specific) forces cause an output from the vertical accelerometer equal and opposite to the

acceleration due to gravity. If the platform is "tilted" through an angle θ_ε, a component of the vertical acceleration will be sensed by the horizontal accelerometers. The magnitude of that acceleration is given by the equation:

$$\ddot{x}_\varepsilon = g \sin(\theta_\varepsilon) \cong g\,\theta_\varepsilon$$

where g is the acceleration due to gravity and θ_ε is the "tilt" angle. When this inadvertent feedback path is included in the block diagram of the horizontal channel of a semi-analytic (vertical-tracking) INS, the diagram is as shown in Figure 2.1.3.4. The only difference between Figures 2.1.3.3 and 2.1.3.4 is that the feedback due to platform tilt is shown explicitly in the latter figure. The performance equation of the vertical tracker represented by the block diagram in Figure 2.1.3.4 can be derived by multiplying the transfer functions shown in the diagram. The overall closed-loop dynamic performance equations for computed position, x_c, and computed platform angle, θ_c, are thus:

$$\ddot{x}_c + (g/R_E)\,x_c = \ddot{x} + g\,\theta_p$$

$$\ddot{\theta}_c + (g/R_E)\,\theta_c = (1/R_E)\,\ddot{x} + (g/R_E)\,\theta_p$$

These equations indicate that the electromechanical vertical tracker behaves as an undamped second-order system with a natural period given by:

$$T = 2\pi\sqrt{R_E/g} \qquad \text{(Seconds)}$$

This is exactly the period of a Schuler pendulum. The preceding analysis thus demonstrates that a servo system designed to track the local vertical is, as previously stated, the equivalent of a Schuler pendulum. The platform angle

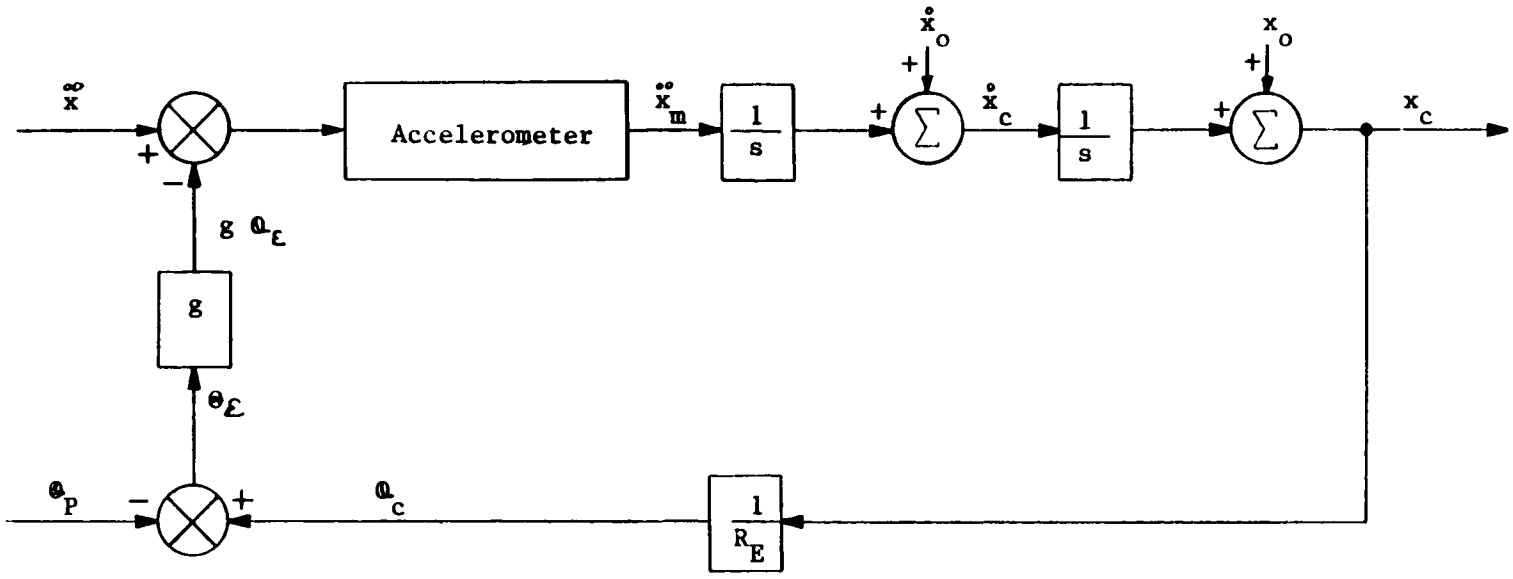

$\ddot{x}$ = True Horizontal Acceleration

$\ddot{x}_m$ = Measured Acceleration

$\dot{x}_c$ = Computed Velocity

x_c = Computed Position

$\dot{x}_o$ = Initial Velocity

x_o = Initial Position

θ_c = Computed Platform Angle

θ_p = Actual Platform Angle

θ_ε = Platform Angle Error (Tilt)

Figure 2.1.3.4 -- Vertical-Tracking Electromechanical Servo with Platform Tilt

response of the vertical tracker to a step input is illustrated in Figure 2.1.3.5. The performance equations also indicate that, in the steady state ($\ddot{x}_c = \dot{x} = 0$ and $\ddot{\theta}_c = \dot{\theta} = 0$):

$$x_c = x$$

and

$$\theta_c = \theta_p$$

as required.

The absence of a damping term in the performance equation, (a term proportional to computed velocity, $\dot{x}_c$, or computed platform angle, $\dot{\theta}_c$), indicates that the system is undamped and that the oscillation depicted in Figure 2.1.3.5 would continue indefinitely if some method were not provided for damping the Schuler "loop". One such method would be velocity feedback, as shown in Figure 2.1.3.6. The effect of the negative feedback is to produce velocity-proportional damping as evidenced by the velocity-proportional term in the performance equation. This method of damping would indeed damp the Schuler oscillations. It would also, however, introduce constant-velocity following errors in the vertical tracker. Those errors, unfortunately, would be prohibitively large. Therefore, an alternative means of damping is employed as shown in Figure 2.1.3.7. As indicated in that diagram, velocity feedback is still employed; but the computed velocity fed back is differenced with a reference velocity derived from an independent measurement (such as that from a Doppler radar navigation system). The result is "velocity-error" feedback. As long as the computed velocity, $\dot{x}_c$, is equal to the reference velocity, $\dot{x}_R$, no feedback occurs, the damping term in the performance equations goes to zero, no damping is applied to the system, and there is no constant-velocity following error. If the reference velocity is

$$\theta_c(t) = \theta_{co} + \Delta\theta \left[1 - \cos\left(\sqrt{\frac{g}{R_E}}\, t\right)\right]$$

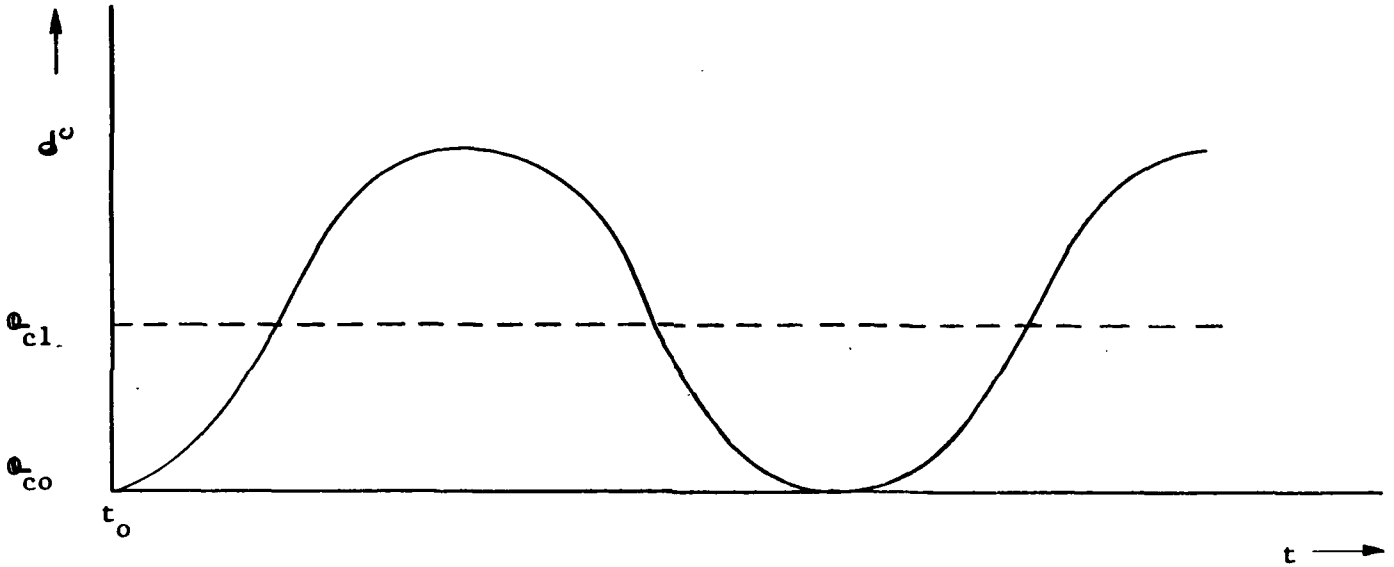

θ_c = Platform Angle

θ_{co} = Initial Platform Angle (before step input)

θ_{c1} = Commanded Platform Angle (after Step Input)

$\Delta\theta$ = Commanded Step Input = $\theta_{c1} - \theta_{co}$

Figure 2.1.3.5 -- Time Response of Local-Vertical-Tracking Positional Servo

(a) Block Diagram

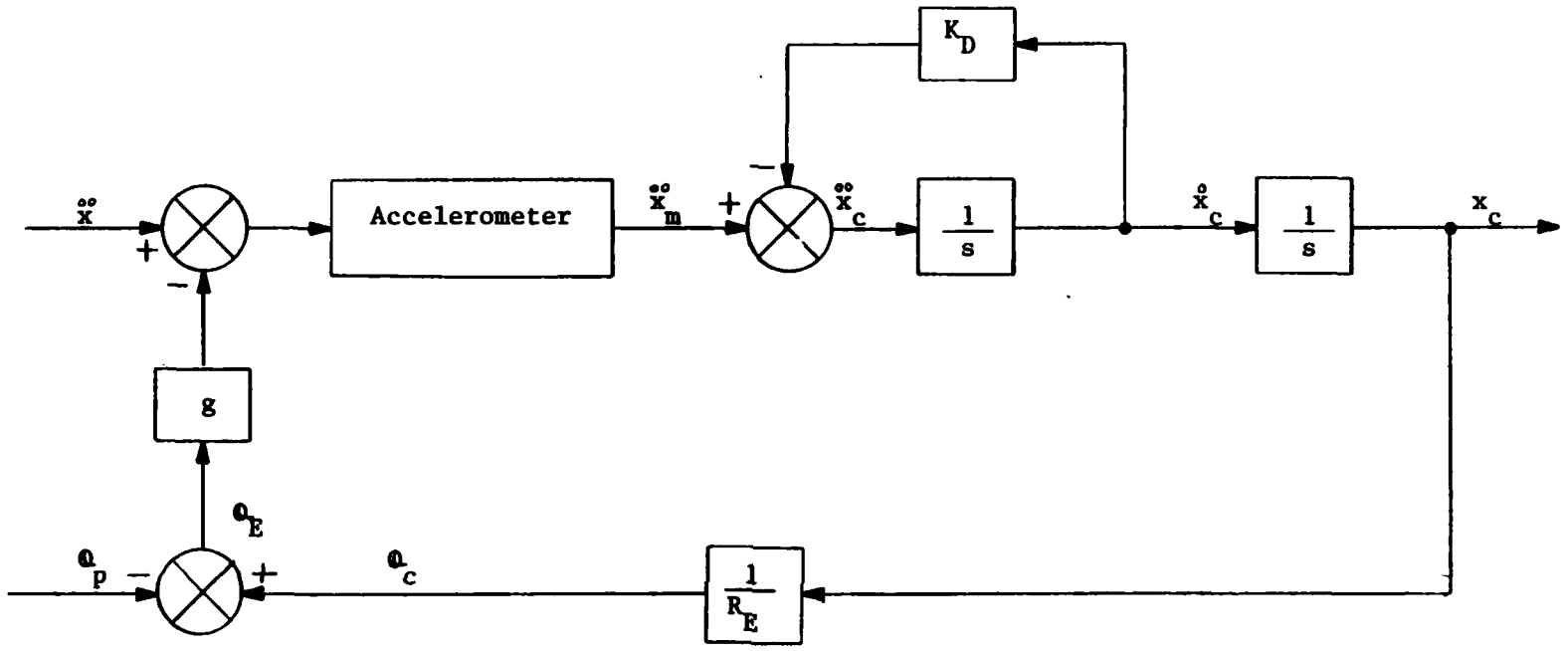

(b) Performance Equations

$$\ddot{x}_c + K_D \dot{x}_c + \left(\frac{g}{R_E}\right) x_c = \ddot{x} + g\,\Omega_p$$

$$\ddot{\Omega}_c + K_D \dot{\Omega}_c + \left(\frac{g}{R_E}\right) \Omega_c = \left(\frac{1}{R_E}\right)\ddot{x} + \left(\frac{g}{R_E}\right)\Omega_p$$

Figure 2.1.3.6 -- Vertical Tracker with Velocity Damping

(a) Block Diagram

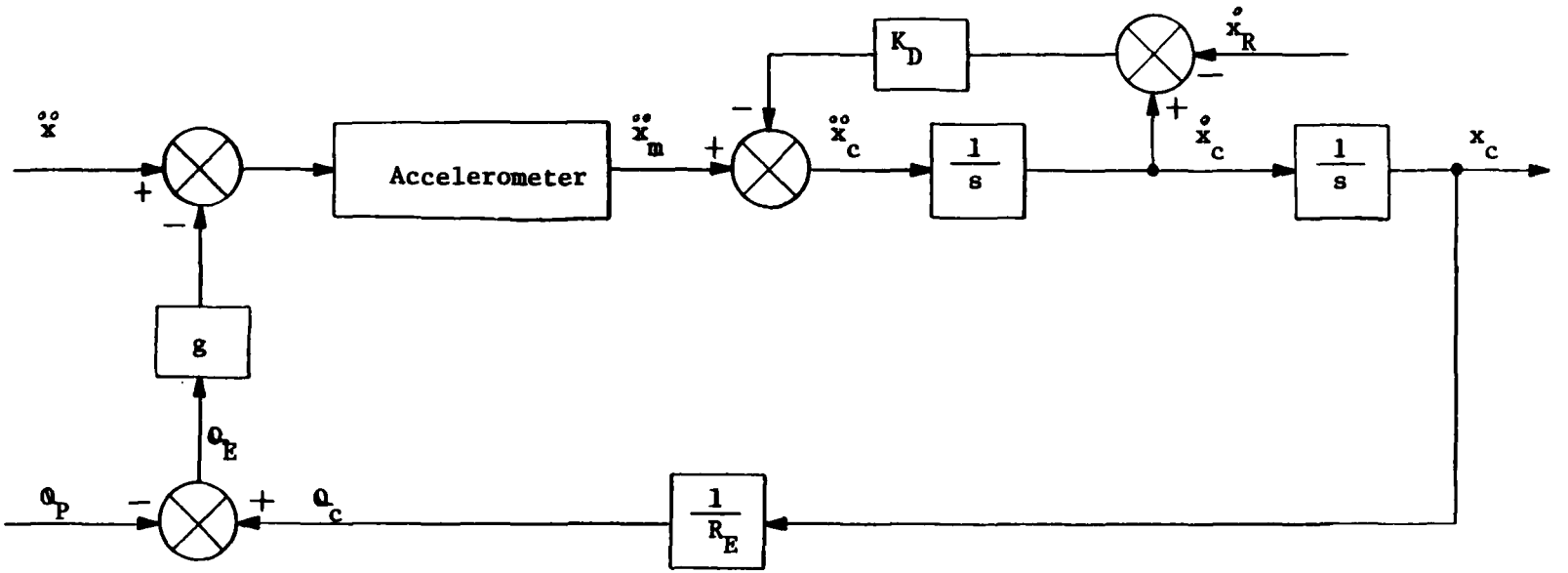

(b) Performance Equations

$$\ddot{x}_c + K_D\left(\dot{x}_c - \dot{x}_R\right) + \left(\frac{g}{R_E}\right) x_c = \ddot{x} + g\theta_p$$

$$\ddot{\theta}_c + K_D\left(\dot{\theta}_c - \dot{\theta}_R\right) + \left(\frac{g}{R_E}\right) \theta_c = \left(\frac{1}{R_E}\right)\ddot{x} + \left(\frac{g}{R_E}\right) \theta_p$$

Where: $\dot{\theta}_R = \frac{\dot{x}_R}{R_E}$

Figure 2.1.3.7 -- Vertical Tracker with Velocity-Error Damping

an accurate measure of the true velocity, $\dot{x}$, then the vertical tracker will be damped only when an error exists in the computed velocity, $\dot{x}_c$. If that error consists of a Schuler oscillation (as often it does), it will be damped out by the velocity-difference feedback. Of course, if the reference velocity, $\dot{x}_R$, is in error, it will introduce errors into the vertical tracker.

In Figure 2.1.3.8 is shown the block diagram for a complete horizontal channel of a semi-analytic (vertical-tracking) INS. Shown in the diagram are all of the inputs and corrections described in preceding sections of this text. Included in the diagram is the correction of platform angle for the component of earth rate required only in the east-west channel. Since the horizontal axes of a semi-analytic INS are maintained perpendicular to the (average) gravitational vector, the only gravitational corrections required are those due to gravitational anomalies. These corrections can be sizeable, however, producing as much as one-nautical-mile errors due to localized geodetic anomalies. High-accuracy inertial navigation systems employ gravity"models" with as many as thirty-two terms. Systems in tactical aircraft generally employ a greatly simplified model (e.g. an elliptical model of the earth), relying upon independent updates to correct accumulating errors.

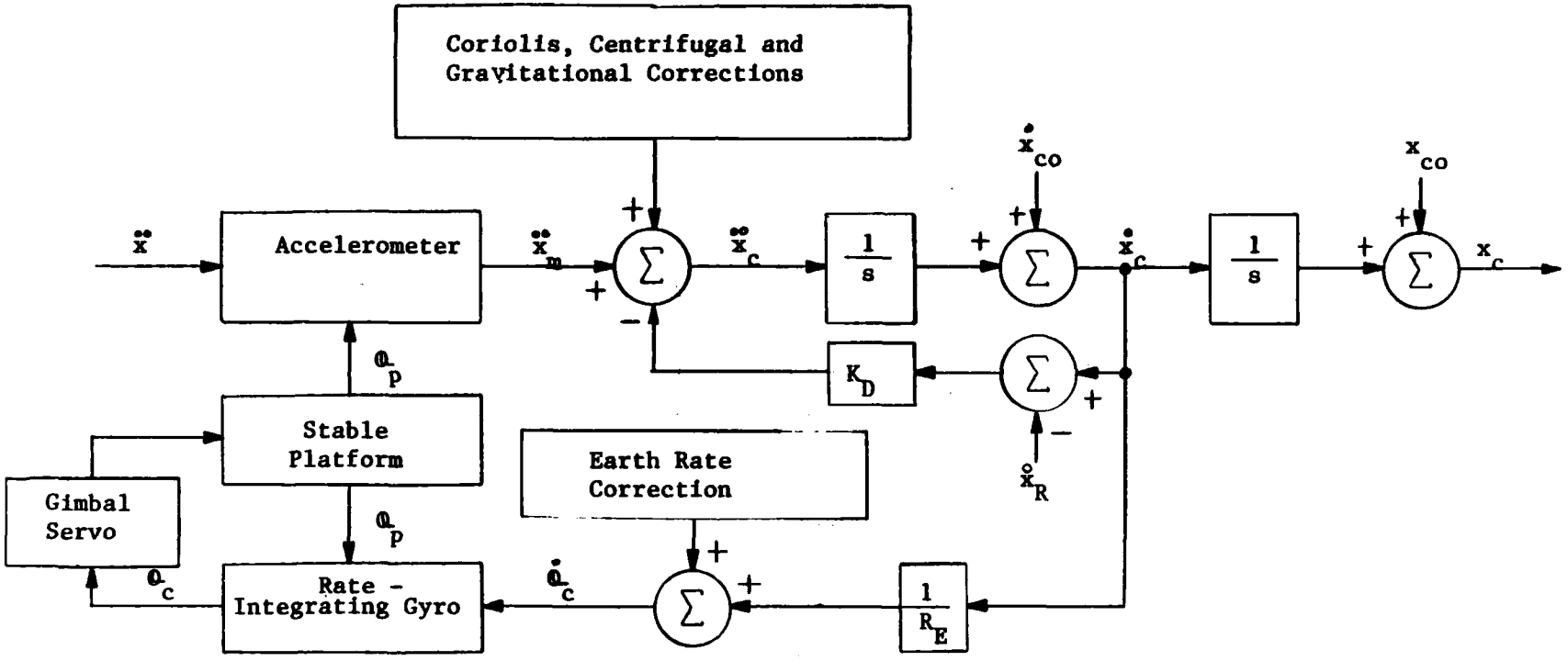

Figure 2.1.3.8 -- Horizontal Channel of Semi-Analytic INS

2.1.4 The Vertical Channel -- Because of the decrease in the gravitational acceleration with increasing altitude, the computation of vertical position (altitude) in an INS is (absolutely) unstable. For that reason, some INS's do not include a vertical channel, relying on other systems (barometric or radio altimeters) for that information. When a vertical channel is included in an INS, it must be stabilized by an altitude-difference feedback similar to that employed in the horizontal channels. The block diagram of an undamped vertical channel (altitude computation) of a semi-analytic INS is shown in Figure 2.1.4.1(a). Incorporated in the altitude computation is the mathematical model for the gravitational acceleration as a function of altitude. The "gravity model" employed is given by the equation:

$$g(h) = g_o - (2g_o/R_E)\,h$$

where g_o is the gravitational acceleration at the surface of the earth (h = o). As previously stated, the accelerometer cannot sense the gravitational acceleration. That acceleration must then be computed and (algebraically) added to the measured (sensed) acceleration. The resultant total acceleration is then doubly integrated to obtain vertical position (altitude). The performance equation of the vertical channel computation is:

$$\ddot{h}_c - (2g_o/R_E)\,h_c = \ddot{h}_m$$

Note the similarity between this equation and that for an undamped horizontal channel. Note, however, that the sign of the zero-derivative term is negative. (It is positive for the horizontal channel). A negative coefficient in the performance (characteristic) equation of a second-order system indicates an absolute

(a) Block Diagram

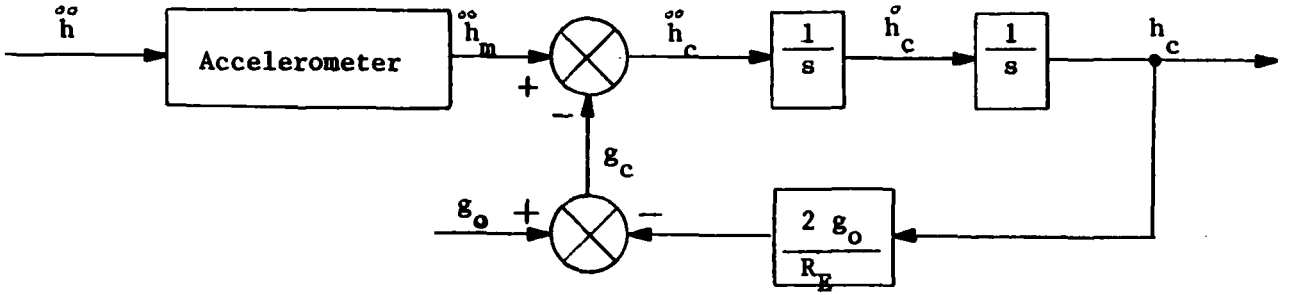

g_c = Computed Gravitational Acceleration

g_o = Gravitational Acceleration at H = 0

h_c = Computed Altitude

$\ddot{h}_m$ = Measured (Sensed) Vertical Acceleration

R_E = Radius of Earth

2.27a

(b) Response to Step Function Input

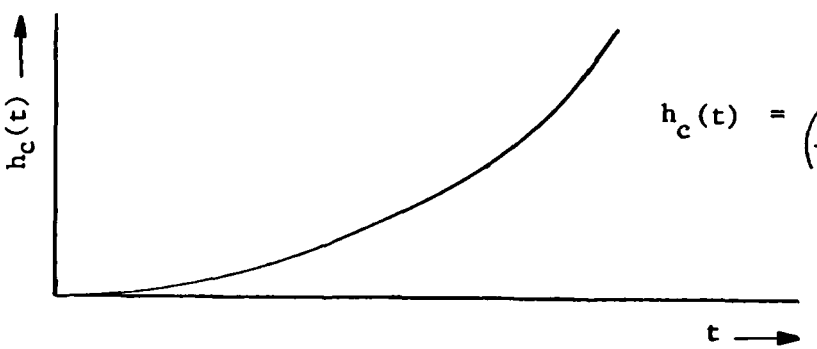

$$h_c(t) = \left(\frac{R_E}{2g_o}\right) \text{Sinh} \left(\sqrt{\frac{2g_o}{R_E}}\ t\right)$$

Figure 2.1.4.1 -- Undamped Vertical Channel of Semi-Analytic INS

instability. (The undamped horizontal channel was neutrally stable.) The absolute instability of an undamped vertical channel is demonstrated by the response to a step function input, as shown in Figure 2.1.4.1(b). A common method of stabilizing the vertical channel of a semi-analytic INS is shown in the block diagram of Figure 2.1.4.2(a). Two negative feedback paths are provided resulting in the position and velocity terms shown in Figure 2.1.4.2(b), with coefficients equal to the K_1 and K_2 feedback gains, respectively. In a manner similar to that employed in the horizontal channels, "position-error" feedback is employed, the computed altitude being differenced with a reference altitude assumed to be an accurate measure of true altitude. The "altitude-error" is fed back around both integrators, thus producing both position and velocity terms in the performance equation, as indicated in Figure 2.1.4.2(b). When altitude-rate-error exists, the feedback through gain K_2 provides velocity-damping. When altitude error exists, the feedback through gain K_1 provides absolute stability for the system as long as:

$$K_1 (h_c - h_r) > (2g_0/R_E) h_c$$

When no altitude error exists, no feedback occurs, thus avoiding feedback-induced errors. As for the horizontal channels, an error in the reference altitude, h_r, will introduce errors in the INS output.

(a) Block Diagram

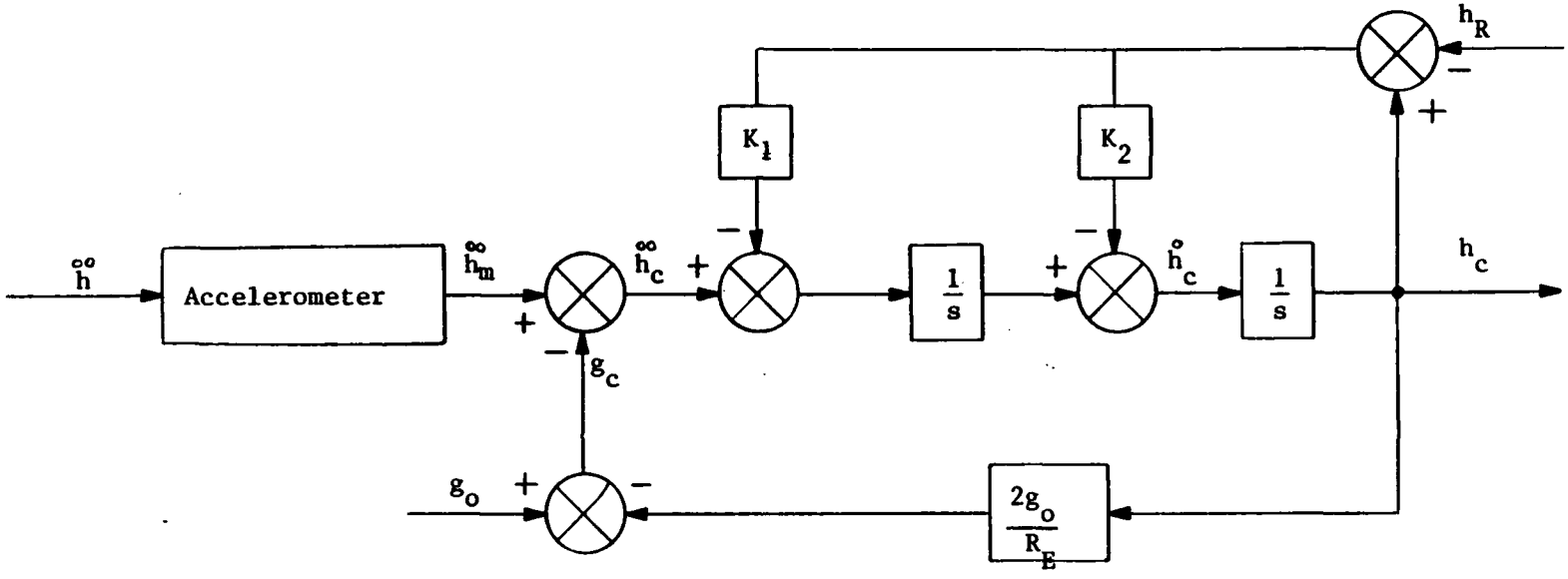

(b) Performance Equation

$$\ddot{h}_c + K_2(\dot{h}_c - \dot{h}_r) + K_1(h_c - h_r) - \left(\frac{2g_o}{R_E}\right) h_c = \ddot{h}_m - g_o$$

Figure 2.1.4.2 -- Damped Vertical Channel of Semi-Analytic INS

2.1.5 The Analytic INS -- As previously indicated, the stable platform in an analytic INS maintains its orientation fixed in inertial space. An analytic INS therefore senses motion and computes velocity and position in an inertial frame of reference. Since it operates in a non-rotating frame of reference, no Coriolis, centrifugal, or earth-rate corrections are required. An all-axis gravitational model is required, however, since major components of gravity can exist in all channels. If the system is intended for terrestrial operation, a coordinate transformation is required from the cartesian inertial coordinates to terrestrial coordinates such as latitude, longitude, and altitude. The block diagram of a terrestrial analytic INS is presented in Figure 2.1.5.1. It should be noted that no gyro torquing (platform realignment) is required, thus eliminating a major source of error (gyro torquing) and also eliminating the position feedback that produces the Schuler-loop oscillations in the semi-analytic INS. It also should be noted, however, that the gravity components computed and fed back introduce (gravity model) errors and also constitute an equivalent position feedback that creates an effective Schuler loop, complete with Schuler oscillations. A terrestrial analytic INS therefore requires stabilization similar to that for a semi-analytic INS. The schematic diagram of a stable platform presented in Figure 2.1.2.11 in Section 2.1.2 of this text is applicable to an analytic INS.

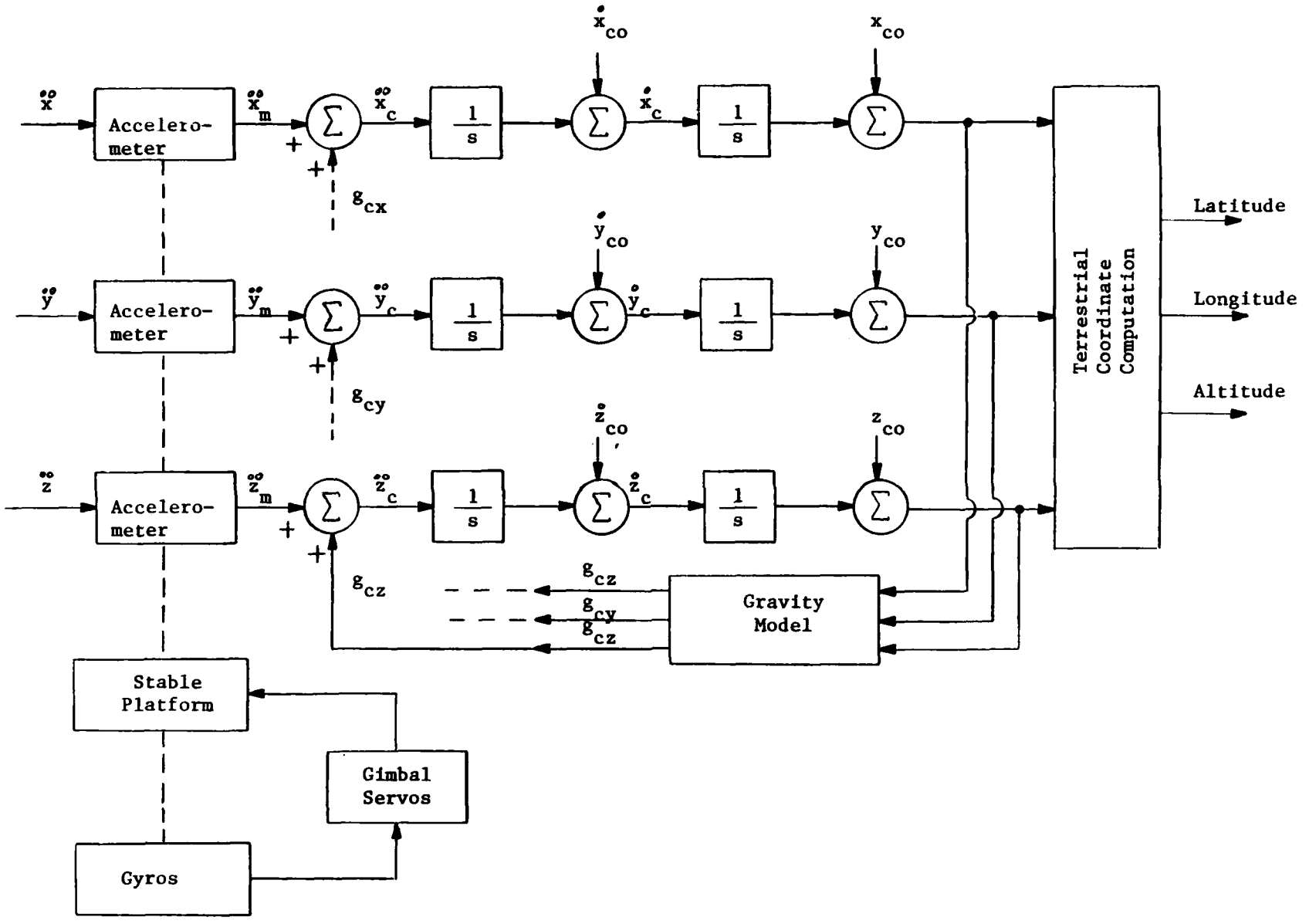

Figure 2.1.5.1 -- Block Diagram, Analytic INS

2.1.6 The Semi-Analytic INS -- As previously indicated, the stable platform in a semi-anayltic INS maintains its orientation fixed with respect to the rotating earth. That is, the vertical axis is maintained aligned with the local vertical ("gravity" vector). The horizontal axes may be maintained aligned with north and east or they may be allowed to deviate from that fixed orientation as in a "wander azimuth" system. In a wander azimuth system, the directions of north and east are, of course, maintained by the system. However, the vertical (azimuth) gyro is not torqued so as to maintain the horizontal axes of the platform aligned with north and east. The horizontal components of acceleration are measured in the directions established by the accelerometer input axes and are then computationally transformed to north and east components, utilizing the known wander azimuth angle with respect to north.

The block diagrams for the east-west, north-south, and vertical channels of an undamped, north-pointing, semi-analytic INS are shown in Figures 2.1.6.1(a), (b), and (c), respectively.

The following definitions apply to the symbols employed in Figures 2.1.6.1

g = Total of accelerations due to gravitation and earth rate.

g_c = Computed value of g.

g_{cy} = North component of gc.

G = Acceleration due to gravitation (earth mass attraction).

h = Altitude of vehicle above earch reference ellipsoid.

R = Distance between earth center of mass and vehicle (sum of R_E and h.)

R_E = Earth reference ellipsoid radius at position of vehicle.

S = Laplace operator

X_e = Computed value of east position coordinate of vehicle.

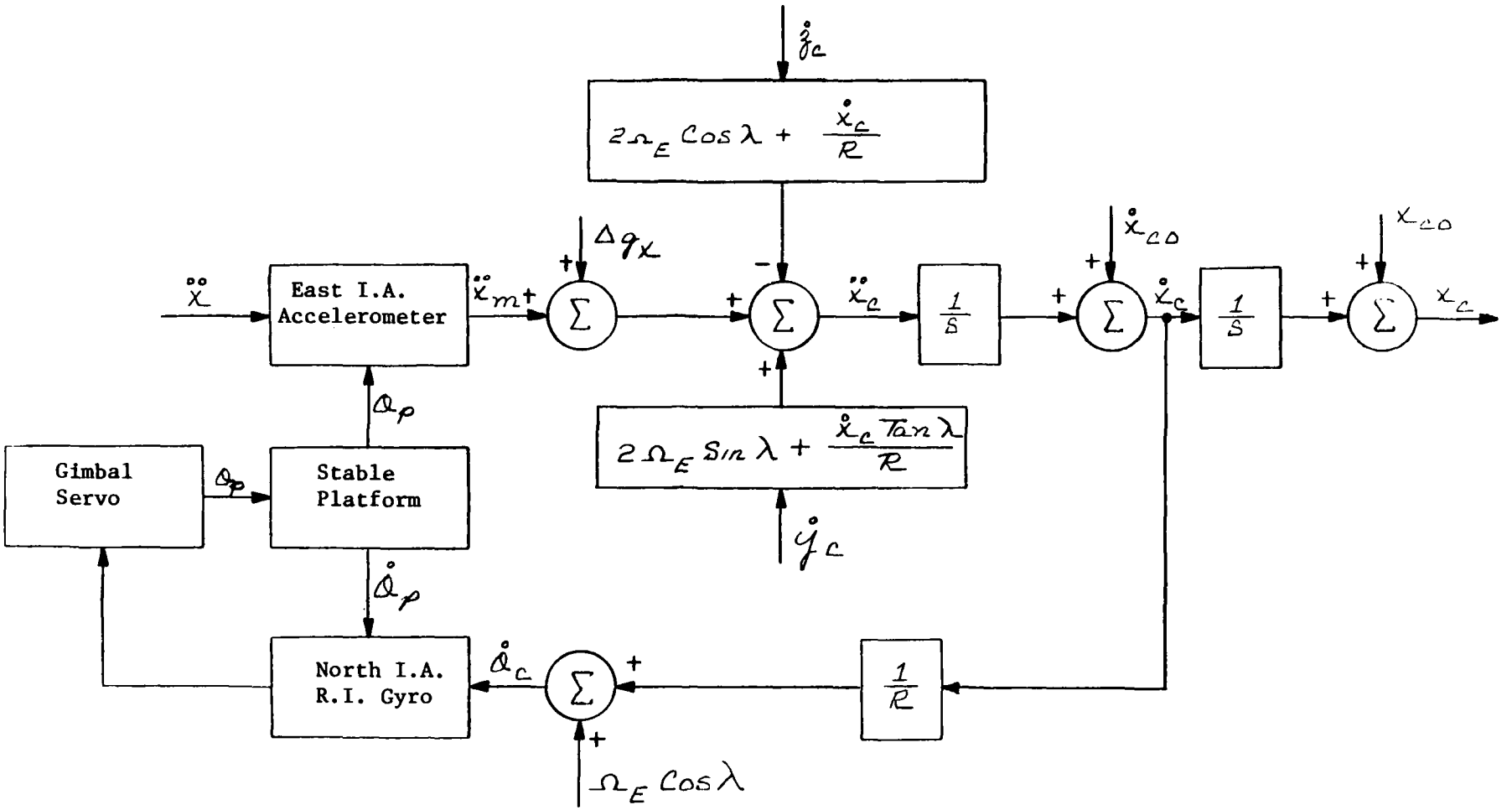

(See Text for Definitions of Symbols)

Figure 2.1.6.1(a) -- East Channel of Undamped, North-Pointing, Semi-Analytic INS

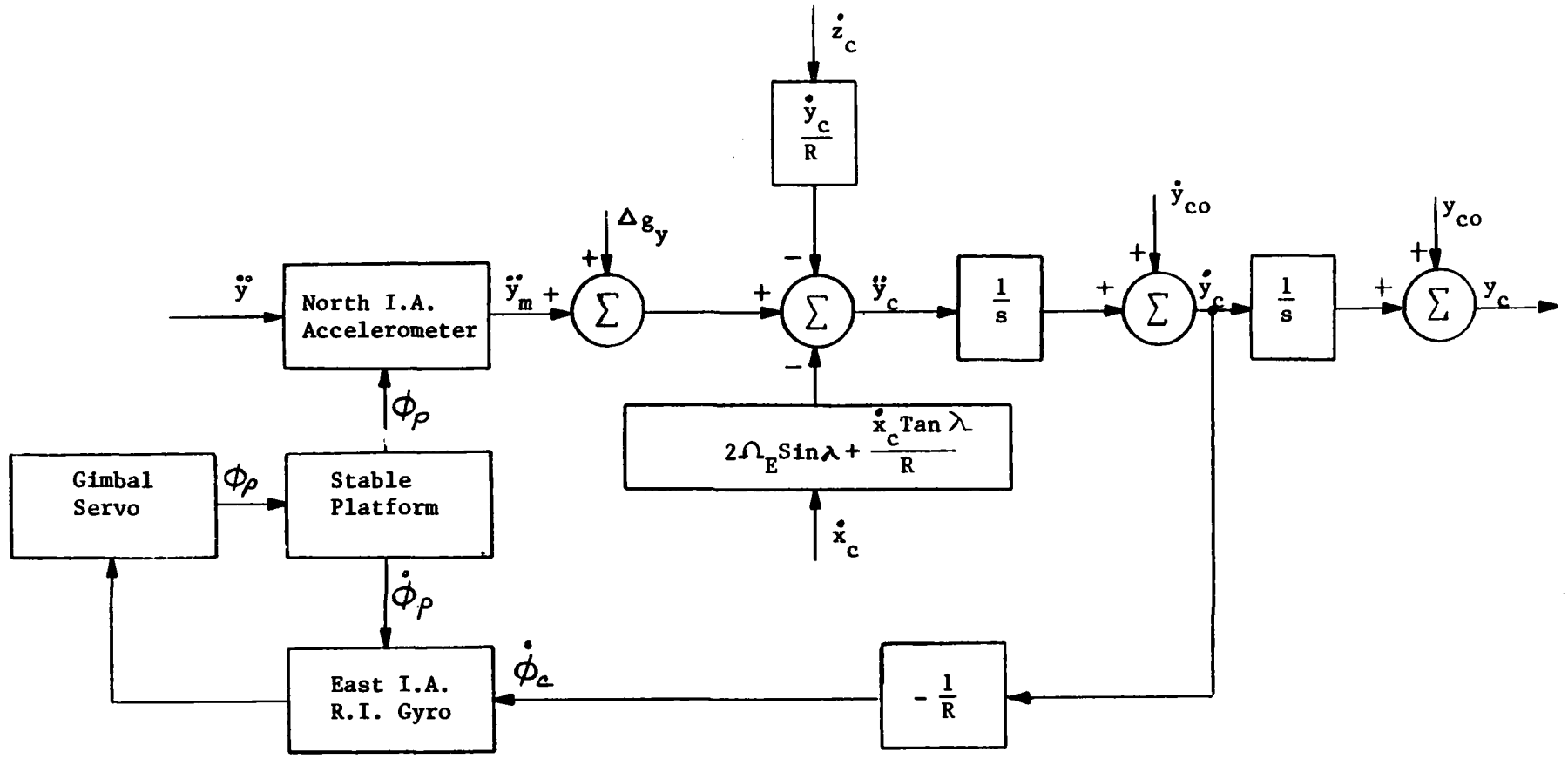

(See Text for Definitions of Symbols)

Figure 2.1.6.1(b) -- North Channel of Undamped, North-Pointing, Semi-Analytic INS

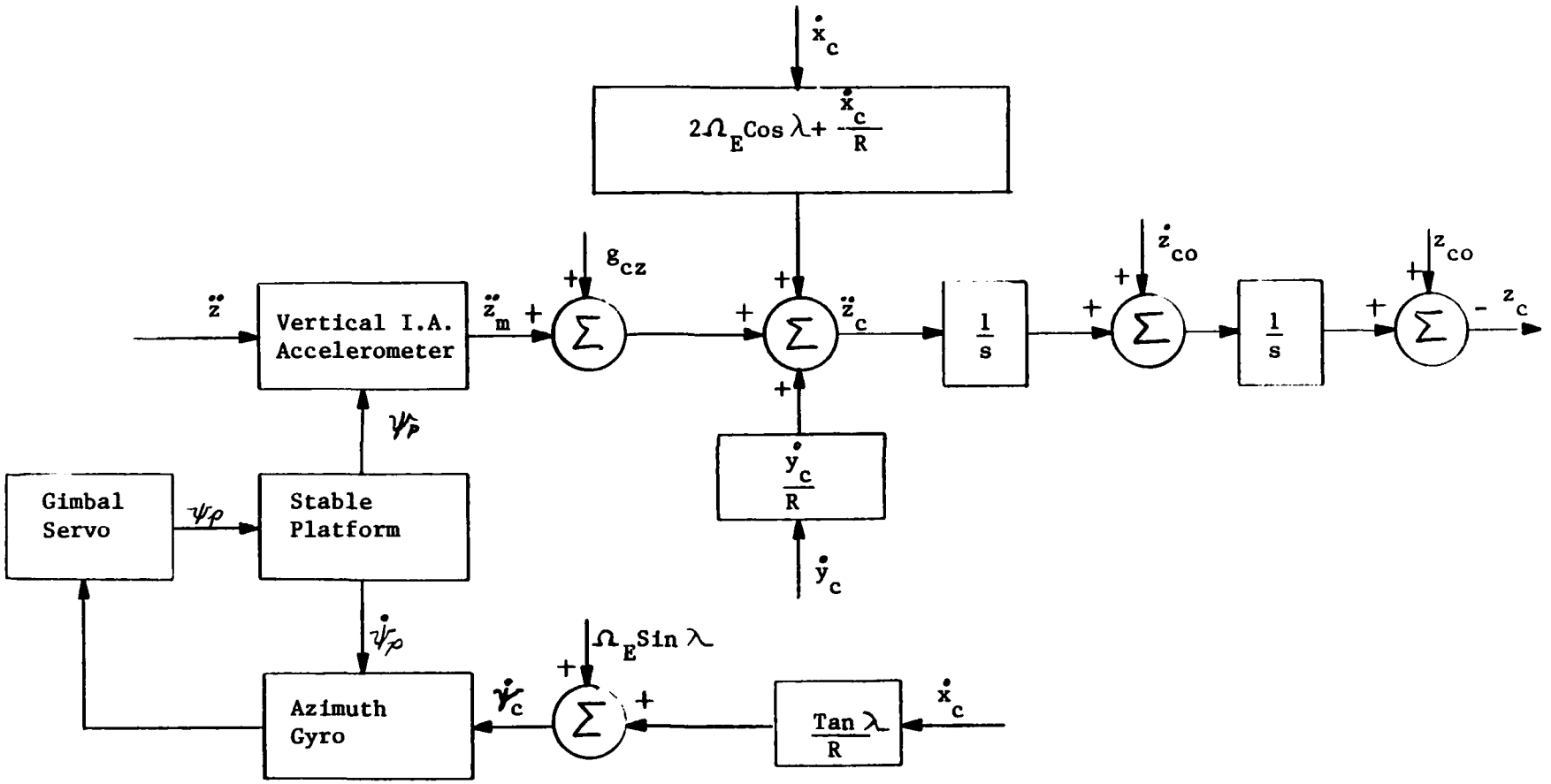

(See Text for Definitions of Symbols)

Figure 2.1.6.1(c) -- Vertical Channel of Undamped, North-Pointing, Semi-Analytic INS

X_{co} = Initial value of X_c

Y_c = Computed value of north position coordinate of vehicle.

Y_{co} = Initial value of Y_c

Z_c = Computed value of vertical position coordinate of vehicle.

Z_{co} = Initial value of Z_c.

θ_p = Stable platform angular position about north-south axis.

θ_c = Commanded (computed) value of θ_p.

ϕ_p = Stable platform angular position about east-west axis.

ϕ_c = Commanded (computed) value of ϕ_p.

ψ_p = Stable platform angular position about vertical axis.

ψ_c = Commanded (computed) value of ψ_p.

λ = Latitude of vehicle.

Ω_E = Angular rate of earth rotation.

Σ = Summation symbol.

The input axes of the horizontal channel accelerometers are mainted perpendicular to the direction of the modeled gravity vector. For that reason, only the gravitational anomalies, Δg_x and Δg_y, need be computed and added to the accelerometer outputs. These corrections are of second order compared to those for the vertical channel (and to those required for analytic and strap-down inertial navigation systems). The "gravity" vector shown in Figure 2.1.6.1 is, by convention, considered to include the centrifugal acceleration due to earth rate. That is:

$$\vec{g} = \vec{G} + \vec{\Omega}_E \times (\vec{\Omega}_E \times \vec{R})$$

where:

$\vec{g}$ = Total "Gravity" Vector

$\vec{G}$ = Gravitational Vector (due to mass attraction)

$\vec{R}$ = Vector Radius from Earch Center of Mass

$\vec{\Omega}_E$ = Angular Velocity Vector of Earth

The magnitude of the gravity vector in the vertical direction, g_z, is then given by:

$$g = G - \Omega_E^2 R \cos^2\lambda$$

where g, G, R, and Ω_E are the magnitudes of the vector quantities and λ is the latitude of the point of measurement. The magnitude of the gravitational vector, G, is given by the equation:

$$G = \frac{\mu}{R^2}$$

where μ is equal to the product of the mass of the earth and the universal gravitational constant and R is the distance of the point of measurement from the center of mass of the earth. Because the gravitational acceleration, G, varies inversely with the square of the distance R as indicated, it can be shown as a function of altitude, h, by the equation:

$$G = G_o \left[1 - \left(\frac{2}{R}\right) h \right]$$

where:

G_o = Gravitational Acceleration at the surface of the earth.

h = Altitude at Point of Measurement.

The inverse dependence of the gravitational acceleration on altitude is responsible for the vertical channel instability discussed in Section 2.1.4 of this text. Due to non-homogeneity and non-ellipsoidicity of the earth, the gravitational acceleration, G, is a function of position. A first-order approximation to the gravitational acceleration is given by:

$$G = (\mu/R^2)\left[1 - (3/4)\, J_2\, (1 - 3\, \cos(2\lambda))\right]$$

where J_2 is a coefficient equal to 8.115×10^{-4}. Highly accurate inertial navigation systems must employ gravity models incorporating many higher-order terms. The coriolis and centrifugal accelerations due to transport velocity of the vehicle are shown algebraically subtracted from the measured accelerations as discussed in Section 2.1.1 of this text. The rate-integrating gyros are shown torqued by the angular rate commands required to maintain the stable platform vertical axis aligned with the local vertical, and the north axis pointing north.

Many terrestrial systems compute in terms of longitude and latitude. The block diagrams shown in Figures 2.1.6.1 are representative of such systems with the substitutions:

$$\text{Latitude} = \frac{X}{R}$$

$$\text{Longitude} = \frac{Y}{R \cos (\text{Latitude})}$$

$$\text{Altitude} = z$$

2.1.7 The Strap-Down INS -- In a strap-down INS, the sensors (gyros and accelerometers) are fixed directly to the airframe. The angular rates and accelerations are, therefore, measured in an entirely unstabilized frame of reference. The components of these quantities in a space-or earth-stabilized frame of reference are then computed employing a time-varying coordinate transformation as shown in Figure 2.1.7.1. To these transformed accelerations are added the components of the gravity vector computed and transformed into the computational frame of reference. In a space-stabilized coordinate system, no coriolis or centrifugal acceleration corrections are required. Computationally, the generation of the airframe-to-computational frame coordinate transformation is extremely demanding. The transformation matrix must be computed in nearly "real time." (Delays of even one microsecond are significant in some systems). The input information for the generation of the transformation matrix is provided by the outputs of the gyros, corrected for the appropriate components of earth rate (for an earth-fixed computational frame). Once computed values of vehicle acceleration in the computational frame of reference are obtained, velocity and position are obtained by integration. No gyro torquing is required.

The relative advantages of the strap-down INS in comparison with the semi-analytic INS are:

(1) The elimination of gimbals.

(2) The elimination of gyro torquing.

(3) The elimination of corrections for the coriolis and centrifugal accelerations due to computing in a rotating coordinate system (for a space-stabilized computational frame).

(4) In general, the substitution of computational functions for hardware functions.

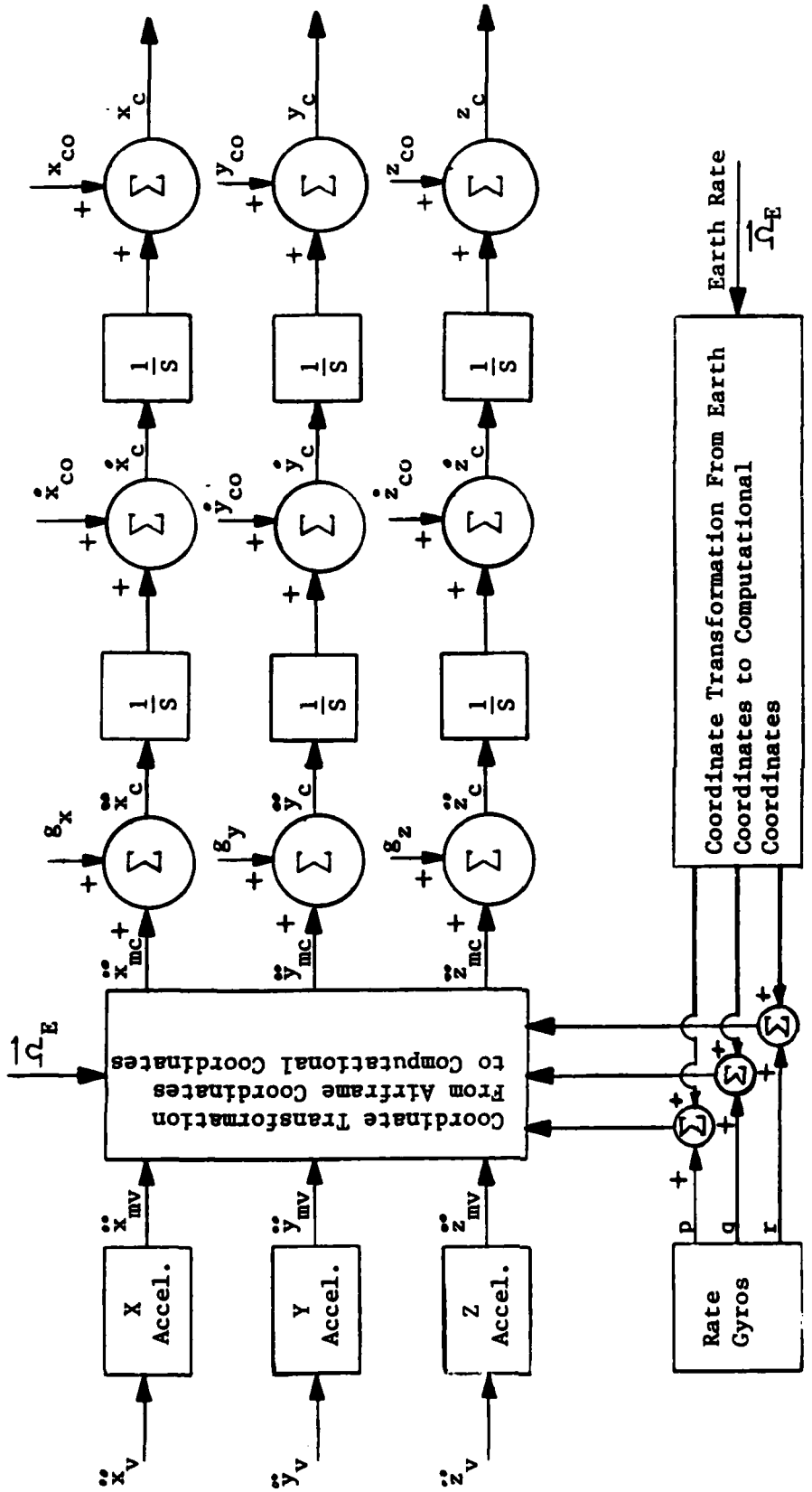

Figure 2.1.7.1 -- Block Diagram, Undamped Strap-Down INS

The relative disadvantages of the strap-down INS are:

(1) Computed gravitational components required in all axes.

(2) Complex, real-time coordinate transformation computations required.

(3) No motion isolation as provided by a stable platform. (Complex error-compensation required.)

(4) In general, reduced accuracy resulting from the above factors.

As indicated for the analytic INS, gravitational computations are a major source of error in an INS. In addition, time-varying orientation with respect to gravitational acceleration induces errors in the accelerometers, gyros, and gimbal systems. In a strap-down INS, the lack of motion isolation requires that the sensors have large dynamic ranges, thereby reducing accuracy at the low acceleration levels generated by transport motions. All of these factors combine to reduce the accuracy of a strap-down INS.

2.1.8 INS Initialization and Alignment -- As previously indicated, an INS is a dead-reckoning navigation system. That is, it deduces position and velocity from acceleration measurements, given initial position and velocity. In addition to position and velocity, an INS requires initial platform alignment (angular orientation). Initialization (or re-initialization) is possible both prior to flight and in-flight. In all cases, initialization and alignment are accomplished by comparison of system parameters with known references. Typical sources of reference quantities are:

Optical benchmarks (Autocollimating)
Master INS (Slaving)
Master INS Angular Rates (Rate Matching)
Visual, Radar, or I/R Checkpoints
The Local Vertical (Leveling)
The Earth's Spin Axis (Gyrocompassing)
The Earth's Magnetic Field (Magnetic Compass)
Celestial Navigation Data
Radio Navigation Data
Doppler Radar Navigation Data

Optical benchmarks are employed in fixed-site applications, such as ICBM silos, to provide alignment. INS slaving involves duplicating the operating state of an already-aligned INS to obtain complete initialization. INS rate matching involves adjusting the alignment of the INS until it indicates the same angular rates, due to vehicular motion, as those indicated by an already-aligned INS. "On-top" and "standoff" checkpoints provide both position and bearing information. The direction of the local gravity vector provides platform leveling information as discussed below. The direction of the earth's spin axis provides azimuth orientation as discussed below. A magnetic compass provides coarse azimuth alignment. Celestial data provides coarse position and fine alignment information. Radio navigation data provides position information. Doppler radar navigation data provide position and ground velocity information used for re-initialization, gyrocompassing, and damping of the INS Schuler oscillations.

Platform Leveling -- Platform leveling for a semi-analytic INS is accomplished, on the ground, by the platform leveling feedback loop shown in Figure 2.1.8.1. (Platform leveling in flight is an integral part of gyrocompassing, discussed below). The loop shown is that for leveling about the north-south axis in a north-pointing system with velocity damping. The loop for leveling about the east-west axis is identical except that the earth-rate compensation is not required. It should be noted that the platform-leveling loop shown is inherent to the normal operation of a semi-analytic INS. Comparison of the block diagram in Figure 2.1.8.1 with that in Figure 2.1.6.1 indicates that the platform leveling loop is identical with the normal navigating loop, with the exception of the leveling gain, K_L. In the navigating mode, the gain K_L is unity. In the platform leveling mode, it is increased to shorten the leveling time. That the platform leveling process is inherent to a semi-analytic INS is a consequence of the pendulum-like nature of such an INS. By nature, its vertical axis (pendulum rod) points in a direction opposite to that of the (resultant) applied acceleration. In this case, the applied acceleration is the result of the force sustaining the aircraft (weight-on-wheels or aerodynamic lift). The platform-leveling process is as follows.

(1) The east-input-axis accelerometer senses a component of the vertical sustaining force due to a platform error (tilt) angle θ_ε.

(2) The output of the accelerometer is integrated, power amplified, and used to torque the north-input-axis rate-integrating gyro.

(3) For the north-south axis shown, the component of earth rate about the north-south axis is added to the commanded rate.

(4) The output of the gyro is amplified and used to rotate the platform, (through the gimbal servo), in the proper direction to reduce the tilt angle θ_ε.

(5) The closed-loop process continues until the platform is level and the accelerometer no longer senses a component of the vertical sustaining force.

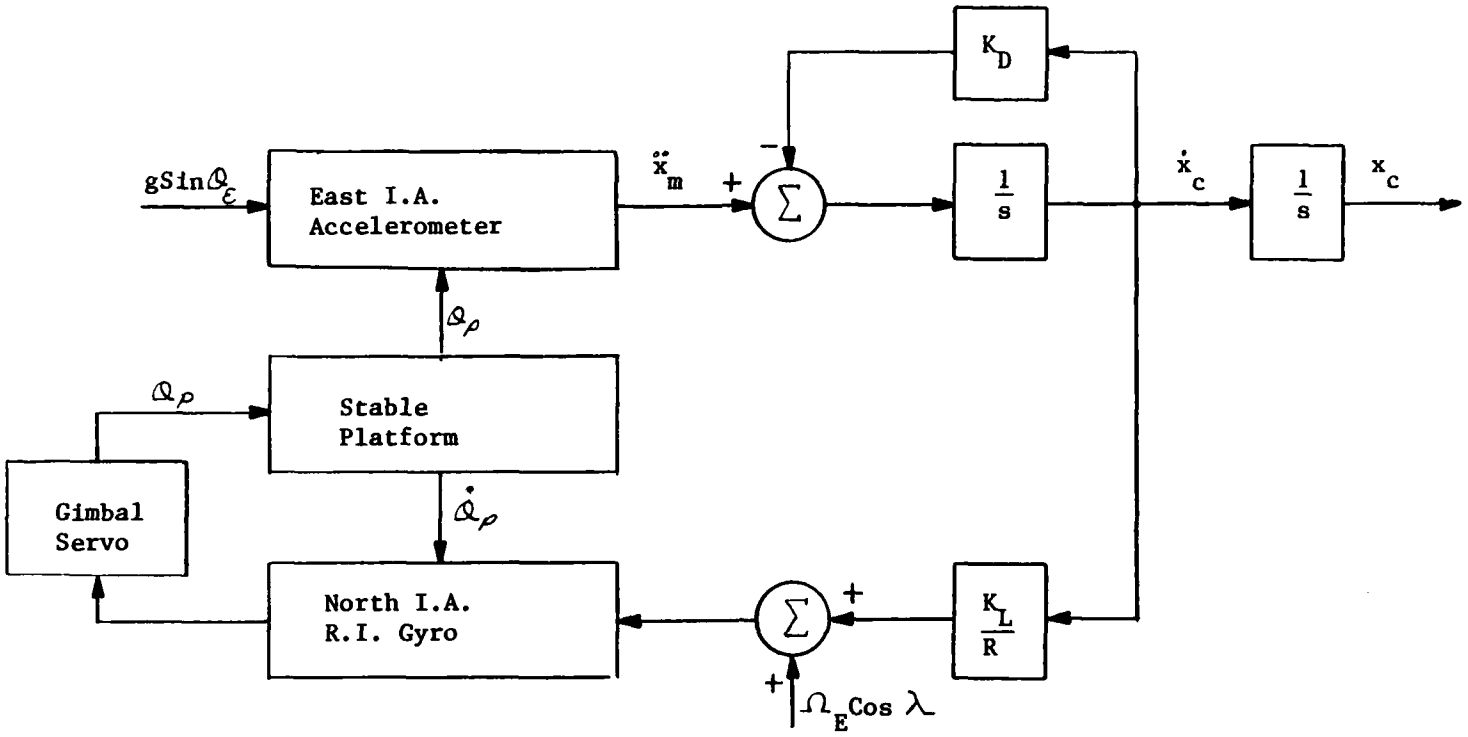

2.37a

g = Acceleration Due to "Gravity"

K_D = Damping Gain

K_L = Platform Leveling Gain

R = Distance From Center of Mass of Earth to Vehicle

$\mathcal{Q}_p$ = Platform Angle About North-South Axis

x = East Position Coordinate of Vehicle

λ = Latitude of Vehicle

Ω_E = Earth Angular Velocity

Figure 2.1.8.1 -- North-South Axis Platform Leveling Loop

Gyrocompassing -- Gyrocompassing is a method of aligning an inertial platform in azimuth by referencing it to the direction of the earth's spin axis. The normal alignment sequence is as follows.

(1) Coarse leveling, to position the platform gimbals at pre-set angles with respect to the aircraft.

(2) Coarse azimuth alignment, to position the platform "north" axis at a pre-set angle, (zero for north-pointing systems), with respect to north as indicated by a magnetic compass.

(3) Fine leveling, to position the platform horizontal axes perpendicular to the earth's gravity vector is described in the preceding section of this text.

(4) Gyrocompassing, to position the platform "north" axis in the plane of the earth's spin axis (for a north-pointing system) or to determine the offset angle of the platform "north" axis with respect to north (for a wander-azimuth system). Fine leveling continues during gyrocompassing. Gyrocompassing and fine leveling can be performed both on the ground and in flight. When performed in flight, the system must have an independent (accurate) measure of ground velocity, as indicated in the following discussion.

The in-flight gyrocompassing configuration for a north-pointing, semi-analytic INS is shown in Figure 2.1.8.2. The gyrocompassing/platform leveling process is as follows.

(1) Due to azimuth misalignment, the east-input-axis gyro senses a component of earth rate.

(2) The resulting gyro output tilts the platform about the east-west axis.

(3) Due to the resulting platform tilt, the north-input-axis accelerometer senses a component of the vertical acceleration due to the force sustaining the vehicle.

(4) The resulting accelerometer output is integrated to produce a false north velocity indication.

(5) The false north velocity is differenced with an independently-determined reference north velocity and the velocity difference signal is used to torque the azimuth gyro in the proper direction to reduce the azimuth misalignment.

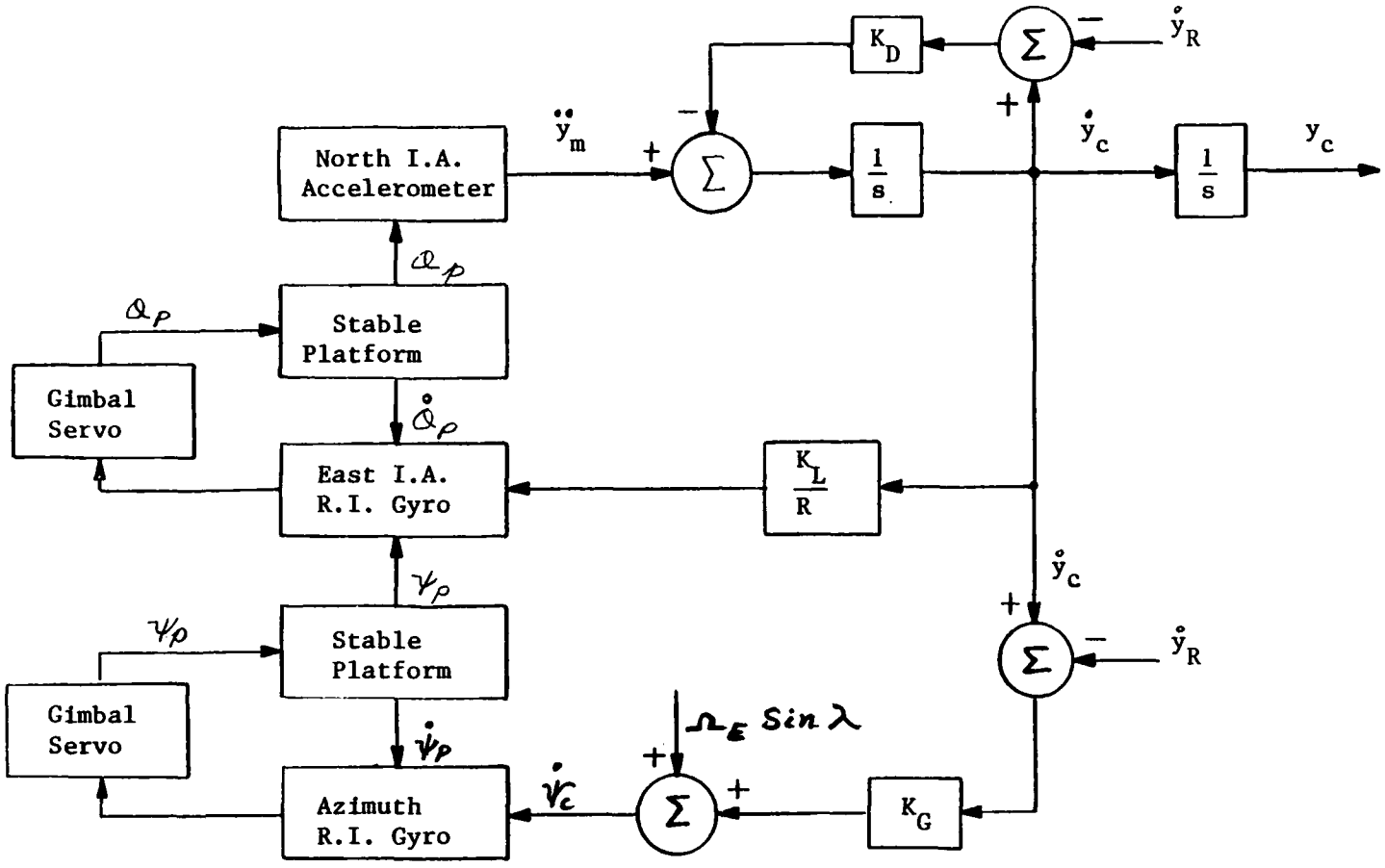

K_D= Damping Gain

K_G= Gyro Compassing Gain

K_L= Leveling Gain

R = Distance From Earth Center of Mass to Vehicle Position

ψ = Platform Azimuth Angle

Ω_E= Earth Angular Velocity

y_R= North Position Coordinate

$\dot{y}_R$= Reference North Velocity

α = Platform Angle About N-Axis

λ = Latitude

Figure 2.1.8.2 -- Gyrocompassing Configuration for a North-Pointing Semi-Analytic INS

(6) The gyrocompassing/leveling process continues until the azimuth misalignment is corrected, the platform is level, the east-input-axis gyro senses no component of earth rate, and the north-input-axis accelerometer senses no component of vertical acceleration.

It should be noted that the gyrocompassing configuration shown in Figure 2.1.8.2 is identical to the navigational mode configurations previously presented, with the exception of the azimuth-gyro-torquing loop containing the gain K_G. The gyrocompassing/leveling process can, in fact, be accomplished while navigating. In the combined navigating/gyrocompassing mode, the gains K_D, K_L, and K_G are reduced (and continuously adjusted) to provide continuing alignment with minimum disturbance to the navigation process. As previously indicated, in-flight gyrocompassing requires an independently-determined north reference velocity.

2.1.9 INS Augmentation -- INS augmentation is the use of independent data sources to improve the performance of an INS. The purposes served by such augmentation are listed below:

Provide Initialization References
Correct Long-Term Gyro Drift
Damp Oscillatory Errors
Stabilize Altitude Computation
Provide In-Flight Updating
Increase Accuracy
Provide Redundancy

The previously-discussed processes of initialization, platform leveling, gyro-compassing, velocity feedback damping, and altitude computation stabilization are all examples of augmentation. The process of in-flight updating consists of correcting position, velocity, or platform alignment errors in accordance with known reference points. The accuracy of navigation can be improved by statistically combining data from two or more redundant navigation systems. In addition, redundant systems provide back-up capability in case of failure.

It should be noted that effective updating of an INS requires the updating of all components of position, velocity, and platform orientation. That is, all of these quantities are cross-coupled by the system. An error in any one quantity propagates into all quantities. For example if, as shown in Figure 2.1.9.1, position error is removed by updating position, without also updating velocity, (the slope of the curve for position), the velocity error will immediately generate position error as indicated in the figure.

The short-term accuracy of an INS generally surpasses that of any other navigation system. The long-term accuracy, however, because of gyro drift effects and other errors that accumulate with time, is inferior to that of some other systems. For that reason, inertial navigation systems are rarely used without some type of augmentation.

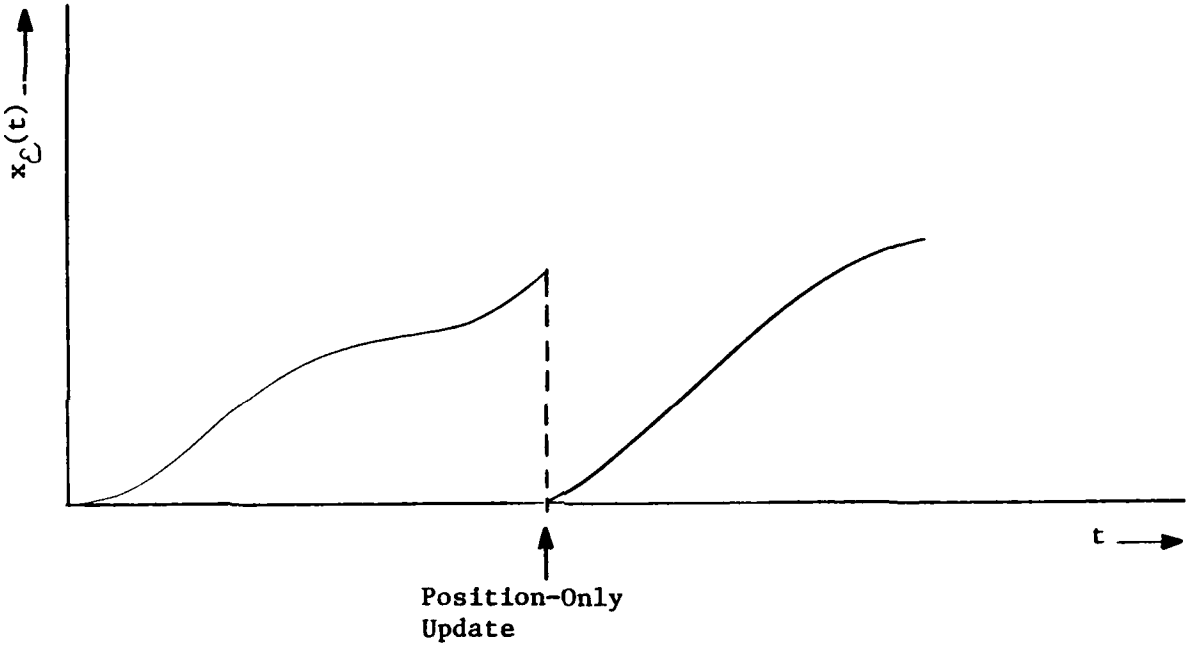

$x_{\mathcal{E}}(t)$= INS Indicated Position Error

Figure 2.1.9.1 -- Effect of Position-Only Update on INS Position Error

2.2 Doppler Radar Navigation Systems

2.2.1 Principles of Operation -- A Doppler radar navigation system, (DNS), is a dead reckoning navigator that determines vehicle ground velocity directly, by measuring the Doppler frequency shift in radar ground returns. In order to resolve the ground velocity into north, east, and vertical components, a DNS requires independent determinations of the direction of north and the direction of the vertical. The north, east, and vertical velocities are then integrated to obtain vehicle position. A block diagram for a Doppler radar navigation system is shown in Figure 2.2.1.1. The Doppler radar utilizes standard techniques for determining the Doppler shift in the ground returns from two or more narrow beams. (A detailed discussion of Doppler radar is included in the text on Radar Systems.) The beams are formed by an antenna array which may be fixed to the aircraft or stabilized with respect to the vertical. If the antennas are stabilized, the vertical reference provides aircraft pitch and roll angle information to the antenna stabilization system. If the antennas are fixed, the vertical reference provides that information to the computer for resolution of the measured velocity into horizontal components. The heading reference provides aircraft heading (and hence antenna array azimuth orientation) information to the computer for resolution of the measured velocity into north and east (or other specified) components. The integrator generates a position indication from an initial position (externally determined) and ground velocity. In addition to geographic position, a Doppler navigator may indicate bearing and distance to a specified target or track angle and cross-track errors with respect to a specified course.

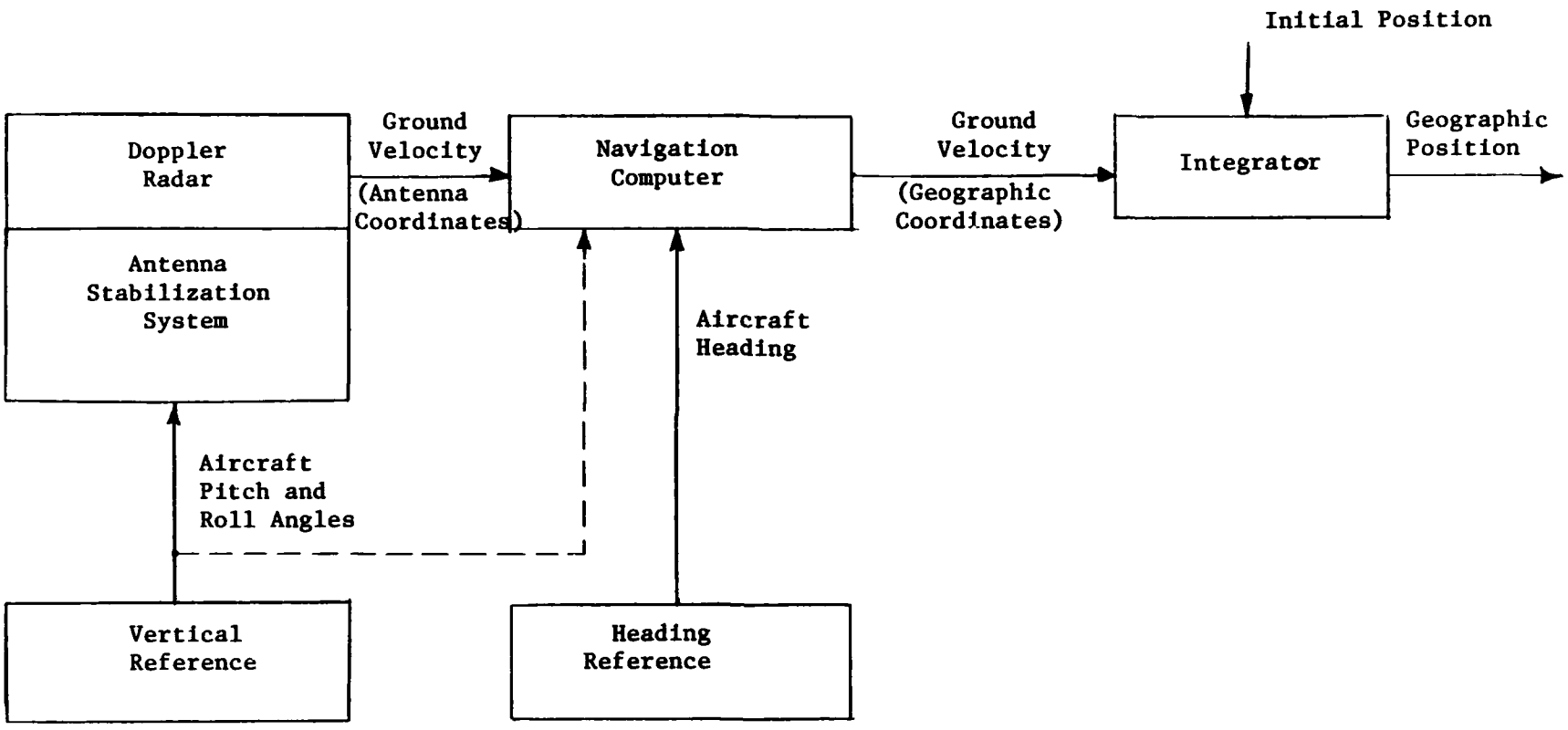

2.41a

Figure 2.2.1.1 -- Block Diagram, Doppler Radar Navigation System

2.2.2 The Doppler Radar Velocity Measurement -- Figure 2.2.2.1 shows the basic geometry involved in the measurement of aircraft ground velocity by means of the Doppler shift in the ground return from a pencil radar beam. (For purposes of illustration only, a single beam is shown, positioned directly ahead of the aircraft.) For the depression angle γ shown, the Doppler shift in the received ground return is given by (see Section 2.11 of the test on Radar Systems):

$$f_d = \frac{2V}{\lambda} \text{ Cos } (\gamma)$$

where:

V = Velocity of Aircraft with respect to Ground

γ = Radar Beam Depression Angle (Angle of Beam with respect to Velocity Vector)

λ = Wavelength of Radar Signal

Because the Doppler shift depends upon depression angle, a beam of finite width results in a spread of return frequencies. The spectrum of a typical ground return is shown in Figure 2.2.2.2. As indicated in the figure, the bandwidth of the ground return, for a beam of width $\Delta\gamma$, is given by:

$$\Delta f_d = \frac{2V}{\lambda} \text{ Sin } (\gamma)\ \Delta\gamma$$

or:

$$\frac{\Delta f_d}{\overline{f_d}} = \text{Tan } (\gamma)\ \Delta\gamma$$

where:

$\overline{f_d}$ = Mean Doppler Shift

Δf_d = Half-Power Return Signal Bandwidth

A typical Doppler navigator beam width is about 4 degrees, giving rise to a typical value of $\frac{\Delta f_d}{\overline{f_d}}$ of about 0.2.

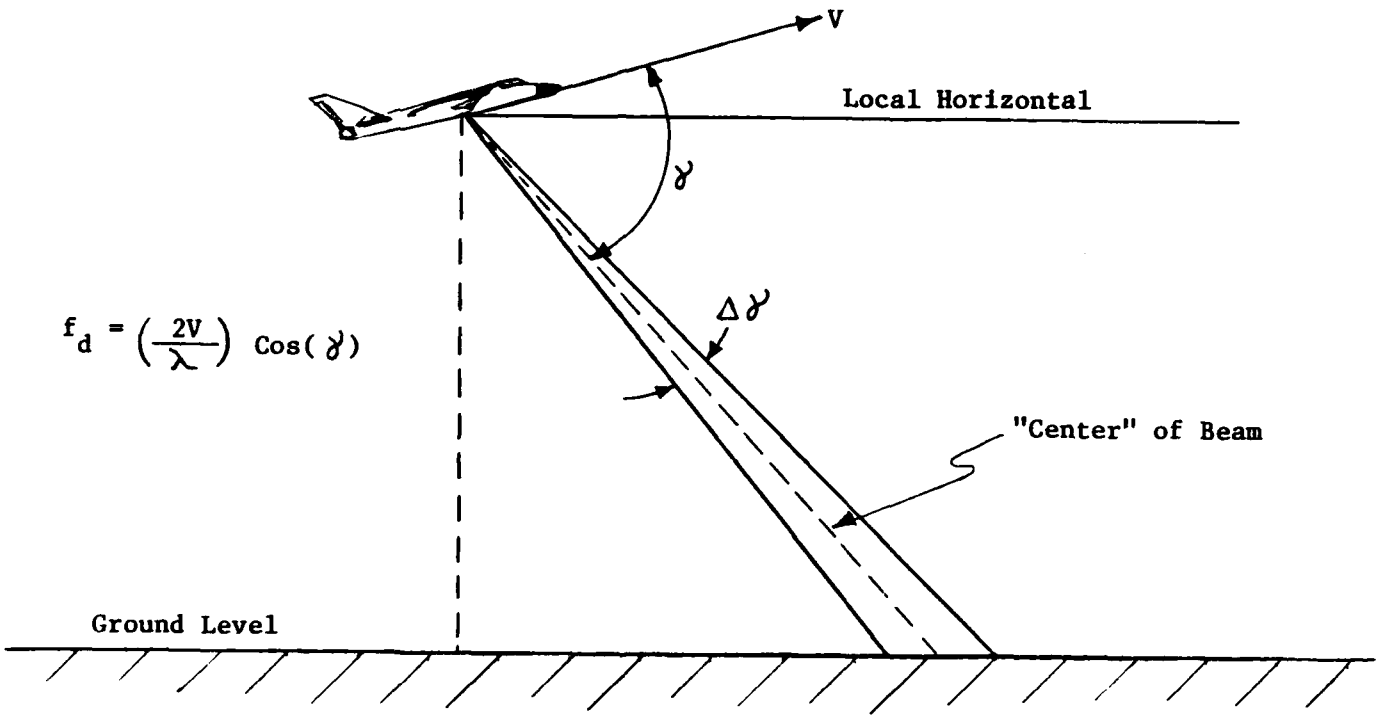

Figure 2.2.2.1 -- Doppler Radar Navigator Beam Geometry

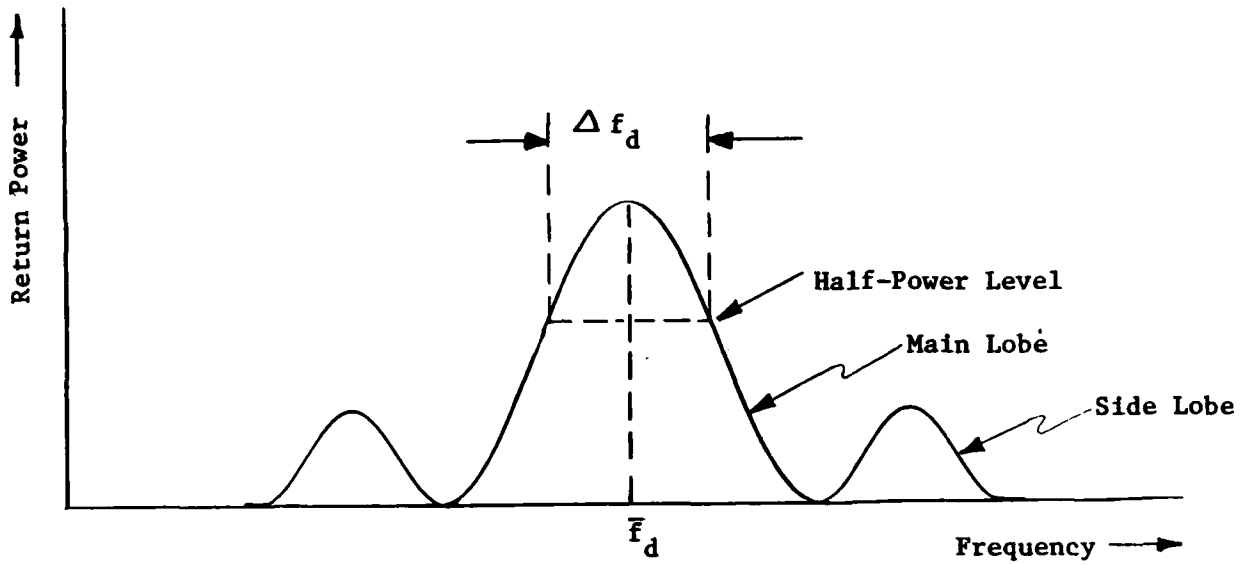

$$\Delta f_d = \left(\frac{2V}{\lambda}\right) \mathrm{Sin}(\gamma)\ \Delta\gamma$$

$$\frac{\Delta f_d}{f_d} = \mathrm{Tan}(\gamma)\ \Delta\gamma$$

Figure 2.2.2.2 -- Spectrum of Doppler Radar Ground Returns

Typical Doppler navigator beam configurations are shown in Figure 2.2.2.3. The two-beam configuration shown in Figure 2.2.2.3(a) requires an independent source of the vertical velocity. The three-beam configurations shown in Figures 2.2.2.3(b) and (c) provide velocities in all three axes. The four-beam configuration shown in Figure 2.2.2.3(d) provides redundancy, which allows consistency checks to verify proper operation. The elongated "footprints" shown in Figure 2.2.2.3(d) yield more return signal without increasing the Doppler bandwidth of the signal. This is accomplished by extending the "footprints" only along the isodops or loci of constant Doppler shift. (The isodops are the lines of intersection between the earth's surface and cones of constant angle, γ, from the velocity vector. As such, they describe hyperbolic curves on the surface of the earth with the axis of symmetry along the ground track as shown in Figure 2.2.2.4.)

(a) Two-Beam Non-Janus

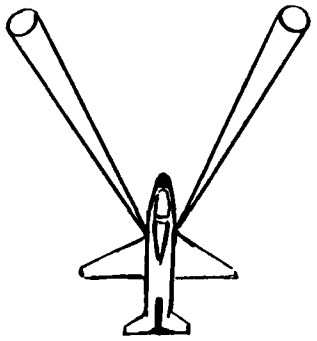

(b) Three-Beam Janus Lambda

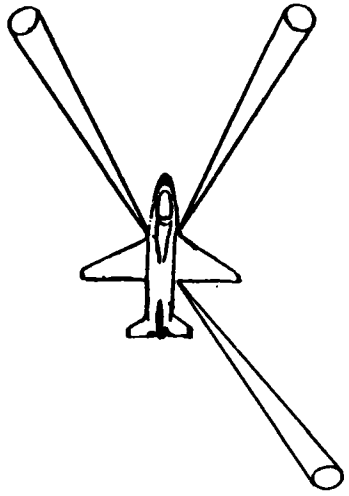

(c) Three-Beam Janus T

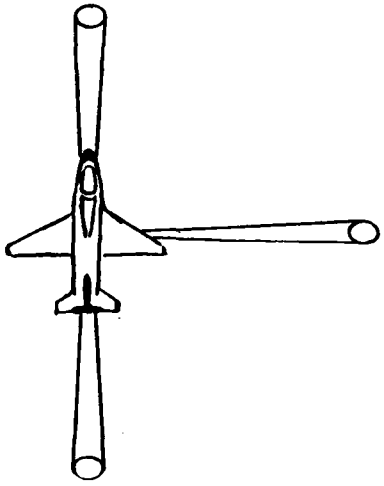

(d) Four-Beam Janus X

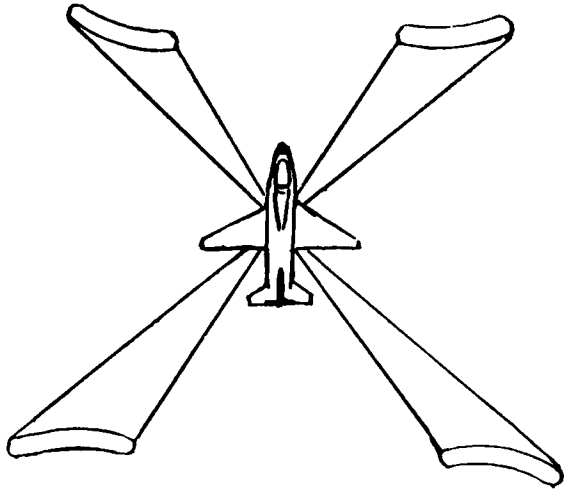

Figure 2.2.2.3 -- Doppler Navigator Beam Configurations

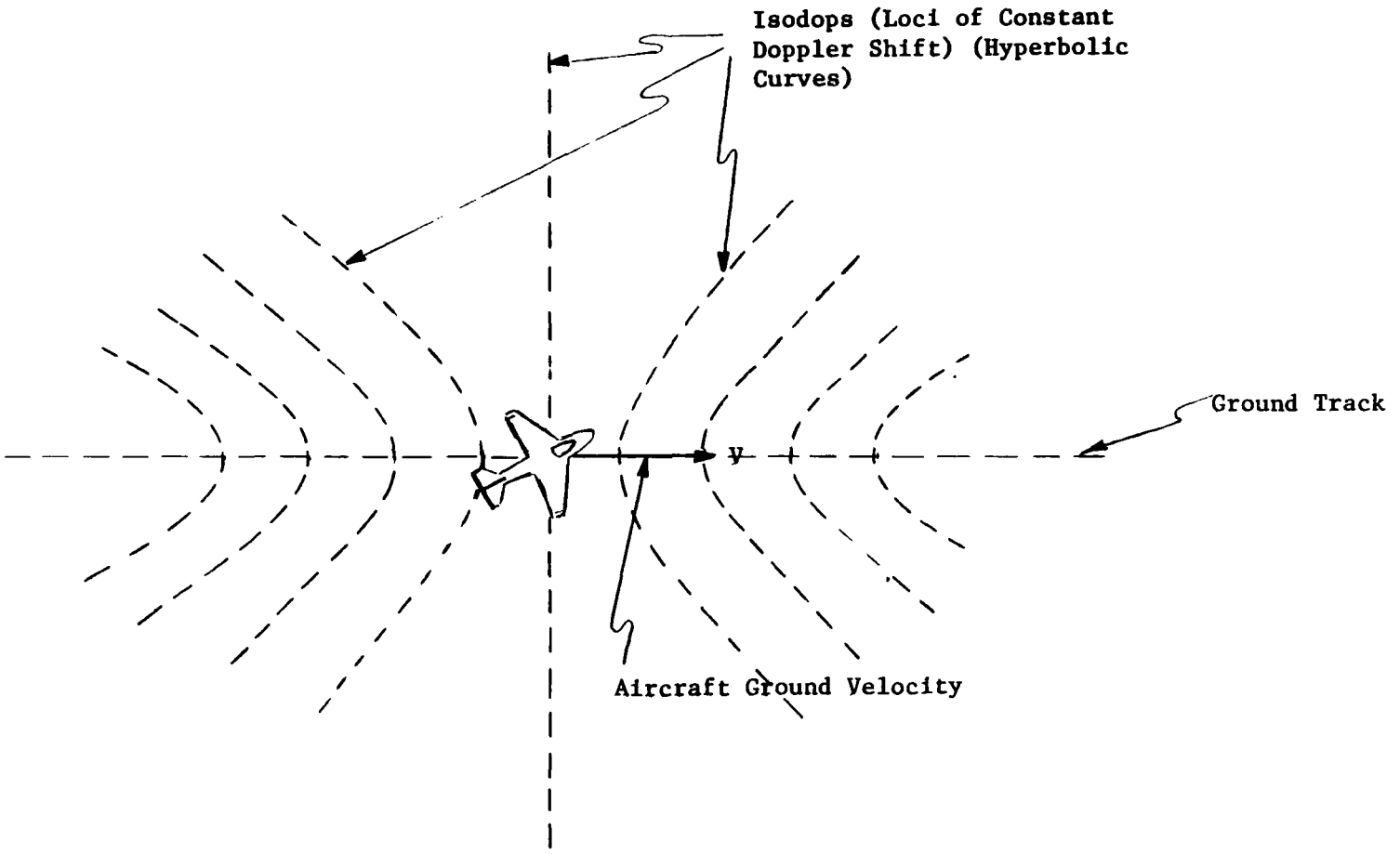

Figure 2.2.2.4 -- Doppler Ground Return Isodops

2.2.3 Antenna Stabilization with respect to the Local Vertical -- As previously indicated, a Doppler navigator requires an independent reference for the local vertical. That information, in the form of aircraft pitch and roll angles, is used either to position (stabilize) the antenna array with its reference axis (centerline) aligned with the vertical or to resolve the measured velocity into horizontal components. In the latter case, the antenna array remains fixed with respect to the airframe. The two cases are illustrated in Figure 2.2.3.1.

In Figure 2.2.3.2 is shown the geometry of a lambda-beam Doppler navigator with a vertically-stabilized antenna array. With such an array, the Doppler measurements are made directly in Ground (horizontal) coordinates and the Doppler frequency shifts are:

$$\bar{f}_{d1} = \frac{2}{\lambda}\left[-V_H \sin\alpha\cos\beta + V_D \sin\alpha\sin\beta + V_V \cos\alpha\right]$$

$$\bar{f}_{d2} = \frac{2}{\lambda}\left[V_H \sin\alpha\cos\beta + V_D \sin\alpha\sin\beta + V_V \cos\alpha\right]$$

$$\bar{f}_{d3} = \frac{2}{\lambda}\left[V_H \sin\alpha\cos\beta - V_D \sin\alpha\sin\beta + V_V \cos\alpha\right]$$

These equations can be solved for the three horizontal components of ground velocity, yielding:

$$V_H = \frac{\lambda\left(\bar{f}_{d2} - \bar{f}_{d1}\right)}{4\sin\alpha\cos\beta}$$

$$V_D = \frac{\lambda\left(\bar{f}_{d2} - \bar{f}_{d3}\right)}{4\sin\alpha\sin\beta}$$

$$V_V = \frac{\lambda\left(\bar{f}_{d1} + \bar{f}_{d3}\right)}{4\cos\alpha}$$

(a) Antenna Array Stabilized with Respect to Vertical

(b) Antenna Array Fixed to Airframe

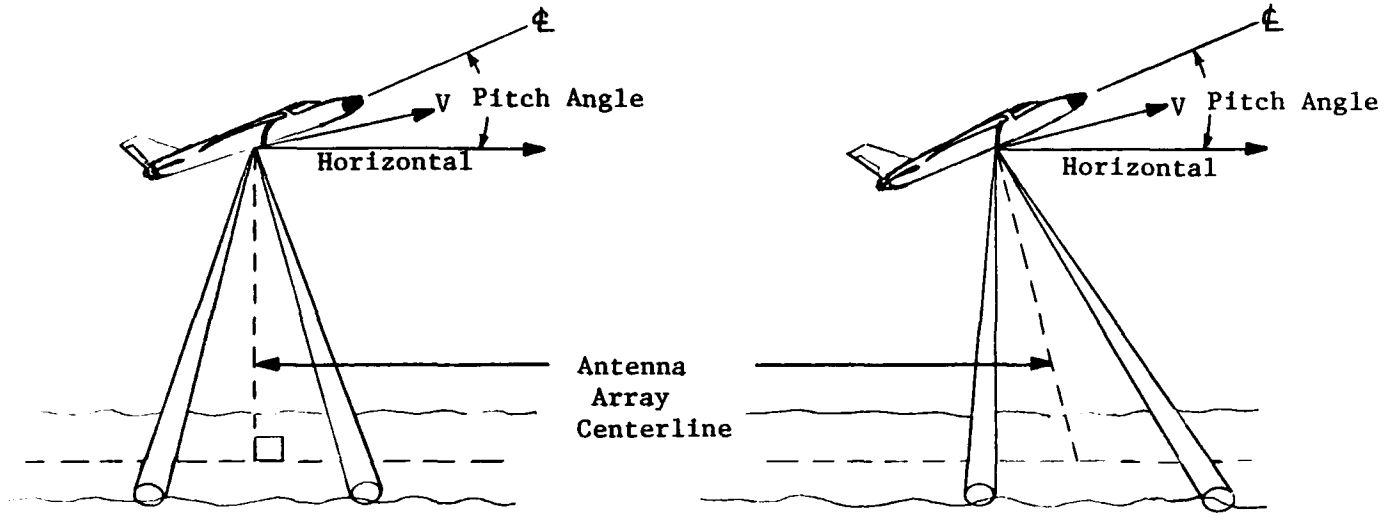

Figure 2.2.3.1 -- Antenna Stabilization with Respect to the Vertical (Pitch Axis Shown)

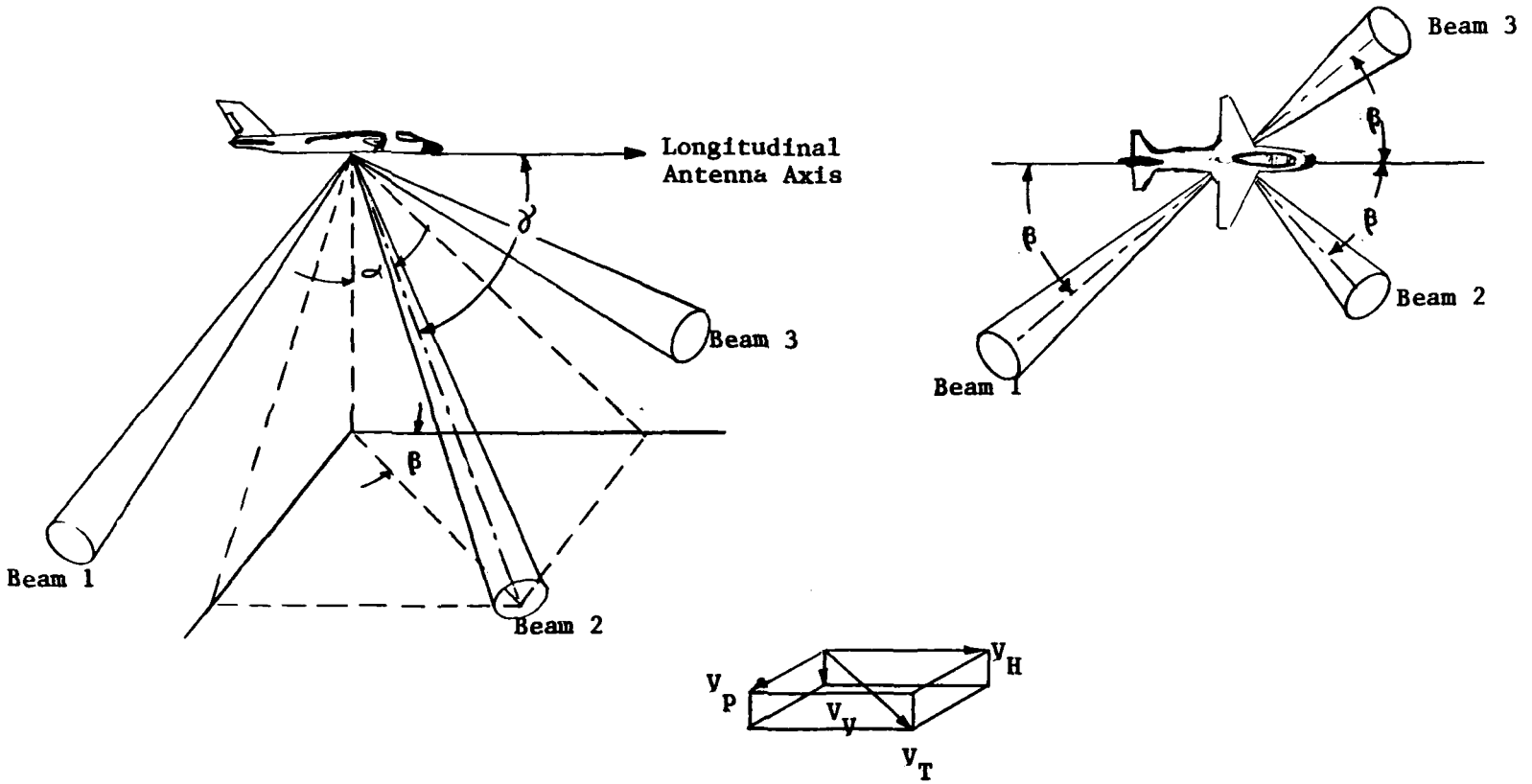

Figure 2.2.3.2 -- Vertically Stabilized Lambda-Beam Doppler Navigator

AD-A130 540 AIRBORNE SYSTEMS COURSE TEXTBOOK: NAVIGATION SYSTEMS TEST AND EVALUATION(U) NAVAL TEST PILOT SCHOOL PATUXENT RIVER MD G W MASTERS 01 SEP 81 2/3

UNCLASSIFIED .F/G 5/9 NL

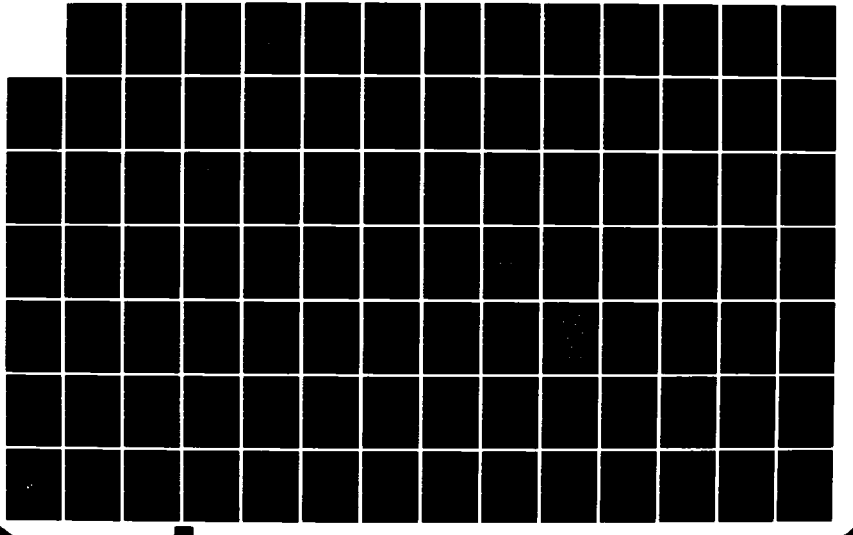

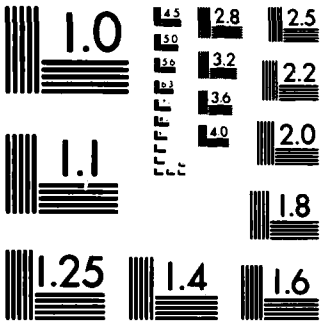

where:

V_H = Horizontal (On-Track) Velocity

V_D = Deflection (Cross-Track) Velocity

V_V = Vertical Velocity

The beam offset angles α and β are defined in the figure and $\bar{f}_{d1}$, $\bar{f}_{d2}$, and $\bar{f}_{d3}$ are the "mean" Doppler shifts in beams 1, 2, and 3, respectively. Thus, the horizontal components of the ground velocity can be determined by summing and differencing the Doppler shifts in the various beams.

If the antenna array is fixed to the airframe, the Doppler measurements are made in a coordinate system fixed to the airframe and must be resolved into horizontal components utilizing the transformation equations:

$$V_H = V_H' \cos\theta + V_D' \sin\theta \sin\phi + V_V' \sin\theta \cos\phi$$

$$V_D = V_D' \cos\theta - V_V' \sin\phi$$

$$V_V = -V_H' \sin\theta + V_D' \cos\theta \sin\phi + V_V' \cos\theta \cos\phi$$

where the primed velocity components are those in the airframe coordinate system, θ is the angle of pitch, and ϕ is the angle of roll.

2.2.4 Antenna Stabilization with respect to the Ground Track -- In addition to being stabilized with respect to the vertical, some Doppler navigator antennas are stabilized with respect to the ground track. That is, they are automatically rotated about a vertical axis until the cross-track Doppler shift is nulled, resulting in the beam orientation shown in Figure 2.2.4.1 (b). Non-track-stabilized antennas are fixed to the airframe and result in the beam orientation shown in part (a) of that figure. For systems with airframe-fixed antennas, the total ground velocity and drift angle are given by:

$$V_{Ground} = \left[V_H^2 + V_D^2 \right]^{1/2}$$

$$\text{Drift Angle} = \text{Tan}^{-1} \left[V_D / V_H \right]$$

For systems with ground-track-stabilized antennas, the ground velocity and drift angle are given by:

$$V_{Ground} = V_H \qquad (V_D = 0)$$

$$\text{Drift Angle} = \text{Antenna Offset Angle}$$

(a) Fixed Antennas

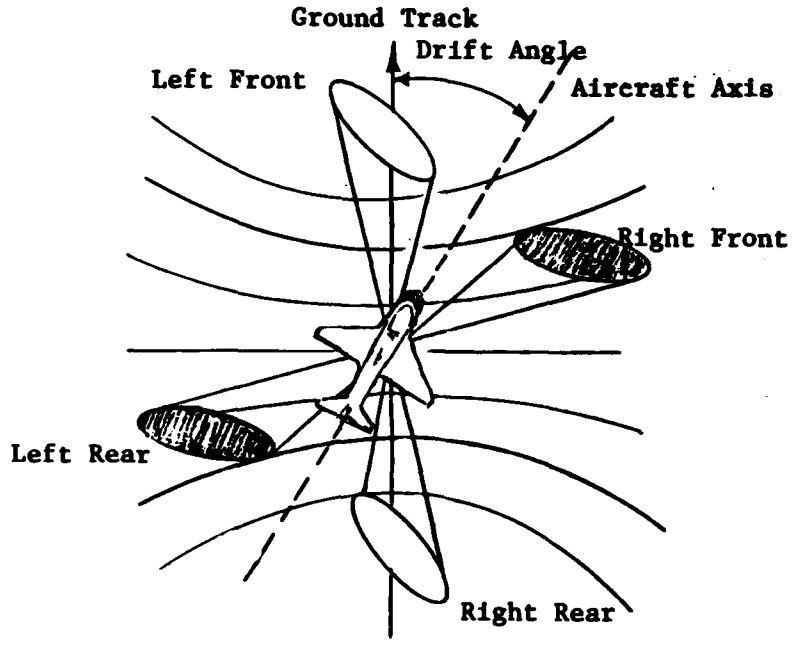

(b) Track - Stabilized Antennas

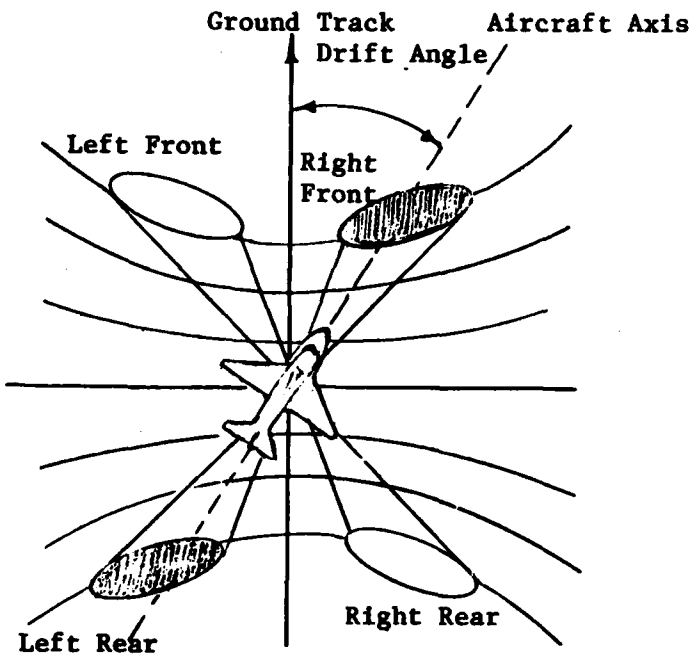

Figure 2.2.4.1 -- Antenna Stabilization with Respect to the Ground Track

2.2.5 Doppler Signal Processing -- As previously indicated, the Doppler frequency shifts exhibited by the Doppler navigator returns cover a relatively wide bandwidth (about twenty percent of the mean Doppler shift). The most difficult operation performed by a Doppler navigator is the recovery, from this broad spectrum, of a single "characteristic" frequency that constitutes a true measure of the ground velocity. The most common approach to the problem is the correlation-tracking loop depicted in Figure 2.2.5.1. The closed-loop arrangement shown in the figure automatically adjusts the frequency of the voltage-controlled oscillator to the value that maximizes the correlation between the broad-band Doppler signal and the single-frequency output of the VCO. The "characteristic" frequency selected by the frequency tracker is not merely the frequency of the largest component of the Doppler signal, but depends, to some extent, upon the characteristics of the correlation detector and the low-pass filter. The operation of the correlation-tracking loop is similar to that of the phase-locked loop described in Section 2.17.9 of the radar text.

Modulation Techniques -- Both pulsed and continuous-wave radars are used in Doppler navigators. Pulsed systems have the advantage of avoiding transmitter-to-receiver leakage as discussed in the text on Radar. Coherent pulse systems also achieve a higher signal-to-noise ratio than do CW systems. (Signal-to-nosie ratio can be a problem at large altitudes and over water or certain terrain.) However, the pulse systems have a serious disadvantage in that they are subject to eclipsing, (as discussed in Section 2.3.8 of the radar text), giving rise to "blind ranges" called "altitude holes". In a Doppler navigator the effect of eclipsing is especially serious. In addition to loss of signal, eclipsing in a Doppler navigator causes a shift in the calibration of the system. As previously

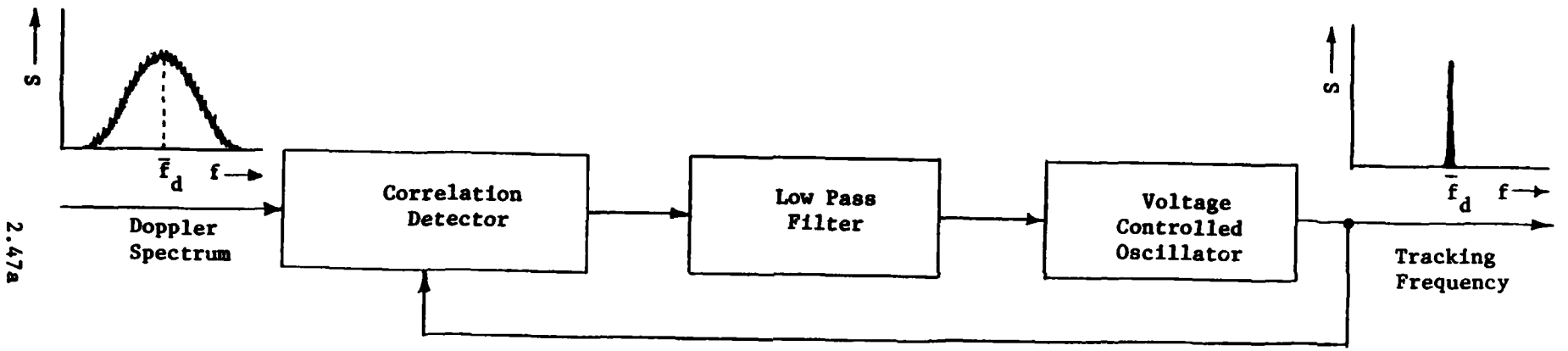

Figure 2.2.5.1 -- Doppler Frequency Tracking Loop

indicated, the Doppler shift is a function of the depression angle γ. Thus, as indicated in Figure 2.2.5.2, the returns from the front of the beam exhibit a greater Doppler shift than do those from the rear of the beam. In addition, the returns from the front of the beam travel a longer distance and, therefore, do not arrive back at the receiving antenna at the same time as do the returns from the rear of the beam. Thus, if eclipsing occurs such that the latter portion of a return pulse (from the front of the beam) is deleted, the high-frequency portion of the Doppler return spectrum is attenuated, thereby shifting the "mean" frequency of the Doppler spectrum to a lower value and altering the system calibration. Eclipsing of the early portion of a return pulse shifts the "mean" Doppler frequency to a higher value. As discussed in the text on radar systems, eclipsing can be alleviated by employing a time-varying pulse repetition frequency (PRF) or by varying the PRF as a function of range (altitude). The effect of eclipsing on Doppler system calibration also can be minimized by shaping the beam as shown in Figure 2.2.2.3(d), or by beam switching as described in Section 2.2.6 of this text.

Continuous wave systems avoid eclipsing (altitude hole) effects and, therefore, function well down to zero altitude. The major problem associated with CW systems is transmitter-to-receiver "leakage". Most CW Doppler navigators solve the leakage problem by frequency modulating the transmitted signal. The FM-CW signal then allows the receiver to distinguish between leakage (undelayed signals) and ground returns (delayed signals). (See Section 2.11.3 of the radar text for a discussion of FW-CW radar.)

Both coherent and non-coherent signal processing are employed in Doppler navigators. The block diagram of a coherent Doppler signal processor is shown in Figure 2.2.5.3.

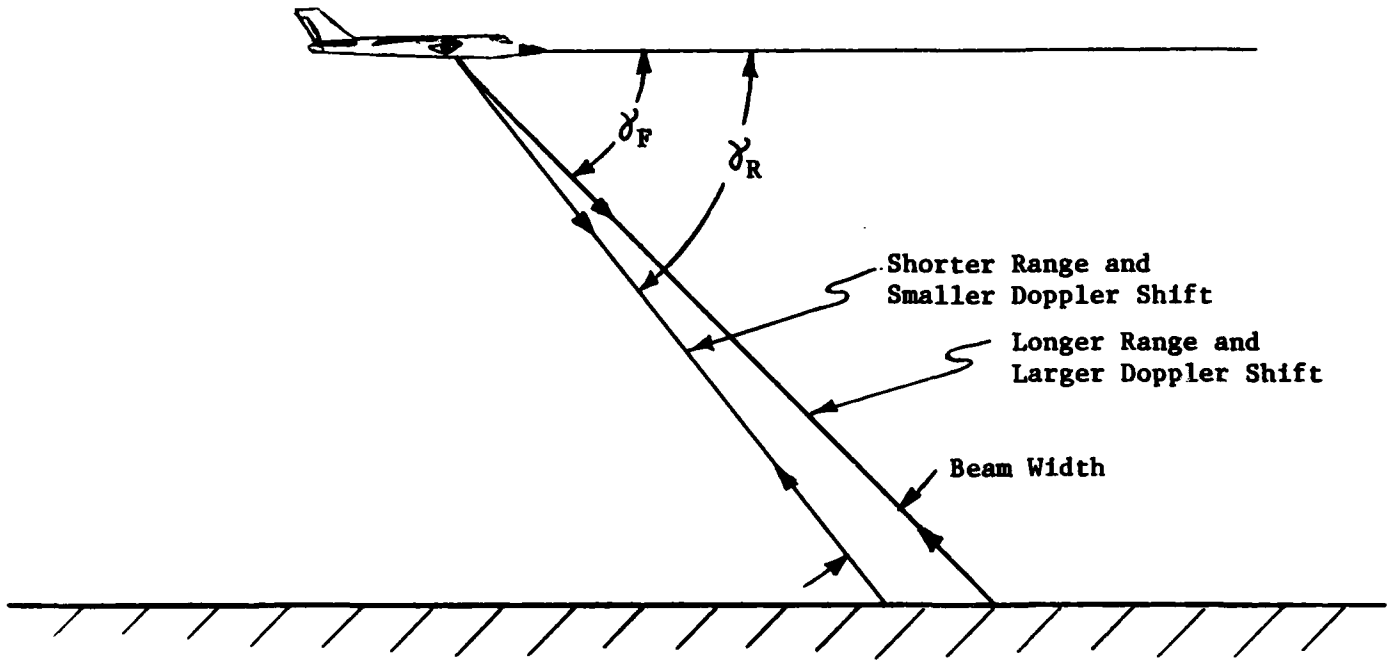

Figure 2.2.5.2 -- Effect of Beam Width on Range and Doppler Shift

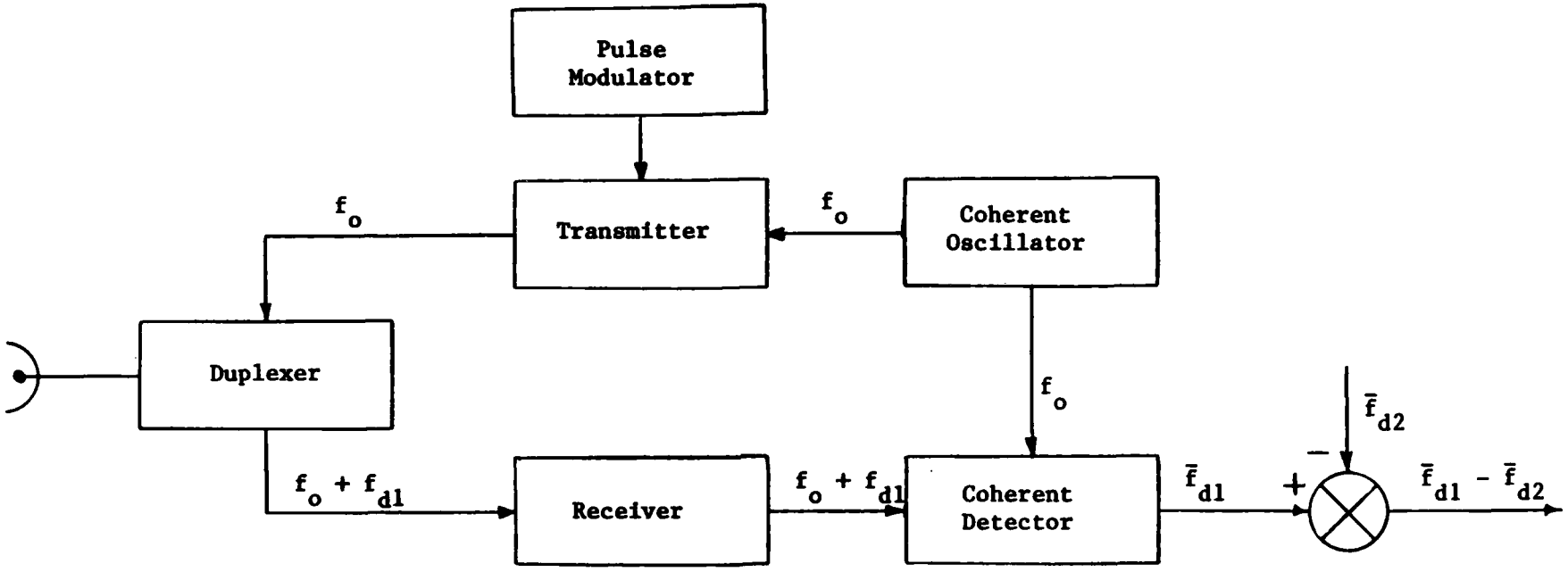

Figure 2.2.5.3 -- Coherent Doppler Signal Processing

The Doppler shift of the return from each beam is determined by comparing its frequency with that of an internal, coherent oscillator. The difference in frequency shifts between two beams is then obtained by differencing the individual beam Doppler shifts as indicated in the Figure. (See Section 2.16.3 of the radar text for a discussion of coherent radar signal processing.) The block diagram for a non-coherent Doppler signal processor is shown in Figure 2.2.5.4. The difference in the Doppler shifts of the returns from pairs of beams is determined by comparing the Doppler-shifted returns with each other. The "beat frequency" created by mixing the returns from two beams is equal to the difference in Doppler shifts as shown. (See Section 2.16.8 of the radar text for a discussion of non-coherent radar signal processing.) The non-coherent Doppler navigator cannot determine vertical velocity or the sign of horizontal velocity. Its principal advantage is simplicity and low cost.

The relative advantages and disadvantages of the four principal types of Doppler navigator signal processing and modulation are presented in the table of Figure 2.2.5.5.

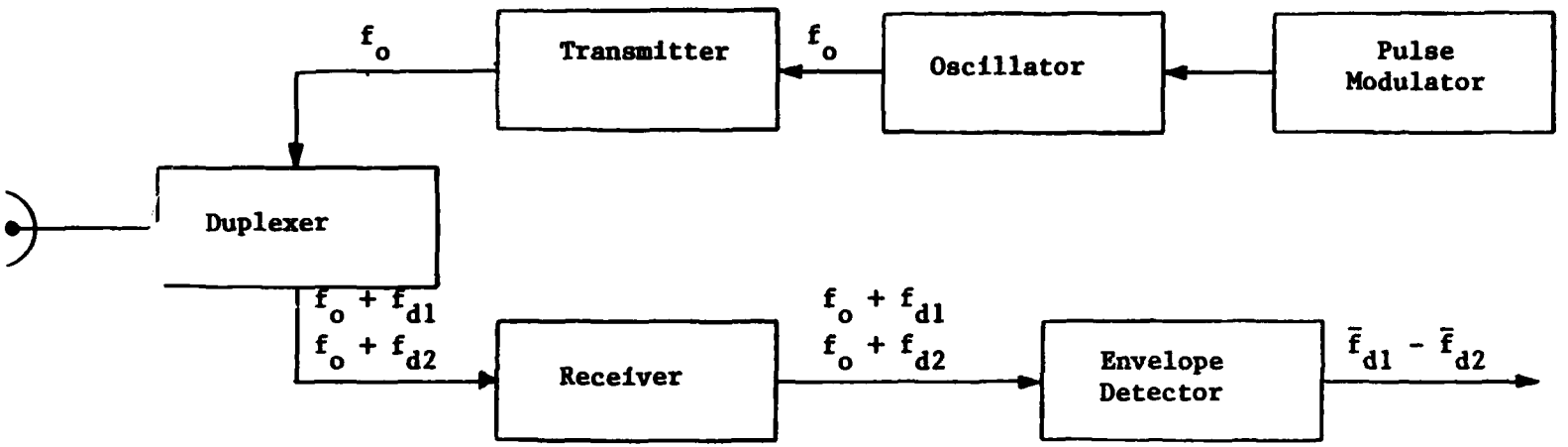

Figure 2.2.5.4 -- Non-Coherent Doppler Signal Processing

Modulation ⟶	CW (Coherent)	FM · CW	Coherent Pulse	Non-Coherent Pulse
Vertical Velocity	Yes	Yes	Yes	No
Velocity Sign	Yes	Yes	Yes	No
Transmitter-to-Receiver Isolation	Poor	Good	Very Good	Very Good
Signal Processing Efficiency	Good	Good	Very Good	Poor
Low-Altitude Performance	Very Good	Good	Poor*	Poor*
High-Altitude Performance	Poor	Poor*	Very Good	Good
System Complexity	No	Yes	Yes	No

*Without special signal processing.

Figure 2.2.5.5 -- Effect of Modulation Techniques on Doppler Navigator Characteristics

2.2.6 Over-Water Operation -- The functioning of a Doppler navigator is affected in several ways by over-water operation. One effect is reduction of signal due to specular reflection. As a result of this loss of signal, a Doppler navigator often will go into "memory" operation. That is, it will switch to a back-up mode in which low-signal measurements of "ground" velocity are rejected and the system dead-reckons using the last reliable value for velocity. Another effect of over-water operation is a shift in system calibration. Also primarily as a result of specular reflection, the back-scattering coefficient for a radar beam reflected from a smooth water surface is a strong function of the angle of incidence of the beam, as shown in Figure 2.2.6.1. As indicated in the figure, the slope of the curve (dependence on angle of incidence) increases as the sea state number decreases. (The sea state numbers indicated in the figures are Douglas sea-state designations, which increase as wave height increases. A sea state of 1 corresponds to a wave height less than one foot. A sea state of 4 corresponds to a wave height between five and eight feet.) As a result of the dependence of reflection coefficient on angle of incidence, the strength of the return from a Doppler navigator beam is a strong function of the beam depression angle, γ, depicted in Figure 2.2.2.1. As previously noted, the Doppler shift also is a strong function of beam depression angle. The joint dependence, on depression angle, of signal return strength and Doppler shift results in a significant attenuation of the high-frequency portion of the Doppler return spectrum, as illustrated in Figure 2.2.6.2. The resulting change in the mean Doppler shift, $\overline{f}_d$, produces a corresponding change in the calibration of the system, as shown in Figure 2.2.6.3.

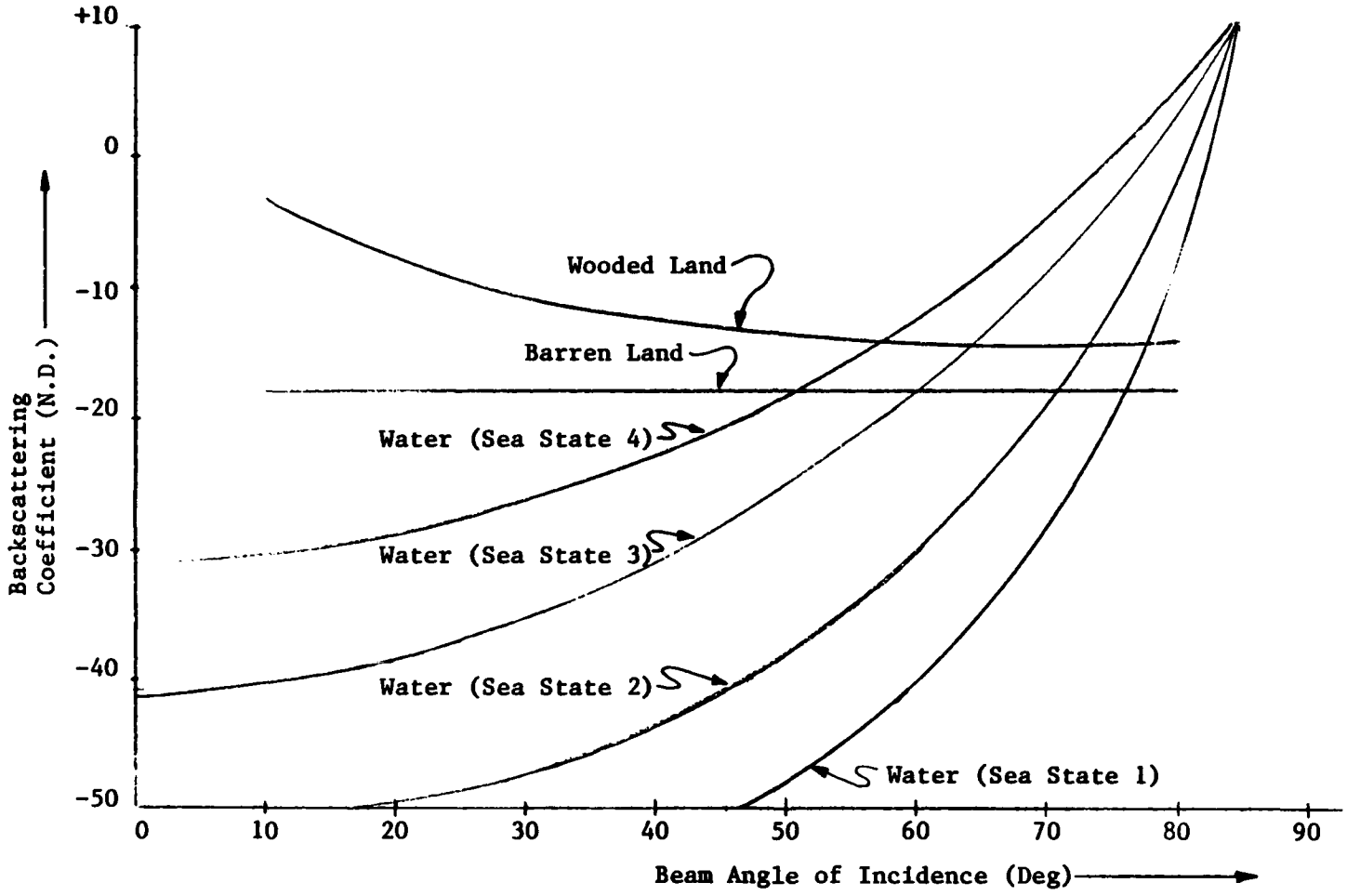

Figure 2.2.6.1 -- Over-Water Radar Backscattering Coefficient as a Function of Beam Angle of Incidence

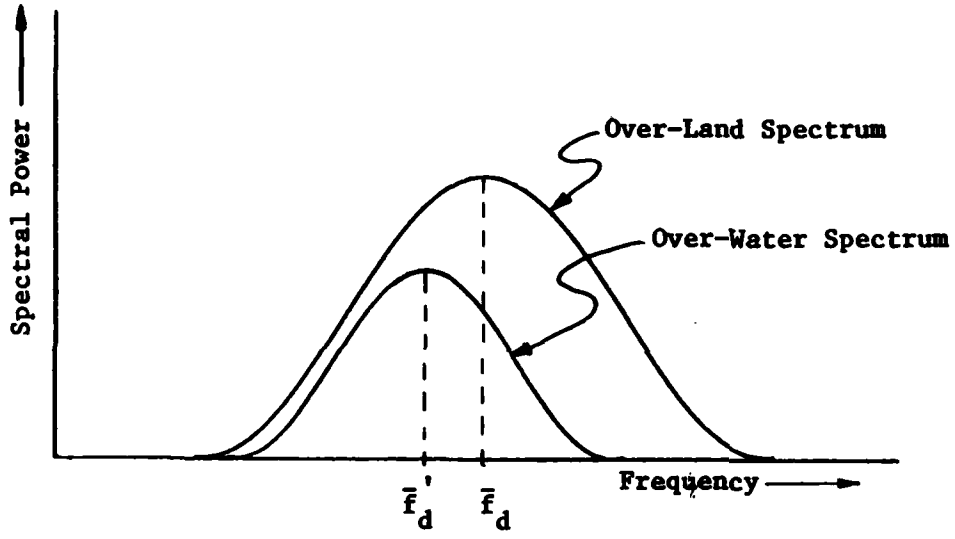

$\bar{f}_d$ = Mean Doppler Shift Over Land

$\bar{f}_d'$ = Mean Doppler Shift Over Smooth Water

Figure 2.2.6.2 -- Effect of Over-Water Operation on Spectrum of Doppler Returns

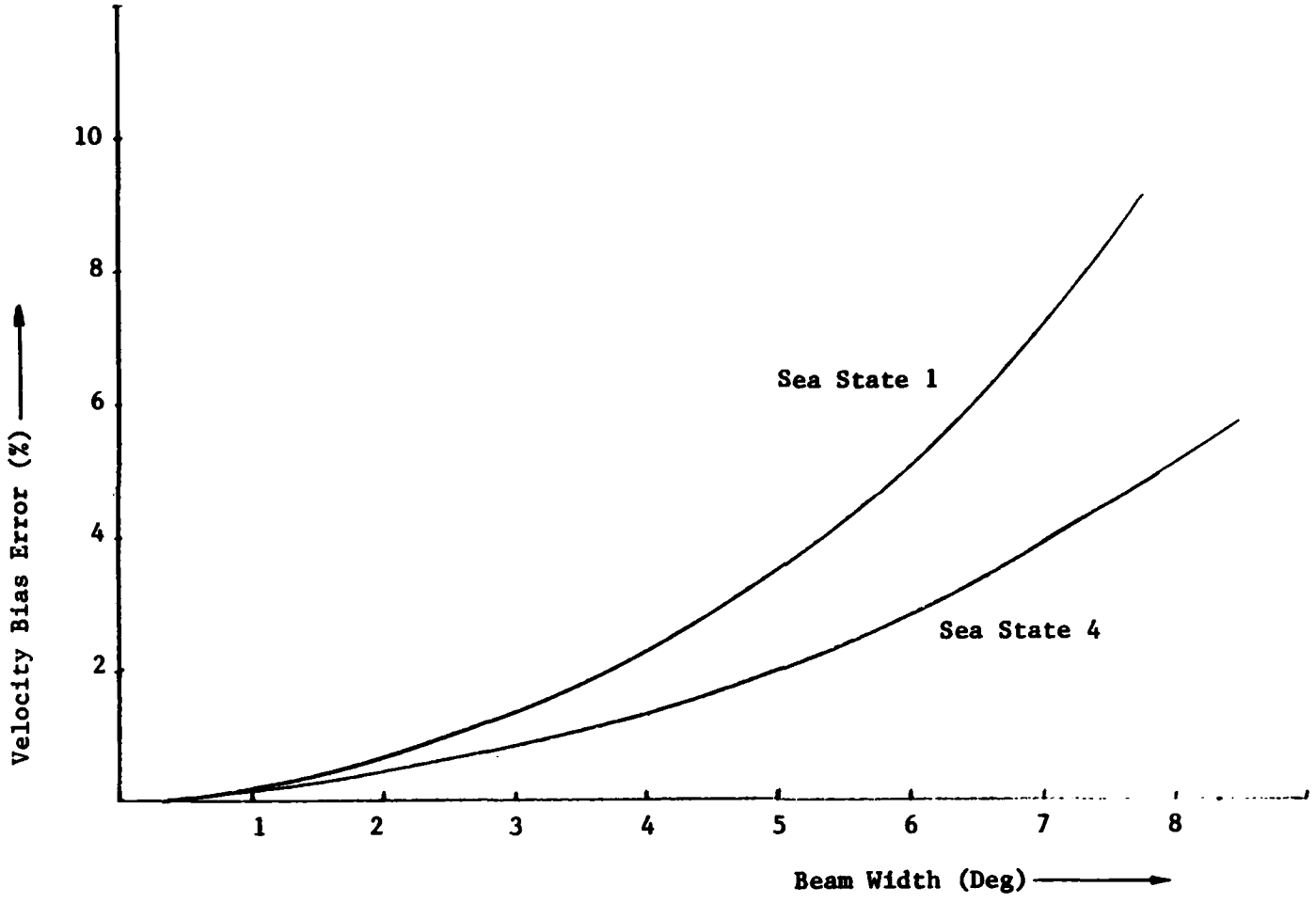

Figure 2.2.6.3 -- Doppler Velocity Bias Error as a Function of Sea State and Beam Width

The signal level and velocity bias effects associated with over-water navigation are major contributors to velocity (and position) errors in Doppler systems. (Similar effects occur over terrain covered by ice, snow, and certain types of vegetation.) Four principal methods are employed to alleviate these effects: switching to back-up (memory) mode, insertion of fixed-value velocity bias, beam shaping, and beam switching. Switching to "memory" mode, previously discussed in this section, avoids the problem by discontinuing Doppler measurements for the duration of the condition, thereby severely degrading the accuracy of the system. Many current systems correct the over-water velocity bias error by introducing a fixed-value, "average" velocity bias into the velocity computation during over-water operation. Since the actual error varies with existing conditions, fixed-bias correction can be significantly in error. Beam shaping, as depicted in Figure 2.2.2.3, narrows the spectrum of the Doppler returns, thereby decreasing the possible error due to attenuation of high frequencies. Beam shaping is often employed in conjunction with one of the other methods of velocity bias correction. The most effective (and also most complex) method of velocity-bias correction is beam switching, as depicted in Figure 2.2.6.4. With this method, the depression angle (and hence angle of incidence) of the beam is alternately switched between two positions as shown in the figure. The two beam positions (two values of depression angle) produce two overlapping return spectra as shown in part (b) of the figure. The system determines the cross-over (equal-power) frequency and uses it to compute velocity. Since the cross-over frequency varies with reflection coefficient much less than does the mean frequency of a single spectrum, beam switching greatly reduces over-water velocity bias error. Beam switching also reduces the altitude-hole error discussed in Section 2.2.5 of this text. A major advantage of the beam-switching technique is the fact that

(a) Doppler Beam Footprints

(b) Doppler Return Spectrum

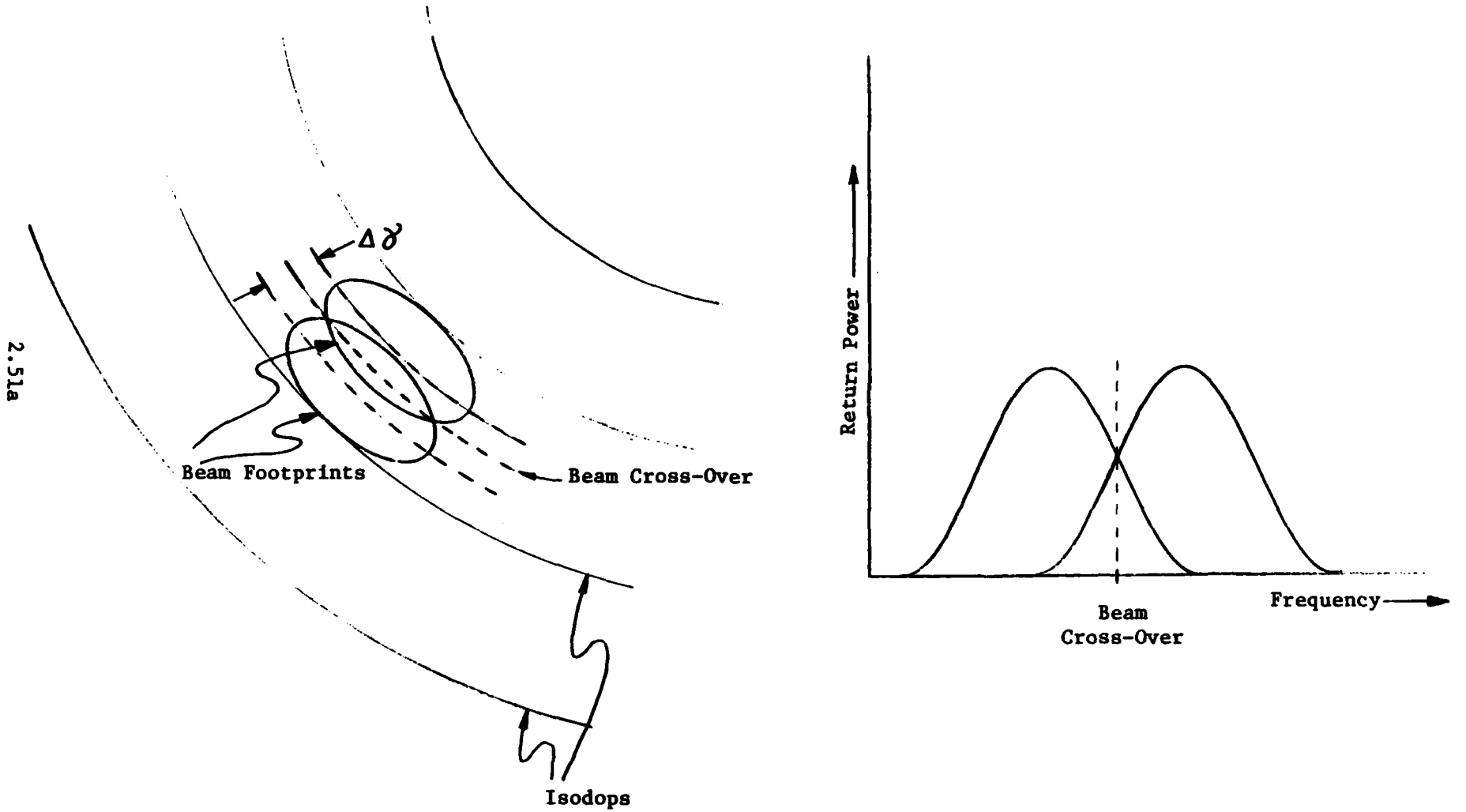

2.51a

Figure 2.2.6.4 -- Doppler Navigator Beam Switching

it automatically reduces velocity errors without human intervention, and for all operating conditions .

In addition to loss of signal and Doppler calibration shift, two other over-water effects are significant. The first effect is velocity error due to flowing water. The "ground" returns of a Doppler system operating over a moving body of water will be shifted by an amount equal to the "ground velocity" of the moving water. The second effect is velocity error due to wind-blown water droplets and to surface motion of the water due to winds. Both of these effects can be significant and, for correction, require a knowledge of surface conditions. Some systems have provision for a correction based upon surface wind velocity. It should be noted that wave motion, per se, does not produce velocity error since, in pure wave motion, the body of water is not in sustained forward motion, but merely oscillates up and down, (and slightly back and forth), with no net movement.

2.2.7 Doppler Navigator Relative Advantages and Disadvantages

The principal advantages of a Doppler navigator, with respect to other navigation systems, are:

(1) Autonomous Operation -- A DNS is not dependent upon external communications as are, for example, radio navigation systems.

(2) Direct Measurement of Ground Velocity -- For a terrestrial navigator, motion in an earth-fixed coordinate system is required. By sensing ground velocity directly, a DNS avoids the wind corrections (and errors) involved with an air-data system, and the cumulative velocity errors produced by the integration of acceleration in an INS.

(3) World-Wide Operation -- A DNS is not subject to the "singular points" exhibited by an INS and it is not affected by the geographic location of ground stations as are radio navigation systems. Except for problems associated with operating over water and mountainous terrain it is unrestricted by geography.

(4) All-Weather Operation -- Since it does not depend upon long-range communication links, a DNS is almost unaffected by weather and atmospherics. Only in heavy, wind-driven rain is its operation seriously degraded.

(5) Continuous Velocity and Position Indications -- Except for periods of violent maneuvering and some over-water operation, a DNS provides continuous, updated position and velocity information.

(6) A DNS requires no pre-flight alignment or velocity initialization.

The principal disadvantages of a Doppler navigator, with respect to other navigation systems, are:

(1) Independent Heading Reference Requirement -- In order to resolve the measured ground velocity into the desired ground coordinate system, a DNS requires an independent heading reference. Commonly employed references are a magnetic compass or an inertial platform.

(2) Independent Vertical Reference Requirement -- In order to resolve the measured ground velocity into the desired horizontal components, a DNS requires an independent vertical reference. A commonly employed reference is a simple mercury-filled leveling switch.

(3) Degraded Operation Over Water -- A DNS encounters two major problems in over-water operation -- a loss of signal and a shift in calibration. The problems associated with over-water operation are discussed in Section 2.2.6 of this text.

(4) Degraded Operation during Aircraft Maneuvering -- In order to prevent inaccurate measurements, limits are placed on DNS operation beyond specified aircraft pitch and roll angles. When these limits are exceeded, the velocity measurement is "frozen" (the system "goes into memory") for the duration of that condition.

(5) Position Initialization Requirement -- As do all dead reckoning navigation systems, a DNS requires initialization in position.

(6) Unbounded (Cumulative) Position Error -- As a result of the time integration of velocity, a DRS exhibits errors that increase (accumulate) with distance traveled (or time).

(7) External Radiation -- Unlike most other airborne navigation systems, a Doppler navigator generates external radiation, thereby disclosing its presence.

2.3 Radio Navigation Systems

2.3.1 General Radio Navigation Principles -- Radio navigation is the practice of determining position by means of externally-generated radio-frequency electromagnetic waves. All radio navigation systems function by determining time-of-arrival, direction-of-arrival, or received frequency of those waves. User position is thereby determined relative to the transmitting stations. Except for rendezvous applications, the position of the transmitters must be known.

A radio navigation system is a "communications" system as defined in the text on communications systems. Therefore, the reader is referred to that text for a detailed discussion of communications theory.

The two principal factors affecting the performance of a radio navigation system are electromagnetic wave propagation effects and externally-generated noise. The wave propagation effects affect performance in three major ways: signal attenuation, multi-path, and variation in the velocity of propagation. As discussed in the text on communications, signal attenuation increases with increasing carrier frequency while external noise increases with decreasing carrier frequency, with no frequency range free of both limitations. Multi-path produces anomalous determinations of signal time - and direction-of-arrival. Variation of propagation velocity produces errors in the time-to-distance conversion unless the propagation velocity is continuously determined. (See Section 2.4.3 of the text on communications systems for a more detailed discussion of the effects of wave propagation and noise.) A significant factor in the generation of radio navigation

errors is geometric dilution of precision (GDOP). GDOP is a function of the angle at which lines-of-position (LOP) intersect and is determined by the geometry of the transmitter and receiver relative locations. (An LOP crossing at right angles yields the most accurate positional "fix.")

The radio navigation systems listed below will be described in the following paragraphs. (Satellite navigation systems are described in Section 2.4 of this text.)

Instrument Low-Approach System (ILS)
Ground-Controlled Approach (GCA)
Microwave Landing System (MLS)
Airborne Direction Finder (ADF)
Distance Measuring Equipment (DME)
VHF Omnidirectional Range (VOR)
Tactical Air Navigation (TACAN)
Long-Range Navigation (LORAN)
Omega

2.3.2 Landing Approach Systems -- The International Civil Aviation Organization (ICAO) designated several categories of instrument-controlled landing conditions as follows:

Category I -- 200 foot "ceiling" and 2600 foot visibility. The pilot must have visual contact with the runway at or above a 200 foot altitude.

Category II -- 100 foot "ceiling" and 1200 foot visibility. The pilot must have visual contact with the runway at or above a 100 foot altitude.

Category IIIA -- 50 foot "ceiling" and 700 foot visibility. Pilot must be able to "see to land".

Category IIIB -- 35 foot "ceiling" and 150 foot visibility. Pilot must be able to "see to taxi".

Category IIIC -- Zero "ceiling" and zero visibility.

In order to control an aircraft landing approach, aircraft position information is required with respect to the runway centerline, the optimum glide slope, and the runway threshold. In order to provide these measurements, three basic types of landing system are currently employed: the instrument low-approach system, the ground controlled approach system, and the microwave landing system. These three systems are described in the following paragraphs.

Instrument Low-Approach System -- The instrument low approach system (ILS) utilizes specially-shaped antenna patterns to "mark a pathway in the sky". The antenna patterns employed are shown in Figure 2.3.2.1. The "localizer" pattern shown in Figure 2.3.2.1(a) provides a signal proportional to lateral angular offset from the runway centerline, out to about plus or minus 4 degrees. A 90 hertz-modulated signal is provided to the left of the centerline, a 150 hertz-modulated signal to the right. The localizer signal carrier frequency is between 108.1 and 111.9 megahertz. The "glide-slope" pattern shown in Figure 2.3.2.1(b) provides a signal proportional to vertical angular offset from the optimum glide slope, out to about plus or minus 0.6 degrees (for a 3-degree optimum glide slope). A 90 hertz-modulated signal is provided above the optimum glide slope, a 150 hertz-modulated signal below. The glide slope carrier frequency is between 329.3 and 335.0 megahertz. The "range marker" pattern shown in Figure 2.3.2.1(c) provides marker signals at discrete aircraft-to-runway threshold distances of about 30,000 feet, 3500 feet (200 foot altitude), and 1000 feet (100 foot altitude). The outer marker is modulated at 400 hertz, the middle marker at 1300 hertz, and the inner marker at 3000 hertz. The middle and inner markers are positioned so as to designate the ICAO Category I and Category II ILS decision heights. The range marker signal carrier frequency is 75 megahertz.

The localizer and glide-slope signals are received by the airborne equipment and are used to position two "crossed" needles in such a way as to indicate the appropriate flight path corrections. Radio wave propagation is by space wave and provides for signal acquisition out to a range of about 15 miles.

(a) Localizer Pattern

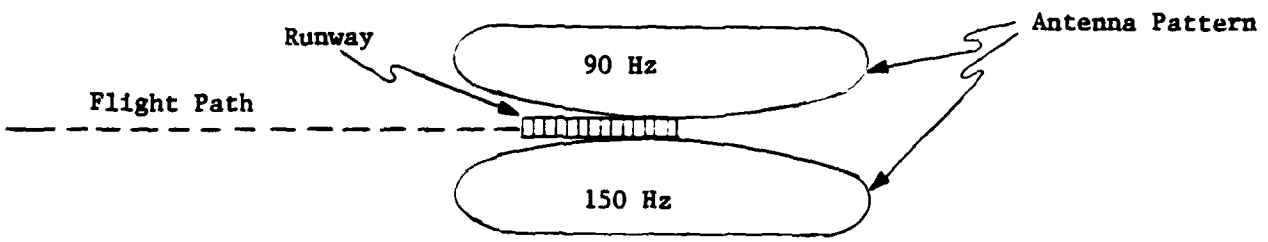

(b) Glide Slope Pattern

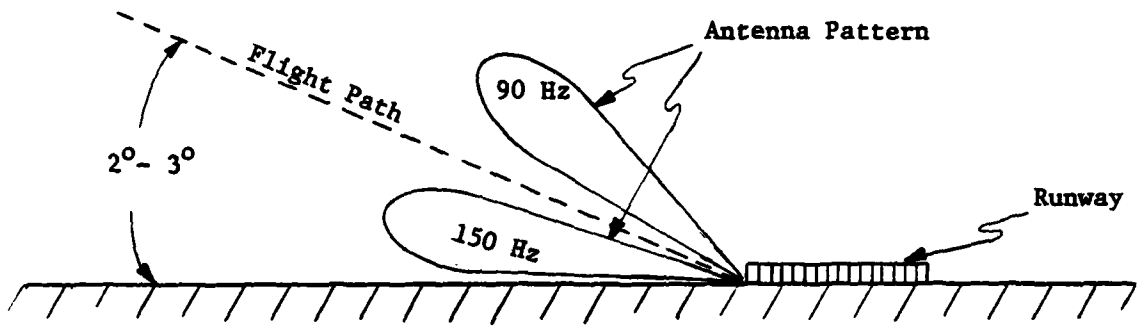

(c) Range Marker Pattern

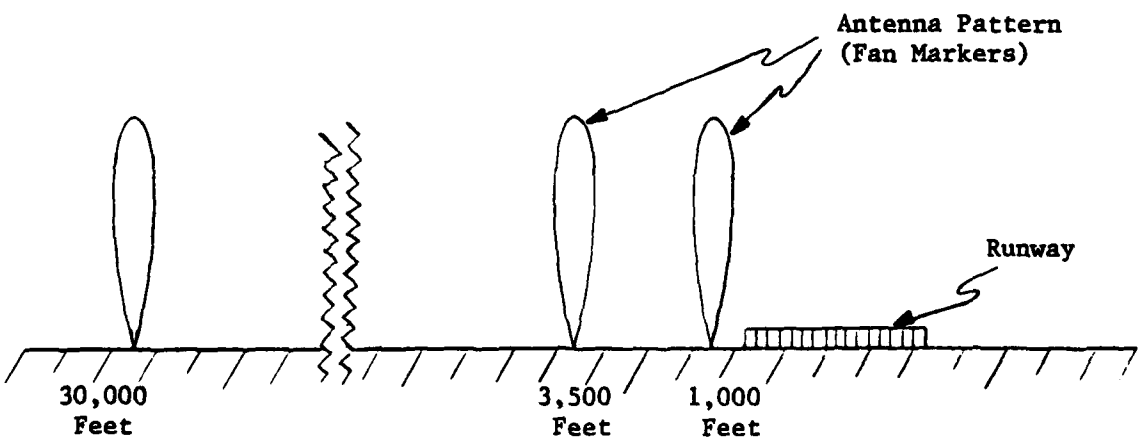

Figure 2.3.2.1--Instrument Low-Approach System Antenna Patterns

An instrument landing system employed by the U. S. Navy is the AN/SPN-41 used aboard aircraft carriers. The antenna patterns are pitch and roll stabilized to compensate for ship motion. Deck "heave" is not compensated for, however, thus making the system unsuitable for use to touchdown. The "accuracy" of an ILS depends primarily upon the shaping and stabilization of the antenna patterns marking the flight path.

Ground-Controlled Approach System -- A ground-controlled approach (GCA), or precision approach radar (PAR), system utilizes a tracking radar to determine the aircraft position with respect to the proper flight path. Appropriate flight-path corrections are then transmitted to the aircraft via radio link. Most GCA-type systems employ a voice uplink. The Aircraft Carrier Landing System (ACLS) employed by the U. S. Navy utilizes an AN/SPN-42 tracking radar and can transmit steering signals to the aircraft by voice link, data link driving a crossed-pointer display, or a data link coupled directly to the aircraft autopilot system. A separate on-board system maintains the proper aircraft angle of attack and airspeed. The commanded flight path is stabilized with respect to ship pitch, roll, and deck heave, thereby giving the system the capability of controlling fully-automatic landings through touchdown. The system also compensates automatically for expected airflow in the vicinity of the flight deck. The AN/SPN-42 tracking radar tracks a radar transponder on the aircraft and achieves acquisition at about 4 nautical miles range. The "accuracy" of a ground-controlled approach system is dependent upon the tracking accuracy of the radar, the accuracy of stabilization of the flight path, and the response of the pilot or autopilot.

Microwave Landing System -- The microwave landing system (MLS), or time-reference scanning beam (TRSB), landing system utilizes two narrow, fan-shaped microwave beams, one scanned in azimuth, the other in elevation. An airborne system receives the pulses produced by the passing beams and, by timing the pulse intervals, computes aircraft position with respect to the runway centerline and glide slope. Range to the runway threshold is determined by utilizing an airborne tranceiver to trigger a ground-based transponder. (See Section 2.3.4 of this text for a description of DME.) The ground station also transmits other information to the aircraft, including wind data. The scanned beams are transmitted at C-band and permit ranges up to 30 miles even under adverse conditions. The DME ranger operates at L-band. The accuracy (100 foot range, 0.1 degrees in elevation, and 0.2 degrees in azimuth), high-rate update (13.5 hertz in azimuth and 40.5 hertz in elevation), and relative freedom from multipath anomalies combine to provide significant performance improvement over ILS.

2.3.3 Airborne Direction Finders (ADF) -- The oldest form of airborne radio navigation is airborne direction finding (ADF). The ADF, or radio compass, utilizes the directivity of a highly directional receiving antenna to determine the relative bearing to a known transmitting station. (The location of the transmitter must be known for a navigational fix.) Two or more such bearings determine user aircraft position by providing a θ, ϕ fix.

Two basic types of directional antennas are commonly used for airborne direction finding: the loop and the Adcock array. The loop, illustrated in Figure 2.3.3.1(a), generally consists of multiple turns of wire and is used at low and medium frequencies (0.03 to 3 megahertz). The adcock array, illustrated in Figure 2.3.3.1(b), consists of two vertical, half-wave dipoles and is used at very high and ultra high frequencies (30 to 3000 megahertz). The high frequency range (3 to 30 megahertz) is not often used for direction finding because, at those frequencies, transmission over long distances is largely by sky wave, an unrealiable method for propagation in direction finding because of phase irregularities. At shorter ranges, low frequencies (ground wave) and very high frequencies (space wave) are more attractive. Ground waves are utilized out to a few hundred miles; space waves are strictly line-of-sight.

For the two types of antenna, the basic principle of operation is the same. That is, the antenna senses the differential in distance from the transmitter to the two vertical portions of the antenna. When that differential is zero, the currents induced in the two sides are equal and in phase opposition. Thus, the received signal vanishes when the antenna is oriented in a plane perpendicular

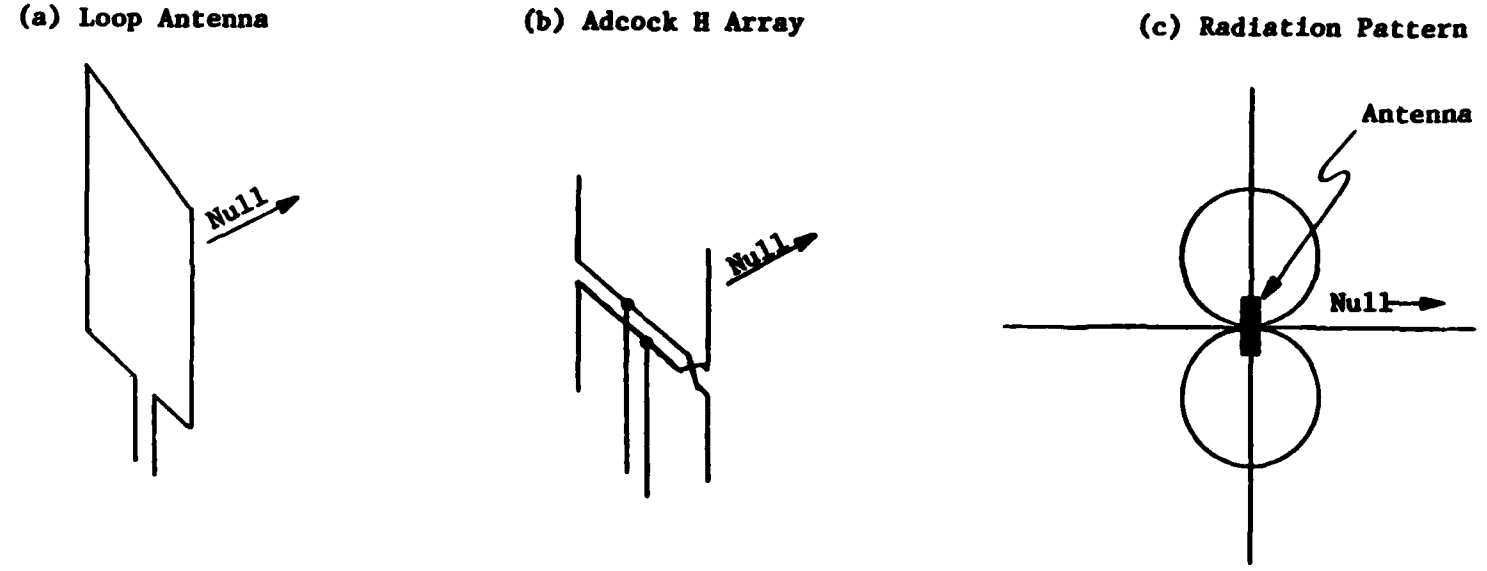

Figure 2.3.3.1--Direction-Finding Antennas

to the line-of-sight to the transmitter, as indicated in the figure. The antenna pattern for both types of antenna is shown in Figure 2.3.3.1(c). The lateral separation of the two vertical portions of the antennas must be less than one-half wavelength in order to avoid multiple nulls.

In some direction finding systems, the antenna is actually rotated to detect the null. In modern airborne ADF's, the problems associated with rotating an antenna are often circumvented by utilizing two crossed, fixed antennas and a goniometer as shown in Figure 2.3.3.2. The inductive goniometer shown in the figure is a variable-coupling milti-phase transformer that resolves the components of a vector field induced in it by currents applied to its stator windings. By rotating the rotor of the goniometer (rather than the antenna) the direction of arrival of the RF wave can be determined. Capacitive goniometers are generally used at VHF and UHF frequencies.

The 180° ambiguity created by the two nulls indicated in Figure 2.3.3.1(c) is usually resolved by the use of a separate "sense" antenna. When an omnidirectional sense antenna is used, the signal it receives will be in phase with that received in one lobe of the directional antenna pattern and 180° out of phase with that received in the other. That phase difference can be utilized to distinguish between the two nulls.

Direction finding also can be accomplished by utilizing the Doppler principle. If a single vertical antenna element is rotated about an offset vertical axis, as shown in Figure 2.3.3.3, the frequency of the received signal will vary sinusoidally with the angle of rotation, being greatest when the element is

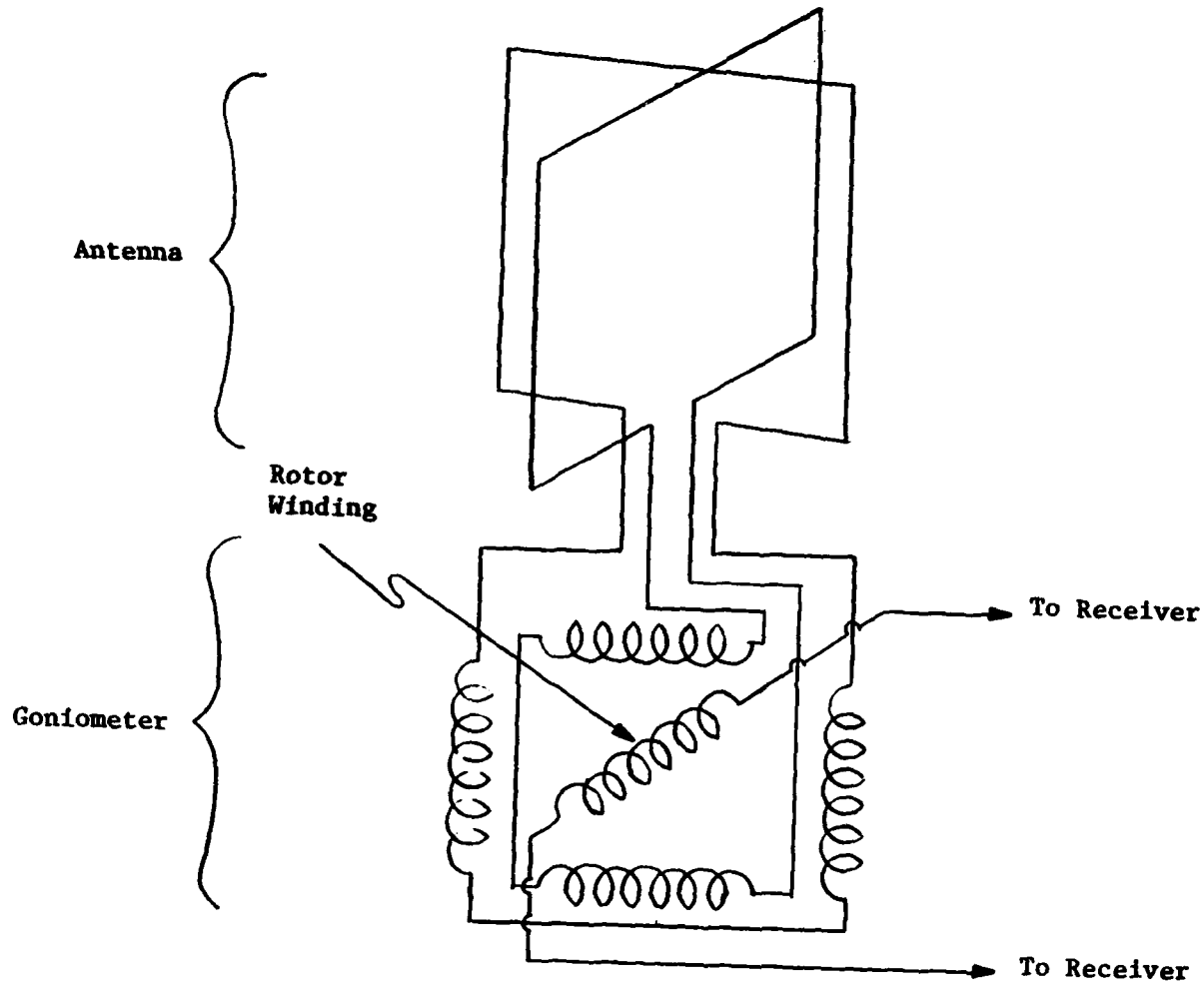

Figure 2.3.3.2 -- Crossed-Loop ADF Antenna Utilizing a Goniometer

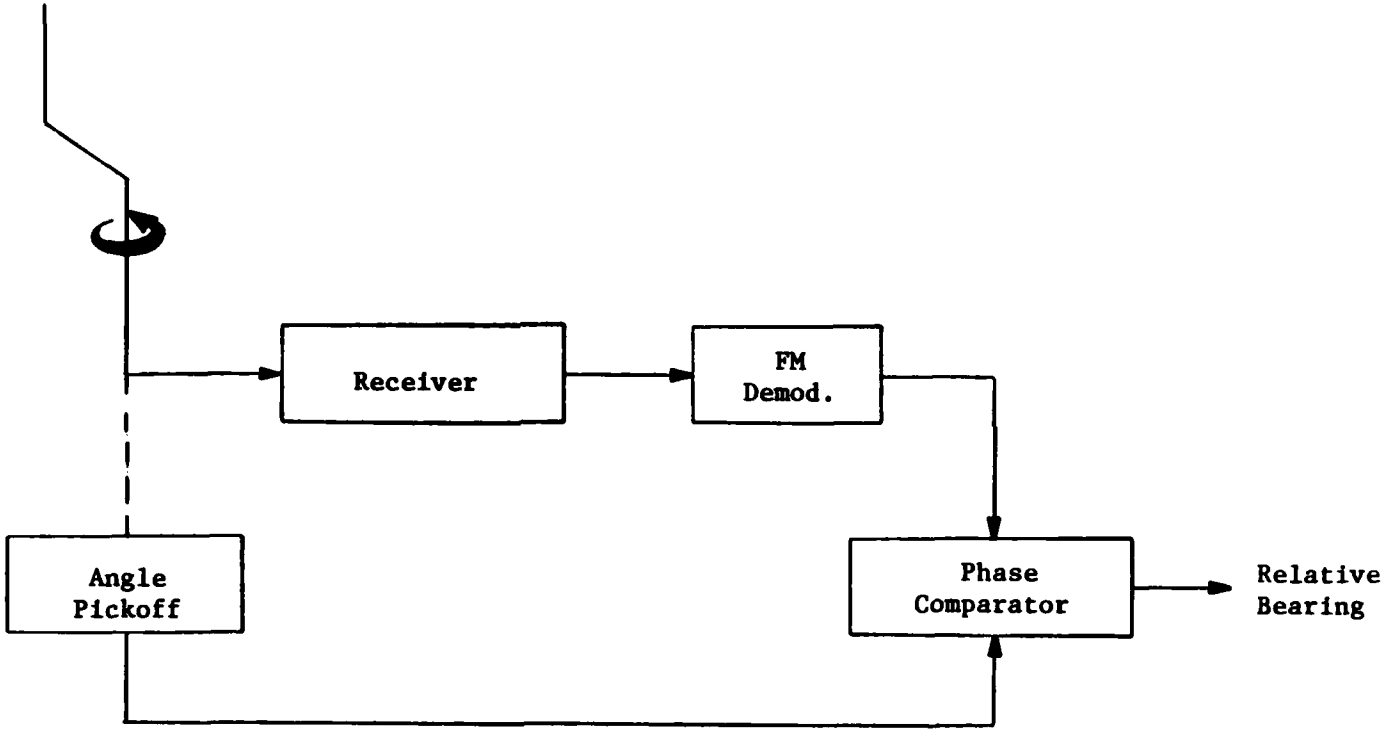

Figure 2.3.3.3--Doppler Airborne Direction Finder

moving in the direction of the transmitter. The direction to the transmitter can therefore be determined by correlating the phase of the sinusoidal frequency variation with the angular position of the rotating antenna, as indicated in the figure.

A major portion of the inaccuracy in an ADF is that due to multipath created by the aircraft structure itself. (Multipath caused by reflecting objects near the receiver affect direction of arrival far more than objects near the transmitter, due to the geometry of the situation.) Another major contributor to ADF inaccuracy is the presence of horizontally-polarized components in the received wave. Such components can be caused by sky-wave contamination of ground-wave signals. In the absence of multipath and sky-wave contamination, ADF accuracies of about $\pm 2°$ are attainable. In the presence of these interfering signals, accuracy may be degraded to $\pm 30°$ or more.

2.3.4 Distance Measuring Equipment (DME) -- A DME system functions in a manner similar to that of a ranging radar with an active transponder for a target. The slant range from the aircraft to a known ground station is determined by measuring the elapsed time from the transmission of a pulse by the airborne transmitter to receipt of the (ground-based) transponder reply pulse by the airborne receiver. A circular line of position is thus established and a positional fix can be obtained from two (or three) such measurements. (Resolution of ambiguity requires a third DME measurement or some other independent determination.) In addition to replying to interrogation pulses, the ground station periodically transmits an identifying code.

The equipment consists of an airborne interrogator (transceiver) and a ground-based transponder, as shown in Figure 2.3.4.1. The triggering circuit generates pulse pairs (3.5 microsecond pulses 12 microseconds apart) which are transmitted by the airborne transmitter and received by the ground-based receiver. After a fixed delay of 50 microseconds, the ground-based transmitter replies with a pulse pair which is received by the airborne receiver. The ranging circuit in the airborne equipment then determines the elapsed time and, hence, the slant range.

In order to prevent transmitter-to-receiver interference in the airborne equipment the transponder replies on a carrier frequency displaced from the airborne transmitter frequency by 63 megahertz, the IF frequency of the airborne receiver. In order to prevent transmitter-to-receiver interference in the ground-based equipment the ground receiver is gated off for about 60 microseconds during and after a ground transmitter pulse. This blanking of the ground receiver can

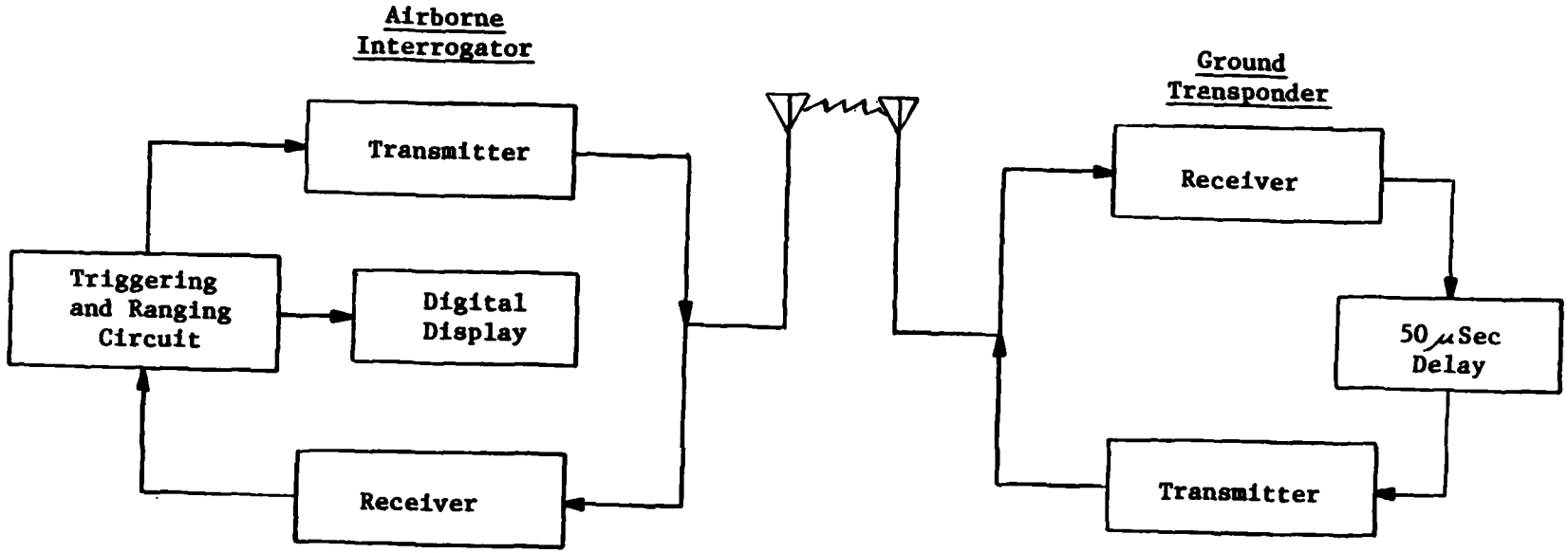

Figure 2.3.4.1--Distance Measuring Equipment (DME) System

result in the loss of up to 20% of the incoming pulses. The system is designed, however, to operate satisfactorily with the resulting missing replies.

The DME system is designed to operate with up to 100 simultaneous users, all operating on the same channel (frequency). The airborne equipment identifies replies to its own interrogations by means of a time correlation technique. It employs a circuit similar to a range gate in a range-tracking radar. (See Section 2.17.8 of the radar text.) The operation of the time-correlating, range-tracking circuit is depicted in Figure 2.3.4.2. In that figure, several sweeps of a simulated scope time line are depicted, with the sweep initiation synchronized with the interrogate pulse transmission times. Each line represents one sweep of the scope. Although random pulse coincidences occur, as shown in the figure, frequent pulse coincidences occur only for that time interval corresponding to the two-way transmission time of the pulses initiated by the airborne interrogator under observation. The DME range gate time, t_g, is referenced to the transmit time, t_o, and is shown bracketing the desired reply pulses. In the search mode, the airborne system sweeps the gate time, t_g, until the received pulses, integrated over a period of time, produce a signal beyond a set threshold. The system then enters the track mode, in which the gate time is controlled so as to keep the reply pulses in the gate, as described in Section 2.17.8 of the radar text. In order to prevent loss of track due to momentary loss of signal, the system is provided with a 10 second tracking memory. In order to reduce the probability that the system will, even momentarily, lock in on the replies intended for another user, the PRI of the interrogate pulses is deliberately varied in a random fashion. To further reduce the probability that the system will respond to extraneous pulses, the system transmits pulse pairs separated by 12 microseconds. Thus, the single pulses shown in Figure 2.3.4.2 actually represent pairs of pulses.

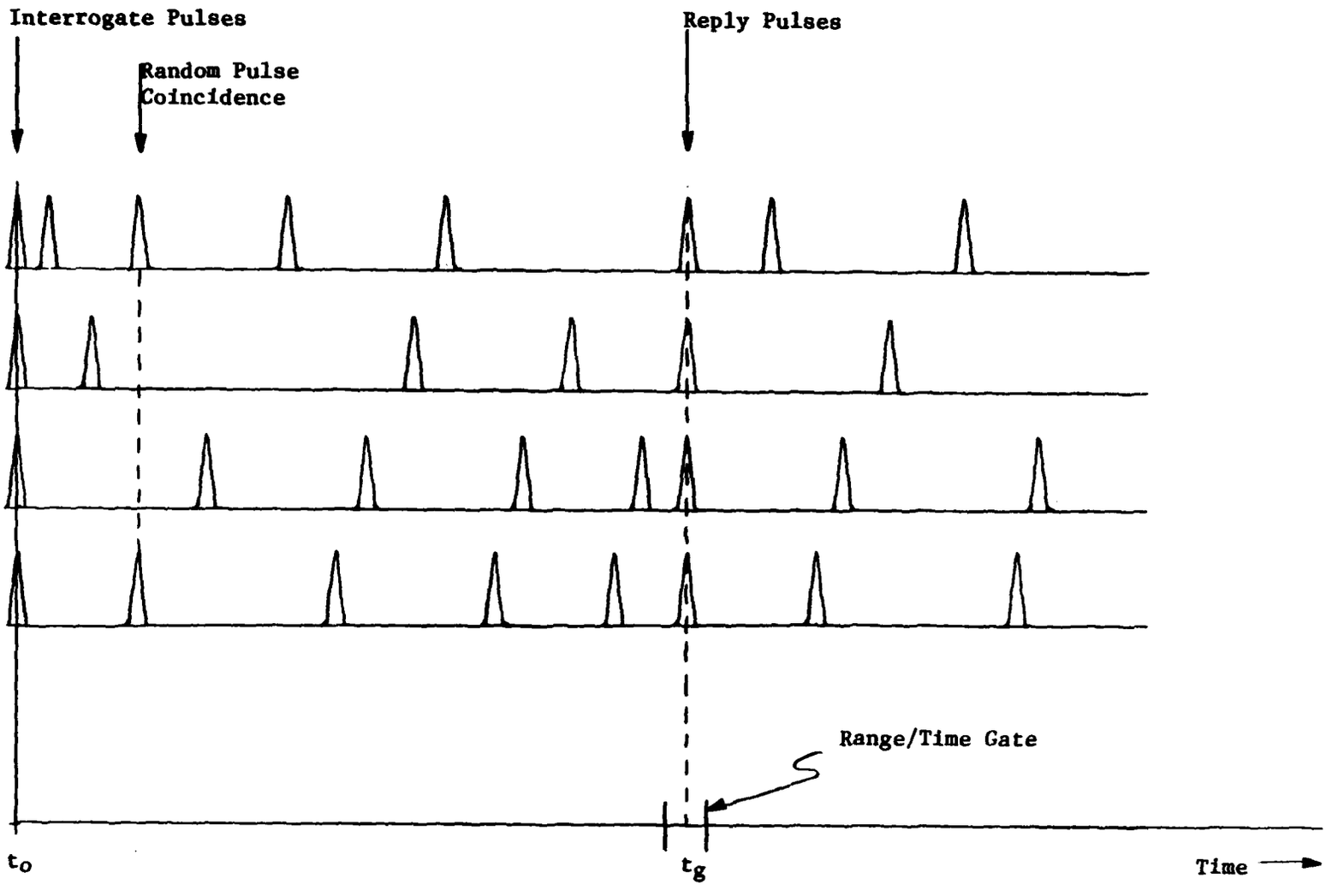

Figure 2.3.4.2--Time-Correlating, Range-Tracking Gate in DME Airborne System

The range gate is 20 microseconds wide and is swept at a rate such that track acquisition time varies between 1 and 20 seconds, depending upon the system design. During track, the PRF of the interrogator is between 5 and 25 pulse pairs per second. During search, the PRF is increased to 150 PPPS in order to shorten the track acquisition time.

In order to attain a constant duty cycle for the transponder, the threshold sensitivity of its receiver is continuously adjusted to obtain a constant 2700 replies per second. In periods of light traffic, most of the replies are in response to noise. In periods of heavy traffic, only the approximately 100 nearest users (strongest signals) are serviced. This limitation is a result of the 2700 reply-per-second operation of the transponder. Although the transponder also has a 100 microsecond recovery time after transmitting a pulse, the *recovery time* is not the limiting factor.

The airborne transmitter operates on one of 126 channels, covering from 1025 to 1150 megahertz, at a power from 50 to 2000 watts depending upon design acquisition range. The ground-based transponder replies on one of 126 channels, separated from the interrogator frequency by exactly 63 megahertz, and covering from 962 to 1024 and 1151 to 1213 megahertz. The output power of the ground-based transmitter is from 1 to 20 kilowatts, generally designed to ensure that the reply to an interrogate pulse will be received by the user. All transmissions are vertically polarized. At these frequencies (UHF), propagation is strictly space wave and useable ranges are from 50 to 300 nautical miles, depending upon the equipment. DME ranging accuracies are between 0.01 miles to 3.0 miles, depending primarily upon user equipment.

2.3.5 VHF Omnidirectional Range (VOR) -- The VHF Omnidirectional Range system, (also called VOR, omnirange, and omni), utilizes a rotating antenna pattern to determine the bearing of the user aircraft from a known ground station. The ground station transmits two signals simultaneously. One is an unmodulated carrier radiated in a directional (cardioid) pattern rotating at 30 revolutions per second. The rotating pattern produces a signal at the airborne receiver that is amplitude modulated, at 30 hertz, with a phase determined by the bearing of the aircraft with respect to the ground station. The other signal transmitted by the ground station is an omnidirectional subcarrier frequency modulated at 30 hertz. The relative bearing of the aircraft from the ground station is determined by comparing the phase of the amplitude modulated signal with that of the frequency modulated reference signal. The rotation of the antenna pattern is synchronized with the frequency modulation on the reference signal so that the two modulations will be in-phase for an aircraft with a magnetic bearing of 0° (due north) from the ground station. The rotating pattern and received signals are illustrated in Figure 2.3.5.1. As shown in the figure, the phase difference between the modulation of the signal due to the rotating pattern (solid line) and the modulation of the reference signal (dotted line) is proportional to the magnetic bearing angle of the aircraft with respect to the ground station.

A block diagram of the VOR receiver/bearing computer is shown in Figure 2.3.5.2. As indicated in the figure, the AM and FM modulation signals are separated and their phases are compared in order to determine the aircraft bearing.

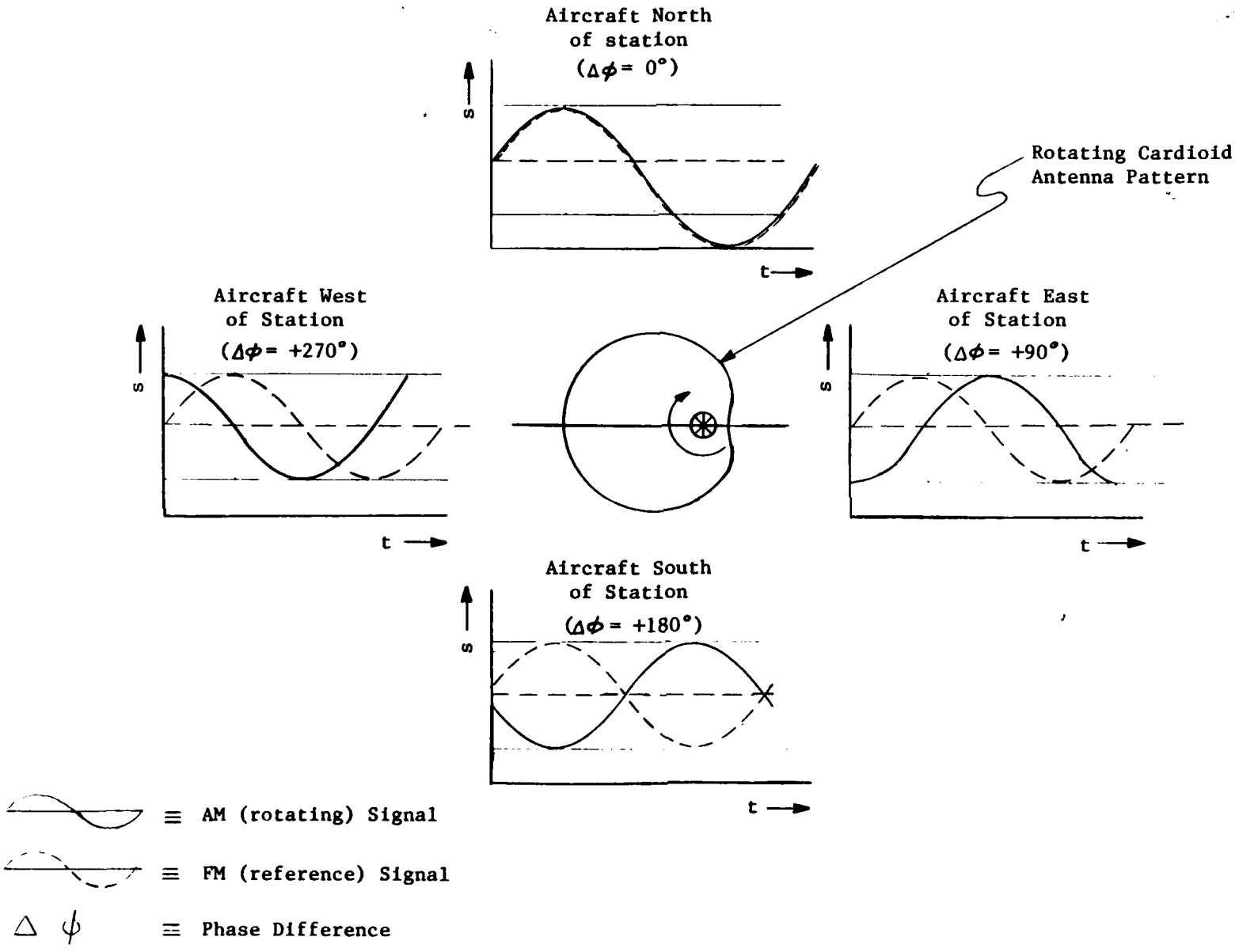

Figure 2.3.5.1--VHF Omnidirectional Range Antenna Pattern and Signals

Figure 2.3.5.2--VHF Omnidirectional Range Receiver/Bearing Computer

The rotating antenna pattern employed by VOR is not produced by actually rotating an antenna array. It is produced by rotating the rotor of a goniometer similar to the one described in Section 2.3.3 of this text. The outputs of the goniometer are then fed through RF distribution circuits (bridges) to four, fixed, Alford-loop antennas located at the corners of a square, as shown in Figure 2.3.5.3. The result is a field pattern rotating at 30 RPS. The FM (reference) signal is generated by a tone wheel driven by the same synchronous motor that drives the goniometer, thereby ensuring synchronization with the rotating field. The FM signal is distributed to the antennas in such a way as to produce an omnidirectional pattern. Both the rotating and the reference signals are horizontally polarized. In addition to the reference signal, the omnidirectional pattern also carries an identification code and can be voice modulated to provide further navigational information.

The ICAO standard VOR operates on one of 20 channels in a frequency band of 108 to 118 megahertz, with a power of 200 watts. Propagation is by space wave (line of sight) with a design maximum range of 200 nautical miles.

The major contributors to VOR bearing inaccuracy are "site error" and instrumentation (receiver/computer) error. Site error is caused by reflections from terrain and other objects in the vicinity of the transmitter and produces a typical maximum error of about 3 degrees. Instrumentation error is about 1 degree, for a total system error of about 3.5 degrees.

In an effort to reduce VOR bearing error, two system modifications have been devised: Doppler VOR and Precision VOR. With Doppler VOR, the bearing-dependent

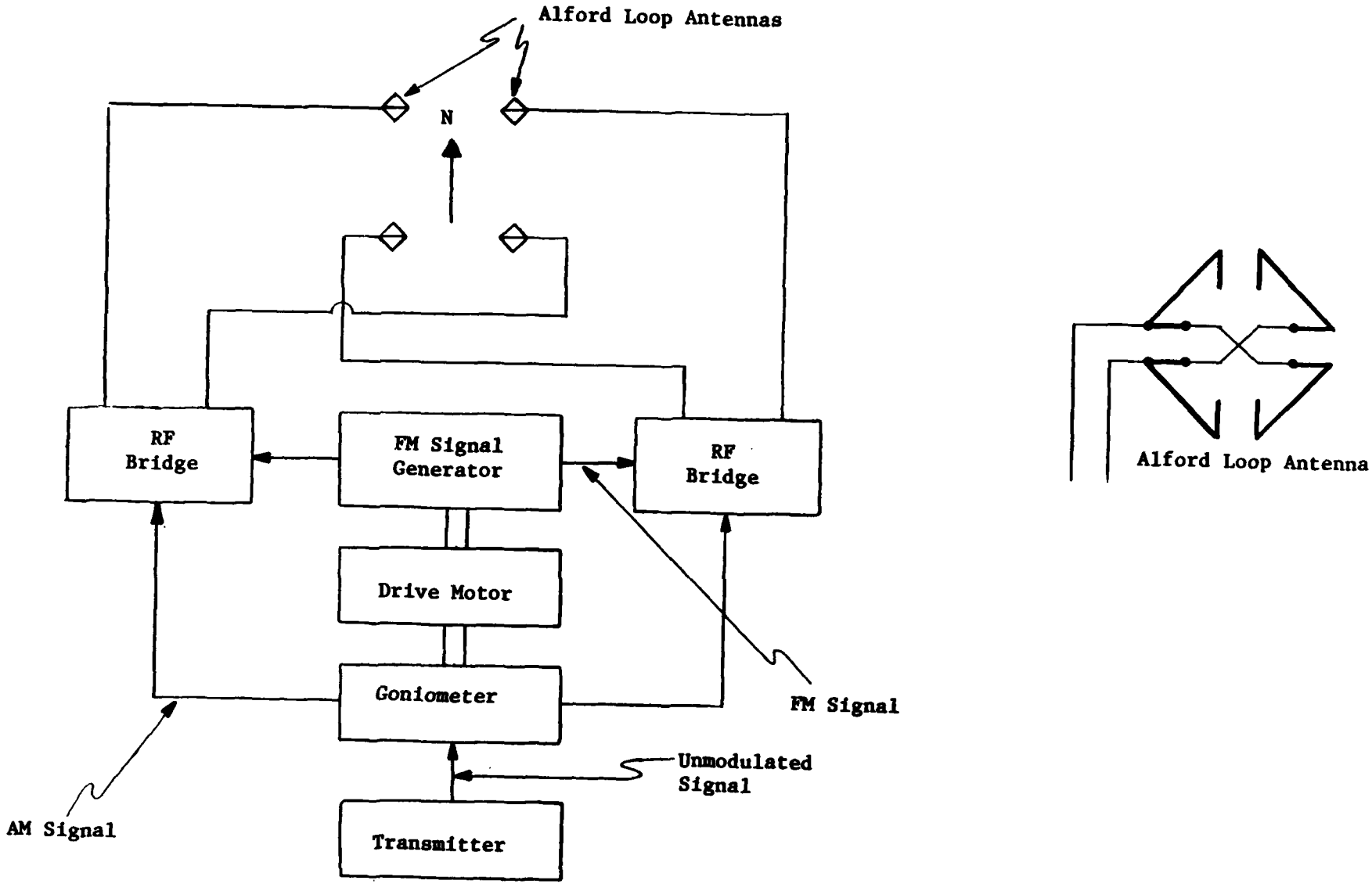

Figure 2.3.5.3--VHF Omnidirectional Range Rotating Pattern Generator

signal is frequency modulated and the reference signal is amplitude modulated. Thus the FM and AM roles are reversed. Otherwise the system of bearing determination is the same as for the standard VOR. The airborne receiver/computer is identical. The bearing-dependent FM signal is produced by a large circular array of Alford loops fed by an unmodulated signal commutated around the array in a rotary fashion. The result at the airborne receiver is an FM signal the phase of which depends upon the bearing of the aircraft from the ground station. Doppler VOR ground stations reduce the site error to about 0.4 degrees.

Precision VOR utilizes a multi-lobed rotating antenna pattern similar to that used by the TACAN system discussed in Section 2.3.6 of this text. With that modification, instrumentation error is on the order of 0.1 degree.

2.3.6 Tactical Air Navigation (TACAN) -- A TACAN system functions, in part, in a manner very similar to that of a VOR. That is, a rotating antenna pattern is used to determine the bearing of the aircraft relative to the ground station. There are two major differences between TACAN and VOR. The first is that TACAN incorporates a DME, similar to that described in Sectiin 2.3.4 of this text, for determining range. Thus a single TACAN station provides a ρ, θ positional fix. TACAN and VOR ground stations are often co-located to allow a ρ, θ fix using the DME for range and the VOR for bearing. A TACAN ground station is, in fact, a DME station modified by: (1) radiating the normal DME transmissions (pulses) through an antenna system with a directional, rotating radiation pattern; and (2) adding rotation angle reference pulses to the normal DME transmissions.

The second major difference between TACAN and VOR is the shape of the antenna pattern. The antenna pattern employed by TACAN has nine lobes, as shown in Figure 2.3.6.1(a). The pulse envelope of the signal received by a user is shown in Figure 2.3.6.1(b). The rotation rate of the antenna pattern is 15 RPS, thus generating a signal level at a user position with a 135 hertz (fine) variation superimposed upon a 15 hertz (coarse) variation, as shown in the figure. The 9-lobed antenna pattern is intended to improve the "sharpness" of the signal "peak" and, thus, the accuracy of the system, over that of the single-lobed VOR system.

Another difference between TACAN and VOR is the nature of the reference signal. Whereas VOR employs a sinusoidally-frequency-modulated phase reference signal,

(a) Rotating 9-Lobed Antenna Pattern

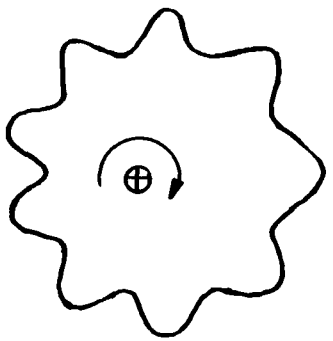

(b) Received Signal

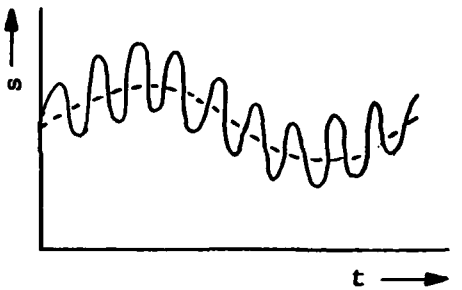

Figure 2.3.6.1 -- TACAN Rotating Antenna Pattern and Induced Pulse Envelope

TACAN employs pulse trains. One pulse train is initiated as the maximum antenna pattern lobe passes through east and therefore provides a "phase" reference for the 15 hertz component of the signal level variations induced by the rotating pattern. Another pulse train is initiated as each of the 9 lobes in the pattern passes through east, thereby providing a "phase" reference for the 135 hertz component of the induced signal level. Utilizing these reference pulse trains, the user is able to determine his bearing from the station from the amplitude modulation of the signal generated by the rotating pattern.

A block diagram of a TACAN receiver/bearing computer is shown in Figure 2.3.6.2. The amplitude-demodulated signal from the receiver is processed, in parallel, to recover: (1) the 15 hertz component of the pulse envelope induced by the rotating pattern; (2) the 15 hertz phase-reference signal from the "coarse" reference pulse train; (3) the 135 hertz component of the pulse envelope induced by the rotating pattern; and (4) the 135 hertz phase-reference signal from the "fine" reference pulse train. The 15 and 135 hertz components of the rotating pattern signal are then passed through electromechanical phase shifters and compared to their respective references. The phase shifter/phase comparator/ servo amplifier/drive motor chain constitutes a closed-loop servomechanism controlling the phase shifter settings. When the phases of the rotating pattern signals, after phase shifting, match the phases of their respective references, the servomechanism is nulled and the readout on the bearing indicator is the required bearing of the aircraft with respect to the ground station. When the servo error (phase mismatch) is greater than $\pm$ 20°, the coarse/fine selector switch is automatically set to the "coarse" position and the 15 megahertz signal

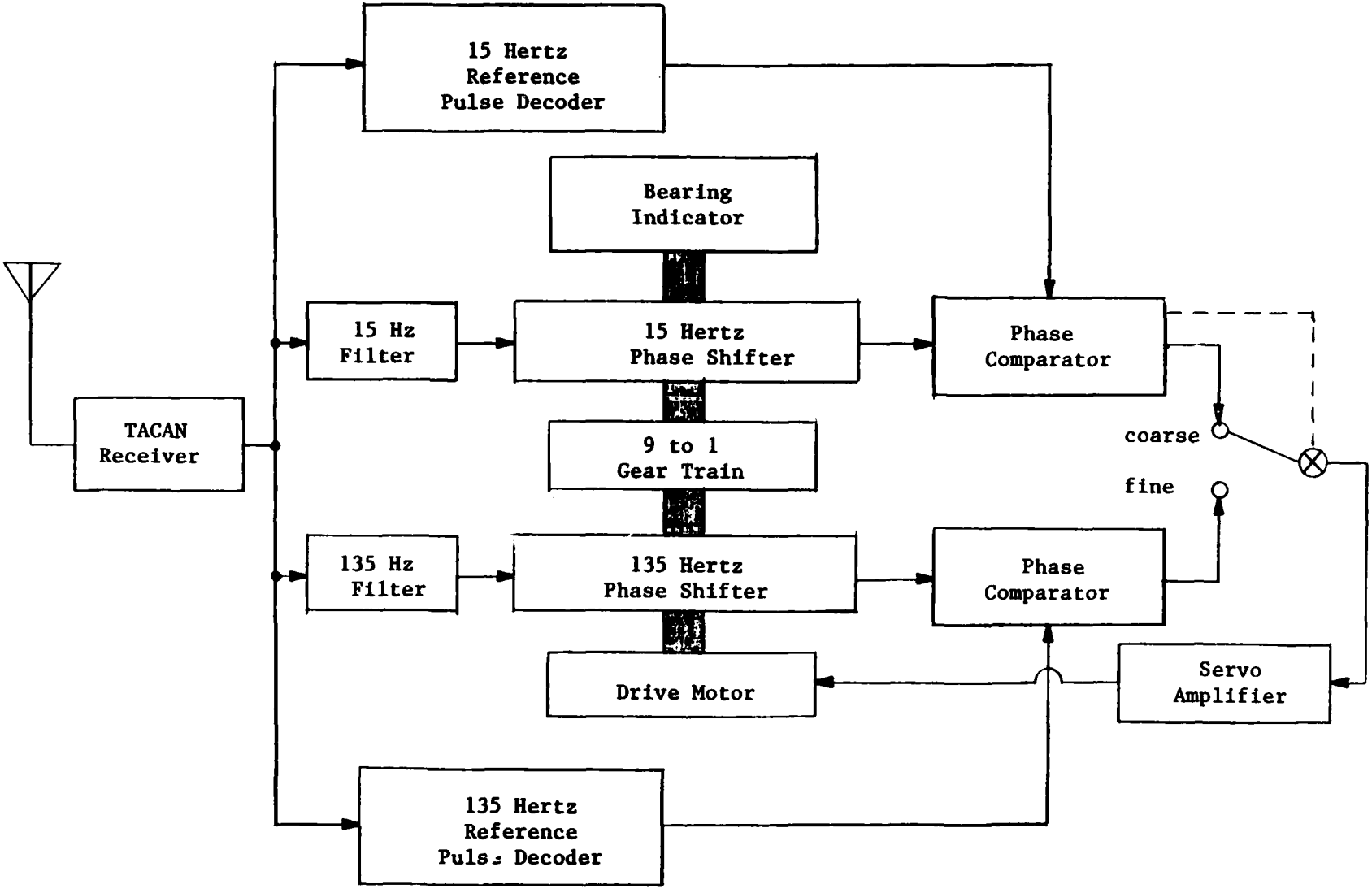

Figure 2.3.6.2--TACAN Receiver/Bearing Computer

controls the servo. When the error is less than $\pm$ 20°, (and the 135 hertz signal is present), the switch is set to the "fine" position and the 135 hertz signal controls the servo. The result is a bearing determination in which the 135 hertz signal provides accuracy and the 15 hertz signal resolves the ambiguity created by the multi-lobed antenna pattern. Occassionally, the system will lock on the wrong lobe, producing a bearing indication in error by exactly a multiple of 40 degrees. As with the VOR system, a TACAN bearing computer possesses a "memory" that prevents loss of bearing during brief signal dropouts.

The rotating antenna pattern used in TACAN is generated by an antenna array with rotating elements as shown in Figure 2.3.6.3. The arrangement utilizes a stationary active radiator in the center. A single parasitic element is mounted on an inner rotating cylinder (to produce the 15 hertz component of the rotating field); and nine equally-spaced parasitic elements are mounted on an outer rotating cylinder (to produce the 135 hertz component of the rotating field). Mounted on the same shaft with the two cylinders, (and therefore rotating at 15 RPS and synchronized with the rotating field), are code wheels which produce the 15 hertz reference pulse train, the 135 hertz reference pulse train, and a 1350 hertz pulse train used for station identification and drive motor speed control. For shipboard installation, the antenna stabilization system maintains the antenna drive referenced to magnetic north. The antenna is also vertically stabilized against the rolling motion of the ship.

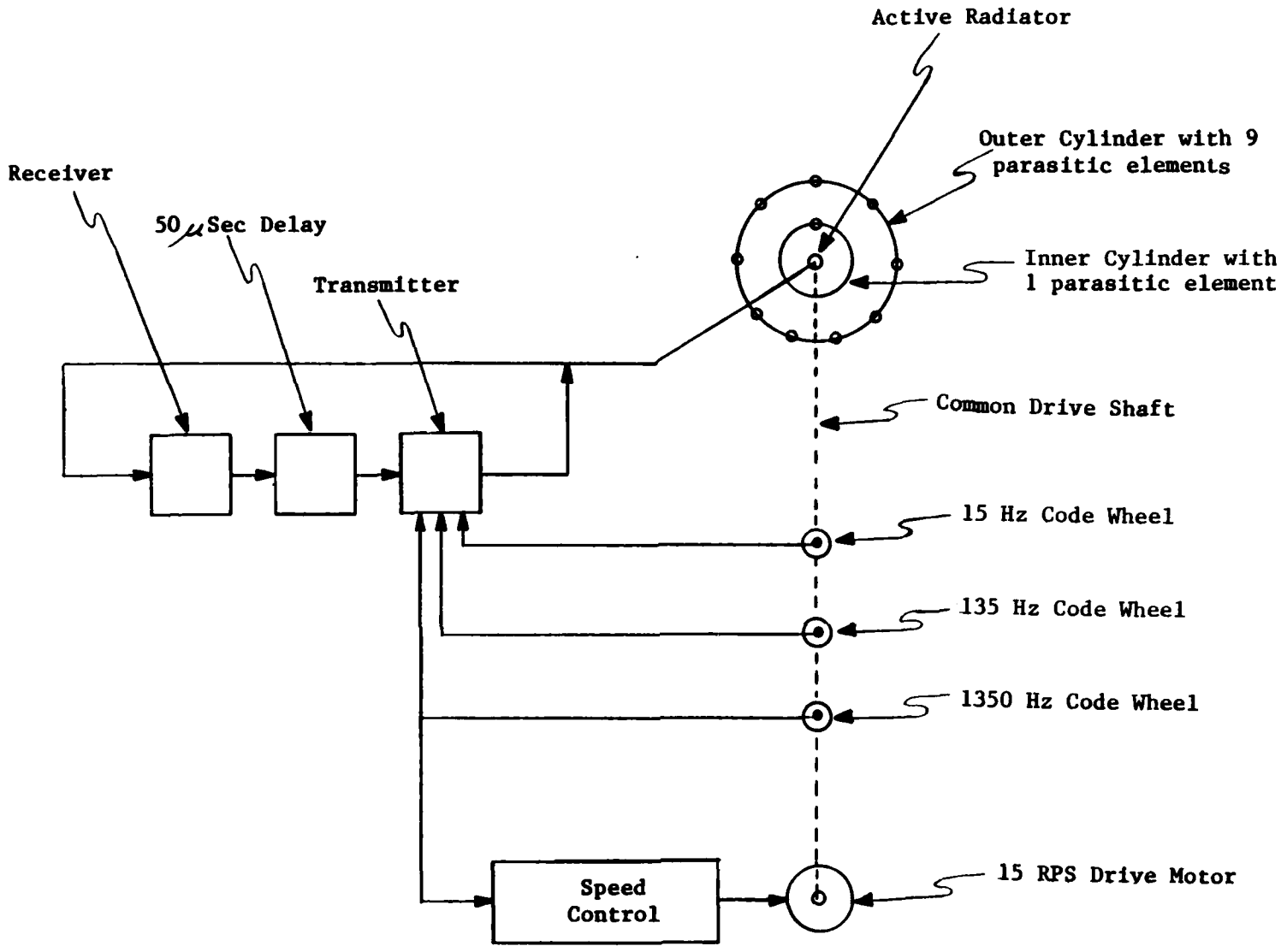

Figure 2.3.6.3--TACAN Antenna Configuration

As is the case for the ICAO standard DME, the carrier frequency of a TACAN ground station is in two bands, from 962 to 1024 and 1151 to 1213 megahertz. The transmitter power is from 1 to 20 kilowatts and propagation is by space wave (line-of-sight). Design maximum range is 300 nautical miles.

The major contributor to bearing error is site error, as discussed in Section 2.3.5 of this text. Design maximum errors are $\pm$ 3.5 degrees in bearing and $\pm$ 0.5 nautical miles in range.

2.3.7 Long Range Navigation (LORAN) -- A LORAN navigation system determines a hyperbolic line-of-position by measuring the difference in times of arrival of pulses transmitted, at a fixed time interval, by two stations of known location. Two pairs of stations provide two such lines-of-position thereby establishing a positional fix. (A third pair of stations may be required in order to resolve ambiguity.) The time interval between the transmissions of the two stations is normally fixed by a master/slave relationship between the stations. That is, the slave station functions as a repeater, triggered by reception of the pulse from the master station. The transmission by the slave station is further delayed so that a user will always receive the transmission from the master station first.

The LORAN station pairs are provided by a LORAN "chain" consisting of a master station and two to four slave stations, typically separated by several hundred miles. A three-station chain is shown in Figure 2.3.7.1. As illustrated in the figure, the lines of position (lines of constant difference in signal time-of-arrival) are hyperbolic curves with the stations as foci. A positional fix usually is obtained by using displayed time difference in conjunction with a special navigation chart with a superimposed LORAN grid. Fully automatic systems have been built that compute and display latitude and longitude directly.

The "transmissions" of both the master and slave stations consist of a series of pulses, rather than a single pulse, thus allowing the signal-to-noise ratio of the processed signal to be greatly improved by means of a "pulse integration" technique similar to that employed in radar. (See Section 2.7 of the radar text

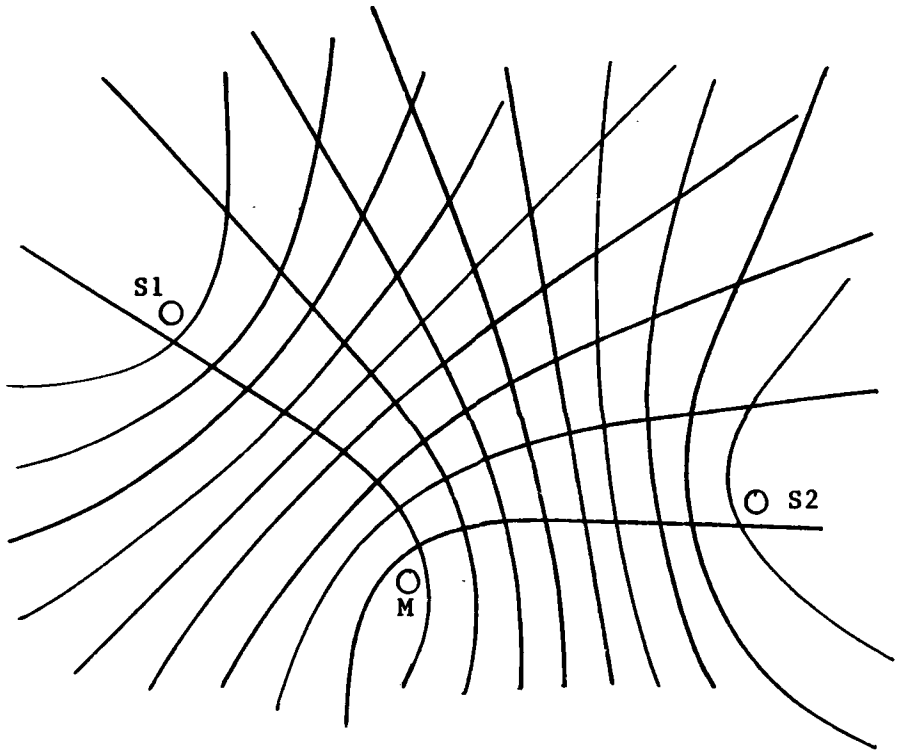

M--Master Station
S1,S2--Slave Stations

Figure 2.3.7.1--LORAN Station "chain" and Hyperbolic Lines of Position

for a discussion of pulse integration.) The master station transmits nine pulses; the slave stations transmit eight. The extra master station pulse serves to identify its signal as that from the master station. The pulse groups consist of pulses 250 microseconds wide, separated by about one millisecond. The groups are repeated ten to twenty-five times per second.

A LORAN receiver is broadly tuned and does not select the desired signal on the basis of carrier frequency. Identification of the chain is provided by assigning a unique pulse repetition interval to each chain. Further identification of the various signals is accomplished by coding the phase of the carrier within each pulse. (The carrier is coherent and synchronized with respect to the envelope of the pulses. Coding can be effected by reversing the carrier phase in selected pulses.) Because of the broad-band tuning (low signal-to-noise ratio), the pulse integration and correlation process utilized by LORAN imposes a signal acquisition time of as much as ten minutes. For that reason, LORAN is best employed as a long-term update for an inertial or Doppler navigation system, when utilized in an aircraft.

Three versions of LORAN have been utilized: LORAN A, LORAN C, and LORAN D. LORAN A was the original (1942) version and employed a carrier frequency of about 2 megahertz. It had an intended maximum range of about 700 nautical miles and a positional accuracy of up to 5 nautical miles at maximum range. LORAN D is a specialized version of LORAN intended for low-altitude, short-range missions. It employs less power and a shorter baseline than standard LORAN. The airborne equipment is identical to LORAN C. LORAN C is the currently operational standard version. It employs a carrier frequency between 90 and

110 kilohertz, has longer range (about 1200 nautical miles), and much greater accuracy than LORAN A.

The improved accuracy of LORAN C is a result of two factors. Some improvement is due to the longer baselines generally used (about 600 to 800 miles). The greatest improvement, however, is due to a technique, called "cycle-matching", in which the LORAN receiver utilizes a specific cycle of carrier within the pulse envelope as the time-of-arrival reference. (LORAN A utilized the envelope itself.) A typical LORAN C pulse is shown in Figure 2.3.7.2. As previously noted, the carrier is coherent and synchronized with the envelope, a specific cycle occurring at a specific time within the envelope. LORAN C "counts" cycles and locks in on the third cycle (indicated in the figure). By utilizing the "fine structure" of the pulse, LORAN C achieves about a ten-fold increase in accuracy over that of LORAN A. The third cycle is used, despite the fact that it is only about one-half the amplitude of the maximum pulse height, in order to avoid sky-wave contamination of the signal. The system is designed to use the first signal to arrive -- that propagated by ground wave. About 30 to 60 microseconds later, depending on the range, the sky-wave signal arrives. In order to avoid interference by the sky-wave signal, the third cycle in the ground wave pulse is utilized, its position being 30 microseconds into the pulse.

As a result of the long base line (several hundred miles), site error is not a major contributor to LORAN positional error. One major error contributor is atmospheric noise, another is sky-wave contamination. When sky-wave propagation is intentionally used, (to obtain greater range), positional accuracy is severely degraded by propagation anomalies. Another error source important

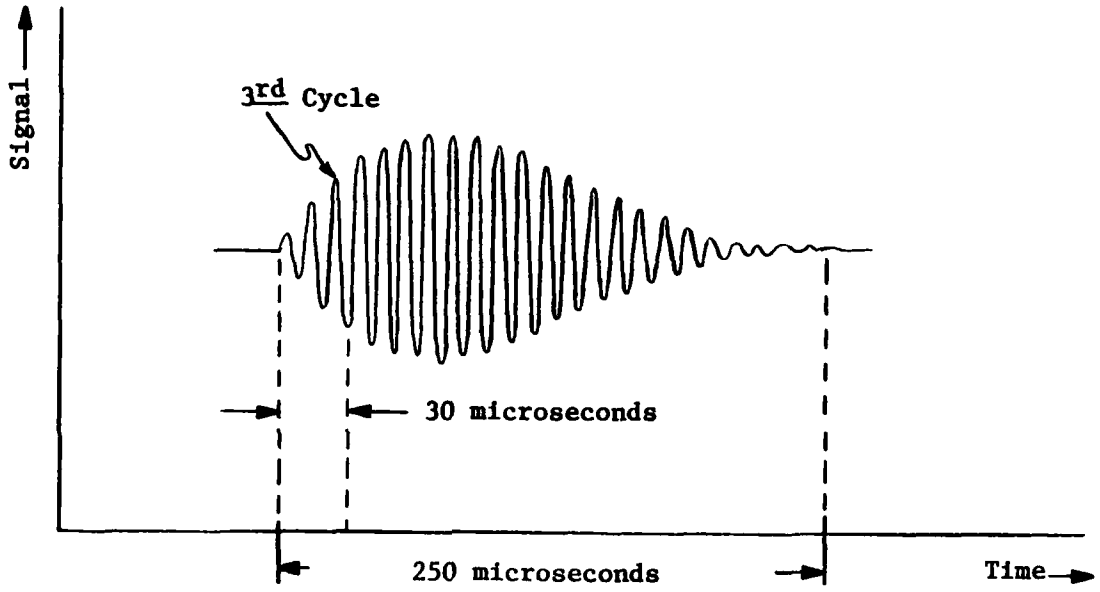

Figure 2.3.7.2--LORAN C Pulse Waveform

for some airborne applications is the so-called "slant range" error. The hyperbolic lines-of-position previously described are actually intersections of three-dimensional hyperbolic surfaces of revolution with the surface of the earth, as shown in Figure 2.3.7.3. As indicated in the figure no "surface-position" error is incurred at zero altitude (or midway between the stations). At altitude, however, the "ground" position of the aircraft is displaced from the hyperbolic line-of-position corresponding to the LORAN signals it would receive. The error involved is small when the altitude of the aircraft is small compared with the ranges to the LORAN stations. The error is also systematic and, therefore, can be removed if the necessary computational facilities are available. Another significant source of error in a LORAN system is geometrical dilution of precision (GDOP). GDOP is the loss of precision resulting from oblique LOP crossings, at the fringes of coverage. (The greatest precision is afforded by LOP crossings at right angles.) The overall positional accuracy of a LORAN C "fix", within the intended coverage area of a chain, is about 0.5 nautical miles.

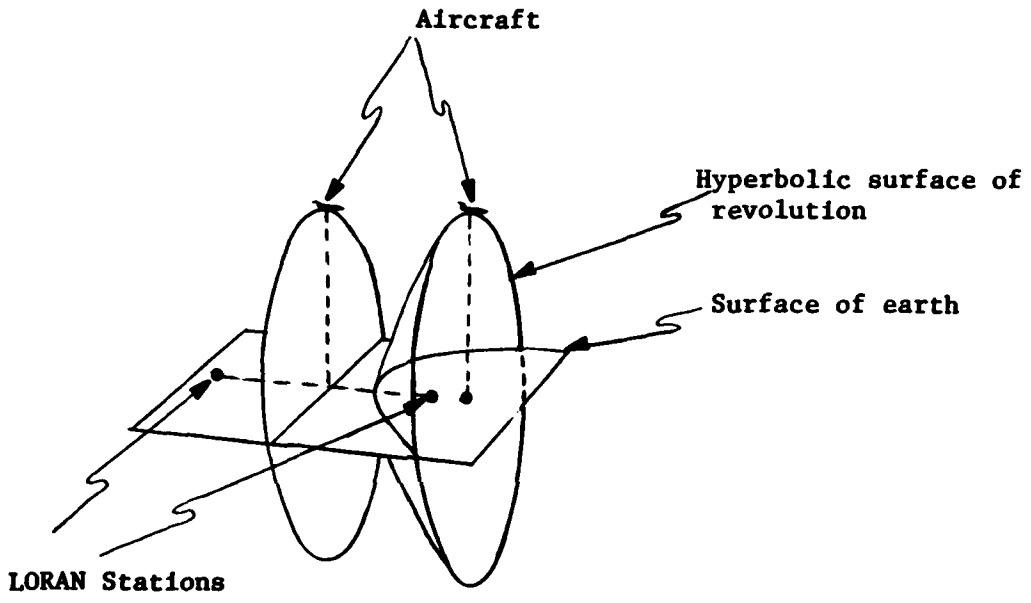

Figure 2.3.7.3--LORAN Hyperbolic surfaces of Revolution

2.3.8 Omega -- In the hyperbolic mode, the Omega radio navigation system establishes a hyperbolic line-of-position by measuring the difference in phase between two continuous-wave (CW) signals transmitted coherently by two known stations. Two pairs of stations provide two such lines-of-position, thereby providing a positional fix. Omega also is used in a direct-ranging mode in which the phase of the signal from a single station is compared to that of an on-board coherent oscillator. Direct-ranging results in circular lines-of-position. The phase of the CW signal received by a user is, of course, a function of the range from the transmitting station to the user (propagation time). The phase measurement is, in effect, a measure of the "time-of-arrival" of the signal. Thus, in the hyperbolic mode, omega is quite similar to LORAN. That is, it is, in effect, a "differential time-of-arrival" system, and therefore, produces hyperbolic lines-of-position. There is, however, a major difference between the operation of Omega and that of LORAN. In LORAN, true time-of-arrival is measured, thereby yielding a unique measure of propagation distance. In Omega, phase difference is measured. Because of the cyclic nature of the phase of a sinusoidal signal, the measured phase difference "folds", or repeats itself, every 360 degrees, thereby yielding an inherently ambiguous measure of propagation distance. The hyperbolic lines-of-position thus repeat themselves indefinitely, as shown in Figure 2.3.8.1. For the phase-difference measured by the receiver at the position indicated, the receiver position could be anywhere on any one of the hyperbolic lines-of-position shown. This inherent ambiguity in the Omega system creates a major problem and can be eliminated only by independent measurements. One source of independent measurement is another navigational system, such as an inertial navigation system, with sufficient accuracy to resolve the ambiguity. A dead-reckoning system such

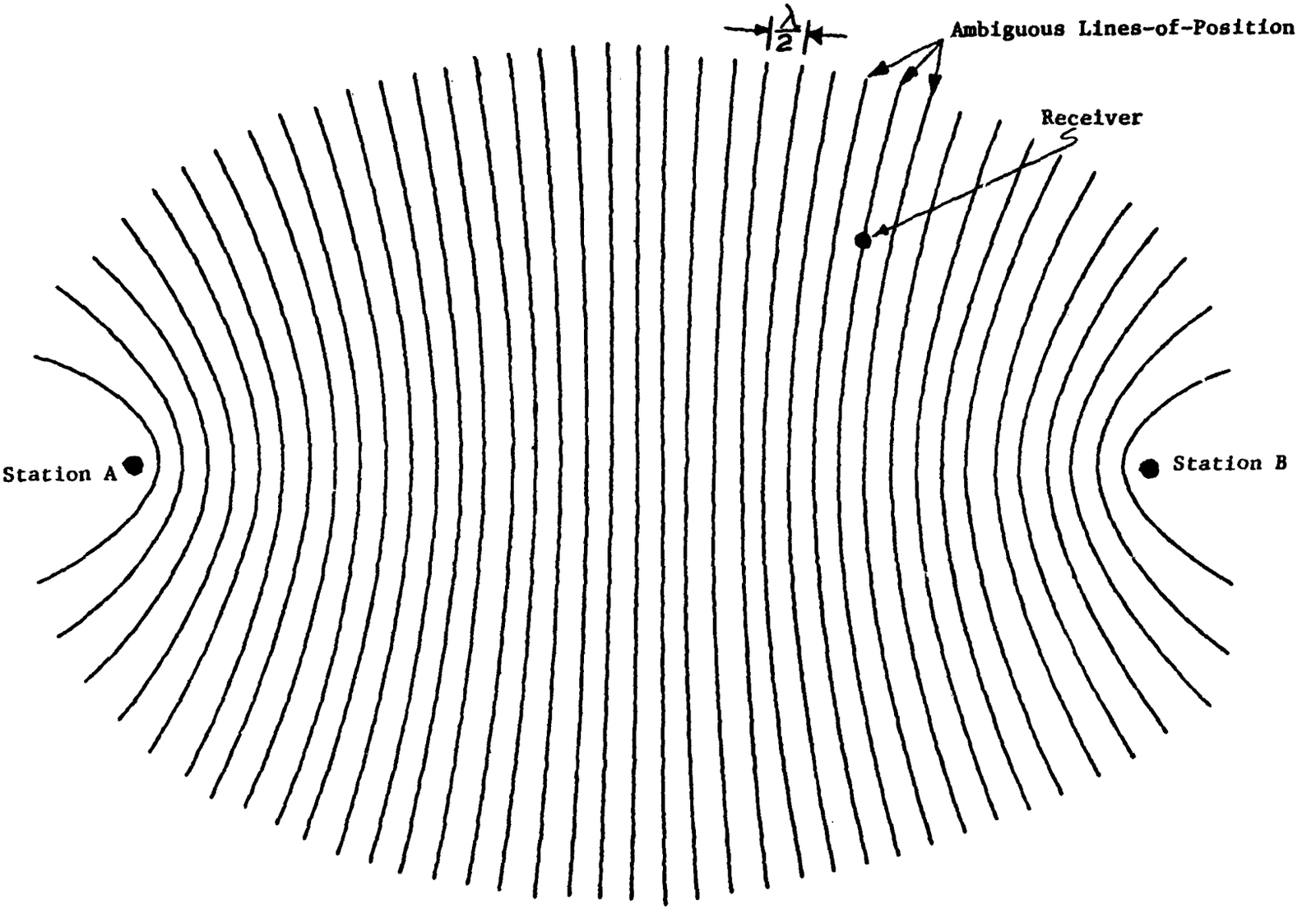

Figure 2.3.8.1--Hyperbolic Lines-of-Position for Omega

as an INS can be used in conjunction with Omega to provide the necessary "memory" required to resolve the Omega ambiguity as the vehicle travels from lane to lane. (The region between two zero-phase-difference LOPs is referred to as a "lane". For the hyperbolic mode, a lane is one-half of a wavelength (8 miles) wide on the baseline between stations. For the direct-ranging mode, it is one wavelength (16 miles) wide). Another type of "memory" is that provided by "lane counting". By counting the number of times a zero-phase-difference LOP is crossed, an omega system can, once initialized, determine which lane it is in, thereby resolving the lane-to-lane ambiguity.

Lane ambiguity can be reduced, (but not eliminated), by utilizing multiple carrier frequencies. Omega stations currently transmit on three frequencies: 10.2, 11.33, and 13.6 kilohertz. Since the physical width of a lane depends upon carrier wave length, the measured phase difference will be different for each of the three frequencies. By combining the results from two or three phase measurements, the effective width of the "composite lane" (region of non-ambiguity) can be extended. (It becomes equal to one-half of the wavelength corresponding to the difference frequency or beat frequency for the two carriers.)

Signal attenuation due to absorption is small at very low frequencies. In addition, the region between the earth and the ionosphere acts as a waveguide at those frequencies. As a result of these two factors, the effective range of omega stations is about 5000 nautical miles. (Because of the relatively low absorption in sea water, Omega transmission can even be received by submerged submarines.) Due to their large effective ranges, only eight Omega stations are required to achieve world-wide navigation coverage. The eight locations are

shown in Figure 2.3.8.2. Although very large transmitting antennas are required, the radiated power of the Omega stations is only 10 kilowatts. (Signal-to-noise ratio is reduced by employing long-integration-time signal filtering in the receivers.)

Omega stations transmit in unique sequences of coherent CW bursts, as indicated in the schedule presented in Figure 2.3.8.3. The coherency of the transmissions is controlled to one part in 10^{12} by the use of atomic clocks (clocks employing Cesium oscillators). (In the direct-ranging mode, the coherency of the on-board oscillator also is controlled by an atomic clock.) As indicated in the schedule, only three stations transmit at any one time, none on the same frequency. (The user equipment incorporates three receivers). In order for a user to compare the phases of the (identical frequency) transmissions of two stations, the user equipment "remembers" the phase of the first station signal by locking the phase of a coherent internal oscillator to that of the signal received from the first station. When the second station transmits that frequency, the user equipment compares the phase of the signal from that station to the phase of its coherent oscillator.

For airborne application, Omega presents several difficulties. One is the size of the required antenna. Precipitation static also is a problem. A loop antenna is the best choice. Another problem with airborne application is the long signal correlation time required (up to two minutes). For an aircraft, the Omega system is useful only in updating a separate, continuously-navigating device. Such a composite system is, in effect, a frequently-updated dead reckoning system.

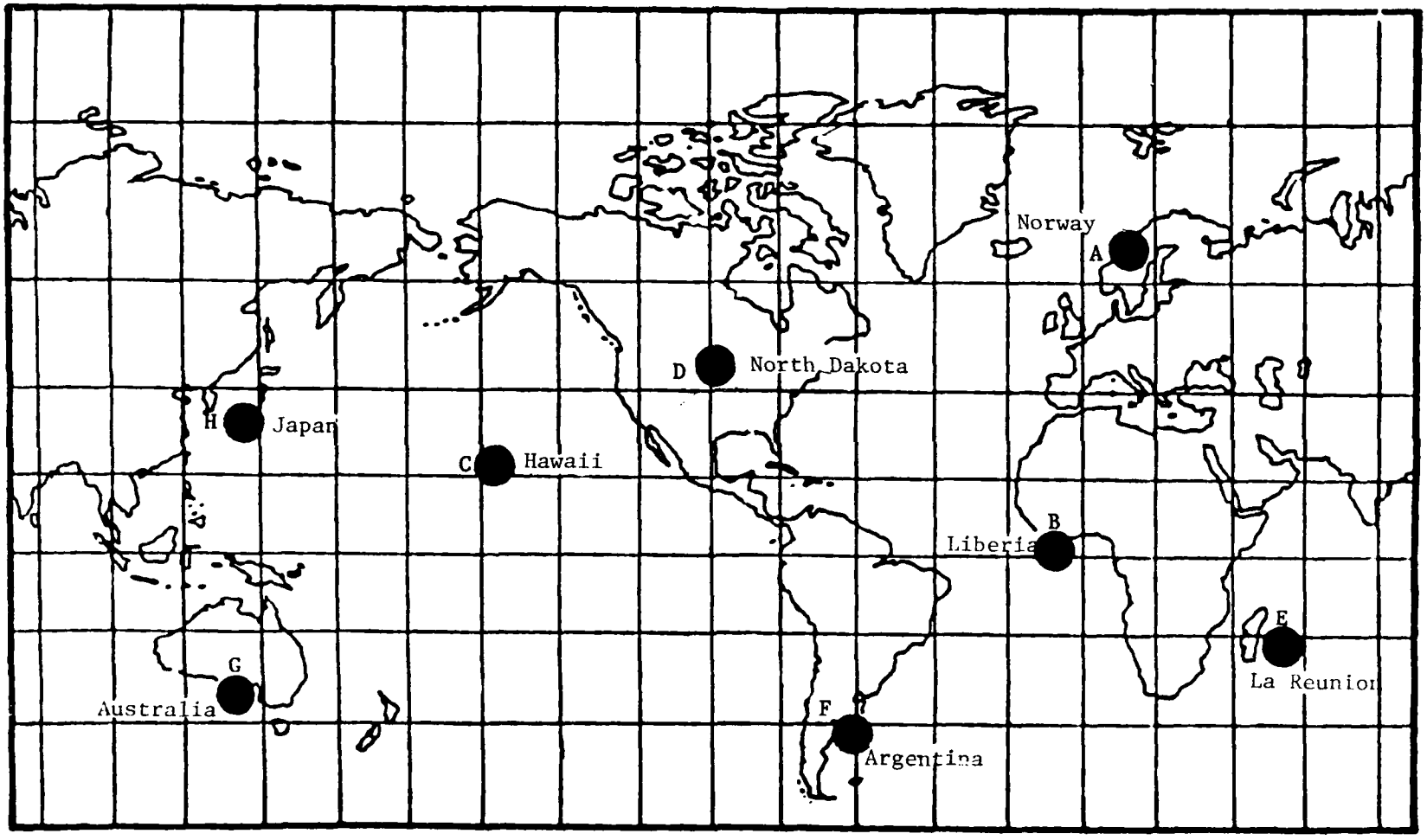

Figure 2.3.8.2-- Omega Station Locations

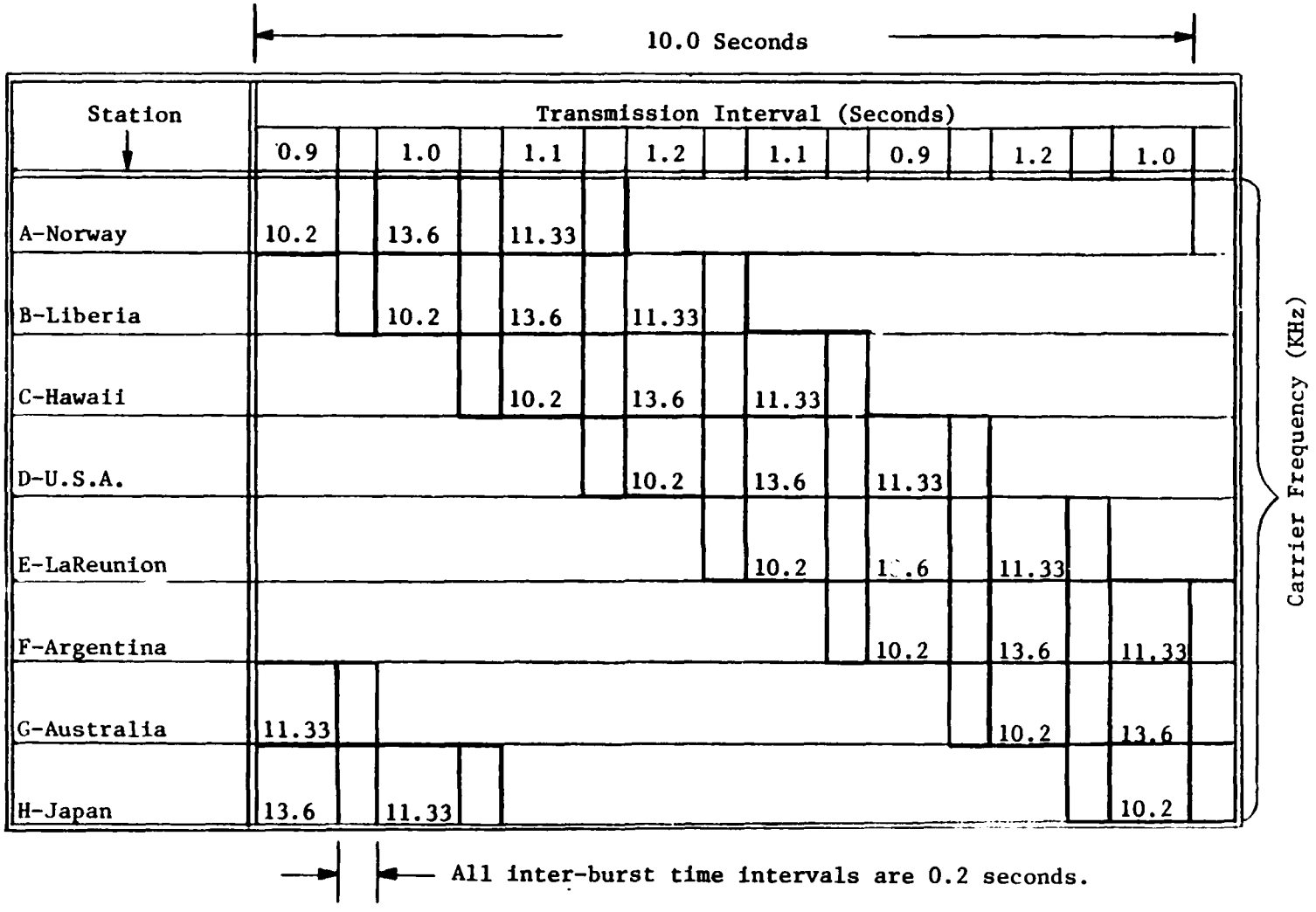

Figure 2.3.8.3--Omega Transmission Sequence

Because of the very large baselines, geometric dilution of precision (GDOP) is small for Omega navigation. The largest source of position error is error in the assumed velocity of propagation of the radio signals. In practice, this error is largely removed by tabulated corrections or by "calibrating" the system by determining the indicated location of a monitor station of precisely known location. In a "manual" system, the operator reads out phase difference from the Omega receiver; applies a tabulated correction based upon solar position, surface conductivity, earth oblateness, the earth's magnetic field, and station-user geometry; and applies the corrected phase difference, in terms of the lane and centi-lane (1/100 of a lane), to a special chart (map) with a superimposed Omega grid. Automated, computerized Omega systems are available which indicate longitude and latitude directly. In addition, the optimum available stations are selected on the basis of signal strength and station-user geometry. Typical positional accuracy for world-wide Omega navigation is one nautical mile for daytime operation and two nautical miles for night time operation. (Night time error is larger because of larger uncertainties in the velocity of propagation of radio waves.) When a nearby monitoring station is used to "calibrate" the system, accuracies of 0.2 nautical miles are attainable.

2.4 Satellite Navigation Systems

2.4.1 General Satellite Navigation Principles -- In a sense, navigation by means of artificial (man-made) satellites is a natural extension of the ancient practice of celestial navigation. There are, however, major differences in the ways in which artificial satellites and natural celestial bodies can be used for navigation. Celestial bodies lend themselves only to line-of-sight angle measurements. Artificial satellites, as a result of their proximity to the earth and the fact that they can carry transmitters, allow range and range-rate measurements as well as angle measurements.

Fundamentally, the satellite navigation process involves the sclution of an oblique triangle similar to the triangle E-S-P shown in Figure 2.4.1.1. That is, it is the task of the navigator to determine any combination of sides and angles that provides a circular line-of-position for the user vehicle. The sides (ranges) and angles (bearings) of the triangle can be measured directly or they can be inferred from measurements of range rate, knowing the relativ velocities of the satellite and the user vehicle. User position also can be determined by differential range measurements, (to two satellites or to a single satellite at two times), yielding hyperbolic lines-of-position.

The essential elements of a satellite navigation system are shown in Figure 2.4.1.2. The user receives information from the satellite, including the satellite's ephemeris and orbital corrections (from which the user determines the position and velocity of the satellite); ranging signals (from which the user determines the range, range-rate, and/or bearing to the satellite); time

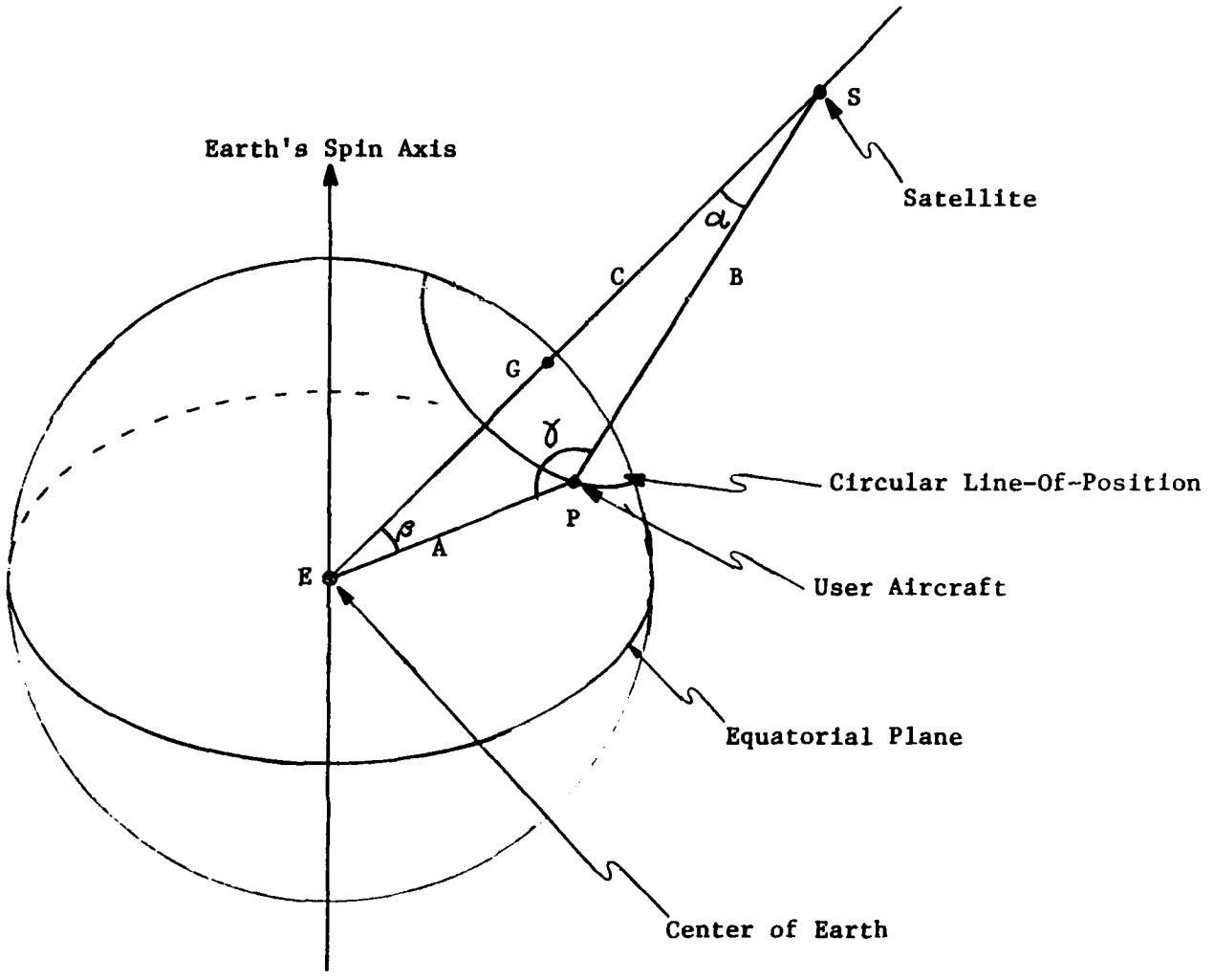

Figure 2.4.1.1.--Satellite Navigation Geometry

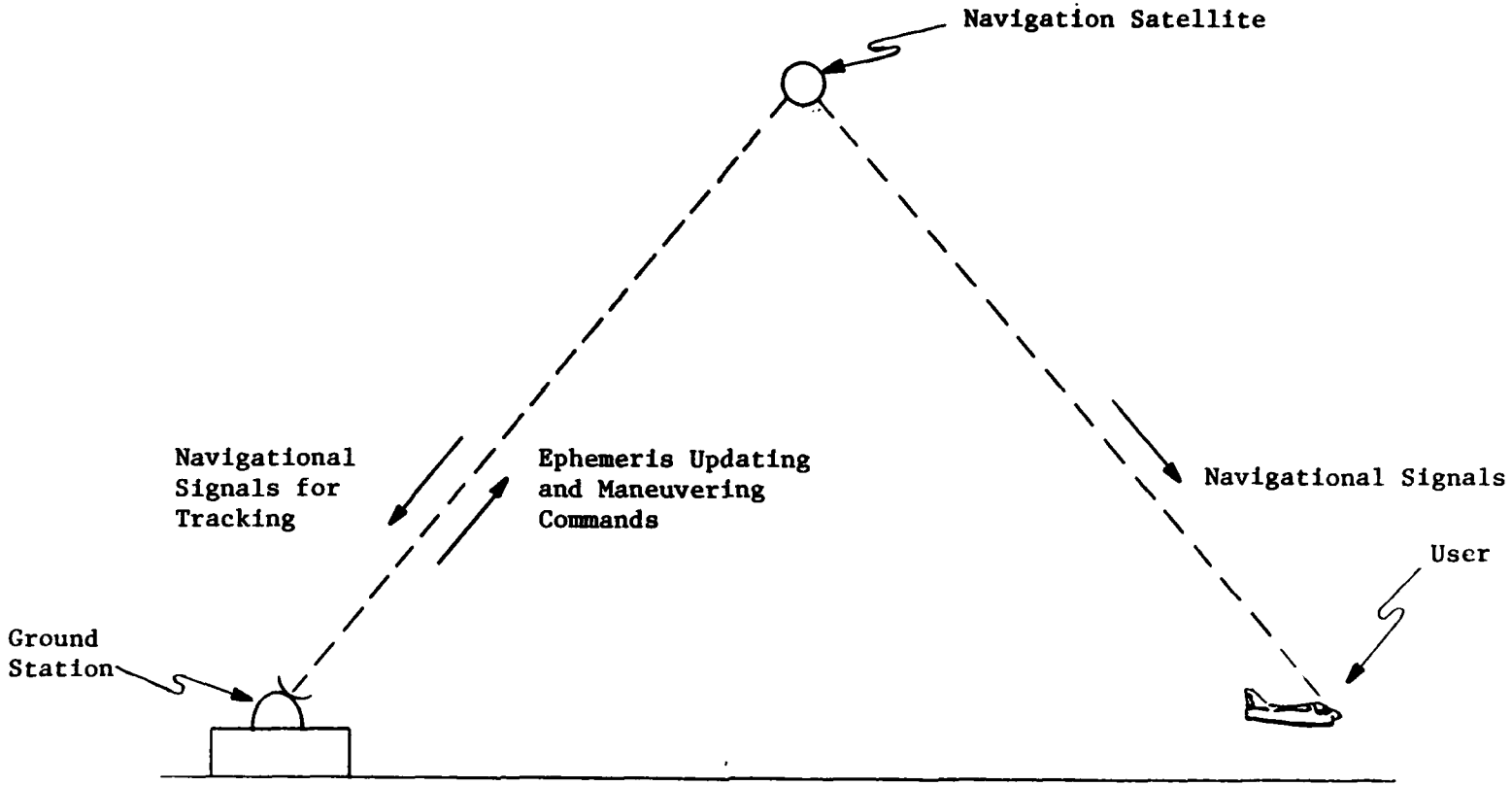

Figure 2.4.1.2--Satellite Navigation Elements

of day; and other information such as signal propagation factors. The ground station tracks the satellite, (from the satellites transmissions or by radar), and uplinks, to the satellite, commands to update the information supplied by the satellite to the user and, possibly, to correct orbital variations.

When user vehicle position is to be determined by measurement of satellite range and/or bearing, the satellite navigation process can be described in the following manner. (Refer to Figure 2.4.1.1.)

(1) From the known satellite ephemeris, determine satellite altitude, C, with respect to the center of the earth, and satellite sub-orbital point, G.

(2) By independent means, (if required), determine the user altitude, A, with respect to the center of the earth.

(3) Measure user vehicle-to-satellite range, B, and/or bearing, γ.

(4) Compute the central angle, β, thereby determining a circular line-of-position for user vehicle location or the projection of that location on the surface of the earth.

(5) Determine a second such line-of-position thereby obtaining a positional fix.

When user vehicle-to-satellite range, B, is measured, compute central angle, β, from the Law of Cosines. That is:

$$\beta = \cos^{-1}\left[\frac{A^2 - B^2 + C^2}{2AC}\right]$$

When satellite bearing, γ, is measured, compute central angle, β, from the Law of Sines. That is:

$$\beta = 180^\circ - \gamma - \sin^{-1}\left[\frac{A \sin\gamma}{C}\right]$$

When satellite range, B, and bearing, γ, are measured, compute central angle, β, from the Law of Sines. That is:

$$\beta = \text{Sin}^{-1}\left[\frac{B \sin\gamma}{C}\right]$$

When user vehicle position is to be determined by measurement of user-to-satellite range rate, the satellite navigation process can be described in the following manner. (Refer to Figure 2.4.1.3.)

(1) From the known satellite ephemeris, determine satellite orbital position and velocity, V, as a function of time.

(2) By independent means, determine user vehicle altitude and velocity.

(3) Measure user-to-satellite range rate by observing Doppler shift in signal transmitted by satellite.

(4) Compute the user-to-satellite range, thereby determining a line-of-position for user vehicle location or the projection of that location on the surface of the earth.

(5) Determine a second LOP, (from a second satellite or the same satellite at a later time), thereby obtaining a positional fix.

Doppler measurements can be utilized in various ways to determine user-to-satellite range. The following development derives an expression for the required slant range in terms of the Doppler shift, f_D, and its time rate of change, $\dot{f}_D$. Referring to Figure 2.4.1.3, the Doppler shift in a signal transmitted by the satellite and received by the user is given by:

$$f_D = \left(\frac{f_o}{c}\right)\dot{R} = \left(\frac{f_o}{c}\right) V \cos\gamma = \left(\frac{f_o}{c}\right) V \sin\theta$$

where:

C = Velocity of Propagation

f_o = Transmitted Frequency

f_D = Doppler Shift

R = User Vehicle-to-Satellite Slant Range

V = Satellite Velocity

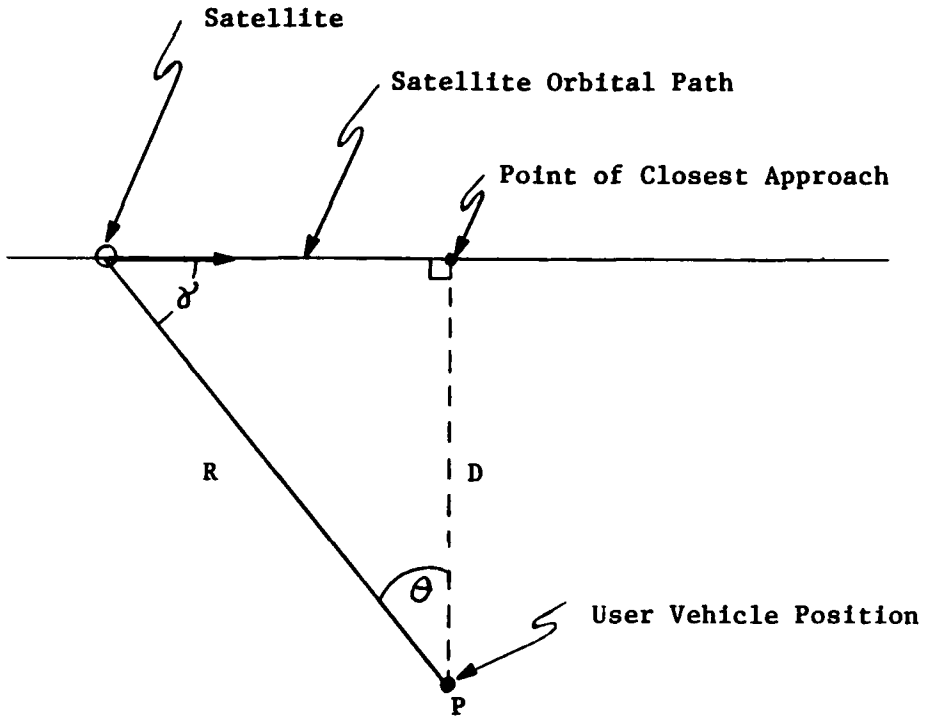

Figure 2.4.1.3 -- Satellite Range Rate Geometry

Thus:

$$\dot{f}_D = \left(\frac{f_o V}{c}\right) \cos\theta \, \dot{\theta}$$

But:

$$\dot{\theta} = \frac{V \cos\theta}{R}$$

So:

$$\dot{f}_D = \frac{V^2 f_o \cos^2\theta}{R c}$$

or, solving for range:

$$R = \frac{V^2 f_o \cos^2\theta}{c \dot{f}_D}$$

where: $$\theta = \sin^{-1}\left[\frac{c \dot{f}_D}{V f_o}\right]$$

The determination of range by means of the above equations is simplified if the Doppler measurement is made at the satellites point of closest approach to the user (as determined by the time of zero Doppler shift). For that case:

$$f_D = 0$$

$$\theta = 0$$

and:

$$R = \frac{V^2 f_o}{c \dot{f}_D}$$

Thus, the satellite location at time of closest approach fixes the location of a plane perpendicular to the satellites orbital path, and the time-rate-of-change of Doppler shift determines the distance, D, in that plane, between the satellite position and the user. The altitude of the user completes the positional fix.

Satellite radio navigation possesses both major advantages and major disadvantages with respect to other methods. The major advantages are:

(1) All-Weather Service -- Direct line-of-sight, primarily exo-atmospheric, propagation is less subject to atmospheric disturbances than that of terrestrial systems. Radio frequencies are much less susceptible to atmospheric absorption than are optical frequencies used in celestial navigation.

(2) Worldwide Service with Few "Stations" -- Orbital altitudes provide wide coverage (remote radio horizons). Non-synchronous satellites "sweep" earth's surface.

(3) Extreme Accuracy at Remote Locations -- Direct propagation path provides accuracy normally associated only with "local" navigation facilities.

(4) Ease of Automation -- Automatic "tracking" (navigation) is less difficult than optical (angle) tracking of celestial bodies.

(5) Secure Operation -- Satellite transmissions can be encoded for wartime military purposes. User equipment can be passive.

The major disadvantages are:

(1) High-Cost "stations" -- Satellites are complex and expensive to place into orbit. Maintenance is also expensive.

(2) Non-Stationary "stations" -- Satellites must be continuously tracked and their orbital parameters transmitted to users. Orbital corrections may be required.

(3) Low Level Signals -- Because of satellite-to-user distances and necessarily low-power transmissions, satellite navigation requires high-gain user receivers and/or antennas.

(4) Satellite Vulnerability -- An orbiting satellite is an attractive military target.

2.4.2 Transit -- The Transit satellite navigation system utilizes low altitude satellites in polar orbits about the earth. (Altitude is about 600 n. miles; orbital period is about 2 hours.) The user measures the Doppler shift of a CW signal transmitted by the satellite, thereby inferring his position with respect to the known position of the satellite. (The analytic relationship between Doppler shift and user-to-satellite range is derived later in this section.) In addition to the "Doppler reference" signal, the satellite transmits its own orbital parameters and the time of day. (These quantities are determined by ground tracking stations and uplinked to the satellites periodically.) The altitude and velocity of the user must be determined independently and input to the Transit computations.

The Transit signals are utilized by the navigator in a way that makes Transit, in effect, a differential range (hyperbolic) navigation system. The user differences the frequency of the (Doppler shifted) received signal with the frequency of an on-board stable oscillator. (The stable oscillator frequency is offset, by a fixed amount, from that of the signal transmitted by the satellite.) The difference between the received and local oscillator frequencies is then integrated (counted) to obtain a measure of the difference in the user-to-satellite ranges at the beginnings and the ends of counting intervals defined by timing signals transmitted by the satellite. Satellite positions and the corresponding user-to-satellite ranges are depicted, in Figure 2.4.2.1, for four demarcation times. As can be seen from the figure, the measurements yield the equivalent of differential ranges to four separate satellites of known position.

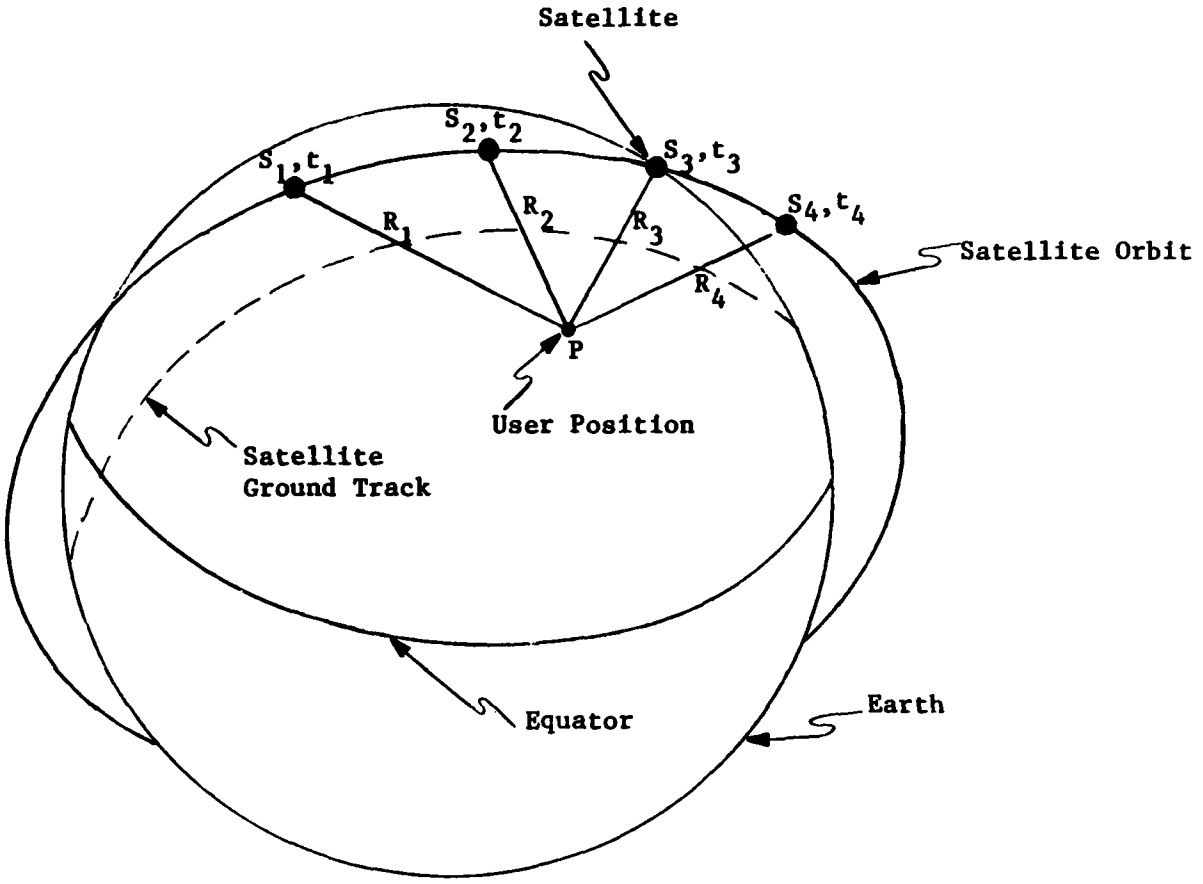

Figure 2.4.2.1 -- Transit Satellite Navigation

In the following development, equations are derived for the user-to-satellite differential ranges in terms of the cycle counts, (integrals of the difference in the received and local oscillator frequencies), for a typical time interval shown in the figure.

The Doppler frequency shift in the signal transmitted by the satellite and received by the user is given by:

$$f_D = f_R - f_T = \frac{f_T \dot{R}}{C}$$

where:
- C = Velocity of Propagation of Signal
- f_D = Doppler Frequency Shift
- f_R = Received Frequency
- f_T = Transmitted Frequency
- $\dot{R}$ = User-to-Satellite Slant Range Rate

Solving for range rate:

$$\dot{R} = \left(\frac{C}{f_T}\right)(f_R - f_T)$$

Indicating the frequency offset between the satellite transmitter and user local oscillator as Δf:

$$\dot{R} = \left(\frac{C}{f_T}\right)(f_R - f_L + \Delta f)$$

where:

- f_L = User Local Oscillator Frequency

Integrating both sides of the equation between the times of receipt of two successive interval-demarcing signals:

$$R_{n+1} - R_n = \left(\frac{C}{f_T}\right) \int_{t_n + \frac{R_n}{C}}^{t_{n+1} + \frac{R_{n+1}}{C}} (f_R - f_L)\, dt + \left(\frac{C}{f_T}\right) \int_{t_n + \frac{R_n}{C}}^{t_{n+1} + \frac{R_{n+1}}{C}} (\Delta f)\, dt$$

where:

R_n = User-to-Satellite Range at $t = t_n$.

R_{n+1} = User-to-Satellite Range at $t = t_{n+1}$.

The first term on the right of the above equation is the total difference-frequency cycle count, $N_{n,\ n+1}$, for the time interval t_n to t_{n+1}.

Thus:

$$R_{n+1} - R_n = \left(\frac{c}{f_T}\right) N_{n,n+1} + \left(\frac{\Delta f}{f_T}\right)\left[(R_{n+1} - R_n) + c(t_{n+1} - t_n)\right]$$

or:

$$R_{n+1} - R_n = \frac{\left(\frac{c}{f_T}\right) N_{n,n+1} + c(t_{n+1} - t_n)\left(\frac{\Delta f}{f_T}\right)}{1 - \left(\frac{\Delta f}{f_T}\right)}$$

Since $\left(\frac{\Delta f}{f_T}\right) \ll 1$:

$$R_{n+1} - R_n = \left(\frac{c}{f_T}\right) N_{n,n+1} + c(t_{n+1} - t_n)\left(\frac{\Delta f}{f_T}\right)$$

If the frequency offset (Δf) were known, the above equation would yield the required differential range in terms of known and measured quantities. When (Δf) is unknown, (though constant over the satellite transit time), successive measurements (intervals) yield the necessary equations to eliminate (Δf). In any event, at least two such measurements (counts) would be required to solve for user position (latitude and longitude). (Altitude is known independently.) In actual practice many successive measurements (counts) are made and the results are combined by least squares to obtain a best estimate of position.

The ranges and range rates depend upon satellite position and velocity as well as user position and velocity. Satellite position and velocity are known for all time as a result of the orbital information broadcast by the satellite. In order to reduce user position to an equivalent latitude-longitude pair, user position must be extrapolated from time-point to time-point by dead reckoning. Also, the effects of user velocity must be removed from the Doppler shift. The short-term navigation requirement, in addition to the requirements to know user altitude and velocity accurately, imply the use of an inertial navigation system or its equivalent. For airborne applications, Transit generally is used as an update for an INS or Doppler navigator.

Sources of Error -- Random errors due to noise in Transit navigation are small as a result of the excellent smoothing provided by the counting (integrating) process. There are, however, several contributors to bias errors. The major contributors are:

Velocity of Propagation (Index of Refraction) Error
Error in User Velocity
Error in User Altitude
Instability in Local Oscillator Frequency
Errors in Dead Reckoning
Errors in Satellite Orbital Parameters

The errors due to anomalies in the signal velocity of propagation are largely removed by signal transmission at two carrier frequencies (150 MHz and 400 MHz.). (Velocity of propagation error is a known function of frequency and can be removed by redundant measurements at two frequencies.) Refraction (propagation) errors are greatest when the satellite orbit is low in the sky. Geometric dilution of precision (GDOP) is greatest when the satellite orbit is directly overhead. Favorable conditions exist when the elevation of the satellite, at the user position, is between 15° and 75°.

All errors are greatly reduced by the use of recursive estimation techniques. (Successive approximations are made of user position and local oscillator offset frequency). The total (RSS) error for a high-quality Transit navigator, under favorable conditions, is less than 100 feet.

2.4.3 Global Positioning System -- The Global Positioning System (also called GPS or Navsat) is a satellite navigation system that provides user position and velocity in three dimensions. Basically, position is determined by passive ranging and velocity is determined by measuring the Doppler shift in the signals received by the user. (In sophisticated systems, position, velocity, and various system parameters are determined, simultaneously, by optimal estimation techniques). Each satellite transmits the following information in a 1500 bit word; at a 50 bit per second rate:

Satellite Ephemeris
Time of Day
Signal Propagation Information
Satellite Operational Status
Acquisition Information on Other Satellites
Special Messages

The satellite ephemeris provides, to the user, knowledge of the position of the satellite. The time signal allows the user to determine the time of transmission of the signals transmitted by the satellite. The signal propagation information allows the user to make corrections to the value for the signal velocity of propagation employed in the range computations. The remaining information assists the user (or his equipment) in selecting and acquiring an optimal set of satellites for navigational purposes.

In order to provide world-wide coverage, the GPS satellite system consists of 18 satellites, 3 in each of six planes. The orbital planes have inclinations of 55 degrees and are spaced 60° apart. The 3 satellites in each plane are equally spaced in their common orbit. All of the satellites are in circular orbits of 10,898 nautical mile altitude and, therefore, have 12-hour orbital

periods. The satellite configuration is depicted in Figure 2.4.3.1. In order to provide maximum uniform coverage (signal strength), directional, shaped-beam antenna arrays are employed on the satellites, which are attitude stabilized with respect to the earth.

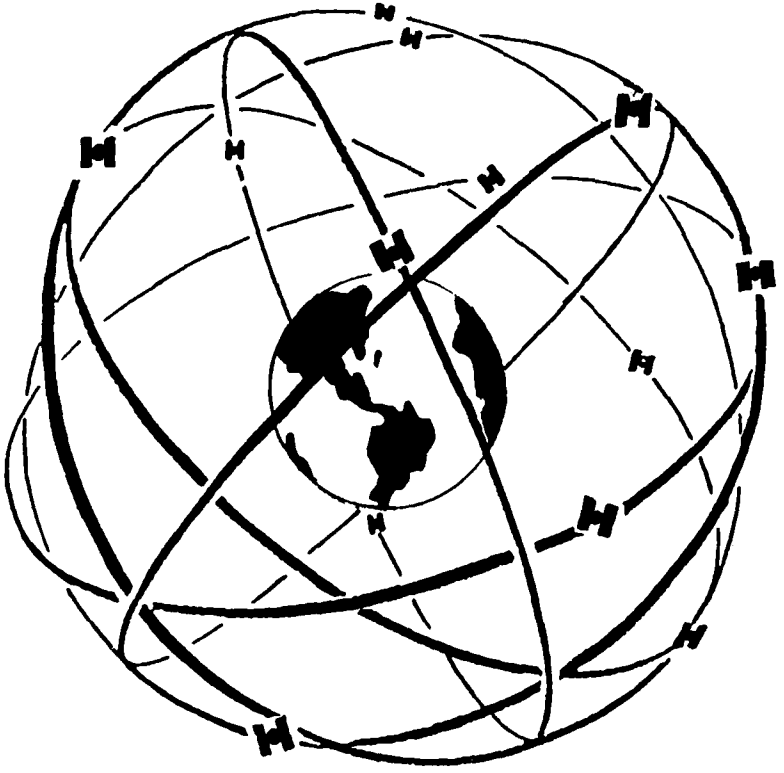

Figure 2.4.3.1 -- Global Positioning System Satellite Orbits

The basic equations used to determine the position of the user are presented below. (Refer to Figure 2.4.3.2.)

$$R_1 = [(x_1 - x)^2 + (y_1 - y)^2 + (z_1 - z)^2]^{1/2} = c(t_{R1} - t_{T1} + \Delta t)$$
$$R_2 = [(x_2 - x)^2 + (y_2 - y)^2 + (z_2 - z)^2]^{1/2} = c(t_{R2} - t_{T2} + \Delta t)$$
$$R_3 = [(x_3 - x)^2 + (y_3 - y)^2 + (z_3 - z)^2]^{1/2} = c(t_{R3} - t_{T3} + \Delta t)$$
$$R_4 = [(x_4 - x)^2 + (y_4 - y)^2 + (z_4 - z)^2]^{1/2} = c(t_{R4} - t_{T4} + \Delta t)$$

where:

C = Velocity of Signal Propagation

R_1, R_2, R_3, R_4 = User-to-Satellite Ranges

$t_{R1}, t_{R2}, t_{R3}, t_{R4}$ = Times of Receipt of Coded Signals

$t_{T1}, t_{T2}, t_{T3}, t_{T4}$ = Times of Transmission of Coded Signals

X, Y, Z = Coordinates of User

X_i, Y_i, Z_i = Coordinates of i^{th} Satellite

Δt = Time Offset in User Clock

As indicated by the equations, the positions of the satellites and that of the user are represented in cartesian coordinates. (The coordinate system employed is geocentric and fixed to the rotating earth.) If the user clock were perfectly synchronized with the clock in the satellite, the user clock time offset, Δt, would be zero; and the above equations would contain three unknown quantities: the coordinates of the user; X, Y, and Z. (All other quantities would be known or measured.) In that case, any three of the equations would contain the necessary information to solve for the user position, and the problem would be one of simple ranging to three known "stations". The positional

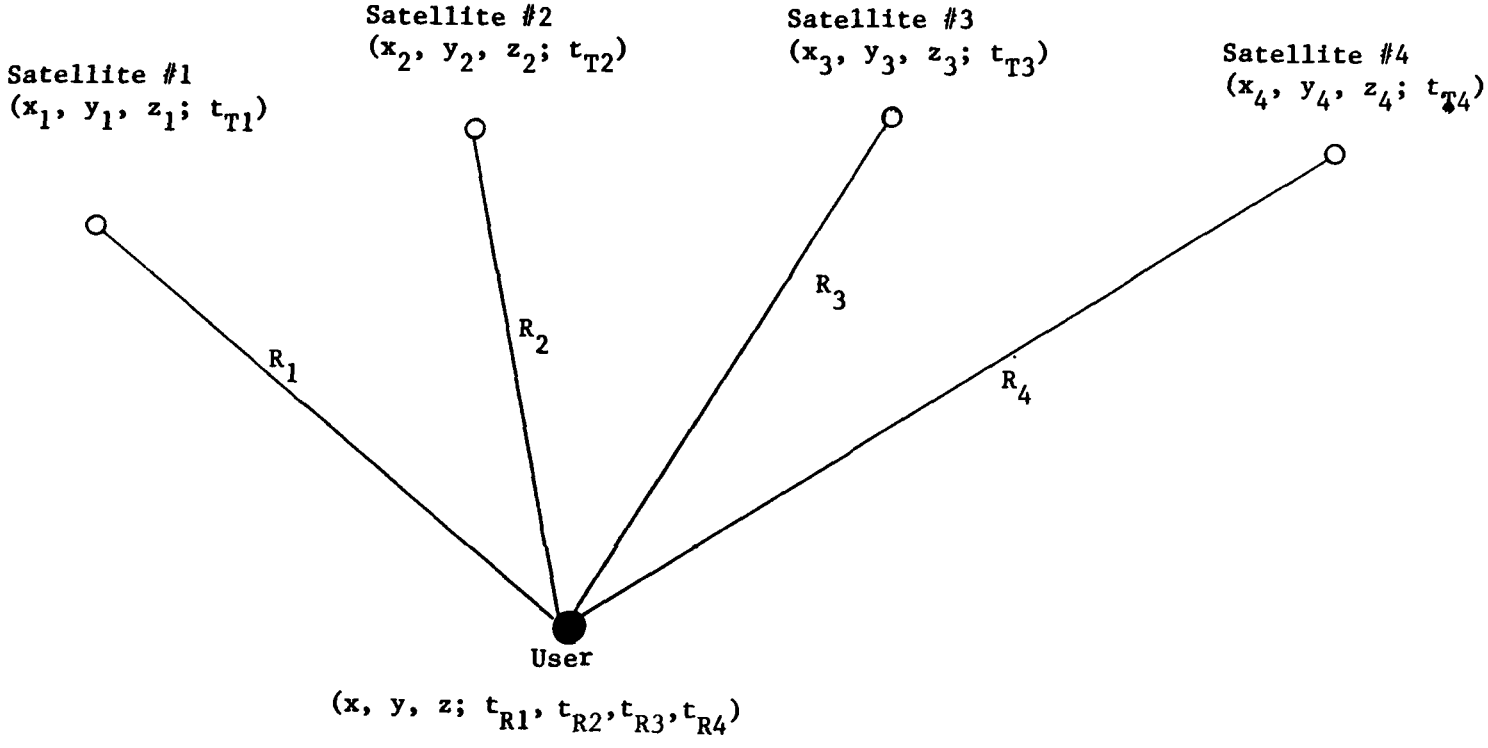

Figure 2.4.3.2 -- Global Positioning System Geometry

fix would then represent the common intersection of three spheres. In general, the time offset, Δt, is unknown and four measurements (four equations) are required to solve for the user position and the time offset. (If user altitude is known, three equations are sufficient to solve for two dimensional user position (e.g. longitude and latitude) and the time offset.) With the time offset unknown, the navigation process is sometimes called pseudo-ranging, since the unknown time offset can be considered as part of a "pseudo-range". That is:

$$R_i = \left[(x_i - x)^2 + (y_i - y)^2 + (z_i - z)^2\right]^{1/2} - c\,(\Delta t)$$

The GPS consists of three parts as indicated in Figure 2.4.3.3: the satellite segment, the user segment, and a ground-based control segment. The function of the control segment is to track the satellites; determine signal propagation corrections, satellite timing errors, and other system parameters; and uplink that information to the satellites, to be re-transmitted by the satellites to the user. The satellite orbital parameters (ephemeris) are determined by analysis of the satellite transmissions received by several monitor stations located worldwide. In order to allow determination of the signal propagation parameters, the satellites transmit on two frequencies: 1227.6 megahertz and 1575.42 megahertz. (Since the velocity of propagation is a known function of frequency, redundant transmissions allow determination of the effective coefficient of refraction.) The satellites incorporate atomic-frequency-standard clocks stable to one part in 10^{13} per day. Nevertheless, the satellite time signals are monitored by the ground stations and corrected by uplink transmissions. (The timing corrections even include a rate offset to compensate for relativistic effects caused by the satellite velocities with respect to an earth observer.)

The GPS ranging function is accomplished by time-coloring the transmitted signals, utilizing pseudo-random binary codes. The 1227 megahertz signal carries only the precision, (P), code, consisting of a 7-day-long, pseudo-random binary sequence. The 1575 megahertz signal carries both the P code and the clear-access, (C/A), code, consisting of a one-millisecond-long, pseudo-random binary sequence. The long P code is intended to provide maximum timing accuracy and maximum security when the P code is employed for encryption. The short C/A code is intended for ease of acquisition. (The user normally acquires (locks on) the C/A code first, and then acquires the P code utilizing data acquired from the C/A code information.

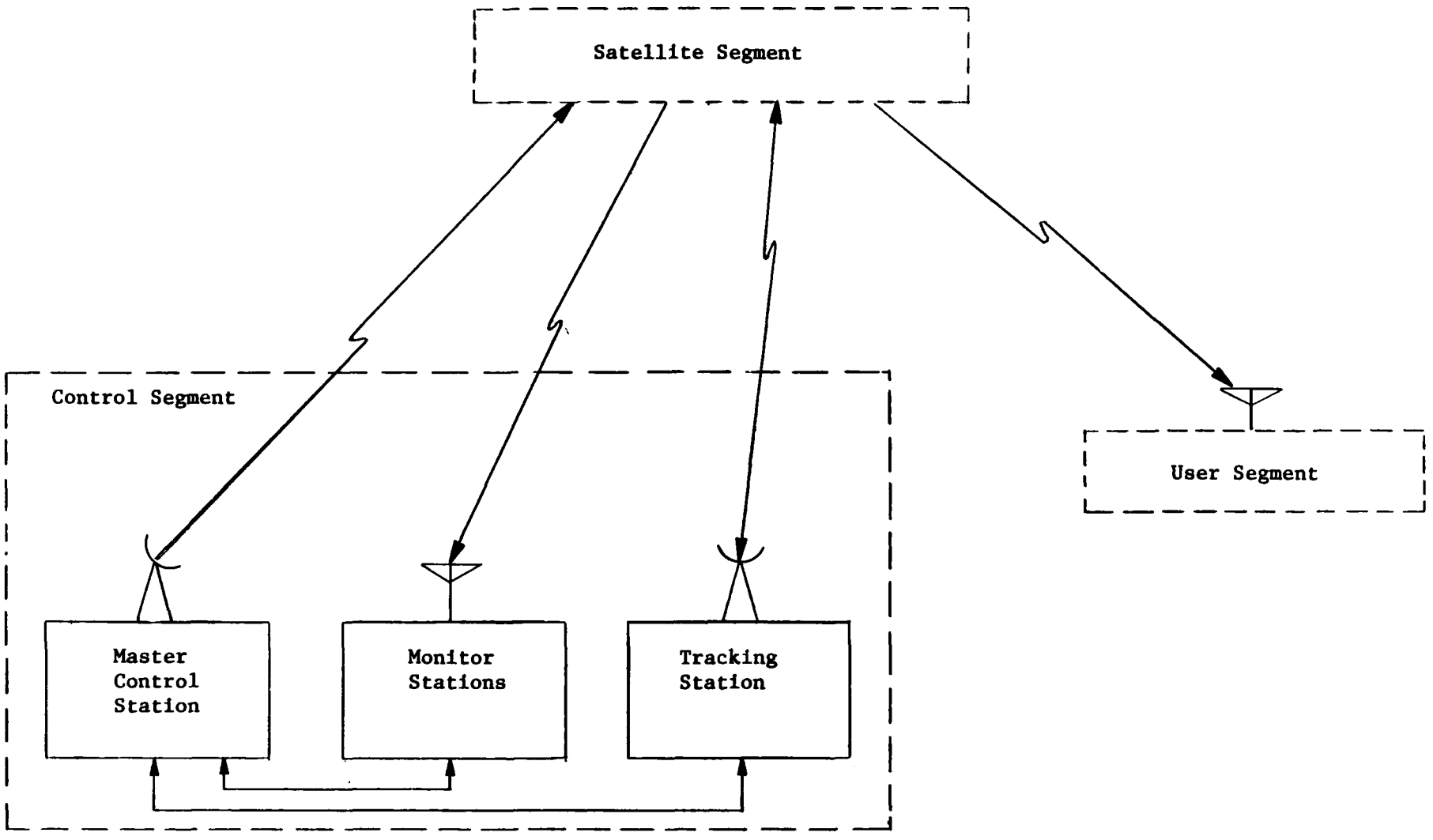

Figure 2.4.3.3 -- The Global Positioning System Network

Timing (ranging) is accomplished by adjusting the phase (timing) of an identical binary sequence (code), generated by the user equipment, until the satellite and user codes match. The necessary phase (time) offset is then a measure of the signal propagation time (range). Depending upon the complexity (accuracy) of the user data reduction process, a positional fix can be obtained in a time ranging from tens of seconds to several minutes. For the latter case, airborne application of GPS would require that it be used as a precision update for an INS or other dead reckoning system.

The major sources of GPS ranging error are listed below with the one-sigma values of the error remaining after correction by the system.

Source	Error (Ft)
Propagation Delays	15
Multipath Effects	7
Satellite Ephemeris and Timing	8
User Equipment Errors	5
RSS Total	19

The one-sigma total (RSS) error in range-rate is less than 0.5 feet per second, for a typical airborne system. Geometric dilution of precision determines the manner in which the above range and range-rate errors propagate into horizontal and vertical errors. Propagation errors are greatest for satellites near the horizon at the user position. GDOP effects depend on the positions of the satellites utilized, and provide the principal basis upon which the satellites are selected, either manually or automatically. With favorable geometry, the one-sigma position, velocity, and time errors are as shown in the following table.

	Position Error (Ft)	Velocity Error (Ft/Sec)	Time Error (Nanosecs)
Horizontal	27	0.3	25
Vertical	41	0.4	

Listed below are the principal characteristics of the GPS satellite navigation system.

- Accurate, 3-Dimensional Position and Velocity
- Accurate Time of Day
- World-Wide Coverage
- All-Weather Operation
- Real-Time, Continuous Information
- Unlimited Simultaneous Users
- Passive User Operation
- Jam-Resistant Operation
- Controlled Access

The above characteristics make GPS suitable for the following applications.

- Enroute Navigation
- Way-Point Steering
- Rendezvous
- Reconnaissance
- Weapon Delivery
- Close Air Support
- Remotely Piloted Vehicles
- Universal Time Standard
- Test Range Instrumentation
- Remote Sensing and Tracking

3.0 Navigation System Characteristics

3.1 General Navigation System Performance Characteristics

3.1.1 The Error Model -- For purposes of functional test planning, the performance characteristics of a navigation system are best expressed in terms of an error model. An error model consists of a set of analytical expressions (equations) relating errors in the output(s) of the system to corresponding errors in the input measurements and parameters of the system. For example, if the output, z, of a system is related to the inputs, x and y, and the system parameters, a and b, by the functional relationship:

$$z = f(x, y, a, b),$$

then the error in the output, Δz, is related to the input measurement errors, Δx and Δy, and the parameter errors, Δa and Δb, by the equation:

$$\Delta z = \left(\frac{\partial f}{\partial x}\right)\Delta x + \left(\frac{\partial f}{\partial y}\right)\Delta y + \left(\frac{\partial f}{\partial a}\right)\Delta a + \left(\frac{\partial f}{\partial b}\right)\Delta b$$

This equation represents the error model for the simple system assumed. An evaluation of the partial derivatives, (a sensitivity analysis), reveals the important error contributors (characteristics) of the system. The error model includes the effects due to geometrical dilution of precision (GDOP) as well as those due to internal system parameters. Note that, for systemswith significant internal dynamics, the partial derivatives can be functions of time.

The statistical nature of system errors should be recognized. Specifically, it should be noted that, from the viewpoint of system evaluation, errors are of two basic kinds: deterministic and random. Deterministic errors are predictable. They are sometimes referred to as "biases"; and, often, can be identified and removed. (Note that such "biases" may be time-varying.) Random errors are unpredictable or uncorrelated in time. Both types of error must be included in the error model. Note that "systematic" errors must be treated as random when only their statistics are known. When determining the total statistically-expected system error due to several random (statistically uncorrelated) error sources, the individual expected errors (average, rms, or one-sigma values) cannot be added directly as implied by the above equation for the total systematic error, Δz. When the individual errors; Δx, Δy, Δa, and Δb; are uncorrelated, the total expected error, Δz, is given by the RSS relationship:

$$\Delta z = \left[\left(\frac{\partial z}{\partial x}\right)^2 (\Delta x)^2 + \left(\frac{\partial z}{\partial y}\right)^2 (\Delta y)^2 + \left(\frac{\partial z}{\partial a}\right)^2 (\Delta a)^2 + \left(\frac{\partial z}{\partial b}\right)^2 (\Delta b)^2 \right]^{1/2}$$

3.2 Inertial Navigation System Functional Characteristics

3.2.1 The INS Error Model -- The major sources of error is an INS are listed below.

Gyroscope Errors

Output Drift Rate
Torquing Error
Scale Factor Error
Acceleration-Induced Error
Nonlinearity
Misalignment

Accelerometer Errors

Output Bias
Scale Factor Error
Cross-Acceleration Error
Nonlinearity
Misalignment

Gimballed-Platform Error

Acceleration-Induced Error
Structural Misalignment
Mass Unbalance
Vehicle Motion Isolation Inadequacy

Computer and Software Errors

Gravity Model Errors
Sensor Compensation Error
Analog-to-Digital Conversion Error
Truncation and Roundoff Error
Computational Algorithm Approximations

Initialization, Update, Gyrocompassing, and Damping Errors

Position and Velocity Errors
Platform Alignment Errors

The error model for a semi-analytic, north-pointing, undamped, un-updated INS can be derived from the block diagrams presented in Figures 2.6.1.1, by injecting each error factor into the system at the proper point and with the proper coefficient. The block diagram of that portion of an INS error model pertaining to the north channel of such an INS is shown in Figure 3.2.1.1. From that diagram and those for the other channels, the following individual north position error equations can be derived. (Similar models apply to the vertical and east channels. Since all channels are cross-coupled, the entire error model (all channels) must be considered in deriving expressions for the error functions.)

Initial Position Error (Δy_o)

$$\Delta y = (\Delta y_o) \text{ Cos } (\Omega_E t)$$

where: Ω_E = Earth Spin Rate

Initial Velocity Error ($\Delta \dot{y}_o$)

$$\Delta y = (\Delta \dot{y}_o / \omega_s) \text{ Sin } (\omega_s t)$$

where: $\omega_s = \sqrt{g/R}$

Accelerometer Bias ($\Delta \ddot{y}_o$)

$$\Delta y = (\Delta \ddot{y}_o) \quad (R/g) \quad [1 - \text{Cos } (\omega_s t)]$$

Initial Platform Alignment Error about east-west axis ($\Delta \phi_o$)

$$\Delta y = (\Delta \phi_o) \; R \; [1 - \text{Cos } (\omega_s t)]$$

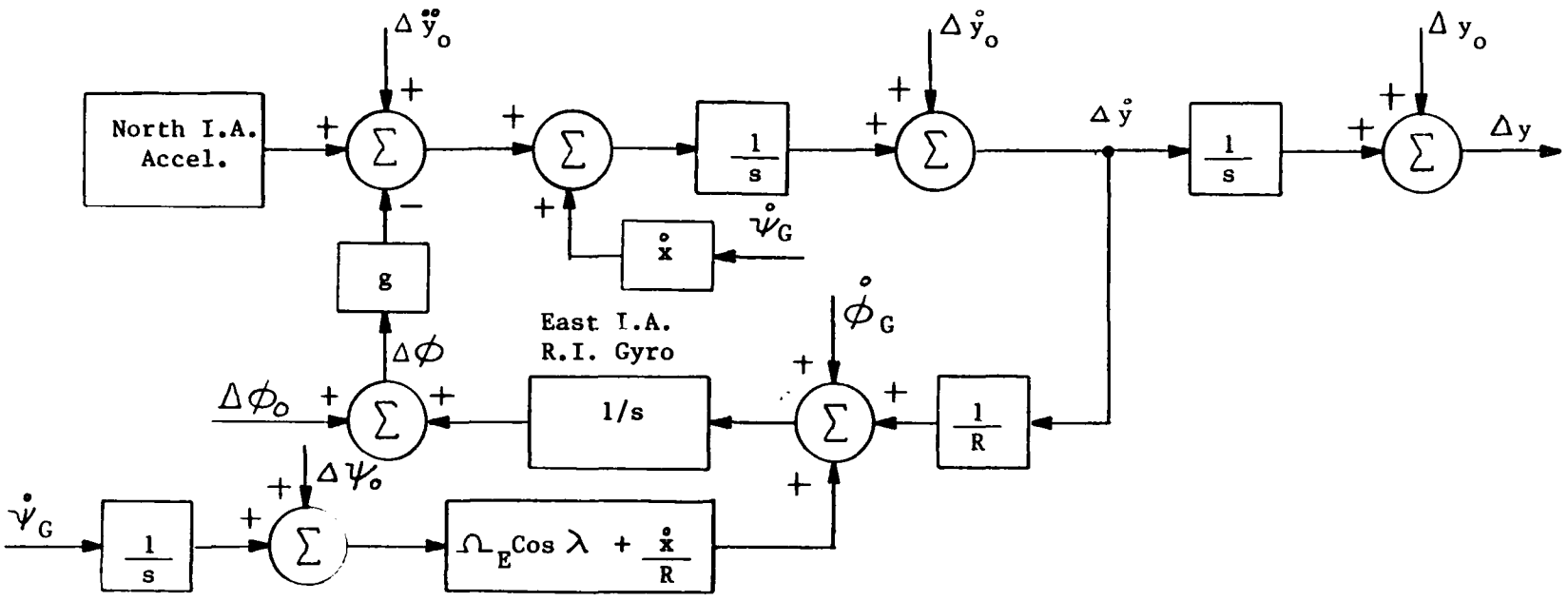

g = Gravitational Acceleration

R = Earth Radius

$\dot{x}$ = East Velocity

$\dot{\phi}_G$ = East I.A. Gyro Drift Rate

Δy = Error in Computed North Position

$\Delta \dot{y}$ = Error in Computed North Velocity

Δy_o = Error in Initial North Position

$\Delta \dot{y}_o$ = Error in Initial North Velocity

$\dot{\psi}_G$ = Azimuth Gyro Drift Rate

λ = Latitude

Ω_E = Earth Spin Rate

$\Delta \ddot{y}_o$ = Error in Initial North Acceleration

$\Delta \phi$ = Error in Platform Angle about East-West Axis

$\Delta \phi_o$ = Error in Initial ϕ

$\Delta \psi_o$ = Error in Initial Platform Azimuth

Figure 3.2.1.1 -- Error Model for North Channel of Semi-Analytic INS

AD-A130 540 AIRBORNE SYSTEMS COURSE TEXTBOOK NAVIGATION SYSTEMS TEST AND EVALUATION(U) NAVAL TEST PILOT SCHOOL PATUXENT RIVER MD G W MASTERS 01 SEP 81 3/3

UNCLASSIFIED F/G 5/9 NL

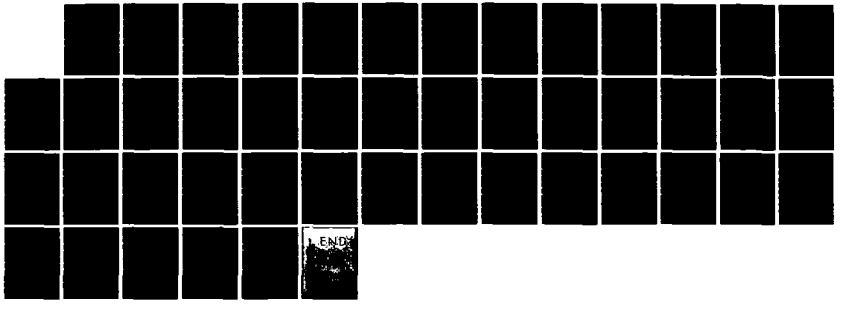

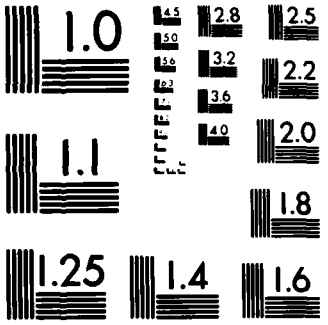

Initial Azimuth Alignment Error ($\Delta\psi_o$)

$$\Delta y = (\Delta\psi_o)\ R\ \text{Cos}\ (\lambda)\ [\Omega_E t - (\Omega_E/\omega_s)\ \text{Sin}\ (\omega_s t) + \text{Sin}\ (\Omega_E t)]$$

Azimuth Gyro Drift Rate ($\dot{\psi}_G$)

$$\Delta y = (\dot{\psi}_G)\ R\ \Omega_E\ \text{Cos}\ (\lambda) \left\{(1/2)t^2 - (1/\omega_s^2)\ [1 - \text{Cos}\ (\omega_s t)]\right\}$$

East-Input-Axis Gyro Drift Rate ($\dot{\phi}_G$)

$$\Delta y = (\dot{\phi}_G)\ R\ [t - (1/\omega_s)\ \text{Sin}\ (\omega_s t) + (1/\Omega_E)\ \text{Sin}\ (\Omega_E t)]$$

As can be seen from the above equations, there are constant errors, errors that increase with time, errors that oscillate at the Schuler frequency, and errors that oscillate at the earth rate frequency.

Time plots for typical individual INS errors are presented in Figures 3.2.1.2. It should be noted that some inertial navigation systems attempt to determine, and compensate for, errors due to many of the error sources included in the error model shown in Figure 3.2.1.1. When that is the case, the error coefficients of interest are those remaining after compensation. It also should be noted that, on a statistical basis, the errors due to individual, statistically-uncorrelated error coefficients must be RSS'd.

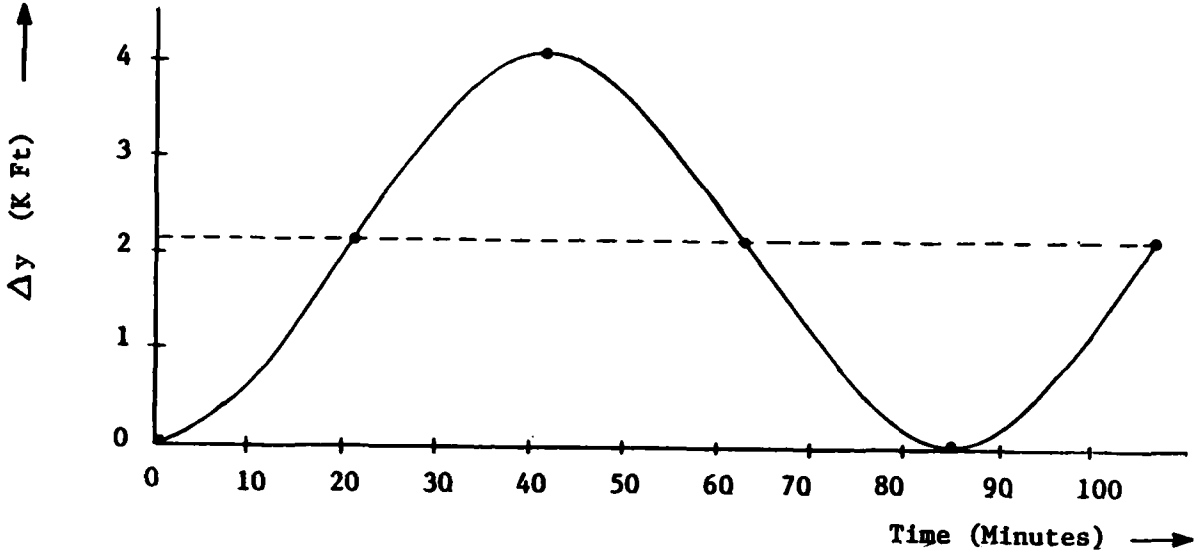

$$\Delta y = R\left[1 - \cos(W_s t)\right](\Delta \phi_o) \quad \text{(Feet)}$$

$$R = 2.1 \times 10^{7} \text{ (Ft)}$$

$$\omega_s = 1.25 \times 10^{-3} \text{ (Rad/Sec)}$$

$$\Delta \phi_o = 1.0 \times 10^{-4} \text{ (Rad)}$$

Figure 3.2.1.2 (a) -- INS North Position Error Due to Initial Platform Misalignment About East - West Axis

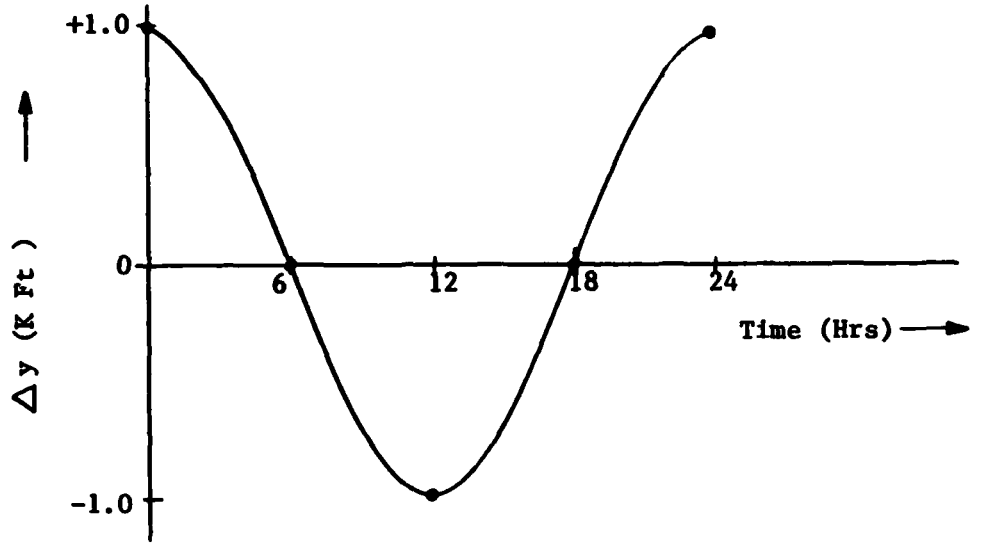

$$\Delta y = \text{Cos}\ (\Omega_E t)\ (\Delta y_o) \quad \text{(Feet)}$$

$$\Omega_E = 7.3 \times 10^{-5} \ \text{(Rad/Sec)}$$

$$\Delta y_o = 1.0 \times 10^{3} \ \text{(Ft)}$$

Figure 3.2.1.2(b)--INS North Position Error due to Initial Position Error

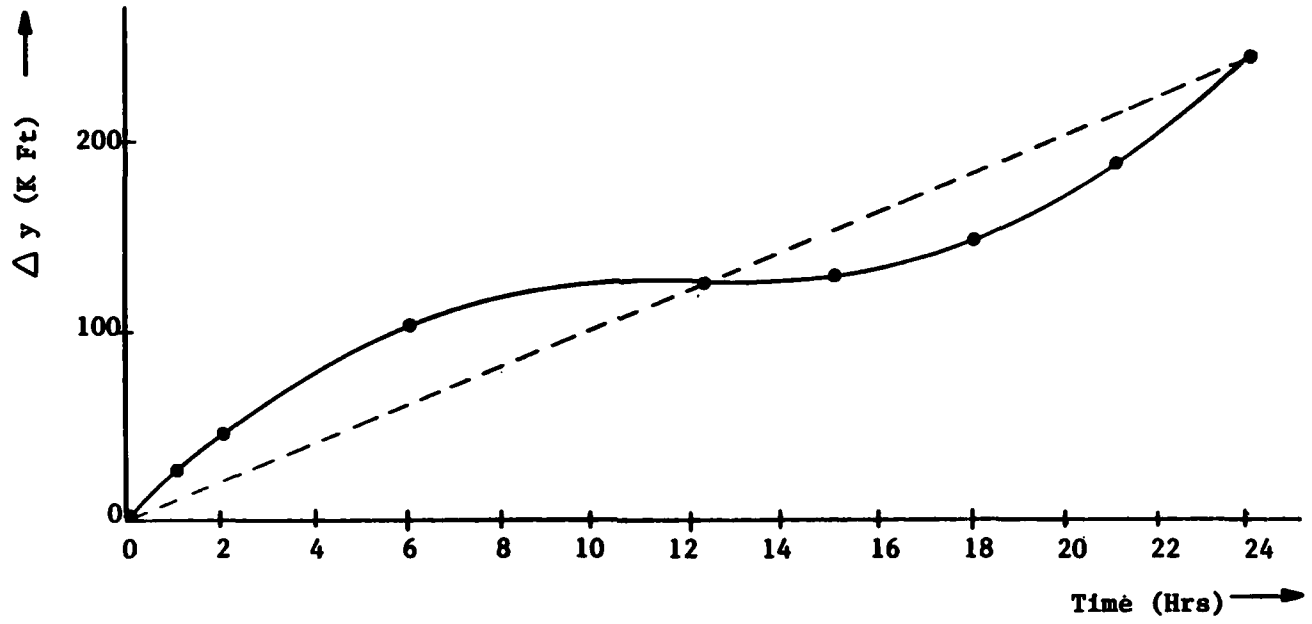

$$\Delta y = R \cos(\lambda)\left[\Omega_E t - (\Omega_E/\omega_s) \sin(\omega_s t) + \sin(\Omega_E t)\right] (\Delta\Psi_o) \quad \text{(Ft)}$$

$R = 2.1 \times 10^7$ (Ft)

$\cos(\lambda) = 0.9$ (N.D.)

$\Omega_E = 7.3 \times 10^{-5}$ (Rad/sec)

$\omega_s = 1.24 \times 10^{-3}$ (Rad/sec)

$\Delta\Psi_o = 1.7 \times 10^{-3}$ (Rad)

Figure 3.2.1.2(c)--INS North Position Error due to Initial Platform Misalignment in Azimuth

3.2.2 Other INS Characteristics -- In addition to the quantitative characteristics represented by the error model, an inertial navigation system exhibits other important functional characteristics. A list of the most important of these characteristics is presented below.

Installation Function
Warm-Up Time
Leveling Time and Performance
Gyrocompassing Time and Performance
Gimbal Limits
Attitude-Rate Limits
Velocity and/or Acceleration Limits
Update Function Performance
Operating Mode Switching
Back-Up Mode Performance
Latitude Limitations
Controls and Displays Suitability
Self Calibration Performance
Built-In-Test Function
Interfaces with Other Systems
Carrier Suitability

3.2.3 Typical INS Characteristics -- For a description of typical, currently-operational inertial navigation systems, the reader is referred to the separate, classified volume devoted to airborne system hardware descriptions.

3.3 Doppler Radar Navigation System Performance Characteristics

3.3.1 The Doppler Navigator Error Model -- The error model for a Doppler radar navigation system differs from that for an INS in that the effects of the internal dynamical characteristics of a Doppler system are minimal in determining the output errors due to various error sources. (Only the integration of the velocities to obtain position can be considered a dynamic relationship.) Thus, no extensive dynamical error model is generally needed. The error model for each output quantity consists entirely of an equation of the form (see Section 3.1.1 of this text):

$$\Delta z = \left(\frac{\partial f}{\partial x}\right)\Delta x + \left(\frac{\partial f}{\partial y}\right)\Delta y + \left(\frac{\partial f}{\partial a}\right)\Delta a + \left(\frac{\partial f}{\partial b}\right)\Delta b$$

where

z = System Output

x,y = System Inputs

a,b = System Parameters

Δ = Variational Operator

For a given system, the error sensitivity coefficients (partial derivatives) must be evaluated in order to identify the important error contributors.

The major error sources in a Doppler radar navigator are listed below.

- Doppler Radar Errors
  - Transmitted Frequency Fluctuation
  - Doppler Return Frequency Fluctuations
  - Frequency Tracker Error
  - Altitude-Hole Effects
  - Calibration Errors
- Heading Reference Errors
- Beam Direction Stabilization Errors

Computational Errors
Terrain Effects
Over-Water Effects
Maneuver-Induced Errors

Typical, one-sigma residual magnitudes for the errors listed above are shown in the following table.

Error Source	1σ Error
Doppler Radar	0.1%
Heading Reference	0.3%
Beam Stabilization	0.1%
Computation	<<0.1%
Terrain Effects	<0.1%
Over-Water Effects	0.1%
Maneuvering	<0.1%
RSS	0.36%

As can be seen from the tabulated errors, the RSS total error is dominated by the contribution due to error in the external heading reference. Note that these errors represent the residual errors after systematic error reduction. Some errors, such as those due to over-water operation will be much greater in the absence of appropriate error correction. For a 1000 nautical mile test flight over land, typical Doppler navigation system errors were found to be about 0.25% of distance traveled in the along-track direction and 0.50% of distance traveled in the cross-track direction. The greater cross-track error reflects the sensitivity of cross-track errors to errors in heading.

3.3.2 Other System Characteristics -- In addition to the quantitative characteristics represented by the error model, a Doppler navigation system exhibits other important functional characteristics. The most important of these characteristics are listed below.

Velocity and/or Acceleration Limits (Low & High)
Attitude (Roll and Pitch) Limitations
Attitude Rate Limits
Altitude Limitations (Min. and Max.)
Altitude Holes
Terrain Effects
Over-Water Flight Effects
Atmospheric Effects (Rain, Etc.)
Airspeed Effects
Aircraft Configuration Effects
Update Function Performance
Back-Up Mode Performance
Recovery from Transients
Antenna Stabilization Limits
Antenna Stability
Controls and Displays Effectiveness
Built-In-Test Function
Interface with Other Systems
Carrier Suitability

It should be noted that a Doppler navigator is principally a radar system. For that reason, the reader is referred to the text on radar system testing.

3.3.3 Typical Doppler Navigation System Characteristics -- For a description of tvpical, currently operational Doppler navigation systems, the reader is referred to the separate, classified volume devoted to airborne system hardware descriptions.

3.4 Radio Navigation System Performance Characteristics

3.4.1 The Radio Navigation Error Model -- Due to a lack of significant internal dynamics, the error model for a radio navigation system does not generally require that such effects be included. The error model for each output quantity is usually assumed to consist of a single, non-dynamic equation relating the individual contributing error factors to the error in the output (position and/or velocity). The major error sources for a radio navigation system are listed below.

Signal Propagation Anomalies
Multipath Effects
Timing Errors
Noise Effects
Signal Granularity
User Equipment Errors
Dynamic (User-Motion-Induced) Errors

The magnitudes of the errors contributed by the major error sources are presented in Figure 3.4.1.1. An essential part of the error model for a radio navigation system, (or any navigation system navigating with respect to "stations" of known location), is geometric dilution of precision (GDOP). As previously described, GDOP is the relationship between errors in the measured quantities, (such as range and bearing from a given station), and errors in the user position quantities, (such as latitude and longitude). GDOP is best presented as a "map" of error coefficient contours superimposed upon a map showing the locations of the navigation "stations".

System	Navigation Error			
	Propagation	Multipath	User Equipment	Total Error
ADF	0^{o} - 25^{o}	1^{o} - 5^{o}	1^{o} - 2^{o}	1^{o} - 30^{o}
VOR	---	3^{o}	1^{o}	3.5^{o}
DME	---	---	60 - 18,000 Ft.	60 - 18,000 Ft.
TACAN	--- ---	3^{o} ---	0.5^{o} 200 - 3,000 Ft.	3.5^{o} 200 - 3,000 Ft.
LORAN C	500 Ft.	0 - 3,000 Ft.	100 Ft.	500 - 3,000 Ft.
OMEGA	5,000 Ft.	0 - 6,000 Ft.	500 Ft.	1,200 - 12,000 Ft.

Figure 3.4.1.1 -- Radio Navigation System Errors

3.4.2 Other System Characteristics -- In addition to the quantitative characteristics represented by the error model, a radio navigation system exhibits other important functional characteristics. The most important of these characteristics are listed below.

Velocity and/or Acceleration Limits (Low & High)
Aircraft Attitude (Antenna) Limitations
Altitude Limitations (Low & High)
Airborne Antenna Patterns
Aircraft Configuration Effects
Airspeed Effects
Reliable Signal Coverage (in space and time)
ffects of Signal Propagation Anomalies
Terrain Effects
Ionospheric Effects
Tropospheric (Atmospheric) Effects
Station Selection and Signal Acquisition
Update Function Performance
Back-Up Mode Performance
Recovery from Transients
Receiver Sensitivity
Receiver Signal Overload Characteristics
Lane Ambiguity Resolution
Dead Reckoning Performance (Omega, Satellites)
Controls and Displays Effectiveness
Built-In-Test Performance
Interfaces with Other Systems
Carrier Suitability

It should be noted that a radio navigation system is essentially a radio communication system. For that reason, the reader is referred to the text on communication system testing.

3.4.3 Typical Radio Navigation System Characteristics -- For a description of typical, currently operational radio navigation systems, the reader is referred to the separate, classified volume devoted to airborne system hardware descriptions.

3.5 Satellite Navigation System Performance Characteristics

3.5.1 The Satellite Navigation System Error Model -- As for the case of the other radio navigation systems, no dynamical error model is generally required for the internal dynamics of a satellite navigation system. The major error sources are listed below.

Signal Propagation Anomalies
Multipath Effects
Satellite Ephemeris Errors
Error in User Altitude (Transit)
Error in User Velocity (Transit)
Timing Errors
Noise Effects
Errors in Dead Reckoning (Between Fixes)
User Equipment Errors
Dynamic (User-Motion-Induced) Errors

The error characteristics of the Transit navigation system are discussed in Section 2.4.2 of this text. The error characteristics of the GPS navigation system are discussed in Section 2.4.3 of this text.

3.5.2 Other System Characteristics -- It should be noted that a satellite navigation system is, in fact, a radio navigation system. The system characteristics listed in Section 3.4.2 of this text, therefore, apply to satellite navigation systems.

3.5.3 Typical Satellite Navigation System Characteristics -- For a description of the GPS satellite navigation system, the reader is referred to the separate, classified volume devoted to airborne system hardware descriptions.

4.0 Airborne Navigation System Performance Test and Evaluation

4.1 The Philosophy of Testing

4.1.1 Stages of Testing -- Testing can be categorized as developmental, functional, or operational, depending upon the stage of development of the test item. Developmental testing is concerned with the evaluation of design features for the purpose of design development. The end result of developmental testing is the proposed final design. Functional testing is concerned with the performance evaluation of the final design as a whole. The principal method of evaluation is the quantitative measurement of the ability of the test item to perform its intended functions. The end result of functional testing is final design acceptance or rejection. Operational testing is concerned with the evaluation of the final design and production implementation of the test item. Of primary interest is the ability of the test item to accomplish its intended operational mission. The end result of operational testing is acceptance or rejection of the test item for service use and the recommendation of operational procedures.

4.1.2 Testing Criteria -- The basic purpose of any stage of testing determines the criteria used to evaluate the test results. The testing criteria, in turn, are reflected in the tests to be performed and the test methods employed. Testing criteria derive from one of three objectives: data acquisition, determination of specification compliance, and evaluation of mission performance. In developmental testing the intent is to acquire comprehensive information on the characteristics of the item under test. Usually, no a-priori criteria are

imposed for performance acceptance or rejection. Functional testing, however, is primarily intended to evaluate the performance of the test item against specific criteria -- that is, for specification compliance. As previously indicated, operational testing is primarily concerned with mission performance. While some specific, quantitative requirements are imposed, test criteria for operational testing often are of a qualitative nature.

It should be recognized that the three states of testing; developmental, functional, and operational; are not mutually exclusive. That is, the differences are primarily ones of emphasis. For example, functional testing often produces data that result in a design change. Thus, functional testing often takes on some aspects of developmental testing. For that reason, it is necessary, in functional testing, to test to a depth sufficient to allow engineering analysis of the problem. A "go" or "no-go" answer is not sufficient. On the other hand, functional testing cannot ignore mission suitability in evaluating a new design. Compliance with published specifications is not sufficient if functional testing reveals an operational problem. Thus, while the following sections of this test will be concerned primarily with quantitative tests for specification compliance, it should be noted that functional testing should reflect mission requirements, including non-quantitative considerations when appropriate.

In general, functional testing is required when any one of the following circumstances applies:

(1) a new system is introduced
(2) an existing system is significantly modified
(3) the mission of an existing system is significantly extended
(4) an existing system is installed in a new aircraft with significantly different environment.
(5) an existing installation is extensively modified

With a digital system, some functional testing should be performed for even seemingly minor software changes.

4.1.3 Test Regimes -- Functional airborne system tests are performed in the laboratory, in the aircraft on the ground, and in flight. For various reasons, testing is usually performed in that order. Tests performed on the bench in the laboratory are most convenient, quickest, cheapest, and safest. Flight tests are least convenient, take the longest time, are most costly, and present the greatest danger to personnel and equipment. They also are most susceptible to uncertainties in the weather and availability of equipment. For the above reasons, tests should be performed in the laboratory, before installation in the aircraft, when feasible. Tests that can only be performed installed in the aircraft should be performed on the ground when feasible. Flight tests should be performed only when necessary and only when laboratory and ground tests have reduced the uncertainties to the greatest extent possible. Of course, some tests can be performed only in flight; and, in any event, flight performance eventually must be evaluated.

Flight tests sometimes can be performed in a test-bed aircraft. Such an arrangement allows in-flight tests to be performed with instrumentation far more extensive than would be possible with the system installed in the aircraft for which it was intended. In addition, a test bed aircraft can be employed for which flight operations are more convenient, less hazardous, and less costly. Testing in a test bed aircraft, however, cannot satisfy all flight testing requirements. The performance characteristics of all airborne systems are, to some extent, susceptible to the environment of the installation. Other factors influenced by the vehicle are the electrical power, cooling, electromagnetic interference, vibration,

acceleration, and other environmental effects. In a digital system, software interaction is an important area for evaluation.

An alternative to some flight testing is flight simulation testing. The most useful "simulations" incorporate actual flight hardware for the system under test, utilizing simulations only for generating external stimuli. Such a hybrid test simulation can, in fact, perform tests not possible in actual flight. Test "flights" can, for example, be re-run exactly, or with controlled modifications. The ability of a simulation to exactly duplicate test conditions is especially valuable in testing digital systems, where one-at-a-time modifications of the inputs are necessary to exercise the various logic branches of the software. Furthermore, real-time interrupts in a test simulation make possible the examination of internal system quantities not available in an actual flight situation.

This text is devoted to test methods peculiar to navigation system parameter determination and performance testing. Topics of general concern to airborne systems test and evaluation, such as test planning, test performance, instrumentation, data acquisition, and data analysis, are discussed in the test on Integrated Airborne Systems Test and Evaluation.

In the following sections, a brief description is given of the methods employed to determine system compliance with the major navigation system functional specifications. General testing, such as environmental, electromagnetic compatibility, reliability, and maintainability testing, is discussed in a separate text devoted to tests common to all airborne systems.

4.2 General Airborne Navigation System Testing

The function of a navigation system is that of mensuration. That is, a navigation system "measures" the motion (position and/or velocity) of a vehicle. In view of this measurement function, the primary task of an evaluator is to determine the accuracy of those measurements by comparing the results of the measurements to "truth data" obtained from an accurate, independent source. For an airborne navigation system, the principal sources of truth data are those listed below.

Fly-Over Checkpoints
Ground Instrumentation
Another Navigation System

Fly-over checkpoints can be visual references (e.g. towers or other structures), radiating installations (e.g. Tacan stations), or objects detectable by radar, infrared, or other sensor. In all cases, the location of the checkpoint reference must be accurately known, (though not necessarily fixed). The use of fly-over checkpoints requires minimal instrumentation, but provides only position information, yields discontinuous data, and constrains the test route to one for which known checkpoints exist. The accuracy of visual fly-over checkpoint data is about one-half the altitude. Typical fly-over altitudes vary between 200 and 2000 feet AGL. Fly-over accuracy can be greatly improved by the use of vertical-axis cameras.

Ground instrumentation usually consists of visual (theodolite), radar, laser tracker, or radio ranging (DME) equipment. Truth data derived from such sources has the advantage that it is essentially continuous and can yield position, velocity, and,

(by profile-matching of cine-theodolite images), approximate vehicle attitude information. The principal disadvantage of ground instrumentation data is the fact that it constrains the test flight path to the volume of coverage of the ground-based sensors. The position accuracy of ground instrumentation varies from about $\pm$ one foot (for laser trackers) to $\pm$ 1000 feet (at large ranges). Multiple trackers provide extended accuracy.

When it is feasible, the most useful source of navigation truth data is a second, accurate navigation system installed on the test vehicle. While it is desirable, it is not necessarily required, that the source of truth data be more accurate than the system under test. When properly applied, modern regression analysis techniques allow the recovery of error coefficients in the presence of other errors many times greater than those being determined. In the case of inertial navigation system testing, the ideal on-board source of truth data is another INS. Another INS yields the continuous data on position, velocity, and aircraft attitude required for the recovery of the INS error coefficients. The Global Positioning System (GPS) is another excellent source of position and velocity data. Because of the accuracy of the GPS data, it can, for most purposes, be considered a true measure of the actual position and velocity of the test vehicle. Where space and cost permit, the optimum on-board navigation reference is a high-quality, GPS-updated inertial navigation system. The position accuracy of such a system is approximately $\pm$ 10 feet over an extended area.

In addition to the quantitative evaluation of the ability of a navigation system to determine position and/or velocity, a comprehensive performance evaluation must examine various subsidiary functions. Examplesof such functions are: (1) the ability of a radio navigation receiver to select and acquire an optimum set

of transmitting stations, (2) the adequacy of antenna track stabilization in a Doppler navigator, (3) the gyrocompassing performance of an INS, and (4) the time required for a satellite navigation system to obtain a fix. All such relevant functions must be tested under conditions representing those expected in the mission for which the system under test is intended. In addition, testing also should be performed in a manner designed to reveal anticipated weaknesses in the system, including possible worst-case situations. There are two justifications for testing outside of the expected mission envelope. One is the possibility of future extensions of that envelope. The other is the need to identify the performance limitations of the system.

4.3 Inertial Navigation System Performance Testing

4.3.1 INS Accuracy Testing -- It is evident from the error model presented in Section 3.2.1 of this text that INS errors are of a dynamical nature. For that reason, they can be determined only by measurements taken over an extended period of time. Furthermore the measurements must be taken either continuously or at time intervals small compared with the smallest system time constants of interest. For example, if the error components oscillating at the Schuler frequency are to be determined, measurements must be taken over an appreciable portion of a Schuler period (84 minutes). In addition, they must be taken at intervals such that several values per cycle are recorded. (In theory, at least two readings per cycle are required. In practice, however, several readings are advisable.)

In order to "excite" the many terms in the INS error model, and thus reveal the error coefficients, the flight path of the test aircraft must be "shaped". Various directions and speeds should be included in the flight plan, and maneuvers with high turn-rates should be executed. It is expedient to fly a west-to-east course, at maximum speed, in order to test the velocity limit of the system. In order to excite the Schuler oscillations, closed paths with 84 minute flight times should be included in the flight plan. In order to examine the 24-hour oscillatory errors, the test plan should include an extended flight (at least 12 hours), if appropriate for the aircraft. Testing should include flights which involve operation in the vicinity of computationally significant points, such as the equator, the poles, and the International Date Line. Aircraft maneuvers should be executed

that are designed to test the attitude, linear and angular acceleration and velocity responses of the system. It is especially important to perform those maneuvers routinely employed in the intended missions for the aircraft under test. In order to distinguish between "forced" and "unforced" errors, it is useful to record at least one Schuler cycle while stationary (one the ground) both before and after the flight test. These data also allow an examination of the total accumulated errors. The pre-flight data allow evaluation of alignment (gyrocompassing) performance. The performance of the INS must be evaluated in all modes (Alignment, Inertial, Doppler-Inertial, Etc.).

Data should be recorded at about 5 or 10 minute intervals throughout the test flight. While manual recording of position, velocity, and time requires the least instrumentation, automatic recording is desirable because of the large number of data points required. Automatic data recording also provides essentially continuous data and allows a large number of other quantities to be recorded, if desired.

The minimum data required for each time point includes indicated position (latitude, longitude, and altitude), actual position, and time. Other quantities of interest are listed below.

System Status
INS Velocities
Ground Speed
Ground Track Angle
True Airspeed
True Heading
Magnetic Heading
Magnetic Variation
Barometric Altitude
Wander Angle
INS Pitch and Roll Angles

Computed Wind Velocity
Drift Angle
Command and Event Marker Tones
Outputs from other Systems for
Comparison with INS Outputs

The recorded data are generally processed to obtain north-south and east-west position errors. In addition, radial error is usually derived. In order to facilitate the identification of individual error coefficients, it is useful to resolve the errors into the INS computational coordinate system. (If the system is a wander azimuth system, the computational coordinates are oriented to the wander angle.) From the above error data, the circular error probable (CEP) can be determined as a function of navigating time. In addition, the mean, standard deviation, rms value, and other statistics can be determined.

INS accuracy testing results are best presented as a function of navigating time. In Figure 4.3.1.1 is shown a plot of radial position error, as a function of time, derived from actual test data. As indicated in the figure, the test flight path consisted of a number of 84-minute orbits. The first approximately six hours were flown in the free inertial (I) mode, followed by about two hours on the Doppler-Inertial (DI) mode. The proper functioning of the Doppler damping is evident in the error time history. It is likely, (though not obvious), that a large part of the apparent increase of average radial error with time is, in fact, the first portion of an oscillatory, 24-hour period, error component.

4.3.2 Other Inertial Navigation System Testing --

In addition to accuracy testing, the INS characteristics listed in Section 3.2.2 of this text must be evaluated. In large part, the accuracy tests described above allow adequate examination of these other characteristics. Some characteristics, however, require special tests. Those tests which can be performed

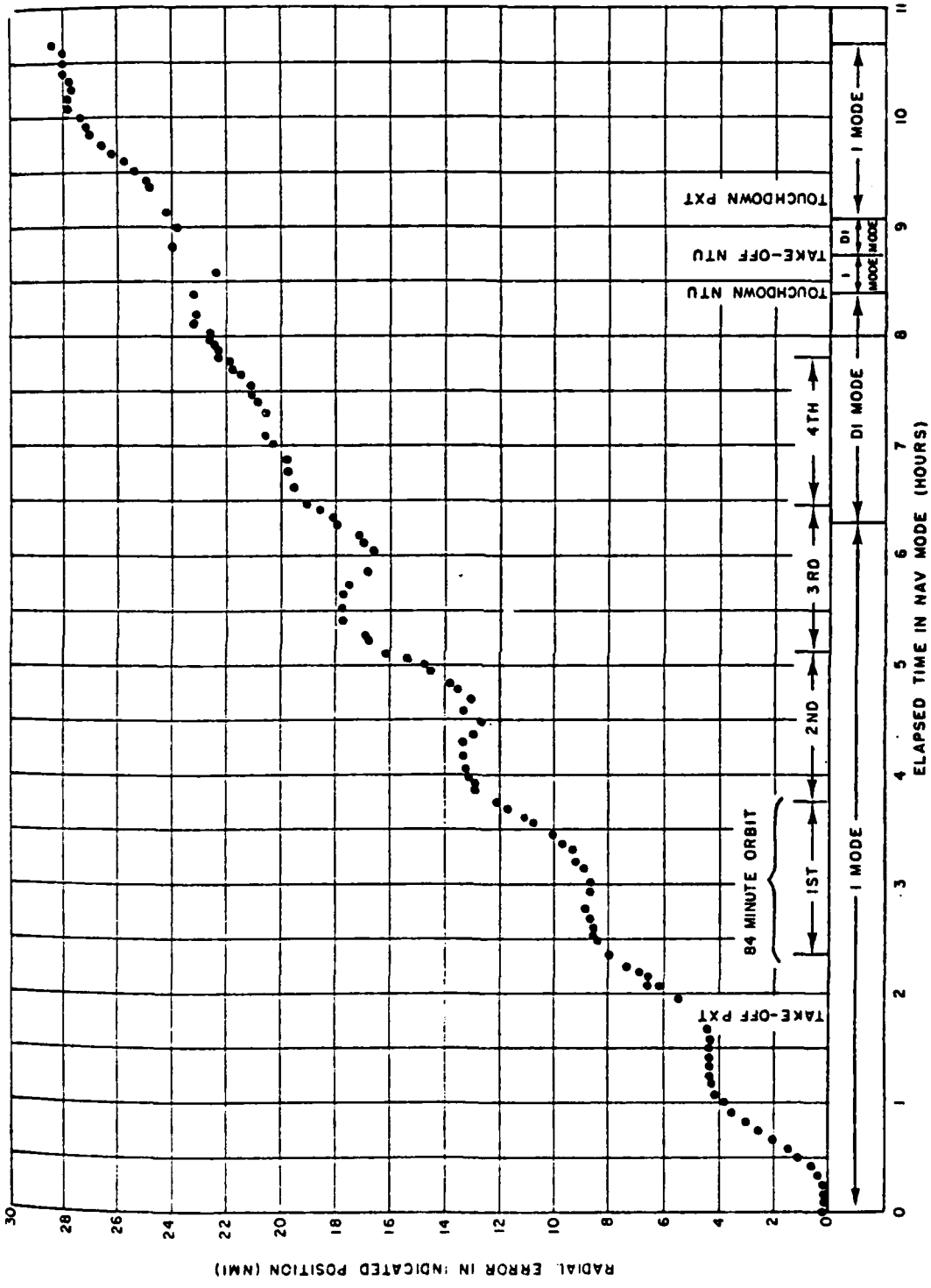

Figure 4.3.1.1 -- Inertial Navigation System Radial Position Error

on the bench (in the laboratory), on the ground (installed in the aircraft), and in flight are indicated in the following lists.

Bench Tests

Operational Mode Selection
Warm-Up and Leveling Times
Self-Alignment Time and Accuracy
Acceleration Input Response
Attitude Rate Response (Earth Rate and Rate Table)
Update Function
Self-Calibration
Built-In-Test
Acceleration and Velocity Limits
Gimbal Limits
Attitude Rate Limits
Controls and Displays Suitability
Interfaces with Other Systems (Simulated Inputs & Outputs)
Response to Transients (Mode and Power)

Ground Tests

Installation
Operation Mode Selection
Warm-Up and Leveling Times
Self-Alignment Time and Accuracy
Static Drift Test
Update Function
Self-Calibration
Built-In-Test
Controls and Displays Effectiveness
Interfaces with Other Systems (Inputs & Outputs)
Taxi Tests (Navigation and Alignment Interrupt)

Flight Tests

Operational Mode Selection
Warm-Up and Leveling Times
Self-Alignment Time and Accuracy
Self-Calibration
Built-In-Test
Aircraft Maneuvering Effects
Gimbal Limits
Attitude Rate Limits
Acceleration and Velocity Limits
Update Function
Back-Up Mode Performance
Latitude Limitations (Singularity & Gyrocompassing)
Singular Point Effects
Controls and Displays Effectiveness
Interfaces with Other Systems
Carrier Suitability

4.4 Doppler Navigation System Performance Testing

4.4.1 Doppler Navigator Accuracy Testing -- The errors in a Doppler navigation system are primarily functions of the distance traveled. There also is some dependence of the errors on time. (A constant offset (bias) at the input of the velocity-to-position integrator results in an error that increases linearly with time). Both distance-dependent and time-dependent errors must be evaluated by measurements taken over an extended period of time.

The flight path employed in Doppler navigator accuracy testing must be "shaped" in order to induce errors from the sources listed in Section 3.3.1 of this text. In order to induce errors in the Doppler radar velocity measurements, the test flights should include periods of high ground speed and acceleration. In order to evaluate errors due to the heading reference, the tests should include prolonged operation at each of several constant headings. In order to evaluate altitude sensitivity and altitude-hold effects, operation at various altitudes is necessary. In order to evaluate the adequacy of antenna stabilization, aircraft maneuvers about all three axes are required. The test flights must be planned to include operation over various types of terrain and over water in various sea states. Prolonged periods of hovering are needed for helicopter installations in order to detect velocity bias errors. The test flights should, of course, include any maneuvers or conditions expected to be encountered in the missions for which the system is intended.

Truth data for Doppler navigator evaluation is obtained by the same methods employed for the evaluation of an INS or other navigation system. Because of the

nature of the basic Doppler velocity measurements, however, the task of error analysis is greatly facilitated if velocity, as well as position, truth data are obtained. Unfortunately, ground velocity truth data of sufficient quality are not easily obtained. One possible source is the use of ground-based Doppler radars. Another is the use of ground-based laser trackers. Similarly, the task of error analysis is greatly facilitated if heading truth data are obtained. (The greatest single source of error in a Doppler navigator is heading error.) Accurate determinations of true heading are, however, even more difficult to obtain than are determinations of ground velocity. An on-board INS is one possible source of accurate heading data. Data should be recorded at about 15 minute intervals throughout the test flight. Position, velocity, altitude, and time constitute a minimum data set. Other quantities of use in data analysis include:

System Status
Ground Track Angle
True Heading
True Airspeed
Magnetic Heading
Magnetic Variation
Barometric Altitude
Aircraft Attitude (Pitch and Roll)
Doppler Return Signal Strength
Command and Event Marker Tones
Outputs from Other Systems for Comparison with Doppler Navigation Outputs
Weather Conditions

The recorded data are generally processed to obtain along-track and cross-track position and velocity errors. (The major errors in a Doppler navigation system tend to be evident in a ground-track-oriented coordinate system.)

When errors are examined in a along-track/cross-track format, care must be taken to "desensitize" the apparent accumulated error to changes in heading. In order to be meaningful the along - and cross-track errors at a given point must be

associated with the flight path that produced those errors. One way to achieve such association is to divide the actual flight path into successive, straight-line (constant heading) segments and to determine the incremental along - and cross-track errors associated with each segment. The total errors at any point in the flight then would be the sum of the individual errors for each segment. Another way to isolate along - and cross-track errors from changes in heading is to include in the actual flight path extended runs at constant heading. The errors accumulated during each run then can be evaluated separately.

Useful information also can be obtained by resolving the errors into a north-oriented coordinate system. (Errors due to some magnetic heading reference errors are more evident in a magnetic-north-oriented coordinate system.)

Doppler navigator accuracy testing results are normally presented in a plot of position and velocity error as a function of distance traveled. (Both heading reference errors and velocity scale factor errors tend to accumulate with distance traveled.) The quantity plotted can be the error for each individual flight or it can be the CEP, RMS, or mean and deviation of the data ensemble from a number of flights. Also useful is a plot of error growth rate with distance traveled versus distance traveled.

Shown in Figure 4.4.1.1 is a typical plot of Doppler navigator error as a function of distance traveled. As indicated in the drawing, two major changes of heading were executed. The apparent changes in the slope of the cross-track errors indicate an error in the system magnetic heading reference (single-cycle compass deviations.) Along-track errors are relatively insensitive to heading errors, as

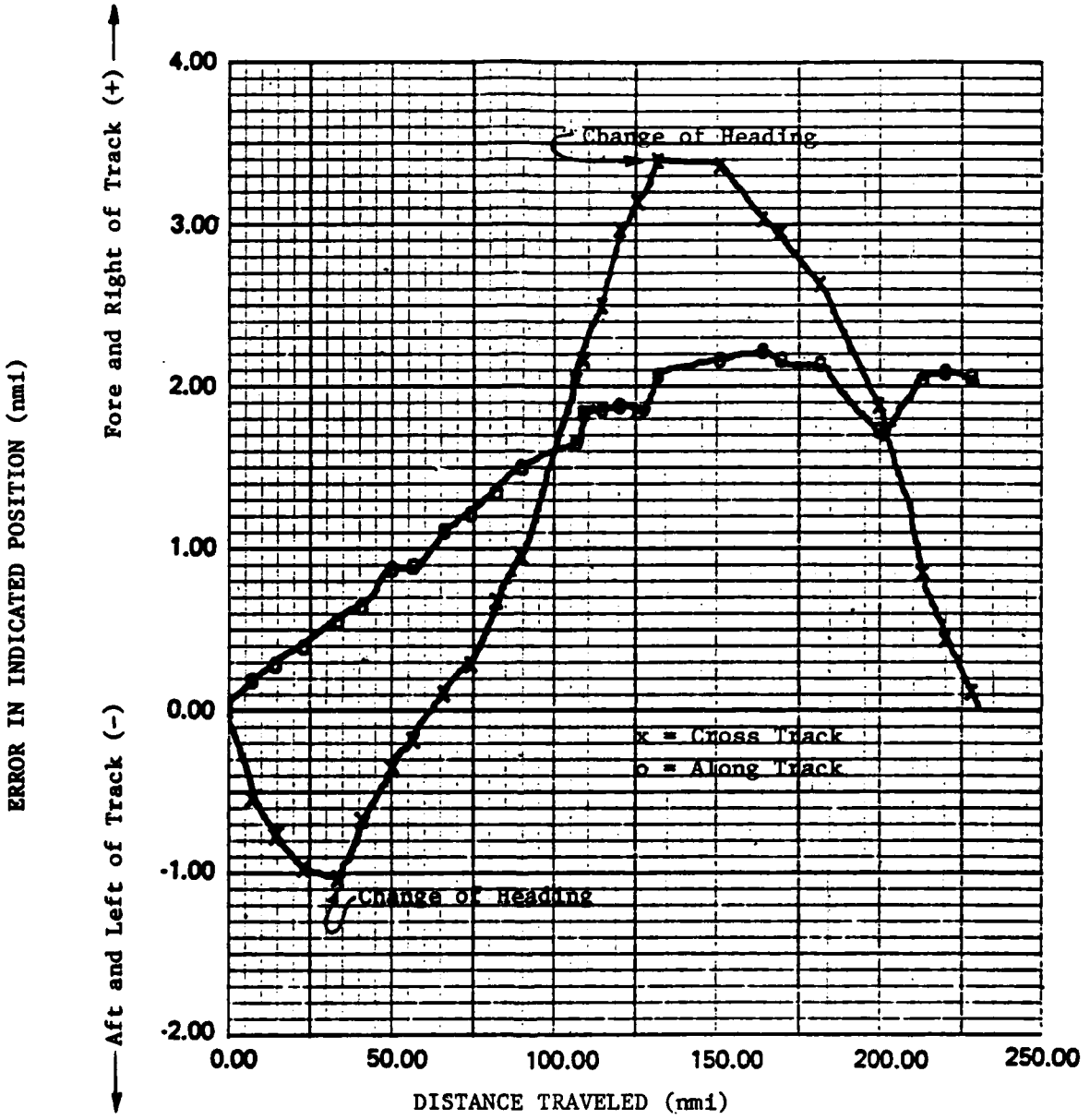

Figure 4.4.1.1 -- Doppler Navigation System Error as a Function of Distance Traveled

indicated by the minor effect of heading change on the along-track error curve. The relatively constant initial slope of the along-track error curve suggests a Doppler radar bias or scale-factor error. (A velocity change would have distinguished between the two.) The reduction in slope of the latter portion of the along-track error curve indicates that another, heading-dependent error source also is contributing to along-track error.

4.4.2 Other Doppler Navigation System Testing -- In addition to accuracy testing, the Doppler navigator characteristics listed in Section 3.3.2 of this text must be evaluated. Those tests which can be performed on the bench (in the laboratory), on the ground (installed in the aircraft), and in flight are indicated in the following lists.

Bench Tests

Operational Mode Selection
Response to Simulated Velocity Inputs
Response to Simulated Heading Inputs
Response to Simulated Aircraft Attitude Inputs
Position Update Function
Built-In-Test
Controls and Displays Effectiveness
Interfaces with Other Systems

Ground Tests

Installation
Operational Mode Selection
Position Update Function
Built-In-Test
Controls and Displays Effectiveness
Interfaces with Other Systems
Antenna Stabilization Limits

Flight Tests

Operational Mode Selection
Velocity and Acceleration Limits
Attitude Limits
Attitude Rate Limits
Altitude Limitations (Min and Max)
Altitude Holes
Terrain Effects
Over-Water Effects
Atmospheric Effects (Rain, Etc.)
Airspeed Effects
Aircraft Configuration Effects
Update Function Performance
Back-Up Mode Performance
Recovery from Transients
Antenna Stabilization Limits
Antenna Stability
Controls and Displays Effectiveness
Built-In-Test
Interface with Other Systems
Carrier Suitability

4.5 Radio Navigation System Performance Testing

4.5.1 Radio Navigation System Accuracy Testing -- The errors in a radio navigation system are caused primarily by wave propagation effects and are functions of the position of the user with respect to the transmitting stations. Except for seasonal and daily variations in signal propagation, there is little time dependence of the error model. Similarly, except for signal correlation and smoothing times, there are no significant internal dynamic effects. Motion of the user induces significant errors in some systems. When long solution times would otherwise cause unacceptable errors, dead reckoning is generally employed to avoid the effects of user motion. In such cases, errors in dead reckoning affect the overall accuracy of the system.

Because of the position dependence (rather than time dependence) of radio navigation system errors, it is more important, in testing such systems, to test over a range of positions than to test over a period of time. (The daily and seasonal variations noted above make it necessary to test at various times of day and times of the year.)

The flight path employed in radio navigation accuracy testing should be "shaped" to exercise the geometric dilution of precision (GDOP) and propagation errors of the system. The flight path, therefore, must be appropriately oriented with respect to the positions of the stations. If the "stations" are in motion, (e.g. satellites), the position of the user with respect to the station is a function of the user position, the satellite ephemeris, and the time of day.

In order to obtain the information required for a statistical analysis of the errors, redundant data must be obtained with respect to user-station relative position.

As is the case for all airborne systems testing, radio navigation system testing should include flight paths designed to test the extremities of the operation envelope as well as those designed to represent expected missions. Of special importance in radio navigation system testing is the effect of aircraft attitude (receiving antenna patterns) and altitude (transmitting antenna patterns). Aircraft external configuration can greatly affect the receiving antenna patterns.

Truth data for radio navigation testing is obtained by the same methods employed for other navigational systems. There are, however, two situations of special interest. One is the testing of short-range, precision landing systems (ILS, GCA, MLS). Because of the precision required, special instrumentation (e.g. optical or laser trackers) is necessary. Fortunately, such precision instrumentation is feasible over the small test volumes of interest. The other special situation is the testing of world-wide navigation systems such as Omega or GPS. Because of the tremendous test volume involved, it is difficult to obtain complete, continuous, consistent coverage. The testing of precision systems such as GPS is especially difficult because of the accuracy required. (GPS is an accurate source of continuous truth data for the testing of other world-wide navigational systems.) The most convenient current method of obtaining world-wide navigational truth data is the use of several precise, short-range navigation aids. Fly-over checkpoints provide a non-continuous source of such data. Fortunately, because of the lack of internal dynamic effects in a radio navigation system, absolute continuity of the truth data is not generally critical.

Radio navigation test data should be recorded at position intervals which depend upon the user-to-transmitter geometry. In areas of high time of arrival-to-position gradient, data must be taken at correspondingly small intervals. Position, velocity, altitude, time, and date constitute a minimum data set. Other quantities of interest include:

System Status
Signal Strength
Signal-to-Noise Ratio
Aircraft Attitude (Pitch and Roll)
Aircraft Magnetic Heading
Aircraft True Heading
Magnetic Variation
Barometric Altitude
Stations Selected
Received Signal Phases
Solution Variances (when available)
Weather Conditions
True Airspeed
Ground Speed
Ground Track Angle
Command and Event Markers

The recorded data are generally processed to obtain north-south and east-west errors as well as errors in a coordinate system consistent with user-to-station geometry (GDOP).

Radio navigation system errors can be presented as contours of constant error superimposed upon a map showing the locations of the transmitting stations (or satellite ground track.) The quantity plotted can be those errors for a given flight or it can be a statistical measure of the error from a number of flights (RMS, CEP, Mean, Standard Deviation).

When statistical error data applicable to a given area of coverage are of interest, the error information can be presented without reference to position within that

area. Such data can be presented as a geographical distribution pattern (north-south error versus east-west error) as shown in Figure 4.5.1.1; or it can be presented in statistical form as a plot of cumulative probability distribution versus radial error, as shown in Figure 4.5.1.2. (The information presented in Figure 4.5.1.2 represents data taken for flight paths covering the entire continental United States.)

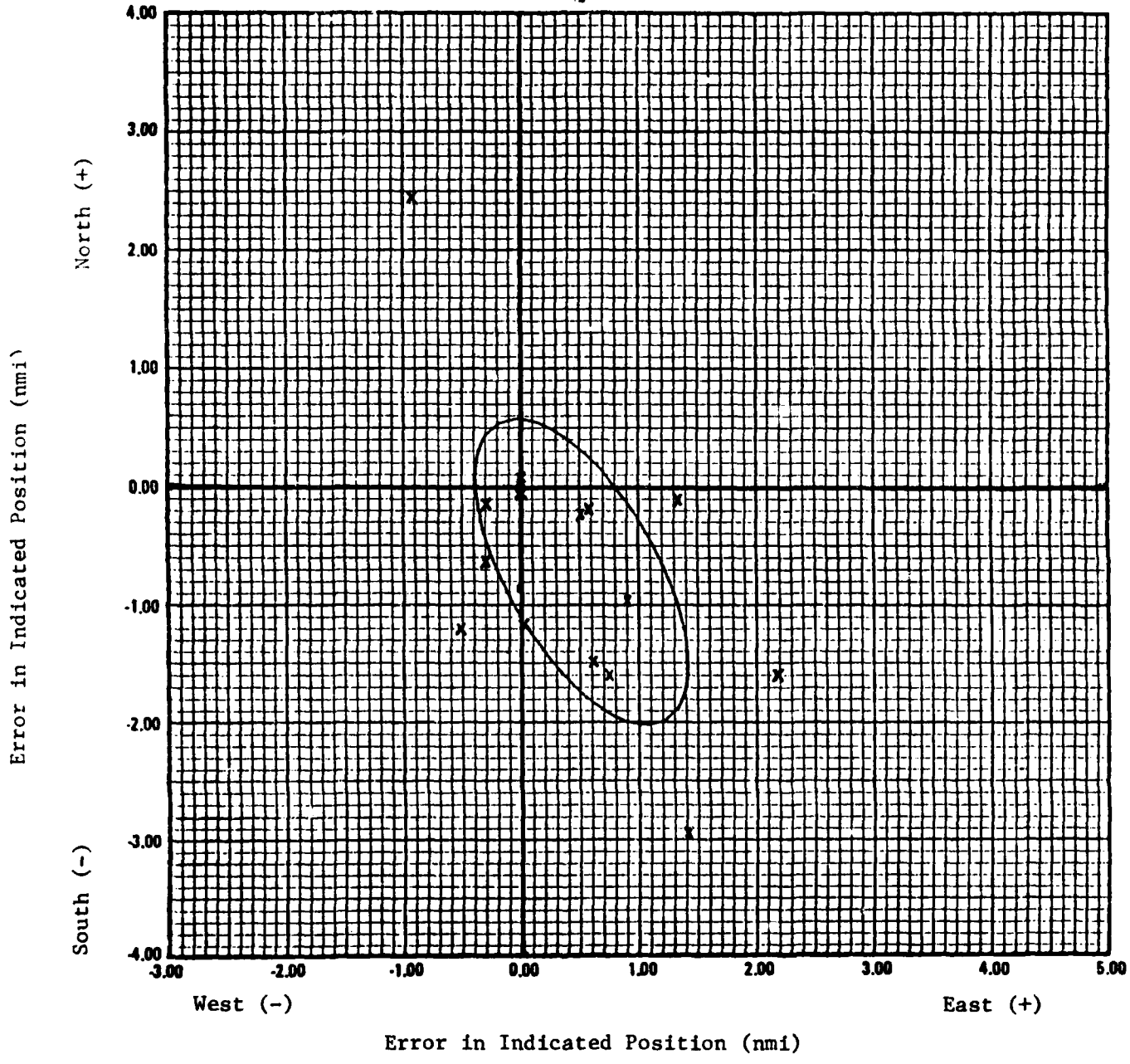

Figure 4.5.1.1 -- Omega Radio Navigation System Position Error

4.5.2 Other Radio Navigation System Testing -- In addition to accuracy testing, the radio navigation system characteristics listed in Section 3.4.2 of this text must be evaluated. Those tests which can be performed on the bench (in the laboratory), on the ground (installed in the aircraft), and in flight are indicated in the following lists.

Bench Tests

Operational Mode Selection
Receiver Sensitivity
Receiver Signal Overload Characteristics
Response to Simulated Radio Inputs
Response to Simulated Auxiliary System Inputs
(Airspeed, Groundspeed, Heading, Drift Angle,
Inertial Velocity, Altitude, Etc.)
Position Update Function
Lane Ambiguity Resolution Performance (Omega)
Built-In-Test
Controls and Displays Effectiveness
Interfaces with Other Systems

Ground Tests

Installation
Operational Mode Selection
Receiver/Antenna Sensitivity
Antenna Patterns
Aircraft Configuration Effects
Station Selection and Acquisition Performance
Position Update Function
Built-In-Test
Interfaces with Other Systems
Controls and Displays Effectiveness

Flight Tests

Operational Mode Selection
Station Selection and Signal Acquisition
Airborne Antenna Patterns
Aircraft Configuration Effects
Airspeed Effects
Aircraft Maneuvering Limitations
Velocity and/or Acceleration Limits
Attitude Limitations
Altitude Limitations
Reliable Signal Coverage
Effects of Signal Propagation Anomalies
Terrain Effects
Ionospheric Effects
Tropospheric (Weather) Effects
Lane Ambiguity Resolution
Dead Reckoning Performance
Back-Up-Mode Performance
Controls and Displays Effectiveness
Built-In-Test Performance
Interfaces with Other Systems
Carrier Suitability

4.6 Satellite Navigation System Performance Testing

Current satellite navigation systems are, in fact, radio navigation systems. The differences in their characteristics from those of earth-based systems (and, hence, the differences in their testing) are primarily a result of the fact that satellites are in motion. For that reason: (1) their ephemeris must be obtained, and (2) the geometric dilution of precision depends not only upon user position but also the satellite position. The differences in testing produced by the nature of satellite navigation stations are relatively minor and are primarily ones of degree, rather than kind. For example, because of the motion of the satellites, time-of-day becomes more critical. On the other hand, the large "baseline" afforded by satellites makes GDOP less critical. Without exception, the characteristics of interest and test considerations presented in Section 4.5 of this text apply to the testing of satellite navigation systems.

END

FILMED

8-83

DTIC